The Convection Dispersion Equation- not the Question, the Answer!

Anion and Cation Transport through Undisturbed Soil Columns during Unsaturated Flow

A thesis presented in partial fulfilment of the requirements for
the degree of
Doctor of Philosophy in Soil Science
at Massey University

Iris Vogeler

1997

Abstract

Prediction of solute movement through the unsaturated zone is important in determining the risk of groundwater contamination from both "natural" and surface applied chemicals. In order to understand better the mechanisms controlling this water-borne transport, unsaturated leaching experiments were carried out on undisturbed soil columns, about 3 litres in volume, for two contrasting soils. One was the weakly-structured Manawatu fine sandy loam, and the other the well-aggregated Ramiha silt loam. Anion transport was satisfactorily described using the convection dispersion equation (CDE), provided that anion exclusion for the Manawatu soil, and adsorption for the Ramiha soil were taken into account. At water flux densities of about 3 mm h^{-1}, a dispersivity of about 40 mm was obtained for the Manawatu soil, and a dispersivity of about 15 mm for the Ramiha soil. The difference was probably due to the contrasting structures of the two soils. Increasing the water flux density in the Manawatu soil to about 13 mm h^{-1} resulted in a slightly higher dispersivity of about 60 mm.

Flow interruption resulted in a subsequent drop in the effluent concentration for the Manawatu soil but not in the Ramiha soil. This suggests that the lag time for transverse molecular diffusion from "mobile" to "immobile" water domains was important in the Manawatu soil, but not in the Ramiha soil.

In both soils cation transport was described satisfactorily with the CDE in conjunction with cation exchange theory, providing that only 80% of the cations replaced by 1 *M* ammonium acetate were assumed to be involved in exchange reactions.

Column leaching experiments were also carried out using a rainfall simulator and larger columns of about 22 litres of the Manawatu soil with a short pasture on top. Solid chemical was applied to both a dry and a wet soil surface. Neither the pasture nor the initial water content had a significant effect on solute movement. Slightly higher dispersivities of about 70 mm were found.

Time Domain Reflectometry (TDR) was found to be valuable for monitoring solute transport in a repacked soil under transient water flow conditions. But in undisturbed soils TDR only proved to be accurate under steady-state water flow when absolute values of solute concentration were not sought.

The CDE was thus found to satisfactorily answer the question of how to describe transport of non-reactive and reactive solutes under bare soil and under short pasture. This applied during both steady-flow and transient wetting.

Acknowledgements

Thanks to god for creating such a wonderful soil, and for taking the time to separate the soil water into "mobile" and "immobile" fractions (or not?).

Special thanks to David Scotter for his excellent supervision, understanding and encouragement throughout my study. Dave, aside from being an expert in the field of soil physics, was always concerned for my future and well-being. Apart from tons of help and advice, he showed plenty of patience in watching bubbles throughout sleepless nights.

Thanks also to Brent Clothier for his patient discussion and constructive criticisms during the research and writing of my thesis, as well as for his friendship.

Appreciation and thanks are also extended to Russell Tillman and Steven Green. Steve's introduction to the TDR-system and modelling was much appreciated.

The Department of Soil Science and the Environment Group of HortResearch as a whole have always been friendly, and gave help whenever I needed it.

Finally I would like to express my gratitude to my parents, brother and also to Shane for their love and support.

Table of Contents

CHAPTER 4

CHAPTER 5

CHAPTER 6

CHAPTER 7

List of Tables

Chapter 4

Chapter 5

List of Figures

Chapter 2

Chapter 3

Chapter 4

Chapter 5

Chapter 6

List of Symbols

Roman Symbols

a	empirical constant	[m^3 kg^{-1}]
a_1 , a_2	variables in computer program	-
b	empirical constant	-
b_1, b_2	variables in computer program	[kg or mol m^{-3}]
c	propagation of an electromagnetic wave in free space	[m s^{-1}]
c_1, c_2	variables in computer program	[(mol m^{-3})^2]
c_3	empirical constant	-
d	empirical constant	-
f	fraction of exchange sites in immobile water domain	-
f_c	temperature correction coefficient	-
$f_t(Q)$	solute probability function of cumulative infiltration	[m^{-1}]
$f_t(t)$	solute travel-time probability function	[s^{-1}]
g	solute life-time probability function	[s^{-1}]
h_o	pressure head	[m]
l	column length or calibration length	[m]
l_a	apparent TDR probe length	[m]
l_t	TDR probe length	[m]
n	constant in Eq. 2.22 and Eq. 2.40	-
q_d	diffusional flux exchange between mobile and immobile water	[kg or mol m^{-2} s^{-1}]
q_i	solute flux in immobile phase	[kg or mol m^{-2} s^{-1}]
q_m	solute flux in mobile phase	[kg or mol m^{-2} s^{-1}]
q_w	water flux density	[m s^{-1}]
q_s	solute flux density	[kg or mol m^{-2} s^{-1}]
r	voltage reflection coefficient	-
t	time	[s]
t'	input time	[s]
v	pore water velocity	[m s^{-1}]

v_p	relative velocity setting on TDR instrument	-
v_e	propagation velocity of an electromagnetic pulse	[m s^{-1}]
x	variable in computer program	[kg or mol m^{-3}]
y	variable in computer program	[kg or mol m^{-3}]
z	depth	[m]

A_s	cross-sectional area	[m^2]
A	ion species	-
B	ion species	-
C	concentration in soil solution	[kg or mol m^{-3}]
$C_a(z)$	depths-dependent initial soil solution concentration	[kg or mol m^{-3}]
C_{ai}	total initial anion concentration	[kg or mol m^{-3}]
C_A	concentration of cation species A in soil solution	[kg or mol m^{-3}]
C_B	concentration of cation species A in soil solution	[kg or mol m^{-3}]
C_f	flux-averaged solute concentration	[kg or mol m^{-3}]
C_i	resident soil solution concentration in immobile phase	[kg or mol m^{-3}]
C_m	resident soil solution concentration in mobile phase	[kg or mol m^{-3}]
$C_o(t)$	time-dependent input solution concentration	[kg or mol m^{-3}]
C_r	resident soil solution concentration	[kg or mol m^{-3}]
C_s	soil solution concentration of ion species *s*	[kg or mol m^{-3}]
C_T	total cation concentration in soil solution	[kg or mol m^{-3}]
C_1	constant concentration	[kg or mol m^{-3}]
D_s	hydrodynamic dispersion coefficient	[m^2 s^{-1}]
D_i	diffusion coefficient in soil	[m^2 s^{-1}]
D_m	dispersion coefficient in mobile phase	[m^2 s^{-1}]
D_w	soil water diffusivity	[m^2 s^{-1}]
D_o	diffusion coefficient in water	[m^2 s^{-1}]
F_{in}	solute mass flux entering soil volume	[kg or mol s^{-1}]
F_{ex}	solute mass flux leaving soil volume	[kg or mol s^{-1}]
I	ionic strength	-
J_c	convective solute flux in mobile water	[kg or mol m^{-2} s^{-1}]

J_{disp}	dispersive solute flux in mobile water	[kg or mol m^{-2} s^{-1}]
J_E	diffusional flux exchange between mobile and immobile water	[kg or mol m^{-2} s^{-1}]
J_L	longitudinal diffusional flux	[kg or mol m^{-2} s^{-1}]
K_{A-B}	selectivity coefficient for cation species A and B	-
K_{M-D}	selectivity coefficient in Gapon equation	[(mol kg^{-3})$^{1/2}$]
K_d	distribution coefficient	[m^3 kg^{-1}]
K_G	geometric constant of TDR probe	[m^{-1}]
K_s	saturated hydraulic conductivity	[m s^{-1}]
K_w	hydraulic conductivity	[m s^{-1}]
L_D	diffusion/dispersion length parameter	[m]
L_{diff}	diffusion length parameter	[m]
L_{dis}	dispersion length parameter	[m]
L_{mim}	mobile/immobile exchange length parameter	[m]
M_o	pulse of solute applied to soil surface	[kg or mol m^{-2}]
M	total solute concentration	[kg or mol m^{-3}]
M_i	solute mass in immobile phase	[kg or mol m^{-3}]
M_m	solute mass in mobile phase	[kg or mol m^{-3}]
P	Pèclet number	-
R	retardation factor	-
R_C	radius of cylinders of porous soil	[m]
R_H	radius of cylindrical macropores	[m]
R_S	radius of spheres	[m]
Q	cumulative drainage or infiltration	[m]
R	solute retardation factor	-
S	sorptivity	[m $s^{-1/2}$]
S_s	amount of solute adsorbed	[kg or mol kg^{-1}]
T	travel time of electromagnetic pulse	[s]
V_o	zero reference voltage	[V]
V_f	final reflected voltage at very long time	[V]
V_i	voltage of incident step	[V]
V_r	voltage after reflection from probe end	[V]

X_A	charge concentration of cation species A on exchanger	[$mol_c\ kg^{-1}$]
X_{CEC}	charge concentration of adsorbed cations	[$mol_c\ kg^{-1}$]
Z_o	characteristic impedance	[Ω]
Z_L	impedance of TDR probe	[Ω]

Greek Letters

α	mass transfer coefficient	[s^{-1}]
β	constant	-
δ	Dirac delta function	-
ε	dielectric constant	-
γ	constant	-
λ	dispersivity	[m]
λ_{eff}	effective dispersivity	[m]
λ_m	dispersivity in mobile water	[m]
λ_{meff}	effective dispersivity in mobile phase	[m]
λ_{num}	numerical dispersivity	[m]
μ_l	mean of the lognormal distribution	[s]
ρ_b	soil bulk density	[$kg\ m^{-3}$]
σ	bulk soil electrical conductivity	[$S\ m^{-1}$]
σ_l	variance of the lognormal distribution	[s]
σ_s	surface conductance	[$S\ m^{-1}$]
σ_w	pore water electrical conductivity	[$S\ m^{-1}$]
τ	tortuosity factor	-
θ	volumetric water content	[$m^3\ m^{-3}$]
θ_a	residual water content	[$m^3\ m^{-3}$]
θ_i	immobile water fraction	[$m^3\ m^{-3}$]
θ_m	mobile or effective water fraction	[$m^3\ m^{-3}$]
θ_n	initial water content	[$m^3\ m^{-3}$]

θ_s	saturated water content	[m^3 m^{-3}]
θ_x	excluded water fraction	[m^3 m^{-3}]
ω	attenuation coefficient	-

Subscripts

n	depth position
j	time index
Ca	calcium
D	divalent
K	potassium
Na	sodium
M	monovalent
Mg	magnesium
CM	calcium plus magnesium

Abbreviations

BTC	breakthrough curve
CDE	convection dispersion equation
CEC	cation exchange capacity
CLT	convective lognormal transfer function
E_l	expected mean travel time at reference depth l
E_z	expected mean travel time at depth z
MIM	mobile/immobile concept
pdf	probability density function
REV	representative elementary volume
REA	representative elementary area
TDR	time domain reflectometry
Var_l	variance at reference depth l
Var_z	variance at depth z

Chapter 1

1. Introduction

Leaching of contaminants such as agricultural chemicals, pesticides, and leachates from waste disposals and landfills through the unsaturated zone into the underlying groundwater has become an important area of environmental research worldwide. The development of models for simulating contaminant transport is a key component for environmental impact assessment, as it can take decades for groundwater contamination to become apparent. One of the most important parts of solute transport modelling is to identify the relevant transport processes. Although during recent years much effort has been directed toward the identification of these processes, it still remains unclear as to which physical, chemical and biological processes are most important for describing contaminant transport (Kutílek and Nielsen, 1994). Furthermore the ranking of importance is likely to be as variable as soils are in Nature!

The recognition of the need to develop solutions for various agricultural and environmental problems such as pollution of surface and groundwater resources has led to the development of environmentally-based laws and regulations, such as New Zealand's Resource Management Act (1991). The regional and district plans within this Act are directed towards ensuring sustainable surface application of agricultural chemicals. Irrigation management requires efficient use of water to minimize the hazardous potential of agrichemicals on the environment, such as the leaching of soil nutrients into the groundwater. An understanding of the processes affecting solute transport is necessary to achieve this.

In an attempt to advance the understanding of the transport processes various models have been proposed (Nielsen and Biggar, 1961; van Genuchten and Wierenga, 1986). Early models considered only non-reactive chemicals, with transport affected only by convection and dispersion. During the last decade, more and more complex models have been developed to simulate multispecies transport. However, the relative capabilities of existing models and the credibility of their results is still an important concern (Jury, 1983; Wagenet, 1983). This is due primarily to the unavailability of

appropriate data to confirm the assumptions of these different models and to estimate their accuracy. Thus, as Engesgaard and Christensen (1988) pointed out: ... "future research should be directed towards validation studies ...rather than developing still more complex models".

1.1 The Purpose of the Study

The most-commonly used model to predict solute movement in soil is the convection-dispersion equation (CDE). However despite its widespread use, the validity of the CDE has been questioned. The main concerns are that diffusive mass transfer in aggregated soils containing immobile water, solute dispersion growth with transport distance (Khan and Jury, 1990; Jury and Roth, 1990), and flow down preferential pathways appear to make it invalid in many situations (Schulin *et al.*, 1987b).

The CDE has been found to describe satisfactorily one-dimensional solute transport through homogeneous columns of repacked soil. However in soil columns packed with large aggregates, or in structured soils, or in the field, the CDE has sometimes been found wanting (Biggar and Nielsen, 1976; van Genuchten and Wierenga, 1976; Nkedi-Kizza *et al.*, 1982; White *et al.*, 1984). Solute movement at variance with the CDE has been explained by nonequilibrium in solution concentration between mobile and immobile water regions (van Genuchten and Wierenga, 1976), dead end pores, bimodial pore size distributions (Gerke and van Genuchten, 1993; Zurmühl and Durner, 1996), and solute diffusion into and out of aggregates. One objective of this study is to determine if the classical CDE can be used to describe solute transport during unsaturated flow in undisturbed soils, or alternatively if nonequilibrium models, such as the mobile immobile model are needed.

Molecular diffusion and local convection are among the most important processes affecting solute transport in undisturbed soils (van Genuchten *et al.*, 1988). These processes are controlled by the structure of the soil, and in particular the size, shape, and spacing of the pores. However, as a detailed description of the complex pore geometry of a soil is not feasible, when the CDE is used the effects of diffusion and dispersion are

lumped into a hydrodynamic dispersion coefficient (Rao *et al.*, 1980; Brusseau and Rao, 1990). The hydrodynamic dispersion coefficient is often assumed to be linearly related to the water flow velocity (De Smedt and Wierenga, 1978), with the proportionality constant termed the dispersivity. However, while the hydrodynamic dispersion caused by convective transport of solutes is obviously dependent on the velocity of flow, molecular diffusion occurs at a rate independent of water flow velocity. The question arises then, can the dispersivity be assumed constant under various water flow rates? Alternatively does diffusive mass transfer between mobile and immobile water need to be explicitly considered? In a study on repacked aggregated soils Brusseau (1993) found the approach of a "lumped" dispersivity, which is velocity invariant, to be inadequate. Thus another objective of this study is to investigate the effect of the water flow velocity on solute dispersion in undisturbed soils, and to determine the conditions under which it is appropriate to use a velocity-invariant dispersivity.

Many studies in the field, and on intact soil cores in the laboratory have revealed a preferential flow of solutes, that by-passes most of the soil matrix (*e.g.* Elrick and French, 1966; Kissel *et al.*, 1973; White *et al.*, 1984; Beven and German, 1982; Roth *et al.*, 1991). This preferential and far-reaching flow of water and solutes is obviously then of importance in evaluating the potential risk of management practices on the contamination of the groundwater resources. Whereas by-passing reduces the leaching of chemicals that are present in the resident soil water, early appearance of surface-applied chemicals in the groundwater may occur, thereby resulting in undesirable pollution, and a lower application efficiency for fertilizers. Preferential flow is generally attributed to macropores, that are the result of cracks, or channels formed by plant roots or soil organisms. Significant water flow through macropores however only occurs when they are water filled (Brusseau and Rao, 1990), such as under ponded or near-saturated conditions. In New Zealand however leaching is likely to occur predominately under non-ponding unsaturated conditions, and the CDE may then satisfactorily describe solute transport. So whether or not preferential flow occurs during unsaturated leaching will also be addressed in this study.

Earlier studies suggest that preferential flow can also be induced during transient wetting of initially dry soil (White *et al.*, 1986), or by vegetation funelling the incident water (Saffigna *et al.*, 1976; Kanchanasut and Scotter, 1982). So, the effects of the initial water content, and of the vegetation on solute transport during unsaturated flow will also be assessed in this thesis.

Most leaching studies to date have focused on conservative solutes. Little attention has been devoted to the transport of reactive solutes, such as cations, although the importance of exchange reactions had been recognized in 1963 by Biggar and Nielsen. Studies on cation transport have been largely confined to repacked soil columns, although the transport of these might be quite different to the transport in structured soils, due to non-equilibrium effects, which might be either of a chemical or physical nature. Thus, cation transport in undisturbed soils will also be investigated in this study. A related objective is to assess the ability of the CDE, in conjunction with cation exchange theory, to describe cation transport through undisturbed soil columns.

A factor limiting research on the transfer processes in the unsaturated zone is the lack of adequate instrumentation to measure *in situ* simultaneously the water content and the solute concentration. Within the last decade Time Domain Reflectometry (TDR) has become widely used for measuring the soil's water content. Now TDR is also being seen as a means by which the changing concentration of electrolyte in the soil solution can be observed (Kachanoski *et al.*, 1992). The ability to take measurements continuously and automatically, in a non-destructive way, makes TDR a potentially valuable tool for observing solute transport. However, so far application of this technique to monitor solute transport through structured soils during nonsteady water flow remains a largely unmet challenge. Consequently, another objective of this study was to investigate the feasibility of time domain reflectometry (TDR) to characterize water and solute movement in the laboratory in both repacked and undisturbed soil columns.

In summary, this study set out to answer the following three questions:

1. Can the convection dispersion equation be used to describe solute transport through undisturbed soil columns under various unsaturated water flow regimes typical in the field? In particular, under which conditions is the use of the CDE appropriate, and when do we need more sophisticated models such as the mobile/immobile water concept? Is the assumption of a velocity-invariant dispersivity in the CDE appropriate? Can we use the CDE in conjunction with cation exchange theory to describe cation movement through undisturbed soil?

2. How does the soil surface, in particular the vegetative cover, and the initial water content prior to solute application affect solute transport?

3. Can we use Time Domain Reflectometry (TDR) to monitor solute transport under transient and steady-state water flow through repacked and undisturbed soil columns, and what are the limitations associated with TDR?

1.2 The Experimental Procedure of the Study

While experiments in both the laboratory and field are needed to understand fully the processes involved in solute transport (Hutson and Wagenet, 1995), the studies described here are confined to controlled laboratory studies. Although field testing of a transport models is a necessary component of research, if confidence in model predictions are to be achieved, they have the disadvantage of lack-of-control. Solutes have to be collected within the soil using porous cups, low suction lysimeters, or by destructive sampling. These methods give only local estimates of the solute concentration which may however vary significantly in space. Also in the field it is much harder to control, and define the boundary and initial conditions, and so the testing of a model is troublesome.

Alternatively, laboratory studies on large undisturbed soil columns can provide volume averaged solute concentrations. Crucial for meaningful average solute transport

behaviour is the column size needed. This depends on the scale of variability of the soil, and especially the soil surface, *e.g.* the vegetative cover. Furthermore, the control possible in the laboratory offers the possibility to study in detail the effects of certain factors, such as the water flow rate, and intermittent leaching events, on solute transport behaviour.

Although water flow in the field is often transient, over winter, when a large fraction of the leaching occurs, the amount of water in the soil various little, and the water content can be considered fairly constant. The leaching experiments described here were hence mainly carried out under steady-state water flow. However unsteady water flow is also considered, as solute flow patterns under intermittent water flow might be quite different, due to solute movement from rapid flow paths into soil micropores or aggregates. In order to evaluate the likely role and extent of preferential flow under situations that mimic the field, the leaching experiments described here were carried out at water contents below saturation.

1.3 The Structure of the Study

The present study is divided into a theoretical part (Chapters 2 and 3) and an experimental part which includes modelling (Chapters 4, 5 and 6). The literature relevant to the various parts is reviewed in the appropriate chapters. The experimental part is presented in the form of papers. These papers have been submitted to various international journals, and have either already been accepted for publication, or are still in review. Minor changes have been made to achieve consistency, and the references have been moved to the end of the thesis. All papers have multiple authorships. The contribution of the authors was as follows:

Iris Vogeler:	**Principle Investigator**
carried out:	all the planning and execution
	data collection and model development
	physical and chemical analysis
	manuscript preparation and writing

David R. Scotter:	**Advisor**
aided the study by:	discussing methodology and results
	data collection
	model development
	editing and discussion of the manuscripts

Brent E. Clothier:	**Advisor**
aided the study by:	discussing methodology and results
	editing and discussion of the manuscripts

Russell W. Tillman:	**Advisor**
aided the study by:	discussing methodology and results

Steven R. Green:	**Advisor**
aided the study by:	model development
	discussing results

The titles, locations and status of the various papers are as follows:

Characterizing Water and Solute Movement by TDR and Disk Permeametry
Chapter 4.2. By Iris Vogeler, Brent E. Clothier, Steven R. Green, David, R. Scotter, and Russell W. Tillman. *Soil Science Society of American Journal, 1996*, 60, 5-12.

TDR Estimation of the Resident Concentration of Electrolyte in the Soil Solution
Chapter 4.4. By Iris Vogeler, Brent E. Clothier, and Steven R. Green. *Australian Journal of Soil Research*, 1997 (3).

Anion Transport through Intact Soil Columns During Intermittent Unsaturated Flow.
Chapter 5.2. By Iris Vogeler, David R. Scotter, Brent E. Clothier, and Russel W. Tillman. *Soil Technology*, in press.

Solute Movement through Undisturbed Soil Columns Under Pasture During Unsaturated Flow.

Chapter 5.3. By Iris Vogeler, David R. Scotter, Steven R. Green, and Brent E. Clothier. *Australian Journal of Soil Research*, submitted.

Cation Transport During Unsaturated Flow Through Two Intact Soils

Chapter 6.2. By Iris Vogeler, David R. Scotter, Brent E. Clothier, and Russel W. Tillman. *European Journal of Soil Science*, submitted

In Chapter 2, the theory of solute transport is described to provide a general understanding of the mechanisms that govern chemical transport, such as convection, diffusion, dispersion, anion exclusion, and adsorption. Furthermore various transport models are considered. The initial and boundary conditions needed to solve the model equations are described, and analytical and numerical solutions are outlined. Chapter 3 covers the theory of time domain reflectometry (TDR) to describe water and solute transport. In Chapter 4 the use of TDR to monitor solute transport through repacked and undisturbed soil columns is discussed, and consideration is given to difficulties in solute concentration measurements by TDR. Several previous studies have shown that the rate of water application affects the leaching of solutes. This is investigated in Chapter 5, which deals with the transport of anions through undisturbed soil columns under various water flow regimes. Firstly, solute transport under bare soil is considered there, and then solute transport under pasture. The role of different transport mechanisms in affecting solute transport would appear capable of clarification by intermittent leaching. So experiments incorporating this are also described. Chapter 6 is concerned with the nature, extent, and the way in which cation exchange reactions influence the leaching of solutes. Finally Chapter 7 summarizes the results and insights gained during the study. Appendix A describes the numerical solutions used in the main computer programs, and in Appendix B some of these programs are listed.

Chapter 2

2. The Theory of Solute Movement in Soils

2.1 Introduction

In this chapter various approaches to describe solute transport through soils, will be outlined and compared. Initially the interaction between the soil-solid phase and solute is assumed to be negligible, and the solute is considered to be conservative with no decay or production. However as most nutrients and pollutants react chemically with the soil, later in the chapter exchange reactions are considered. Although solute transport in the soil is coupled with the transport of water, the theory of water transport is not explicitly discussed here. A brief description of water transport under nonsteady conditions is given in Chapters 4 and 5.

2.2 Micro- and Macroscopic Views

Modelling the transport of solutes through the soil implies some understanding of the complex soil system and the processes involved. One simplified physical picture of the soil is shown in Fig. 2.1. The soil is idealised here as a system of larger pores of various shapes and sizes. These are termed macropores, and are embedded in a soil matrix containing smaller pores, or micropores. In saturated soils all pores contain water. However, under unsaturated conditions some fraction of the macropores will no longer contain nor transmit water. Water and solute move by convection and diffusion through the soil. We could assume that only the water in the macropores moves by convection, and hence is mobile, and that the water in the micropores is effectively immobile. At the microscopic scale, the convective flow through the macropores is not uniform, but variable both within pores and between pores of various sizes. These variations in the flow velocity, and the different pathlengths of water movement induced by tortuosity, cause mechanical dispersion of a solute within the flow. Furthermore, the macropores might intersect occasionally, which results in convective interchange of solute between them, and thereby reduces the dispersion, and affects the way it scales with depth.

Solute exchange between the immobile water in the micropores and the mobile water in the macropores occurs by transverse molecular diffusion. During wetting of dry soils solute exchange between the two domains may also occur by convection. Depending on the spacing between the macropores, and the water flow velocity within them, molecular diffusion could also lead to exchange between the macropores. Longitudinal molecular diffusion also occurs, tending to reduce concentration gradients in the direction of water flow. In fact it will be argued later that if the Darcy flux density is less than about 1 mm d^{-1}, this is likely to be the dominant solute-mixing process. The combined effect of mechanical dispersion, molecular diffusion and convective mixing is termed hydrodynamic dispersion (Kutílek and Nielsen, 1994).

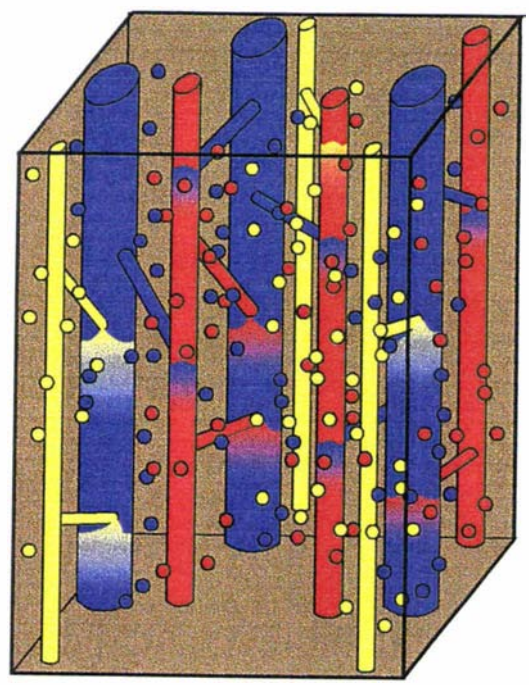

Fig. 2.1 Simplified picture of the soil with macropores of various sizes, and soil matrix with micropores. Molecular diffusion is indicated by the spots.

2.2.1 Representative Elementary Volume and Representative Elementary Area

A description at the microscopic scale of all these processes occurring in the soil system is not feasible. Solute transport needs to be viewed at a different scale. Bear (1972) introduced the concept of a representative elementary volume (REV). In an REV the microscopic processes are volume averaged to produce a macroscopic scale representation of the processes. It is assumed that an REV encompasses all the microscopic variabilities, thereby allowing the definition of a meaningful average value of the parameters, or properties of interest. The concept of what constitutes an REV is intuitive, and depends on the soil's properties. To illustrate the idea of an REV, consider the porosity of a soil. At a point with infinitely small volume, the porosity is either one or zero, depending on whether the point falls into the void (or pore) space, or into the solid matrix. With increasing sample size, the porosity changes as different mixes of pores and matrix are incorporated. With further increase in sample size these variations in the porosity with sample size become smaller. When the size of an REV is reached they become "negligible". For porosity measurements soil samples of about 100 cm^3 or 10^{-4} m^3 are usually found to be representative. Analogously to the REV, the representative elementary area (REA) is the minimum area needed to provide a meaningful average value of a cross section of the porosity. It might be argued that for solute transport the REV and the REA need be larger than for porosity. Solute transport behaviour depends not only on the porosity but also depends on the pore size distribution and pore connectedness.

Solute transport is often studied in the laboratory on soil columns, characterised by a length scale of the order of tens of centimeters. This scale has been termed laboratory scale (Dagan, 1986). At the laboratory scale, the columns are assumed homogeneous in the sense that the irregular pore structure reproduces itself in various parts of the column. A point of dispute is how the parameters obtained at the laboratory scale can be applied to the larger field scale of m or km. When the sample volume is increased substantially above the laboratory scale, to the field scale, the regional scale, or even the soil series scale, the rate of change in variability of soil properties is likely to also change. Solute transport parameters obtained from field studies have often been found

to be highly variable (Biggar and Nielsen, 1976; Jury *et al.*, 1982). However the high variability of solute transport parameters observed by Biggar and Nielsen (1976) would have been largely due to the ponded conditions in their study. A review by Jury (1983) on various transport studies in the field suggests that the variations in solute velocity become smaller under non-ponded conditions. Spatial variability can be analysed using geostatistics. However it is beyond the scope of this study to discuss the spatial variability occurring at the field scale. A general discussion is given by Kutílek and Nielsen (1994).

2.2.2 Flux and Resident Concentrations

When describing solute transport through the soil, it is important to distinguish between solute flux concentrations and solute resident concentrations. In both cases the concentrations are defined macroscopically. In the case of a resident concentration it is an average value over an REV, or in case of the flux concentration averaged over an REA. The resident concentration (C_r) is a volume-averaged concentration, defined as the mass or number of moles of solute per unit volume of soil solution [kg or mol m^{-3}].

Resident concentrations can be measured by direct soil sampling, or by electrical resistance measurements, such as Time Domain Reflectometry. In contrast, the flux concentration (C_f) is a flux-averaged concentration [kg or mol m^{-3}], and is the ratio of the solute flux density q_s [kg or mol m^{-2} s^{-1}] to the water flux density q_w [m s^{-1} or m^3 m^{-2} s^{-1}] (Kreft and Zuber, 1978). It is the effective concentration in the moving water in the soil. Flux concentrations are obtained from the outflow of column leaching experiments and lysimeter studies. The difference between flux and resident concentration is illustrated in Fig. 2.2. The resident concentration represents the solute concentration in the "mobile", and in the "immobile" water at a certain time. In contrast, the flux concentration represents only the concentration in the mobile water as sampled over a certain time period. Thereby C_f is weighted by the velocity at which water, and so solute move through the various pathways.

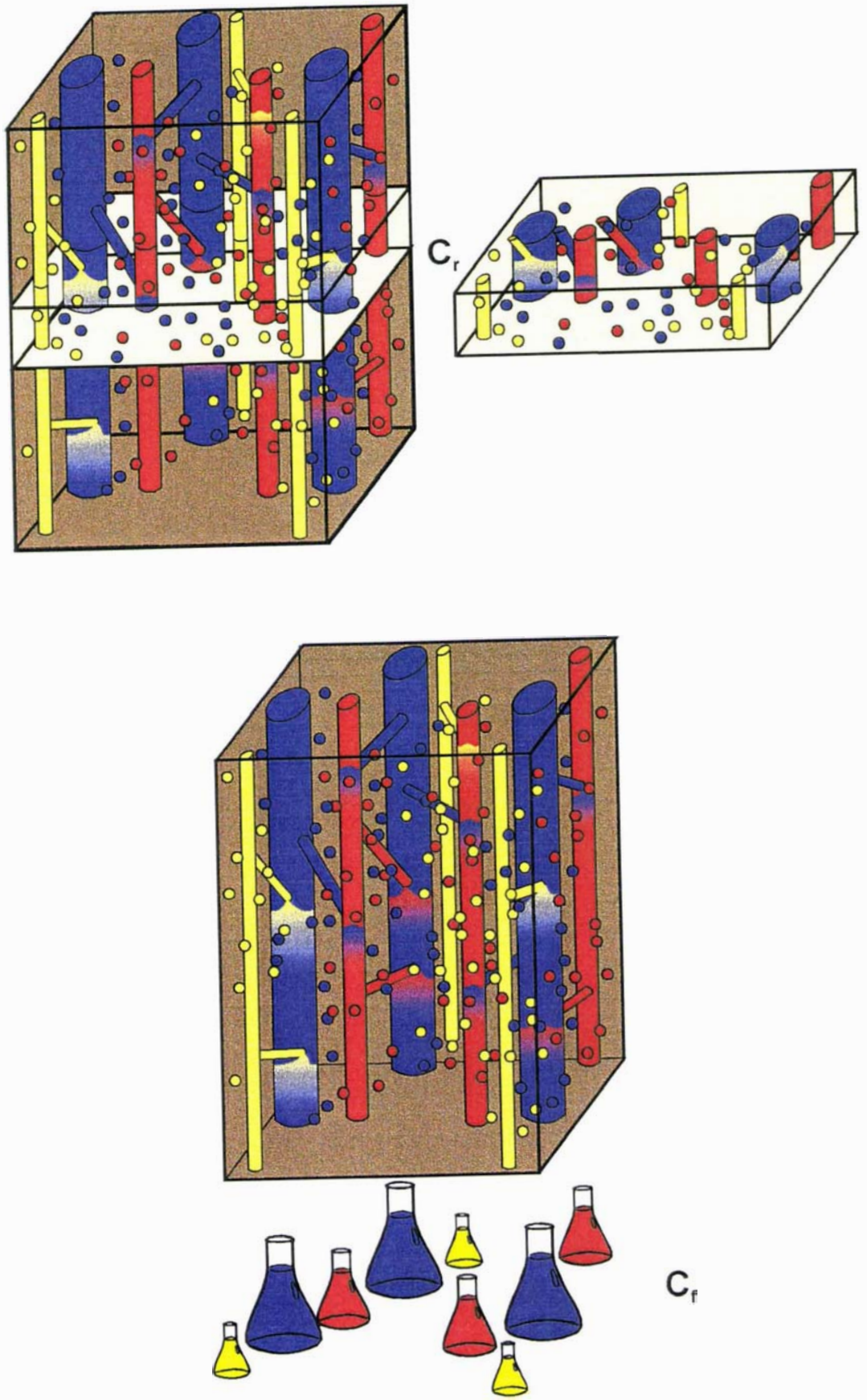

Fig. 2.2 Resident concentration (C_r) and flux concentration (C_f).

For steady-state water flow a consideration of mass conservation implies that the flux and resident concentration for nonreactive solutes are related by,

$$\frac{\partial C_r}{\partial t} + q_w \frac{\partial C_f}{\partial z} = 0 \qquad [2.1]$$

where t is the time [s] and z the depth [m].

2.3 The Language of Models

Solute transport models are most commonly represented as either transfer functions, or as partial differential equations (pdes). Whereas pdes can be used for transient water flow conditions, transfer functions are restricted to steady-state flow, or at least conditions, where the water flow pathways are not considerably changed and the soil water content changes little. However, the transfer function approach does offer a framework within which predictions from different models can be compared.

2.3.1 Transfer Function Approach

In transfer function models, the solute transport processes are based on random variables, which are characterized by a probability density function (pdf). A random variable is a function that assigns either a number (discrete random variable), or a certain range (continuous random variable) to every outcome. Thereby random variables have a probability assigned to them. Given a large number of observations the frequency of a random event will approach a fixed value, which is called the probability of that event. The probability is hence a measure of the likelihood that an event will occur. The pdf then describes how probability is distributed over the possible values a random variable can take, and satisfies the following conditions,

$$f(x) \geq 0 \qquad \text{for all } x$$
$$\int_{-\infty}^{\infty} f(x) = 1 \qquad [2.2]$$

where x is a random variable. Other important concepts of a random variable are the mean, the expected value of x, $E(x)$, and the variance $E[x\text{-}E(x)]^2$.

Process orientated models can also be presented as transfer functions. Transfer function models are limited to linear time-variant systems, which means that at any time the output is a linear combination of present and past values of the input. But provided changes in soil water storage are small, non-steady flow may be described by using a surrogate variable for time, such as cumulative infiltration or drainage.

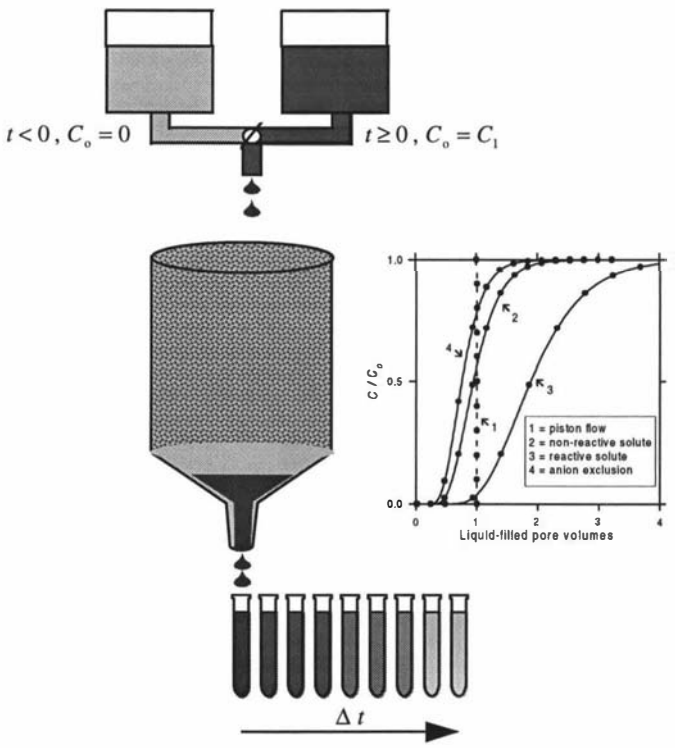

Fig. 2.3 Column leaching experiment with breakthrough-curves for pison flow, non-reactive and reactive solutes, and anion exclusion.

Solute transport is often studied using column leaching experiments. A solution with solute concentration C_f (0,t), is applied to the surface of a soil column of length l, and the concentration measured at the exit surface at the base of the column (C_f (l,t)) is plotted against time, giving a breakthrough curve (BTC). This is shown in Fig. 2.3 for a non-reactive and a reactive solute. The shape and the position of the BTC provide information on the physical and chemical properties of the soil. If no mixing between the initial and incoming solution would occur, the BTC would be a vertical line, which is termed piston flow. A curved BTC indicates mixing. Shifting of the curve to the left indicates exclusion or bypass from some fraction of the soil solution. Shifting to the right indicates solute adsorption by the soil solids.

If we denote the solute input flux by $F_{in}(t)$ [kg or mol s^{-1}], and the output flux by $F_{ex}(t)$ [kg or mol s^{-1}], we may write $F_{ex}(t)$ as the convolution integral of $F_{in}(t)$ and the lifetime pdf g (t-t' | t'), where t' is the time when the solute entered the system,

$$F_{ex}(t) = \int_0^t g\left(t - t' \middle| t'\right) F_{in}(t')\,\mathrm{d}t' \qquad [2.3]$$

where F_{in} and F_{ex} are given by,

$$\begin{aligned} F_{in}(t) &= C_f(0,t)\,q_w(0,t)\,A_s \\ F_{ex}(t) &= C_f(l,t)\,q_w(l,t)\,A_s \end{aligned} \qquad [2.4]$$

where A_s is the surface area [m^2], which is assumed to be the same for the input and the output surface, and l is the length of the soil system studied [m]. Note that g in the above equation may depend on the time of solute application to the surface t'.

Combining the above equations, and assuming steady state water flow leads to the basic transfer function for conservative solutes,

$$C_f(l,t) = \int_0^t C_f(0,t')\,f_t(l,t-t')\,\mathrm{d}t' \qquad [2.5]$$

where t is a random variable, and f_t (l, t-t') is the travel time probability density function (pdf) [s^{-1}], often termed the impulse-response function. The pdf gives the probability that a solute, which has been applied to the soil surface at $t = 0$, will be flowing passed l at time t, and characterizes the solute transport properties of the soil. The pdf is based on the assumption that the solute transport mechanisms are time-independent and conservative. However by using a lifetime pdf, the effect of physical, chemical or biological processes, leading to source-sink terms can be included (Jury and Roth, 1990).

In the simplest case of a Dirac delta input, for which the δ-function is defined by,

$$\delta(t)=0 \qquad t\neq 0$$
$$\int_{-\infty}^{\infty}\delta(t)\,dt=1 \qquad , \tag{2.6}$$

the pdf is equal to the normalized solute flux concentration at the exit. Note that the Dirac delta function is in a mathematical sense not a function. If a pulse of magnitude M_o [kg or mol m^{-2}] is applied when $t = 0$,

$$f_t(l,t)=\frac{C_f(l,t)}{\int_0^{\infty}C_f(l,t')\,dt'}=\frac{C_f(l,t)q_w}{M_o} \quad . \tag{2.7}$$

Under steady-state water flow, the net-applied water form of the transfer function approach can be used, for which the pdf $f_t(l, Q)$ [m^{-1}] for a Dirac delta input is given by,

$$f_t(l,Q)=\frac{C_f(l,Q)}{\int_0^{\infty}C_f(l,Q')\,dQ'}=\frac{C_f(l,Q)}{M_o} \tag{2.8}$$

where Q is the cumulative infiltration [m].

Two important properties of a probability density function are the mean and the variance. The expected value, or mean travel time, $E(t)$, is given by,

$$\mathrm{E}(t) = \int_0^\infty t\, f(t)\, dt \qquad [2.9]$$

and the variance of t, which describes the mean square deviations of t about the average value is given by,

$$\mathrm{Var}(t) = \int_0^\infty \left[t - \mathrm{E}(t)\right]^2 f(t)\, dt = \mathrm{E}\left(t^2\right) - \mathrm{E}^2(t). \qquad [2.10]$$

These two values are unique for any pdf. If the parameters of the pdf are constant in time and space (*i.e.* $f(l,t)$ is a stationary function), as well as independent on the type and concentration of solute, then the transfer function is useful as a predictive tool. To predict solute transport beyond the measurement depth, mechanistic assumptions are required. Examples will be given in section 2.4 and 2.5.

Transfer functions can be written describing flux and resident concentrations, and for both flux and resident pulse inputs. The relationship between them is discussed by Jury and Scotter (1994).

Transfer function models are not restricted to the simple case of the input of a non-reactive solute to the soil surface under steady-state water flow. They also can be used to simulate the transport of indigenous soil solutes (Magesan *et al.*, 1994; Heng *et al.*, 1994), as well as quasi-transient conditions by using the net-applied water form of the transfer function equation (Jury and Roth, 1990), and its pdf [eq. 2.8]. However implicit in the use of transfer function models to describe solute transport is the assumption, that the transport properties are not significantly affected by intermittent drying and wetting cycles. Otherwise water and solute pathways through the soil would change, and f_t would not be unique for a particular system. Also, solute transport is assumed to be a function of the net amount of water applied, but not of the rate at which

the water is applied. Linear source and sink terms can be included provided they are proportional to time or the net amount of water applied (Heng and White, 1996). For transport of reactive and non-conservative solutes, Roth and Jury (1993) coupled the transfer function approach with linear adsorption kinetics and first order decay.

2.3.2 Partial Differential Equations

Solute transport models are based on conservation and flux laws. The mass conservation law is given by,

$$\frac{\partial M}{\partial t}+\frac{\partial q_s}{\partial z}=0 \qquad [2.11]$$

where M is the total amount of solute present in a unit volume of soil [kg or mol m^{-3}].

As mentioned before, solute movement is due to the combined effect of convective mass flow of water and molecular diffusion. If convection is the only transport process operating and both the water flux density and the resident concentration are locally uniform, then the solute flux density is given by,

$$q_s = q_w\, C_r \qquad [2.12]$$

The second transport process is molecular diffusion, which always occurs when there are solute concentration gradients within the pore water. Diffusion of solutes can occur longitudinally in the direction of flow, thereby increasing the dispersion. This will only be significant at low velocities. If the resident concentration at any depth is not locally uniform, molecular diffusion also occurs transverse to the direction of mass flow, thereby reducing any local concentration differences induced by different local velocities. Molecular diffusion is described by Fick's first law,

$$q_s = - D_i \, \theta \frac{\partial C_r}{\partial z} \qquad [2.13]$$

where θ is the volumetric water content [m^3 m^{-3}], and D_i is the effective diffusion coefficient in the soil [m^2 s^{-1}], which is related to the diffusion coefficient in water by,

$$D_i = \tau \, D_o \qquad [2.14]$$

where τ is the tortuosity factor, which accounts for the increased pathlength in the soil compared to the water, and D_o is the molecular diffusion coefficient in water. Typically D_o in liquids is about 1.5 x 10^{-9} m^2 s^{-1}, and τ in wet soil is about 0.5. This means that diffusion occurs over a length scale of mm during time periods of the order of days.

2.4 Stochastic-Convective Approaches

The stochastic-convective approach is consistent with solute movement being solely due to convection. Stochastic convective transfer functions are consistent with the soil behaving as if it consists of independent pathways, or stream tubes with different travel times. Water and solutes move by convection through these tubes. In each tube the mean velocity v is assumed constant. The various tubes however have different velocities, the distribution of which is described by a continuous random variable (Jury *et al.*, 1986). Solute mixing between the different tubes is assumed negligible.

The expected or mean travel time is given by,

$$E_z(t) = \frac{z}{l} E_l(t) \qquad [2.15]$$

where E_z and E_l are the expected travel times for a certain depth z and the reference depth l.

The spreading of a solute for the stochastic convective transport behaviour, as described by the variance, grows quadratically with depth,

$$\mathrm{Var}_z(t) = \left(\frac{z}{l}\right)^2 \mathrm{Var}_l(t) \qquad [2.16]$$

where Var_z and Var_l are the variances for a certain depth z and the reference depth l.

2.4.1 Convective-Lognormal Transfer Function

If the velocities in the various tubes are assumed to be lognormally distributed, then f_t is given by (Jury and Roth, 1990):

$$f_t(t,z) = \frac{1}{\sqrt{(2\pi)}\,\sigma_1\, t} \exp\left(-\frac{\left(\log(t\,l/z) - \mu_l\right)^2}{2\sigma_1^{\,2}}\right) \qquad [2.17]$$

and

$$\mathrm{Var}_z(t) = z^2 \frac{\exp(2\mu_1)}{l^2}\left[\exp(2\sigma_1^{\,2}) - \exp(\sigma_1^{\,2})\right] \qquad [2.18]$$

where μ_l and $\sigma_l^{\,2}$ are the mean and variance of the distribution of the logarithm of travel time ($\log t$) measured at a reference depth l.

Implicit in the above pdf [eq. 2.17] is the assumption, that the processes contributing to the travel time are the same for all depths.

2.4.2 Burns' Leaching Equation

Another stochastic-convective approach is the Burns' leaching equation (1974). Implicit in the Burns' equation is the following stochastic-convective pdf (Scotter *et al.*, 1993),

$$f(z,Q)=\frac{(z\theta)^2}{Q^3}\exp\left(\frac{-z\theta}{Q}\right). \qquad [2.19]$$

2.4.3 Transfer Function Approach linked with the Hydraulic Conductivity-Water Content Relationship

Scotter and Ross (1994) recently suggested that a transfer function derived from the soil's hydraulic properties could be useful for determining the upper limit of solute dispersion. Again solute flow is assumed to be purely convective. The distribution of the soil water velocities is found from the unsaturated hydraulic conductivity-water content relationship ($K(\theta)$). The velocity distribution is then used to calculate the solute travel time distribution, thereby giving the travel time probability as,

$$f(z,t)=-\frac{1}{K_w}\frac{\mathrm{d}K_w(\theta)}{\mathrm{d}t} \qquad [2.20]$$

where K_w is the hydraulic conductivity [m s^{-1}]. However implicit in this approach is the assumption that the velocity distribution can be inferred from the K_w (θ) relationship. This is only true if all the dependence of K_w on θ is due to flow in the pores emptying or filling, so that the velocity in pores staying filled is unaffected. The irregular geometry of soil pores might mean this is not always a realistic assumption. Equation [2.20] does provide an upper limit for the amount of dispersion however, as Scotter and Ross (1994) suggest.

2.5 Convective-Dispersive Approach

In the convective-diffusion approach solute movement is assumed to be due to non-interacting convection and diffusion. Diffusion is described by eq. [2.13], and convection by eq. [2.12], provided that the water flux density (q_w) and the solute resident concentration (C_r) in the soil are locally uniform. However convection is not describable by [2.12], and convection and diffusion interact as described in section 2.2. In the CDE, the effects of nonuniform q_w and diffusion are lumped into the hydrodynamic dispersion coefficient. Further it is assumed that hydrodynamic dispersion can mathematically be described as a diffusion-like process, with the total solute flux given by,

$$q_s = -\theta D_s \frac{\partial C_r}{\partial z} + q_w C_r \qquad [2.21]$$

where D_s is the hydrodynamic dispersion coefficient [$m^2\ s^{-1}$].

If this equation is valid, the solute flow can be called convective-dispersive. The velocity of flow partly determines which of the dispersion processes dominates; mechanical dispersion, molecular diffusion, or convective mixing. Under fast enough flow rates, longitudinal molecular diffusion will be small compared to mechanical dispersion (Gardner, 1965). The dispersion coefficient is then approximately proportional to the pore water velocity (Campbell, 1985). The shape of a BTC measured for non-reactive solutes should then be independent on the pore water velocity. However for slow flow, diffusion is often considered as a main mechanism of dispersion. Diffusion should be independent of water flow, so if it is important, the shape of the BTC does depend on the pore water velocity.

The velocity-dependency of the hydrodynamic dispersion coefficient (D_s) is often described by (De Smedt and Wierenga, 1978; Brusseau, 1993),

$$D_s = \lambda v^n + \tau D_o \qquad [2.22]$$

where λ is the dispersivity [m], v is the pore water velocity defined by q_w / θ [m s^{-1}], and n is a constant, often assumed to be one (Hutson and Wagenet, 1995).

2.5.1 Convection-Dispersion Equation as a Partial Differential Equation

Combining the solute flux equation with the mass conservation law [eq. 2.11] yields the classical convection dispersion equation (CDE). For non-reactive solutes, M equals θC_r, so we get,

$$\frac{\partial(\theta C_r)}{\partial t} = \frac{\partial}{\partial z}\left(\theta D_s \frac{\partial C_r}{\partial z}\right) - \frac{\partial}{\partial z}(q_w C_r) \; . \qquad [2.23]$$

When the water flow is transient, this equation must be solved simultaneously with the water flow equation, *e.g.* Richards' equation. This is described in Chapters 4 and 5. Under steady-state flow conditions, the CDE can be simplified to (van Genuchten, 1981; Kutílek and Nielsen, 1994),

$$\frac{\partial C_r}{\partial t} = D_s \frac{\partial^2 C_r}{\partial z^2} - v \frac{\partial C_r}{\partial z} \; . \qquad [2.24]$$

In the CDE given above, resident concentrations are used. Alternatively, the CDE can be stated in terms of flux concentrations (Parker and van Genuchten, 1984). The CDE for flux concentrations is identical to the above equation, but C_r is replaced by C_f. The flux concentration can also be inferred from the resident concentration by using [2.21] as,

$$C_f = \frac{q_s}{q_w} = C_r - \frac{D_s}{v}\frac{\partial C_r}{\partial z} \; . \qquad [2.25]$$

The above equation shows that the discrepancy between flux and resident concentration increases with increasing dispersivity (λ), which can be defined as D_s / v, if $n = 1$.

In terms of the cumulative infiltration Q [m], the CDE is given by,

$$\theta \frac{\partial C_r}{\partial Q} = \lambda \frac{\partial^2 C_r}{\partial z^2} - \frac{\partial C_r}{\partial z} \qquad [2.26]$$

Note that in the above equation λ is not necessarily independent of the pore water velocity.

These basic equations can be extended to include a wide range of sources or sinks, such as biological and chemical transformations, solute-soil interactions and plant extraction. A few such situations, relevant for the study will be discussed below.

2.5.2 Convection-Dispersion Equation as a Transfer Function Model

Most commonly the CDE is presented as a differential equation, as described above. An alternative way to represent convective-dispersive solute transport is to use transfer functions, based on the response of a soil system to a solute input.

For a Dirac delta input of solute to the soil surface, the solute travel time pdf for convective-dispersive solute flow [eq. 2.21], is given by (Jury and Roth, 1990):

$$f_t(z,t) = \frac{z}{2\sqrt{\pi D_s t^3}} \exp\left(-\frac{(z-tv)^2}{4 D_s t}\right). \qquad [2.27]$$

The above pdf is often termed the Fickian pdf [s^{-1}]

As shown by Jury and Roth (1990), the parameters in the Fickian pdf [eq. 2.27] and the lognormal pdf [eq. 2.17] can be chosen to give similar shapes for the outflow concentration at a particular depth. However the main difference between the two functions is in the way dispersion increases with travel distance.

The mean travel time for the CDE is,

$$E_z = \frac{z}{v} . \qquad [2.28]$$

As already mentioned, for the stochastic convective process the spreading of a solute grows quadratically with transport distance [eq. 2.16]. In contrast, for the convection-dispersion process the spreading grows linearly with transport distance (Jury and Roth, 1990),

$$\mathrm{Var(t)} = \frac{2 D_s z}{v^3} . \qquad [2.29]$$

This basic difference between the two models is due to contrasting assumptions. Whereas the CDE is consistent with eventual mixing of the solutes in regions with different local velocities, the CLT allows no mixing between the tubes. A detailed discussion of the depth dependence of the mean and variance as implied by the convection-dispersion and stochastic-convective assumptions has been given by Jury and Roth (1990).

When considering solute movement in structured field soils it remains unclear if the dispersivity is constant, as found by Roth *et al.* (1991), or grows with depth as found by Jury *et al.* (1982) and Butters and Jury (1989). Rigorous tests on this aspect in the field seem unrealizable, due to the heterogeneity typically found in soil profiles. Increased spreading with depth could be due to a change in the soil structure within the profile. The use of depth-dependent parameters in the CDE would then appear appropriate. As shown by Jury *et al.* (1991, p.179), by defining a dispersivity that grows proportionally with depth, the pdf implied in the CDE becomes stochastic-convective.

2.5.3 Bolt's Approach for Describing Solute Dispersion

To visualize better the phenomenon of dispersion as described by equation [2.26], the approach of Bolt (1982) seems valuable. In this approach the effect of diffusion, water velocity variations, and exchange between mobile and immobile water on solute dispersion are described in a simple, yet quantitative way, by using a diffusion/dispersion length parameter. The dispersivity is replaced by a diffusion/dispersion length parameter L_D, which can be thought of as the sum of the three component length parameters,

$$L_D = L_{diff} + L_{dis} + L_{mim} \qquad [2.30]$$

where L_{diff} is the diffusion length parameter, L_{dis} is the dispersion length parameter, and L_{mim} is the mobile/immobile exchange length parameter.

The first length, L_{diff} accounts for longitudinal molecular diffusion and is given by,

$$L_{diff} = \frac{\theta D_o \tau}{q_w} \qquad [2.31]$$

where D_o is the diffusion coefficient in water, and τ is the pore tortuosity. Assuming that D_o = 1.5 x 10^{-9} m^2 s^{-1}, τ = 0.5, θ = 0.5 m^3 m^{-3}, and q_w = 1 mm h^{-1}, L_{diff} is about 1.3 mm. Note that the slower the water flux density q_w, the more time there is for molecular diffusion, and the greater the smearing, as L_{diff} is inversely proportionally to the water flux density.

The second component L_{dis} is a measure of the non-uniformity of velocity in various flow pathways, and the average distance between intersection of those pathways. Given that the pathways do not change with the water flow rate, L_{dis} is independent of q_w, and L_{dis} is then constant. This could imply that molecular diffusion is fast enough to make disparities in local solute concentrations between "mobile" and "immobile" water unimportant. For structureless soils such as sand, Bolt suggests that L_{dis} should be

similar to the grain diameter. In aggregated soils, L_{dis} characterizes the scale of the structure (Beven *et al.*, 1993).

However in structured soils, diffusion might be too slow, and/or the water flow velocity too fast, for local equilibrium between the solute concentration in the "mobile" and "immobile" water to be approximated. Provided that water and solute transport are not too preferential, the effect of this disequilibrium on solute dispersion can be approximated by defining an equivalent length parameter L_{mim}. For porous spheres Bolt (1982), following the approach of Passioura (1971), gives the following approximate expression for L_{mim},

$$L_{mim} = \frac{R_S^2 q_w \theta_i}{15 D_o \theta^2} , \qquad [2.32]$$

where R_S is the radius of the aggregates (or a characteristic length), θ_i is the immobile water content, and D_o is here the diffusion coefficient inside the spheres. The mobile/immobile exchange length, L_{mim}, is proportional to q_w, and inversely proportional to the molecular diffusion coefficient. It is also proportional to the square of the characteristic length indicating the spacing between the mobile and the immobile water. Thus the faster q_w, the more important L_{mim} becomes relatively.

From equation [2.32] it follows that,

$$R_S = \left(\frac{15 L_{mim} D_o \theta^2}{q_w \theta_i} \right)^{1/2} . \qquad [2.33]$$

For other, non-aggregated soils, another geometric view is to treat soil water flow as occurring through hollow cylindrical macropores of radius R_H, embedded axially in adjacent cylinders of porous soil with radius R_C. Van Genuchten and Dalton (1986) show that for this geometry

$$L_{mim} = \frac{\left[2\ln(R_C/R_H)-1\right]\theta_i\, q_w\, R_C^{\,2}}{4\, D_o\, \theta^2} \quad . \qquad [2.34]$$

As the logarithmic term in this equation is only weakly dependent on R_C / R_H, if we arbitrarily chose a value of 100 for R_C / R_H, it then follows that,

$$R_C \approx \left(\frac{L_{mim}\, \theta^2\, D_o}{2\, q_w\, \theta_i} \right)^{1/2} \quad . \qquad [2.35]$$

It is important to recognize that in this consideration the macropore geometry has a large influence on the characteristic length obtained for a soil. Consider a soil with L_{mim} = 40 mm, q_w = 3 mm h^{-1}, θ = 0.5, θ_i = 0.45, and D_o = 1.5x 10^{-9} m^2 s^{-1}. If we assume that the soil consists of porous spheres, eq. [2.33] implies that the spheres are 50 mm in diameter. However if we assume that the soil consists of porous cylinders enclosing around axial macropores, these would, according to eq. [2.35], have a diameter of only 9 mm.

This approach offers a quantitative way to describe the influence of the three components of L_D on dispersion under various water flow rates, and provides an intuitive physical meaning for L_D. For Darcy flux densities greater than 1 mm h^{-1}, L_{diff} is generally negligible relative to the other components of L_D, which in undisturbed soils is much higher (Beven *et al.*, 1993). Thus measured L_D values may usually be thought of as the sum of L_{dis} and L_{mim} and both increase with flow rate. If q_w could be varied, without changing θ and thereby the flow geometry, experiments at different flow rates would allow the two components (L_{dis} and L_{mim}) to be found. But in unsaturated soil a change in q_w is linked with a change in θ. So any increase in L_D might then either be due to a greater range of flow velocities (increasing L_{dis}), or to an increased disequilibrium between solute concentrations in the mobile and immobile water (greater L_{mim}). Thus deconvoluting L_{dis} and L_{mim} for unsaturated flow seems experimentally fraught with difficulty.

2.6 The Mobile/Immobile Model

Although the equilibrium CDE is the most common approach to describe solute transport, it has often been found inadequate during saturated flow in structured soils. Early arrival, and tailing of solutes have often been observed. Apart from stochastic convective approaches to describe such transport behaviour, a variety of nonequilibrium models based on convective-dispersive solute flow has been developed (Skopp *et al.*, 1981; van Genuchten and Dalton, 1986). These are either based on physical, or chemical nonequilibrium (Nielsen *et al.*, 1986). Physical nonequilibrium may be the result of an heterogeneous water flow regime, while chemical nonequilibrium can be caused by kinetic adsorption (Selim *et al.*, 1976). However, the equations resulting from physical and chemical nonequilibrium are mathematically equivalent for linear adsorption isotherms (van Genuchten, 1981; Nkedi-Kizza *et al.*, 1983; Brusseau and Rao, 1990). This stressses the need for caution in implying which mechanism is responsible for the observed behaviour.

2.6.1 Mobile/Immobile Approach as a Partial Differential Equation

The main nonequilibrium model used is the mobile-immobile concept (MIM) based on the model of Coats and Smith (1964), and van Genuchten and Wierenga (1976). In this model the pore space is divided into two conceptually different domains, a dynamic domain, which contains mobile water (θ_m), and a stagnant domain, which contains immobile water (θ_i). Convective-dispersive transport occurs in the mobile water fraction only. For non-reactive solutes the MIM is given by,

$$\theta_m \frac{\partial C_m}{\partial t} + \theta_i \frac{\partial C_i}{\partial t} = D_m \frac{\partial^2 C_m}{\partial z^2} - q_w \frac{\partial C_m}{\partial z} \qquad [2.36]$$

where C_m is the resident soil solution concentration in the mobile phase [mol m^{-3}], and D_m is the dispersion coefficient in the mobile phase [m^2 s^{-1}].

Solute transport between the mobile and immobile domain is assumed to be diffusion controlled, and described by a first order equation (van Genuchten and Wierenga, 1976),

$$\theta_i \frac{\partial C_i}{\partial t} = \alpha (C_m - C_i) \qquad [2.37]$$

where the subscripts m and i denote the mass in the mobile and immobile domain, and α is the diffusional transfer coefficient for solute exchange between mobile and immobile regions (s^{-1}).

2.6.2 Mobile/Immobile Approach as a Transfer Function

Alternatively the mobile/immobile concept can be presented as a transfer function. This is discussed in detail by Sposito *et al.* (1986). They obtained the probability density function of the MIM by numerical inversion of the Laplace-transformed pdf. The effects of convection, dispersion, mobile/immobile water fractions, and mass transfer coefficient on the shape of the travel time pdf were demonstrated. Also given were the mean and variance of the solute travel time for the mobile/immobile concept. The mean solute travel time is the same as for the CDE, and the variance also growths linearly with travel distance. However the variance is influenced by the immobile domain, and increases with an increase in the immobile water fraction, or a decreasing transfer coefficient.

2.6.3 Critique on the Mobile/Immobile Approach

The mobile/immobile concept of van Genuchten and Wierenga (1976) has shown some improvements over the CDE in describing the frequently observed early breakthrough and tailing, for both repacked and undisturbed soil columns (Rao *et al.*, 1980; Nkedi-Kizza *et al.*, 1983; Seyfried and Rao, 1987; De Smedt and Wierenga, 1984; Vanclooster *et al.*, 1993). At a statistical-fitting level, this is however not surprising as the mobile/immobile concept contains two more fitting parameters. As Jury *et al.* (1991) demonstrated, by varying θ_m/θ, α, or the mobile dispersion coefficient D_m, various

shapes of BTC's can be obtained. The drawback of the model is that none of these parameters is directly measurable, without making some assumption about the other parameters. For example, Clothier *et al.* (1992) recently proposed the disc permeameter technique for determining the immobile water fraction, after dispersive effects had faded away. However, they assumed that α was negligible. Jaynes *et al.* (1995) on the other hand considered that hydrodynamic dispersion was negligible, and thereby determined α. It therefore seems more applicable to use the much simpler classical CDE, in which the effects of matrix diffusion are lumped into the hydrodynamic dispersion coefficient (Valocchi, 1985).

Another point of dispute is the relationship between θ_i and the pore water velocity v (De Smedt *et al.*, 1986; Nkedi-Kizza *et al.*, 1983, van Genuchten and Wierenga, 1977; Kutílek and Nielsen, 1994). The fraction of the immobile water can either be considered constant, or assumed to depend on the total water content. A constant immobile water fraction can be assumed if the soil consists of distinct aggregates (Zurmühl and Durner, 1996).

Although the mobile/immobile concept of van Genuchten and Wierenga (1976) has often been found successful in describing solute transport through structured soils, the question remains whether this model is appropriate. Originally developed to describe preferential flow and asymmetric BTC's, the concept is not based on clearly definable physical processes. Furthermore, for reactive solutes, the mobile/immobile model is not the only conceptual model capable of describing asymmetric BTC's. The use of nonlinear isotherms performs equally well in describing these observed phenomena. This will be discussed in section 2.8. It would seem more useful to describe preferential flow in terms of the transfer function approach, or the classical CDE with some assumptions as to how the parameters change with flow rate and perhaps with depth.

2.6.4 The Link Between the Mobile/Immobile Approach and Bolt's Approach

Bolt (1982) suggested an approximate relationship between the mobile/immobile exchange length L_{mim} and other parameters of the MIM is,

$$L_{mim} = \left(\frac{\theta_i}{\theta}\right)^2 \frac{q_w}{\alpha} \quad . \qquad [2.38]$$

The validity of eq. [2.38] was tested numerically, and simulations are shown in Fig. 2.4 for two different column lengths of 300 and 500 mm, and L_D = 50 mm, L_{dis} = 10 mm, and L_{mim} = 40 mm. Assuming that θ = 0.5, θ_i = 0.25, and q_w = 5 mm h^{-1}, the value for α is found with eq. [2.38] to be 0.03 h^{-1}. Note that L_D in the CDE is the dispersivity λ, and that L_{dis} in the MIM is the dispersivity in the mobile phase λ_m. The agreement between the predictions based on the two different models, and using the approach of Bolt is good. However the major limitation of the MIM remains the inability to measure the parameters θ_i and α independently, and that different combinations of θ_i and α can give the same value of L_{mim}, and the same macroscopic solute behaviour.

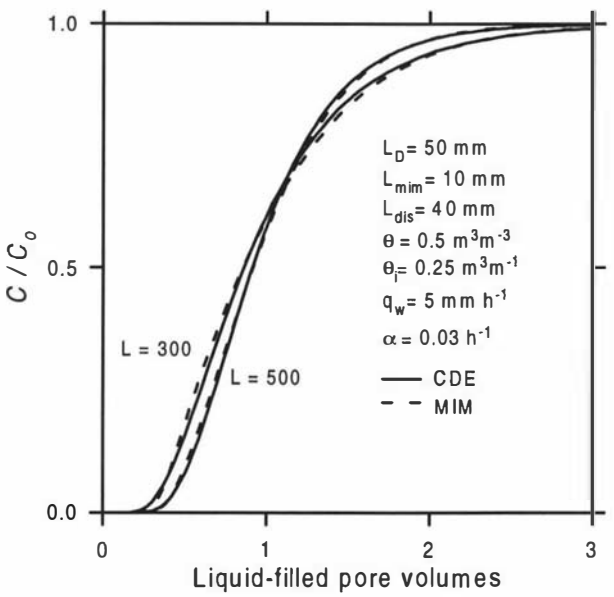

Fig. 2.4. Comparison between simulations using the CDE and MIM, based on the approach of Bolt (1982).

2.7 Layer and Mixing Cell Models

A simple and useful approach for describing solute transport is the use of layer or mixing cell models, where the soil profile is divided into a number of horizontal layers or cells. The incoming water and solutes are usually assumed to mix instantaneously and completely with water and solutes already present in each cell during each time step. Such models have been used to study both the transport of non-reactive and reactive solutes (van Ommen, 1985; Bajracharya and Barry, 1993). Van der Ploeg *et al.* (1995b) recently proposed a mixing cell model, which can be considered as a simplified version of the CDE. They compared predictions using analytical solutions of the CDE with their approach. They found good agreement for both flux and resident concentrations, provided that the Pèclet number $P > 6$, where P is defined as L / λ. Dispersivities in field soils commonly range from 1 - 200 mm (White, 1985b). So in the case of a highly dispersive soil with a λ of 200 mm, the mixing cell model should only be used for depths ≥ 1.2 m.

Apart from being computationally very simple, this mixing cell model has the advantage that nonuniform initial solute distributions in the soil, and even transformation processes (van der Ploeg *et al.*, 1995a) can be easily included. Under these conditions, analytical solutions for the CDE are not readily available.

2.8 Reactive Solutes

So far, discussion has centered on solutes which do not react with the soil matrix. Many chemicals of agricultural or environmental interest are, however, attracted to soil mineral or organic surfaces. This exchange critically controls the depths and pattern of leaching. Two different types of exchange on the soil matrix have to be considered, a constant, and a variable surface charge. While the constant surface charge is independent of the solution concentration, the variable surface charge is determined by the nature of the adsorbed ions, the concentrations of the ions in solution, and the pH of the soil solution (Parfitt, 1980; Bolan *et al.*, 1986). Both anions and cations are to varying degrees subject to adsorption and exchange reactions on the soil matrix.

Nitrate, chloride, bromide and tritium are usually considered to be non-reactive solutes. However adsorption or exclusion of these solutes has also been observed to some extent, depending on the chemical properties of the soil (Biggar and Nielsen, 1962, Krupp *et al.*, 1972).

In this section adsorption reactions onto the soil matrix are described by different processes, and their effect on solute transport is discussed. The basic CDE presented above [eq. 2.24] is modified to include adsorption isotherms, or exchange reactions.

2.8.1 Solute Adsorption

The total amount of solute in the soil M [mol m^{-3}] is assumed to be partitioned into two phases, the concentration on the adsorber S_s [mol kg^{-1}] and the concentration in the soil solution C_r. Thus,

$$M = \rho_b \, S_s + \theta \, C_r \qquad [2.39]$$

where ρ_b is the soil bulk density [kg m^{-3}]. The relationship between the concentration on the exchanger, and that in the soil solution at equilibrium is called an adsorption isotherm. Generally, exchange reactions are assumed to be instantaneous, and equilibrium is assumed between the soil solution concentration and the exchanger. Including the concentration on the adsorber into the CDE results in,

$$\frac{\partial C_r}{\partial t} + \frac{\rho_b}{\theta} \frac{\partial S_s}{\partial t} = D_s \frac{\partial^2 C_r}{\partial z^2} - v \frac{\partial C_r}{\partial z} \; . \qquad [2.40]$$

Adsorption of solutes onto the soil matrix has been described in different ways. One of the main approaches is the use of isotherms $S_s(C)$, which can be linear or of any other functional form. A comprehensive review of adsorption isotherms is presented by Helfferich (1962). One of the most commonly used is the Freundlich equation (Nielsen *et al.*, 1981),

$$S_s = K_d \, C_r^{\,n} \qquad [2.41]$$

where K_d is the distribution coefficient [m^3 kg^{-1}], and n is a constant which can be obtained from isotherm data. The distribution coefficient is generally assumed constant. However in some soils, K_d has been found to be dependent on the ionic strength of the soil solution (Parfitt, 1980, Bolan *et al.*, 1986). An example of such a soil is given in Chapter 5.

When the above adsorption isotherm is inserted into the CDE, it follows that,

$$R \frac{\partial C_r}{\partial t} = D_s \frac{\partial^2 C_r}{\partial z^2} - v \frac{\partial C_r}{\partial z} \qquad [2.42]$$

where the dimensionless retardation factor R describes the velocity of a solute front or pulse relative to the velocity of an non-reactive solute. From [2.40] and [2.42],

$$R = 1 + \frac{\rho_b}{\theta} \frac{d S_s}{d C_r} \; . \qquad [2.43]$$

If eq. [2.43] is valid, it follows that,

$$R = 1 + n \rho_b K_d \frac{C_r^{\,n-1}}{\theta} \qquad [2.44]$$

or for linear adsorption (n = 1),

$$R = 1 + \frac{\rho_b}{\theta} K_d \; . \qquad [2.45]$$

For solutes which are adsorbed, K_d is positive, resulting in $R > 1$. The effect of adsorption is then to hold, or retard the rate of solute movement by the factor R. Dispersion is reduced by the same factor. This means that the adsorbed solute will take R times as long as a non-adsorbed solute to travel a given distance. When solutes are

subjected to anion exclusion K_d is negative, resulting in $R < 1$. This then leads to accelerated leaching of the solute.

The assumption of exchange equilibrium has sometimes resulted in an overestimation of the amount of adsorption occurring during miscible displacement (Davidson and Chang, 1972). As a result, kinetic adsorption models, where the amount of solute sorption is a function of contact time (Lapidus and Amundson, 1952), and two-site linear adsorption models (Selim *et al.*, 1976; Cameron and Klute, 1977) have been developed. In the two- site linear adsorption model, the sorption sites are classified into two types, to one of them sorption is assumed instantaneous, and to the other one sorption is assumed time-dependent. However it is beyond the scope of this review to discuss these models.

2.8.2 Cation Transport

Retention of cations during transport through soils has been described using two different approaches. One of them is the use of an adsorption equation, *e.g.* the Freundlich equation [Eq. 2.41]. Application of this equation to cation exchange in soils does not always, however, take into account competition between cationic species. Another approach is to describe the interaction between the ions in the soil solution and on the exchanger as a reversible and instantaneous exchange reaction. This is then incorporated into the transport model (Robbins *et al.*, 1980). Adsorption of a cation then also depends on other cation species in the soil solution. In a system with cation species Ca^{2+}, Mg^{2+}, K^{+}, and Na^{+}, the total amount of adsorbed cations can be expressed as,

$$X_{CEC} = X_{Ca} + X_{Mg} + X_{K} + X_{Na} \qquad [2.46]$$

where X denotes the charge concentration of adsorbed cations [$mol_c\ kg^{-1}$] and the subscripts represent calcium, magnesium, potassium, and sodium. Although the cation exchange capacity (CEC) of a soil often depends on the pH, and the ionic strength of the soil solution, we first consider here a constant CEC. An example of variable CEC is

given in Chapter 6. Furthermore the discussion here will be limited to a description of binary systems, involving either homovalent or heterovalent exchange.

Since it is assumed that cation exchange reactions are instantaneous and reversible, equilibrium equations can be used to describe the relationship between cation species in the soil solution and on the exchanger. A number of different equilibrium equations have been proposed, and are reviewed by Bolt (1967) and Bohn *et al.* (1985). The most-commonly used equations are probably the mass action, Kerr, Vanselow or Gapon equations. The main difference between these equations is in the treatment of the activities of the involved cations. Firstly we consider cation exchange involving two cation species *A* and *B* of the same valence, and with similar activity. If we assume that the concentrations and activities for both the solution and the adsorbed phase are directly proportional, then all the above equilibrium equations reduce to (Bohn *et al.*, 1985),

$$K_{A-B} = \frac{C_A X_B}{C_B X_A} \qquad [2.47]$$

where $K_{A\text{-}B}$ is the selectivity coefficient, and X_A and X_B are the charge concentrations of adsorbed cations *A* and *B* [$mol_c\ kg^{-1}$]. The selectivity coefficient is generally assumed to be constant (Freeze and Cherry, 1979), but approaches with varying selectivity coefficients have also been used, where $K_{A\text{-}B}$ is a function of the fractional coverage on the exchanger phase (Mansell *et al.*, 1988). The selectivity coefficient can be determined experimentally by measuring the equilibrium ionic composition of several soil solution systems having different exchangeable cation compositions.

Since the cation exchange capacity is assumed constant, it follows for a homovalent system that,

$$X_A = \frac{K_{A-B} X_{CEC} C_A}{C_T + C_A (K_{A-B} - 1)} \qquad [2.48]$$

where $K_{A\text{-}B}$ is the selectivity coefficient, X_{CEC} is the cation exchange capacity of the soil solids [$mol_c\ kg^{-1}$], and C_T the total solution concentration [$mol_c\ l^{-1}$], which for a solution containing only cation species *A* and *B* is given by,

$$C_T = C_A + C_B \ . \qquad [2.49]$$

Retardation for cation transport, assuming a constant C_T is then given by (Selim *et al.*, 1987),

$$R = 1 + \frac{\rho_b\ X_{CEC}}{\theta\ C_T} \frac{K_{A-B}}{\left(1 + (K_{A-B} - 1)\frac{C_A}{C_T}\right)^2} \ . \qquad [2.50]$$

Furthermore if nonpreferential exchange between cation species A and B is assumed ($K_{A\text{-}B} = 1$), the above equation simplifies to

$$R = 1 + \frac{\rho_b\ X_{CEC}}{\theta\ C_T} \qquad [2.51]$$

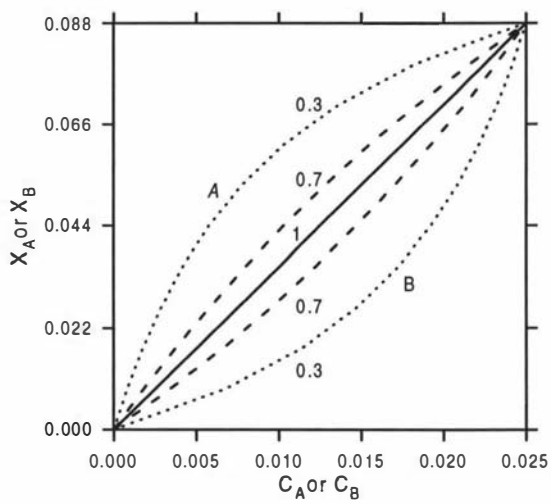

Fig. 2.5 Exchange isotherms for a homovalent system with cation species *A* and *B* for various values of the selectivity coefficient $K_{A\text{-}B}$.

Exchange isotherms for various values of $K_{A\text{-}B}$ are plotted in Fig. 2.5 for a homovalent system. It can be seen that for $K_{A\text{-}B} \neq 1$ the isotherm is nonlinear. For a $K_{A\text{-}B} < 1$ the isotherm becomes favourable for cation species *A* (convex upward), and unfavourable for cation species *B* (concave upwards).

The effect of the two different types of isotherms, unfavourable or favourable, on the shape of the breakthrough curve is shown in Fig. 2.6a and 2.6b. In all cases the simulations were carried out for a Pèclet number of 10, $K_{A\text{-}B}$ values of 0.3, 0.7 and 1, a CEC value of 0.05 $mol_c\ kg^{-1}$, a ρ_b of 1.4 Mg m^{-3}, and a θ of 0.4 $m^3\ m^{-3}$.

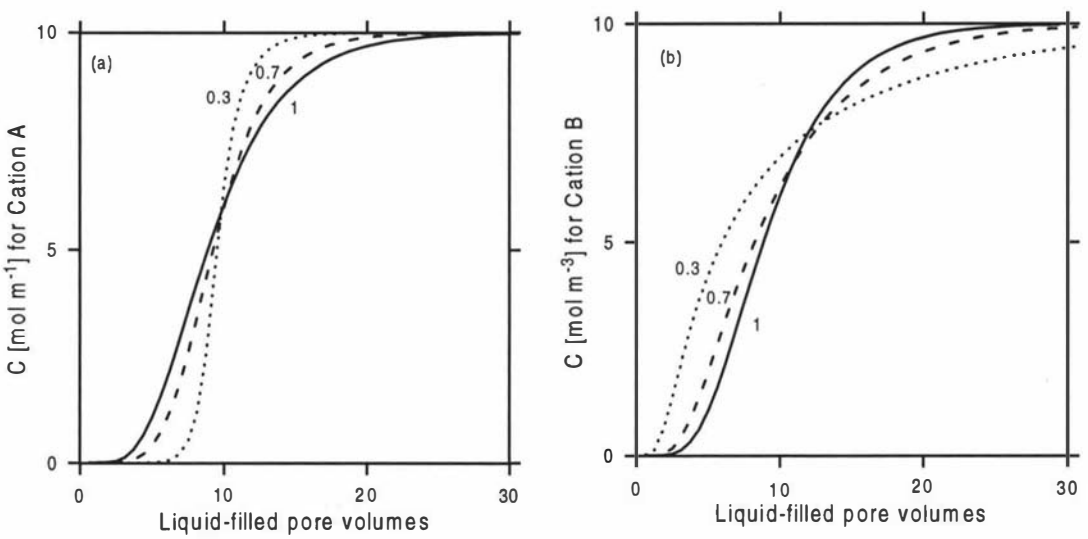

Fig. 2.6 BTC's for a homovalent system with cation species *A* and *B* for various values of $K_{A\text{-}B}$ for (b) an unfavourable isotherm, and (a) a favourable isotherm.

It is evident from Fig. 2.6 that a nonlinear isotherm causes a change in the spreading of the solute front, similar in effect to hydrodynamic dispersion. Two totally different processes can hence have a similar effect on the pattern of solute transport and the shape of the BTC. For an unfavourable isotherm, the spreading increases with increasing nonlinearity in the isotherm. Whereas for a favourable isotherm the spreading decreases with increasing nonlinearity. In the case of an unfavourable isotherm (Fig. 2.6b) adsorption is relatively low at low concentrations, resulting in an earlier concentration rise. With increasing concentration the slope of the isotherm increases, resulting in a tailing effect. For a favourable exchange isotherm (Fig. 2.6a), the opposite effect

occurs, with high adsorption at low concentrations, resulting in a delayed concentration rise. The decrease in the isotherm slope at higher concentrations then sharpens the BTC.

The most-commonly used equilibrium equation to describe cation exchange for heterovalent systems under practical concentration ranges, is the Gapon equation (Bohn *et al.*, 1985),

$$K_{M-D} = \frac{X_D C_M}{X_M (C_D)^{1/2}} \qquad [2.52]$$

where the subscripts M and D denote monovalent and divalent cation species, and K_{M-D} is the selectivity for the monovalent-divalent system [(mol m^{-3})$^{1/2}$].

Equilibrium equations (eqs. [2.47] and [2.52], in conjunction with eq. [2.46] can be directly incorporated into the CDE. This is described in detail in Appendix A.

Exchange equations (eq. [2.48] to [2.51]) in conjunction with the CDE have been used by numerous investigators to describe cation transport through repacked aggregated soil (Selim *et al.*, 1987; Schulin *et al.*, 1989). Predictions based on this have been found to be relatively good. However use of the mobile/immobile concept has often resulted in improved predictions of the observed tailing of breakthrough curves (Selim *et al.*, 1987). Nonequilibrium in cation transport is, however, as Selim *et al.* (1987) pointed out "inconsistent with tritium and ^{36}Cl transport data which indicated local equilibrium". Hence the use of the mobile/immobile concept to describe cation transport seems sometimes to be more pragmatic than fundamentally sound.

It should also be kept in mind that the shape of the isotherm affects the shape of the BTC, as was shown in Fig. 2.6. Nonlinear isotherms can result in increased dispersion and tailing. However tailing can also be simulated by using the MIM with linear isotherms, and by adjusting the ratio between the mobile and the immobile fraction. Although models based on physical or chemical nonequilibrium have often resulted in improved predictions of both anion and cation movement, it seems that these models are

too complicated to be useful as a predictive tool. They require a large number of parameters, which so far cannot be measured independently. Different set of parameters can predict the same solute transport behaviour.

2.9 Boundary Conditions and Solutions for the Convection-Dispersion Equation

2.9.1 Flux and Resident Concentrations

The various formulations of the CDE can sometimes be solved analytically. They can always be crunched numerically. Both analytical and numerical simulations of solute transport require the specification of initial and boundary conditions. The use of the appropriate boundary condition to describe the method of solute application to the soil is critical for the parameter estimation. The choice of solution depends on the type of solute concentration measured, either the flux or the resident concentration (Fig. 2.2). Flux concentrations (C_f) are obtained from measurements of effluent from a soil column, or a lysimeter. Resident concentrations (C_r) are obtained by sectioning soil cores and extracting the soil solution, or by *in situ* electrical resistance measurements of the soil, such as by Time Domain Reflectometry.

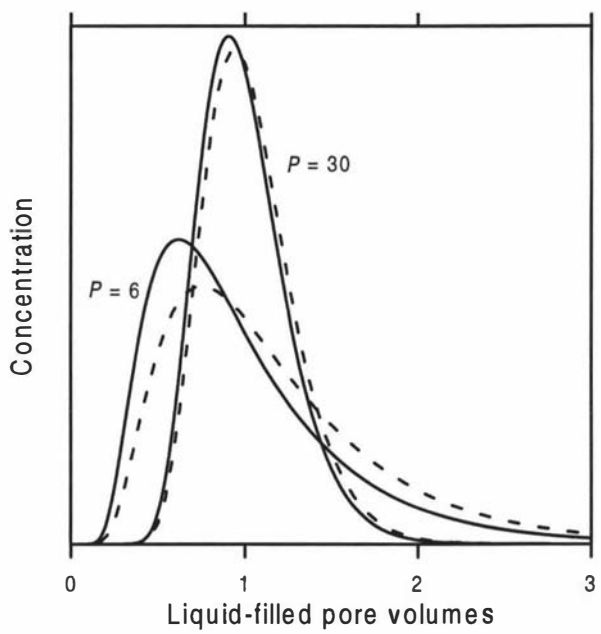

Fig. 2.7 Flux (solid lines) and resident concentrations (broken lines) for two different Pèclet numbers.

The importance of distinguishing between these two types of concentrations when describing convective-dispersive transport was emphasised by Kreft and Zuber (1978), and Parker and van Genuchten (1984), and is shown in Fig. 2.7. In the simulation a solute pulse in the flux concentration was applied to the soil surface, and the concentration at a depth l was simulated as either the flux concentration (solid lines), or the resident concentrations (broken line). Two different simulations are shown, with Pèclet numbers (P) of 6 and 30, where P is defined as l / λ. The difference between the two predictions increases with increasing dispersivity (λ), as is apparent from eq. [2.26]. Misinterpreting the resident concentration as a flux concentration can result in an overestimation of both λ and the retardation factor R.

2.9.2 Boundary and Initial Conditions

The analytical solutions of the convection dispersion equation for a number of boundary conditions are given by van Genuchten and Alves (1982). Here only the solutions for the boundary conditions pertinent to this study are described.

The most-common initial condition is that the initial concentration in the soil is zero, given by,

$$C_r = C_f = 0 \qquad \text{for } t = 0 \quad \text{and } 0 < z \leq l . \qquad [2.53]$$

where C_r is the volume averaged or resident concentration, C_f the flux-averaged concentration, t the time, z the depth [m] and l the length of the column [m]. In certain applications, solutes are initially present in the soil, with the initial concentration of them varying with depth. In this case the CDE requires numerical solution.

The lower-boundary condition for the outlet of finite length columns recommended by Parker and van Genuchten (1984) is that applicable for a semi-infinite domain, that is

$$\frac{\partial C_r}{\partial z}(\infty, t) = 0 . \qquad [2.54]$$

This boundary condition ignores any effects due to the finite length of the column. However as the exit reservoir is not in contact with the liquid phase inside the column, diffusion and dispersion at the outlet end can be neglected. So, this solution can also be used for finite systems, where $0 \leq x \leq l$ (Parker and van Genuchten, 1984).

Much discussion can be found in the literature about the inlet boundary condition most appropriate. Under steady-state water flow conditions, two different input functions are commonly considered, a first- and a third-type condition. The first-type condition defines the solute concentration at the soil surface. For a constant surface concentration C_o it is,

$$C_r = C_o \qquad \text{for } z = 0 \quad \text{and} \quad t \geq 0 \ . \qquad [2.55]$$

The third-type or flux boundary condition defines the solute flux density at the upper surface. For a constant flux density it is,

$$v C_r - D_s \frac{\partial C_r}{\partial z} = v C_o \qquad \text{for } z = 0, t \geq 0 \qquad [2.56]$$

where C_o is the input concentration, C_r the resident concentration, and D_s is the hydrodynamic dispersion coefficient. This third-type condition assumes that molecular diffusion and dispersion above the soil are negligible, which can lead to differences between C_o and C_r at $z = 0$. Hence the discontinuity in the concentration at the inlet end (Parlange *et al.*, 1985) increases with the dispersivity. This third-type boundary condition is generally preferred as it more closely approximates the experimental conditions usually imposed. It is recommended by van Genuchten and Parker (1984) for effectively semi-infinite systems, or finite systems of length l, when $P \geq 5$. This surface boundary condition does not allow solute to diffuse upwards, which means that the symmetry of the diffusion process is broken. The centre of a solute pulse consequently moves downward more quickly and spreads out more slowly than it would in an infinite medium. In very short columns, with a low Pèclet number, it implies an early breakthrough similar to that induced by preferential flow. This is however an artifact of

the soil surface boundary condition, which inhibits backwards dispersion. For a short enough column, early breakthrough (*i.e.* apparently preferential flow) would occur with this surface boundary condition, even if longitudinal molecular diffusion was the only solute-spreading process operative.

The input function at the inlet end depends on the method of solute introduction. It can take on several forms, such as a constant value in time, a pulse-type distribution, or an exponentially increasing or decreasing function (van Genuchten and Alves, 1982). Many column leaching experiments involve a step change in the solute flux density at the inlet end from zero to a constant value. These inputs can mathematically be represented by,

$$\begin{aligned} C_f &= 0 \quad \text{for } z=0 \quad \text{and} \quad t<0 \\ C_f &= C_1 \quad \text{for } z=0 \quad \text{and} \quad t \geq 0 \end{aligned} \qquad [2.57]$$

where C_1 is a constant.

Another commonly-used input is an instantaneous pulse, or Dirac pulse-input, given by

$$C_r = \frac{M_o\, \delta(t)}{\theta\, q_w} \quad \text{for } z=0 \text{ and } t \geq 0 \qquad [2.58]$$

or,

$$C_f = \frac{M_o\, \delta(t)}{\theta\, q_w} \quad \text{for } z=0 \text{ and } t \geq 0 \qquad [2.59]$$

where M_0 [g m^{-2}] is the mass of solute applied to a unit area of soil, and $\delta(t)$ is the Dirac delta function [s^{-1}]. The pulse can either be applied to the soil surface [2.59], or be initially resident in the soil [2.58].

Solute displacement experiments often involve the measurement of flux-averaged concentrations C_f, which if the CDE applies, can be obtained from C_r by eq. [2.26]. The flux concentration at $z \rightarrow \infty$ for semi-infinite systems is assumed to be equal to the resident concentration (Parker and van Genuchten, 1984).

2.9.3 Analytical Solutions

Analytical solutions have been widely used for interpretation of laboratory experiments. Although analytical solutions are limited to conditions of steady-state water flow, uniform water content, linear processes, and restricted initial and boundary conditions, valuable information can be gained by their use. A number of analytical solutions for different boundary conditions for one-dimensional solute transport are given by van Genuchten and Alves (1982).

The solution for the resident concentration following a step change in the input flux concentration [eq. 2.57] is given by (van Genuchten and Wierenga, 1986),

$$C_r/C_o = \frac{1}{2}\,\mathrm{erfc}\left[\frac{z-vt}{2\sqrt{D_s t}}\right] + \left(\frac{v^2 t}{\pi D_s}\right)^{1/2} \exp\left[-\frac{(z-vt)^2}{4 D_s t}\right] - \frac{1}{2}\left(1+\frac{vz}{D_s}+\frac{v^2 t}{D_s}\right) \exp\left(\frac{vz}{D_s}\right) \mathrm{erfc}\left[\frac{z+vt}{2\sqrt{D_s t}}\right] \qquad [2.60]$$

where erfc is the complementary error function.

The resident concentration following a pulse input in the flux concentration [eq. 2.59] is (Kreft and Zuber, 1978),

$$C_r = \frac{M_o}{\sqrt{\pi D_s t}} \exp\left[\frac{-(z-vt)^2}{4 D_s t}\right] - \frac{M_o v}{2 D_s} \exp\left(\frac{vz}{D_s}\right) \mathrm{erfc}\left(\frac{z+vt}{2\sqrt{D_s t}}\right) . \qquad [2.61]$$

The solutions for the flux-averaged concentration (C_f) can be derived directly from the solutions of the resident concentrations by recalling the relationship between the flux-averaged concentration and the volume-averaged concentration [eq. 2.26].

The solution for the flux concentration following a step change in input is given by (Kirkham and Powers, 1971),

$$\frac{C_f(z,t)}{C_0} = \frac{1}{2}\left[\text{erfc.}\left(\frac{z-vt}{2\sqrt{D_s t}}\right) + \exp\left(\frac{vz}{D_s}\right)\text{erfc}\left(\frac{z+vt}{2\sqrt{D_s t}}\right)\right] \qquad [2.62]$$

and for a pulse input the solution is (Kreft and Zuber, 1978),

$$C_f = \frac{M_o\, z}{q_w\, 2\sqrt{\pi D_s t^3}}\exp\left[-\frac{(z-vt)^2}{4 D_s t}\right]. \qquad [2.63]$$

Equations [2.60-2.63] are commonly used analytical solutions of the CDE. These are only valid for the assumptions made in the model, and for the boundary conditions described above.

2.9.4 Numerical Solutions

In situations that mimic the conditions often found in either the laboratory or field, the CDE can only be solved by numerical procedures. Numerical solutions are needed when transient water flow or nonlinear adsorption processes occur. They also offer more flexibility in the initial and boundary conditions and with modern day computers and software, their solution is not too difficult. To solve the CDE numerically a number of different approaches can be used. In all of them, the soil profile is divided into notional compartments each Δz thick, and the time period into notional time steps Δt long. For each compartment initial conditions are specified, *i.e.* for compartment n at the j^{th} time step, the water content is θ_n^j, the solute concentration C_n^j, and the solute mass M_n^j, where the subscripts n and j refer to depth and time. In the numerical schemes used here, a flux type boundary condition [eq. 2.56] is used to define the boundary condition at the soil surface. A zero concentration gradient [eq. 2.54] is assumed deep in the soil

profile. In the numerical procedure this is approximated by adding extra notional layers. The numerical grid is shown in Fig. 2.8.

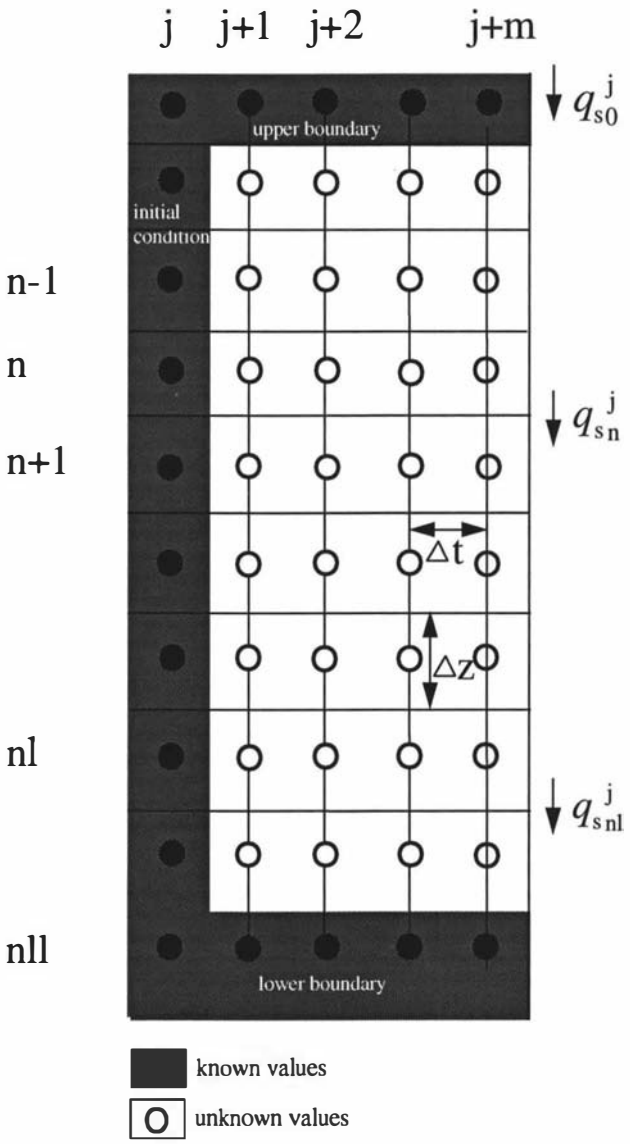

Fig. 2.8 Numerical grid where the depth is downwards and time marches to the right.

The main numerical procedures used in this study are described in Appendix A, and examples of computer programs are given in Appendix B.

2.10 Classification of Solute Transport Models

In the above sections, various approaches to the modelling of solute transport through the soil have been discussed. These, and several other approaches, are discussed and classified in reviews by Addiscott and Wagenet (1985), Brusseau and Rao (1990), and Kutílek and Nielsen (1994). Solute transport models are commonly grouped under two broad headings: deterministic or process models, and stochastic models. In deterministic models, such as the convection dispersion equation (CDE), it is assumed that a given set of events leads to a uniquely-definable outcome. Conversely, in stochastic approaches, the parameters are treated as random variables with a certain probability function (pdf) assigned to them. The value of random variables can be different at each point in the soil. Random variables can also be a function of time. Solute transport behaviour is then treated as a random phenomenon, which means that at any location a number of outcomes can be predicted by the model. Stochastic models include the stochastic version of the CDE (Bresler and Dagan, 1979), Monte Carlo simulation approaches (Amoozegar-Fard *et al.*, 1982), and the stochastic convective stream tube model of Jury and Roth (1990).

On closer examination, however, the above classification seems somewhat artificial, as "stochastic" models do not usually treat solute transport behaviour at either the laboratory or the field scale as a random phenomenon. Although the stochastic-convective model of Jury (1982) has apparently been developed with the idea of randomness, the approach would only be stochastic if a heterogeneous field were visualised as consisting of numerous independent "stream-tubes" in which the transport properties, such as the pore water velocity and the dispersion, are constant in each column but vary randomly between "stream-tubes". In practice the randomness is assumed to occur at a smaller scale, and measurements are not made of individual "stream-tubes". The measured concentration in a certain volume of soil at a certain depth is used to infer the distribution of travel times through a number of notional independent and randomly-distributed pathways or stream tubes, thereby giving for an REV an expected value for the solute travel time and its variance. If these stream tubes are thought of as being macropores, solute concentrations are not really sampled at random. Instead the pdf is assumed to be the same for every REV in the soil, and the

expected value and its variance are constants. Furthermore the travel time distribution, characterised by the probability density function, is assumed to be characteristic for a certain soil, which means that at the scale at which measurements are made, the outcome is not uncertain.

In other classification schemes, models have been grouped into mechanistic and non-mechanistic models. Mechanistic models are believed to be based on the physical processes involved. However the fact that a mechanistic model fits a given data set does not necessarily prove the validity of certain physical mechanisms, but only shows that the operation of those is consistent with the data. Mechanistic models imply that predictions of solute concentrations can be made for all depths. Thus mechanistic models include not only the CDE, but also the stochastic convective stream tube model of Jury and Roth (1990). However the issue of mechanistic or non-mechanistic is quite confusing. For example, Jury (1983) states "The transfer function model has no mechanisms...", and a few pages later the following contradictory statement is given: .. "that convective models such as the transfer function model...". Strictly speaking the only non-mechanistic models would be "black box" approaches, such as the original transfer function model of Jury (1982), applicable to only one depth. However as these models cannot be used to predict solute transport under conditions different from those used for calibration, such models would seem of limited utility. If we want to use models as a predictive tool, we have to open the "lid" of the "black box".

A system is a big black box
Of which we can't unlock the locks,
And all we can find out about
Is what goes in and what comes out.

Perceiving input-output pairs,
Related by parameters,
Permits us, sometimes, to relate
An input, output, and a state.
If this relation is good and stable
Then to predict we may be able,
But if this fails us - heaven forbid!
We'll be compelled to force the lid!

Kenneth Boulding

Additionally, models have been classified with reference to their purpose: research or management oriented. Whereas research-based models aim at a complete understanding of the processes, management-oriented models are thought of as being mainly useful as guides to the best management of soils. However this separation also seems arbitrary, as models are only useful if solute transport under various conditions can be predicted. This seems only be possible if the processes involved are reasonably described. A proper understanding of solute transport does not negate the use of simplified models, but stresses the need to test the validity of these models under various conditions.

In conclusion, clear-cut model classification is difficult. It can give misleading impressions about the differences between models, such as being "stochastic" or "non-mechanistic". In fact it seems that classifying models has increased rather than decreased the confusion as to how they are different. Classification using fuzzy-set logic would seem more appropriate.

2.11 Conclusions

This chapter on solute transport theory and transport models shows that models based on quite different physical and chemical assumptions can result in identical predictions of solute transport.

- The comparison of predicted and observed breakthrough curves can therefore not be considered as a test for the unique validity of any mathematical model or mechanistic description.

- The approach of Bolt was used to demonstrate the relationship between the convection dispersion equation and the mobile/immobile approach.

- Although the MIM is conceptually pleasing, it seems of limited applicability. This is because the same predictions can be made using the simpler CDE, and so far it is not possible to independently estimate the required parameters in the MIM. Consequently, the parameters are generally estimated from BTC's by fitting

procedures. But several sets of parameters usually fit BTC data equally well, but give different predictions for solute transport under different conditions or to different depths. Also it is questionable, if the model parameters obtained by fitting have any physical meaning.

- Some approaches assume well-defined soil geometry to estimate the parameters of the MIM. It seems however that instead of simplifying the soil by assuming a well defined structure (e.g. spherical aggregates), a simplified model such as the CDE should be used, provided it performs satisfactorily.

- The CDE can be used for transient water flow, and it can incorporate exchange reactions and production or decay of solutes. The performance of the CDE will therefore be the focus of this study.

Chapter 3

3. The Theory of Time Domain Reflectometry For Measuring Soil Water Content and Solute Concentration

3.1 Introduction

Monitoring and predicting solute transport at the field-scale is important, and this has been emphasized by several authors (Jury, 1982; Butters and Jury, 1989). Kutílek and Nielsen (1994) concluded that "...without properly taken field data all our effort is futile". To characterize adequately a site, and to obtain a better understanding of water and solute transport at the field-scale, large numbers of measurements are needed, in part because of the high spatial and temporal variability. The traditional technique for measuring the soil's water content involves oven-drying of a soil sample, and determining the weight loss (Gardner, 1986). This so-called 'gravimetric' technique is not only time consuming, but more importantly, it is destructive and hence not suitable for regular *in situ* monitoring of soil water content. An alternative method, and up until recently the most-widely used method for *in situ* measurement of soil water content is the neutron probe (Jury *et al.*, 1991). This method also has many disadvantages, including the attendant radiation hazard, the inability to measure close to the soil surface, and the need for soil specific calibration. There has thankfully been a recent technological advance: Time Domain Reflectometry (TDR).

The traditional method for the determination of the solute resident concentration in the soil is solution extraction from soil samples. However, as with gravimetric water content measurements, this method is also time consuming and destructive. Solute concentration can also be measured using suction cups, but problems include the adsorption of ions by the ceramic material. Furthermore suction cups may only sample water from the mobile regions of the soil water domain. Water in the immobile region might not be drawn into the samplers (van Genuchten and Wierenga, 1977). So there is the uncertainty of whether the sample concentrations represent a resident or a flux concentration (Elrick *et al.*, 1993, Kachanoski *et al.*, 1994). Until very recently

simultaneous measurements of water content and solute concentration have been difficult to make.

Over the last decade, the new technique of time domain reflectometry (TDR) has been proposed to monitor not only the soil's water content, but also the electrical conductivity of the soil solution. The technique has proved successful, provided that appropriate calibrations are available (Topp and Davis, 1985; Dasberg and Dalton, 1985; Heimovaara, 1993). TDR for measuring soil water content, θ, has now become a well-accepted method (Topp and Davis, 1985, Zegelin *et al.*, 1989, Dalton, 1992) and potentially the electrolyte concentration in the soil solution. However, despite numerous applications of this technique to measure the bulk soil electrical conductivity (σ), the relationship between σ and the solute concentration of the soil solution is not yet completely understood (Yanuka *et al.*, 1988). However, with the potential of this dual capacity, TDR offers great scope for monitoring solute transport. Researchers are now using this method increasingly because it is the easiest and most reliable way to measure both θ and σ *in situ*.

Further advantages of TDR are its good spatial and temporal resolution, and its ability to measure very close to the soil surface (Hook *et al.*, 1992), plus the ability to measure the total resident electrolyte concentration in both the mobile and immobile water regions. Multiplexers can be used to automate the measurements (Heimovaara and Bouten, 1990; Baker and Allmaras, 1990; Herkelrath *et al.*, 1991). The ability of automating TDR for the measurement of θ and σ makes TDR a potentially valuable tool for monitoring water and solute movement, allowing a large number of measurements to be made (Heimovaara and Bouten, 1990) to assess variations in space and time. A possible disadvantage of TDR for measuring solute transport is its limitation to detecting only those solutes that alter the electrical conductivity.

This chapter gives a general introduction to the principles and practice of TDR to measure both the soil's water content and solute resident concentration. In the following chapter, calibration measurements from two different soils to determine both the water content and the solute resident concentration are presented. These calibrations

are then used to assess the ability of TDR to monitor solute transport through repacked and undisturbed soil columns. The TDR method is compared with traditional methods of monitoring solute transport.

3.2 The Measurement System

The TDR used here consists of a three-wire probe connected via a coaxial cable to a commercial cable tester (1502 C Tektronix, Beaverton, OR). The coaxial cable consists of an inner conductor and a metal shield, separated by a dielectric material. The dielectric material is generally polyethylene, in which case the wave travels at 0.66 the speed of light. This is the so-called 'velocity of propagation', and the ratio we will later refer to as the relative velocity setting (v_p). The cable tester is operated under computer control using special software developed by Steven Green of HortResearch (pers. comm.).

The cable tester sends out an electromagnetic wave, which travels down the coaxial cable, and enters the probe which is embedded in the soil. The core of the coaxial cable is connected to the centre-wire of the probe, and the shield to the outer two. The probe mimics a coaxial system, thereby obviating the need for an impedance matching balun (Zeglin *et al.*, 1989). A typical setup is shown in Fig. 3.1. The electromagnetic wave consists of an electrical part and a magnetic part. For most soils in the determination of the soil water content, the magnetic part is irrelevant. The electrical part of the travelling wave is influenced strongly by the associated dielectric properties of the soil constituents, especially the water content. The fast-rise, step-shaped voltage pulse of these devices contains a spectrum of frequencies (Fellner-Feldegg, 1969) in the high MHz to GHz range (Topp *et al.*, 1980). The voltage pulse travels from the coaxial cable into the probe. At the end of the probe the signal is reflected. The travel time of the wave along the transmission line is extremely short, usually in the range 1 to 100 nanoseconds, given the typical length of probe length used in the soil.

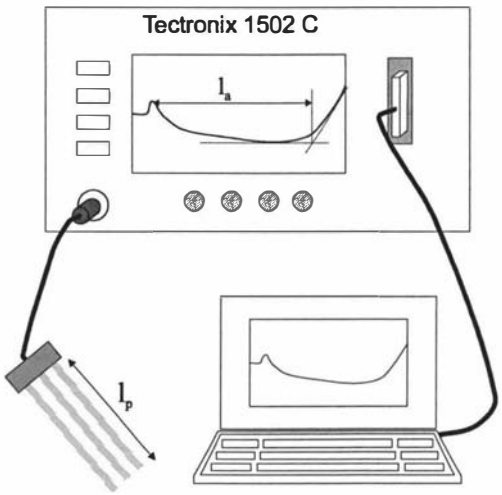

Fig. 3.1 Schematic diagram of the TDR system.

The impedance is the total resistance of a conductor to AC current, and is measured in [Ω]. Any change in the impedance sensed along the line causes partial reflection of the wave, which itself causes a change in voltage between the conductor and the shield. Any reflected wave becomes superimposed upon the waves transmitted from the cable tester. The change in voltage is detected by the TDR and then shown on the oscilloscope as the reflection coefficient (r). This reflection coefficient is the ratio of the voltage reflected back to the receiver, divided by the voltage applied by the TDR unit. The TDR device measures the propagation and reflection of the pulse, as well as its attenuation. The entire curve can be simply called the trace.

In Fig. 3.2 is illustrated an idealized trace. The dielectric constant and the bulk soil electrical conductivity can be calculated from this wave form. Such measurements provide the basis for calculating the volumetric water content around the probes, and the corresponding soil solution electrical conductivity of the soil solution.

The cable tester produces an electromagnetic wave and produces an increase in voltage between the conductor and shield equal to about 0.225 V. The wave then enters the coaxial cable at point A, and travels down the cable to the TDR probe at point B. At this point, some of the voltage pulse is reflected back from the beginning of the probe. The remainder of the pulse is transmitted. Any decrease in impedance at point B results

in a counter phase reflection, and can produce a drop in amplitude compared to the launched voltage pulse. At point C, which corresponds to the end of the probe, the remainder of the transmitted voltage pulse is reflected, in phase, so that the total amplitude becomes twice the transmitted voltage pulse, in the absence of any signal loss. On the way back to point B some of the reflected signal is transmitted through to point A, and the remainder is again reflected back towards point C. This continues until the multiple reflections finally die away, and the final voltage level D is reached.

In summary, any increase in impedance along the cable, or the transmission line, results in an increase in voltage, such as occurs at the end of the probe. Conversely, a decrease in impedance will results in a decrease in voltage, as occurs when the wave travels down the TDR probe.

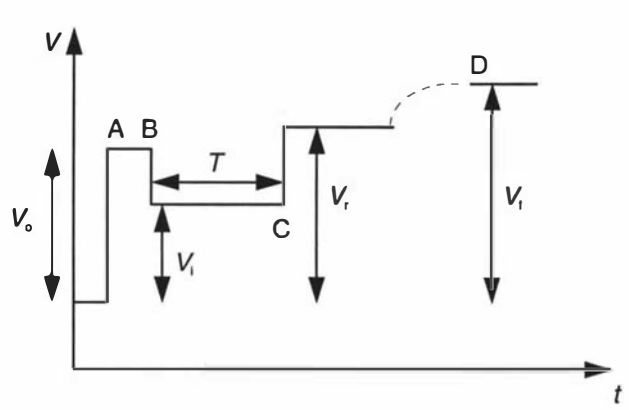

A : output of TDR
B : reflection from probe beginning
C : reflection from probe end
D : final voltage level after multiple reflections
AB: coaxial cable travel time
BC: TDR probe travel time
T : travel time
V_o : zero-reference voltage
V_i : voltage of incident step
V_r : voltage after reflection from probe end
V_f : final reflected voltage at very long time

Fig. 3.2 An idealized TDR voltage trace vs. time.

3.3 TDR for Measuring Soil Moisture Content

The TDR measurement technique was developed Fellner-Feldegg (1969), who used it to measure the apparent dielectric constant (ε) of liquids in a coaxial wave guide. The use of TDR for measuring the dielectric constant of soil was originally proposed by Davis and Chudobiak (1975), and Topp *et al.* (1980). The dielectric constant of soil depends on the volume fractions of the soil constituents and their individual dielectric constants.

Representative values of ε are 80.36 for liquid water, 3-5 for soil minerals, 6-8 for organic matter, and 1 for air, at a frequency of 1 GHz and a temperature of 20^0 C (Weast, 1965). Thus, the ε of a soil is dominated by the volumetric content of water because of its high ε. The dielectric constant consists of a real part, and an imaginary part. The real part of the dielectric constant is a measure of the polarisability of the constituents, while the imaginary part represents the energy absorption by ionic conduction, or dielectric losses. The only polarisable molecules in soils tend only to be water molecules. The relationship between ε and θ developed by Topp *et al.* (1980) has now been widely adopted as a calibration standard for soils with low organic matter content.

The determination of the soil water content by TDR involves the measurement of the propagation velocity (v_e) of the electromagnetic pulse as it travels along a waveguide, or TDR probe, embedded in the soil. The relationship between v_e and ε of a material is given by (von Hippel, 1954):

$$v_e = \frac{c}{\left[\frac{\varepsilon}{2}\left(1+\sqrt{\left(1+\tan^2\delta\right)}\right)\right]^{1/2}}, \qquad [3.1]$$

where tan δ is the loss tangent, which is generally assumed to be <<1 (Topp *et al.*, 1980). Thus eq. [3.1] can be written as,

$$v_e = c\,\varepsilon^{-1/2} \qquad [3.2]$$

where c is the propagation of an electromagnetic wave in free space (viz. $3x10^8$ m s^{-1}), and ε is the dielectric constant of the medium. As already noted, the dielectric constant consists of a real part, and an imaginary part. If the electric loss in the soil is small, then the imaginary part can be neglected (Topp *et al.*, 1980). Hence, only the only real part of the dielectric constant affects the wave velocity, or the pulse transit time in the probe. Over the frequency range 1 MHz to 1 GHz, the real part of the dielectric constant in soil

is not strongly dependent on frequency (Davis and Annan, 1977). Thus, the dielectric constant of the soil measured can be considered only a function of the soil constituents.

The propagation velocity in the soil can be obtained directly from TDR measurements. It is calculated from the time t [s] taken for the reflected signal to travel forth and back along the probe, which corresponds to the interval BC shown in Fig. 3.2. So,

$$v_e = 2\, l_t\, t^{-1} \qquad [3.3]$$

where l_t is the physical length of the probe [m].

By combining Eq. [3.2] and [3.3] it is possible to eliminate v_e and to determine the dielectric constant of a medium from the measured travel time,

$$\varepsilon = \left[\frac{c\,t}{2\,l_t}\right]^2 = \left[\frac{l_a}{l_t \cdot v_p}\right]^2 \qquad [3.4]$$

In commercial TDR cable testers, the term $c\,t/2$ is replaced by an apparent probe length l_a/v_p which is obtained directly from the trace. Here v_p is a fraction, being the relative velocity to the speed of light, which accounts for the specific dielectric of the coaxial cable. This v_p value can either be set manually on the panel of the instrument, or it can be changed under software control.

The volumetric water content of the soil can then be determined by calibration based on a simple measurement of ε. Different approaches have been proposed to relate ε and θ. Some employ mixing laws (Roth *et al.*, 1990b; Dirksen and Dasberg, 1993), while others are empirical (Topp *et al.*, 1980). The empirical relationship found by Topp *et al.* (1980) was initially claimed to be universal, and independent of soil texture, soil density and salinity influences. For this reason it is often referred to as the 'universal relation' (Zegelin *et al.*, 1992). The relationship is:

$$\theta = -5.3\times10^{-2} + 2.92\times10^{-2}\varepsilon - 5.5\times10^{-4}\varepsilon^2 + 4.3\times10^{-6}\varepsilon^3 \ . \qquad [3.5]$$

This empirical relationship has been substantiated by other investigators (Dalton and van Genuchten, 1986; Zeglin *et al.*, 1989). Roth *et al.* (1992) found it appropriate for mineral soils with absolute error in θ of about 0.015 $m^3\ m^{-3}$. If higher accuracy is required, individual calibrations were considered necessary. Since then, other influences on the θ-ε relation have also been studied. These include bulk density (Ledieu *et al.*, 1986), and soil temperature (Roth *et al.*, 1990b). For organic soils this so-called 'universal' relationship has often been found inappropriate. This might be due to the higher amount of bound water associated with organic matter, as bound water has a lower dielectric constant, due to the restricted rotational freedom of the liquid water molecules.

An alternative to eq. [3.5] is, as noted before, the use of mixing models. Here ε is obtained from the individual ε of the three soil components, the soil, the enclosed air, and the volume fraction of water. Major constraints for the use of mixing models include the difficulty in determining the required constants, and the effect of bound water. Empirical θ-ε relations were used in this study.

3.4 TDR for Measuring Solute Concentration

Dalton *et al.* (1984) first proposed the use of TDR for measuring the electrical conductivity (σ) of the soil. They demonstrated that the attenuation of a voltage pulse along the probe could be used to deduce σ. This attenuation was used to infer the solute resident concentration (C_r). Since then several different approaches have been suggested for using the attenuation of the reflected signal to determine σ, and they are based on use of various values of the voltage at different points along the TDR-trace (Fig. 3.2). However, so far it remains unresolved as to which of the alternative expressions is the most appropriate for the calculation of σ.

Dalton *et al.* (1984) used the ratio of the signal amplitude from the start of the probe and the voltage upon its first reflection from the probe, $(V_r - V_i)/V_i$, to find σ (Fig. 3.2). According to electromagnetic field theory (Ramo and Whinnery, 1958), the amplitude of a perfect reflection from the end of a transmission line embedded in an electrically conductive medium with an attenuation coefficient ω, is diminished to

$$V_r - V_i = V_i \exp(2\omega l_t) \qquad [3.6]$$

where V_i is the voltage that enters the transmission line, and l_t is the length of the probe. The attenuation ω is given by:

$$\omega = \frac{60\pi\sigma}{\varepsilon^{1/2}}. \qquad [3.7]$$

and so it follows that:

$$\sigma = \left[\frac{\varepsilon^{1/2}}{120\pi l_t} \ln\left(\frac{V_r - V_i}{V_i}\right)\right]. \qquad [3.8]$$

Later work (Topp *et al.*, 1988) demonstrated that multiple reflections of the signal can occur. These multiple reflections are ignored in the approach of Dalton *et al.* (1984). By using the attenuation voltage at long times (V_f), Yanuka *et al.* (1988) considered the effect of multiple reflections. They found,

$$\sigma = \left[\frac{\varepsilon^{1/2}}{120\pi l_t} \ln\left(\frac{V_i V_f - V_0 (V_i + V_f)}{V_0 (V_i - V_f)}\right)\right]. \qquad [3.9]$$

Zegelin *et al.* (1989) adapted the method of thin-sample conductivity analysis originally proposed by Giese and Tiemann (1975), and they were able to show good agreement between values of σ measured with an AC conductivity bridge, and those measured by TDR. They used the formulation,

$$\sigma = \frac{\varepsilon^{1/2}}{120\pi l_t}\left[\frac{V_i}{V_f}\left(\frac{(2V_o - V_f)}{2V_o - V_i}\right)\right] \quad . \qquad [3.10]$$

It is noted that all of the above formulations (eqs. [3.8], [3.9], [3.10]) require simultaneous measurement of the dielectric constant to determine a value for σ.

Nadler *et al.* (1991) proposed yet another method of determining σ, based on measurement of an impedance of the TDR-probe (Z_L [Ω]). To determine a value for Z_L they used the voltage reflection coefficient r, which is the ratio between the reflected amplitude at long times and the incident signal amplitude. Thus here,

$$r = \frac{Z_L - Z_o}{Z_L + Z_o} \quad , \qquad [3.11]$$

where Z_o is the characteristic impedance of the cable [Ω]. The reflection coefficient can be directly read from the screen of the TDR, thereby allowing an immediate calculation of Z_L. Nadler *et al.* (1991) then converted Z_L to σ using an equation identical to that of Rhoades and van Schilfgaarde (1976),

$$\sigma_{25} = K_G \, f_c \, Z_L^{-1} \qquad [3.12]$$

where σ_{25} is the bulk soil electrical conductivity at 25^0 C, K_G is the probe-geometry constant [m^{-1}], and f_c is a temperature correction coefficient, appropriate for temperatures other than 25^0 C (US Salinity Laboratory Staff 1954, Table 15). The probe-geometry constant is influenced by the length, spacing, and the diameter of the transmission lines. It can, however, be easily determined by immersing the TDR probe into solutions of various known electrical conductivities and measuring the respective impedances (Nadler *et al.*, 1991),

$$K_G = \sigma_{ref} \, Z_L \, f_c^{-1} \qquad [3.13]$$

where σ_{ref} is the electrical conductivity of a reference solution at 25^0 C.

Alternatively, Z_L can be calculated using the respective voltages (Wraith *et al.*, 1993)

$$Z_L = Z_o \frac{(V_i - V_o)+(V_f - V_i)}{(V_i - V_o)-(V_f - V_i)} = \frac{V_f - V_o}{2V_i - V_f - V_o}. \qquad [3.14]$$

The bulk soil electrical conductivity is then calculated using equation [3.12].

The method of Nadler *et al.* (1991) and Wraith *et al.* (1993) for determining the reflection coefficient from voltages after multiple reflections seems to provide a practicable means for the determination of σ, as it does not involve many parameters.

The TDR-measured electrical conductivity of the bulk soil is a function of the water content, the pore-water electrical conductivity (σ_w) due to ionic species in the soil solution, as well as the surface conductance (σ_s). The latter is hopefully small compared to σ_w (van Loon *et al.*, 1991; Mualem and Friedman, 1991). If the surface conductivity can be disregarded, then the pore water electrical conductivity can be obtained from simultaneous measurements of θ and σ, provided the relationship between σ, θ, and σ_w is known. Subsequently, the solute resident concentration (C_r) can then be calculated from known relationships between σ_w and C_r, if the chemical composition of the soil solution is also known. Different approaches can be found in the literature for obtaining σ_w from measured values of σ. Most of these are based on mixing laws, where the determination of various soil parameters is necessary (Rhoades *et al.*, 1976; van Loon *et al.*, 1991). It remains difficult to obtain exact values of σ_w , due to the lack of calibration constants, and the difficulties involved in their determinations. Rhoades *et al.* (1976) suggested that the electrical conductivity of a soil can be approximated by:

$$\sigma = \sigma_s + \sigma_w \theta \tau(\theta) \qquad [3.15]$$

where τ is an electrical tortuosity factor, which is depends on θ. Rhoades *et al.* (1976) proposed a simple empirical relationship between τ and θ given by,

$$\tau = a\theta + b \qquad [3.16]$$

where a and b are soil dependent constants. These constants must be found by calibration.

Ward *et al.* (1994) suggested two different methods to determine the σ-C_r calibration. The first was an indirect method, adopted from Kachanoski *et al.* (1992), and performed on column outflow experiments. This assumes that the final value of σ_w equals that of the input solution. For a multitude of reasons (e.g. immobile water, exchange reactions), this assumption need not always be valid. The second approach is a more direct method, and requires separate experiments, in which the measured impedance is related to solute concentrations at specified water contents.

3.5 TDR for Monitoring Water and Solute Transport

One method for studying water and solute movement is to monitor the flux concentration of solute in the breakthrough-curves (BTC) from column leaching experiments. These BTC's can then be used to assess solute transport parameters (van Genuchten, 1981). Column leaching experiments are, however, time consuming and do not provide information about the variation in the transport parameters with depth. As Jury and Roth (1990) pointed out, transport models based on quite different hypotheses can achieve good agreement with solute outflow concentration data obtained at a single depth. Thus, transport models should be tested using observations obtained at different distances from the surface (Dyson and White, 1987; Jury and Roth, 1990).

Recently TDR has been used to monitor water and solute movement via simultaneous measurement of the soil water content and the solute concentration. The TDR method easily enables the measurement of the solute concentrations at different depths in a soil

column. This then makes TDR a valuable tool for resolving transport parameters. Kachanoski *et al.* (1992) were among the first to measure transport parameters using vertically installed TDR-probes. They monitored the movement of Cl^- ions under steady-state flow conditions in repacked soil columns in the laboratory, as well as in undisturbed soil the field. The parameters they obtained from TDR measurements were compared with those derived from data obtained from either effluent or solution samplers. The agreement between the two different methods was good. In their approach they used TDR measurements of impedance directly, without calibration. This is only possible for steady-state water flow. From the impedance values they determined a travel time probability density function. Vanclooster *et al.* (1993) adapted the method of Kachanoski *et al.* (1992) for use with using horizontally installed TDR-probes. They tested the method on both disturbed and undisturbed soil columns of a sandy material. Wraith *et al.* (1993) monitored Br^- movement using TDR during unsaturated steady-state flow. The values of the transport parameters, the dispersion coefficient (D_s) and the retardation factor (R), obtained from the TDR-measurements were found to be in good agreement with those obtained from the effluent measurements. In all these studies, however, the assumption was made that the measured soil electrical conductivity is linearly related to the solute concentration in the soil solution. This may not always be the case.

3.6 Probe Configuration and Sensitivity

In the first application of TDR for measurement of the soil's water content, coaxial transmission lines with disturbed soil were used (Topp *et al.*, 1980). Later, parallel transmission lines (2-wire probes) with an impedance-matching pulse transformer (balun) were used (Topp *et al.*, 1982). The balun transformer was needed to convert the unbalanced output from the TDR, to a balanced output. Later Zegelin *et al.* (1989) introduced multi-wire transmission lines that have overcome the need for a transformer, by mimicking coaxial conditions. These multi-wire probes improve the reflectance trace (Heimovaara, 1993). The minimum number of wires required is three. In the three-wire probe, the shield of the coaxial cable is mimicked by placing the outer two rods on either side of the central conductor.

Of great importance to TDR-measurements is the volume of the soil sensed by the probe, and the sensitivity of the measurement to the spatial distribution of ε and σ in the soil. This sensitivity was illustrated by Zegelin *et al.*(1989) using the approximate form of the electric field distribution around TDR probes. The main part of the field is concentrated close to the transmission line. This makes TDR most sensitive to the region close to the wires. A high sensitivity to the small volume around the probe was also found by Baker and Lascano (1989). This feature of TDR needs to be taken into account when comparing TDR-measured water contents and with those obtained using other methods. Cracks, root channels, or other kinds of heterogeneity in the soil, can therefore cause deviations, despite both methods providing the correct water content for their respective measuring volumes. To prevent such a restricted sensitivity, Knight (1992) recommended a ratio of rod diameter to rod spacing greater than 0.1.

3.7 Installation of Transmission Lines

Transmission lines can either be installed vertically into the soil, or horizontally from a pit, or into a pedestal. For the installation of horizontal probes some prior excavation is necessary. In either case the measured values of ε and σ are believed to be integrated over the total length of the probe. Thus it is assumed that vertically-installed probes measure the average dielectric constant and bulk soil electrical conductivity over their entire length, integrating any changes with depth (Kachanoski *et al.*, 1994). Horizontally-installed probes on the other hand are assumed to integrate horizontally and measure these properties at a specified depth. They can therefore provide a more precise depth-wise resolution, and a more precise measurement of water content profiles than vertical probes because the range of θ is likely to be less. A great advantage of TDR is that probes can be installed very close to the soil surface with no loss in accuracy. This was shown by Baker and Lascano (1989), who measured water contents with probes placed just 20 mm below the soil surface. Probes of length up to 200-300 mm can also be inserted at an angle to provide spatially integrated measures of θ and C_r in a narrow range close to the surface.

3.8 Conclusion

This chapter provides a short introduction into the theory of TDR-measurements of the soil water content and solute concentration. In the following chapter TDR calibration measurements for two different soils are presented, both for the water content and for the solute concentration. These calibrations were used to obtain relationships between TDR measured dielectric constants, and soil water content; and TDR-measured bulk soil electrical conductivity and the solute concentration resident in the soil. Finally it will be assessed if these ε-θ, and σ-C_r relations can be used to infer solute transport parameters.

Chapter 4

4. Time Domain Reflectometry: Calibration and its Use to Monitor Solute Transport

4.1 Introduction

In the previous chapter, the theory of Time Domain reflectometry (TDR) to measure the soil's water content and solute concentration resident in the soil was outlined. It was noted that a major concern associated with TDR is the need for soil-specific calibrations to relate the TDR-measured impedance to the salt concentration of the pore water, and sometimes also for the water content. For a wide range of soils however, the "universal" calibration curve of Topp *et al.* (1980), given in Chapter 3, can be used to infer the water content from the TDR-measured dielectric constant. The ability to measure simultaneously the water content and the salt concentration make it potentially a valuable tool for studying solute transport under transient conditions.

In this chapter investigations into the applicability of the TDR method to monitor solute transport are described. The use of the TDR-technique is first illustrated on repacked soil columns under transient water flow, using vertically and horizontally installed probes. Also considered is the influence of exchange reactions on TDR-inferred solute transport parameters. The first paper describes the experiments related to these matters. Once it had been demonstrated that the TDR could be used to describe water and solute movement simultaneously, another experiment was conducted in the laboratory on undisturbed soil columns of two different soils. In the second paper this experiment is discussed, and the results are compared with the other more conventional experimental approaches presented in Chapter 5. Different calibration methods are also compared in the second paper.

4.2 Characterizing Water and Solute Movement by TDR and Disk Permeametry

by Iris Vogeler , Brent E. Clothier, Steven R. Green , David R. Scotter, and Russell W. Tillman, 1996.
From *Soil Science Society of American Journal*, 1996, 60, 5-12.

4.2.1 Abstract

To investigate a rapid, non-destructive way of characterizing solute transport properties, TDR and disk permeametry have been used in combination. Calibration measurements had previously related TDR measurements to both the volumetric water content and the pore water concentration of Cl^-. Laboratory measurements from a horizontal TDR probe were used to estimate transport parameters in a soil column by applying a 1-D numerical model in an inverse sense. A vertical TDR probe was used to provide independent verification of these parameters. A repacked column of Ramiha silt loam was used under unsaturated, transient flow conditions. The disk permeameter, set to a pressure head of -50 mm and containing a solution of 0.032 M KCl, was placed straight onto the repacked soil column which possessed an initial water content of 0.32 m^3 m^{-3}. The soil wet to 0.60 m^3 m^{-3}. However in the columns only an envelope of Cl^- concentration could be obtained, due to exchange between the initially-resident Ca^{2+} and the invading K^+. This illustrates why cation exchange needs to be considered when TDR is used to infer solute movement. From the numerical simulations, values for the solute dispersivity and the retardation were found to be 2.3 mm and 1.2. The retardation is shown to be due to the anion exchange capacity varying with the concentration of the invading soil solution.

4.2.2 Introduction

Lack of information on the spatial and temporal variation in soil water content and solute concentration bedevils the description of water and chemical movement through soils. Disk permeametry has improved our ability to describe the hydraulic character of soil, and recent developments in Time Domain Reflectometry (TDR) have enhanced our ability to characterise simultaneously water content and resident solute concentration in

soil. Both techniques offer promise in our quest to obtain better information on soil water flow and chemical transport.

The application of TDR to estimate chemical transport properties has been demonstrated by Kachanoski *et al.* (1992) using vertically-installed probes, and by Wraith *et al.* (1993), using horizontally-installed probes. These studies were conducted under steady-state conditions, using just one probe to monitor water and solute movement. Recently Ward *et al.* (1994) used curved TDR probes in a three-dimensional transport experiment and horizontally-installed probes in a one-dimensional transport experiment. In all cases only the relative soil electrical conductivity was measured, and this was assumed to be the same as the relative solute concentration. Their approach neglected the possible effects of exchange between K^+ and Ca^{2+} ions in the soil on the electrical conductivity. Such effects may have been important in the experiment of Wraith *et al.* (1993) where a silt loam was used. Hussen *et al.* (1994) recently combined TDR and disk permeametry in an experiment performed under steady-state conditions, although details have yet to be published.

We have also combined TDR and disk permeametry. We consider exchange between the invading K^+ and the initially-resident Ca^{2+} in the soil. We use both vertically- and horizontally-installed probes. The horizontally-placed probe allows us to estimate the transport parameters, while the vertically-installed probe can be used for independent verification of these estimates. The objective of this study was to demonstrate the combined use of disk permeametry and TDR, using both vertically- and horizontally-installed probes, to characterise water movement and solute transport. Inverse modelling, by numerical procedures, is used to determine the transport characteristics.

4.2.3 Theory

The experiment described here was conducted in the laboratory on a vertical column of repacked soil. One-dimensional, vertical, transient water infiltration into a homogeneous soil can be described by Richards' equation:

$$\frac{\partial \theta}{\partial t} = \frac{\partial}{\partial z}\left(D_w(\theta) \frac{\partial \theta}{\partial z} \right) - \frac{\partial K_w(\theta)}{\partial z} \qquad [4.1]$$

where θ is the soil's volumetric water content [$m^3\ m^{-3}$], D_w is the soil water diffusivity [$m^2\ s^{-1}$], K_w is the hydraulic conductivity [$m\ s^{-1}$], t is time [s] and z is depth below the soil surface [m]. If the soil has a uniform initial water content of θ_n and the disk permeameter at a pressure head h_o wets the soil to a water content of θ_o, then the boundary conditions are

$$\theta = \theta_n, \qquad z \geq 0 \quad ; t = 0 \qquad [4.2]$$

$$\theta = \theta_o, \qquad z = 0 \quad ; t > 0. \qquad [4.3]$$

For chemical movement, the convection dispersion equation (CDE) can be used to describe the one-dimensional transient flow of reactive solutes (De Smedt and Wierenga, 1984; van Genuchten and Wierenga, 1986). Here then,

$$\frac{\partial (\theta C_r)}{\partial t} + \frac{\partial (\rho_b S_s)}{\partial t} = \frac{\partial}{\partial z}\left(\theta D_s \frac{\partial C_r}{\partial z} \right) - \frac{\partial (q_w C_r)}{\partial z} \qquad [4.4]$$

where C_r is the resident solute concentration of a particular ion in the liquid phase [$mol\ m^{-3}$], S_s is the concentration of that ion adsorbed onto the soil matrix [$mol\ kg^{-1}$], ρ_b is the bulk density of the soil [$kg\ m^{-3}$], q_w is the Darcy flux of water [$m\ s^{-1}$], and D_s is the solute diffusion-dispersion coefficient [$m^2\ s^{-1}$]. This coefficient D_s is commonly considered to be dependent on the pore water velocity v, given by q_w / θ, and defined as (De Smedt and Wierenga, 1978; Brusseau, 1993):

$$D_s = \lambda v + \tau D_o \qquad [4.5]$$

where the proportionally constant λ is known as the dispersivity [m], τ is the tortuosity and D_o is the molecular diffusivity of the ion in free water [$m^2\ s^{-1}$].

If we assume the soil has an uniform initial solute concentration C_{ai}, and that the solute flux density entering the soil is $q_o C_o$, where q_o is the water flux at $z = 0$ and C_o is the concentration of solute in the disk permeameter, then the boundary conditions for solute flow are (van Genuchten and Wierenga, 1986)

$$C = C_{ai}, \qquad z \geq 0; t = 0 \qquad [4.6]$$

$$-\theta D_s \frac{\partial C_r}{\partial z} + q_w C_r = q_o C_o, \qquad z = 0; t > 0. \qquad [4.7]$$

For a non-reactive inert solute the amount of solute adsorbed, S_s, is zero. However for reactive solutes where exchange reactions occur, we need to parameterize S_s by way of an adsorption isotherm. Here we assume a linear relationship between the amount of solute adsorbed onto the soil matrix S_s and the solution concentration C_r given by

$$S_s = K_d C_r \qquad [4.8]$$

with the distribution coefficient K_d [m^3 kg^{-1}] taken to be constant. During flow through a soil maintained at a constant water content, the ratio of the velocity of an inert-solute front to that of a reactive one is called the retardation, R. Under such conditions,

$$R = 1 + \frac{\rho_b K_d}{\theta} \qquad [4.9]$$

so that the retardation of a reactive solute can be used to infer the slope of the soil's adsorption isotherm, namely K_d. Equations 4.1-4.9 form a closed set of equations which can be solved numerically (Green and Clothier, 1994) to describe the transient flow of water and reactive solute through a homogeneous soil column. Under steady-state water flow analytical solutions are available.

4.2.4 Materials and Methods

4.2.4.1 Use of TDR

The theory of TDR has been described in detail by Topp *et al.* (1980), Dalton and van Genuchten (1986), and Nadler *et al.* (1991), among others. Briefly, the TDR technique is based on a measurement of the dielectric constant (ε) and the electrical impedance of the soil (Z_L). Once measured, these properties can then be related, by calibration, to the soil water content and resident solute concentration (Dalton, 1992). The approximately-linear relationship between θ and ε can be influenced by soil type, bulk density, clay content and organic matter (Jacobsen and Schjønning, 1993). The dielectric constant is calculated from (Topp *et al.*, 1980):

$$\varepsilon = \left[\frac{c\,t}{2\,l_t}\right]^2 = \left[\frac{l_a}{l_t\,v_p}\right]^2 \qquad [4.10]$$

where c is the propagation velocity of an electromagnetic wave in free space (*viz.* $3\text{x}10^8$ m s^{-1}), t is the travel time [s], l_t is the real length of the transmission line [m], l_a is the apparent length [m], as measured by a cable tester, and v_p is the relative velocity setting of the instrument.

The resident solute concentration can be related to the bulk soil electrical conductivity (σ) [S m^{-1}] (Dalton, 1992). The bulk soil electrical conductivity can be calculated from the impedance (Z_L) measured at long times, after all multiple reflections have disappeared (Nadler *et al.*, 1991; Kachanoski *et al.*, 1992). Following Nadler *et al.* (1991) and Wraith *et al.* (1993), we assume an inverse relationship between σ and Z_L given by

$$\sigma = K_G\, Z_L^{-1}\, f_c \qquad [4.11]$$

where K_G is a geometric probe constant [m^{-1}], which must be determined empirically, and f_c a temperature-correction coefficient (see Table 15, U.S. Laboratory Staff, 1954). The soil's electrical impedance is calculated using a ratiometric technique similar to that described by Wraith *et al.* (1993). By measuring the zero-reference voltage V_o , the voltage of the incident step V_i , and the final reflected voltage V_f at a very long time, Z_L can be calculated as

$$Z_L = Z_o \left(\frac{V_f - V_o}{2\,V_i - V_f - V_o} \right), \qquad [4.12]$$

where Z_o is the characteristic impedance of the TDR system [Ω].

The geometric probe constant is simply given by,

$$K_G = \sigma_{ref}\, Z_L \qquad [4.13]$$

where σ_{ref} is the electrical conductivity of a reference solution at a temperature 298 K. This constant K_G was determined by immersing the TDR probes into solutions of KCl of various known electrical conductivities and measuring the impedance using Eq. [4.13].

The TDR instrument used for the measurements was a 1502 C Tektronix cable tester (Tektronix Inc., P.O. Box 500, Beaverton, OR 97077). This was connected to a lap-top computer which controlled the settings of the TDR, and recorded and analysed the waveforms. For all measurements three-rod probes similar to those described by Zegelin *et al.* (1989) were used. These probes had a length of 100 mm, a rod diameter of 2 mm, and the spacing between the center and outer rods was 12.5 mm. The three-rod probes were connected via a 50 Ω coaxial cable to a multiplexer that was linked to the cable tester. The multiplexer was similar to that described by Heimovaara and Bouten (1990). Measurements of l_a and Z_L were taken every 30 s and used to calculate ε and σ. The vertical probe was inserted through the disk (Fig. 4.1) immediately after emplacement of the permeameter on the column of soil. It is assumed that the

vertically-installed probe measures the average water content and solute resident concentration over it's entire length, regardless of the distribution. A horizontally-installed probe however measures these properties at a specified depth.

4.2.4.2 Soil Material

The soil was a Ramiha silt loam, which is an Andic Dystrochrept of mixed greywacke origin and contains some volcanic ash. Only material from the Ah2 horizon was used. The soil collected from the field was first air dried then sieved (< 2 mm) to obtain a homogenous material. The cation exchange capacity of this soil is moderate, with Ca^{2+} being the dominant exchangeable cation (Pollok, 1975).

4.2.4.3 TDR Calibration

For the calibration of the TDR system a similar procedure to that of Ward *et al.* (1994) was used. The soil was stepwise brought to a volumetric water of content between 0.3 to 0.6 using 3 concentrations of KCl solution, namely 0.01*M*, 0.03*M* and 0.05*M*. The soil was first mixed thoroughly to achieve a uniform distribution of water and solute. At each water content and solute concentration the soil was then packed into an acrylic column of height 250 mm and diameter 120 mm. A mean bulk density of 0.84 Mg m^{-3} was realised, which is similar to that of the soil *in situ*. For the measurement of the dielectric constant and the electrical impedance of the soil 4 three-rod probes were used. Three were installed horizontally through holes drilled in the acrylic column at 25, 120, and 200 mm depth, and the fourth probe was installed vertically from the soil surface. Duplicate columns were used for each ε-σ combination, which resulted in 8 measurements for each ε-σ combination. The measurements were carried out at temperatures ranging from 290 to 293 K and the appropriate temperature-correction factors were used in Eq. [4.11]. Finally, subsamples of the soil were taken also and the water content determined gravimetrically by oven drying for 24 hours at 378 K. A measure of the pore water electrical conductivity (σ_w) was obtained using a technique similar to that of Dalton *et al.* (1984). This involved centrifuging soil samples at 10,000

RPM for 45 minutes, and measuring the electrical conductivity of the supernatant with a conductivity meter.

4.2.4.4 Positive Charge Measurement

The positive charge of the soil was measured as a function of the ionic strength of the bulk solution because a retardation of Cl^- was observed. We had anticipated KCl to be an inert solute. Only if the anion exchange capacity of the soil increases with increasing strength of the bulk solution can a retardation be detected by the TDR. The positive charge of the soil was measured using an ion retention method as described by Bolan *et al.* (1986) and Marsh *et al.* (1987). This involved a measurement of the amount of Cl^- adsorbed onto the soil at various concentrations of KCl, ranging from 0.005 *M* to 0.05 *M*. For this measurement 2 g of air dried soil was put into a weighed centrifuge tube to which was added 30 ml of the appropriate concentration of KCl solution. For each concentration 4 replicates were used. After shaking for 2 hours the samples were centrifuged, the solution decanted and the soil retained for 4 further washes. After the fifth wash the solution was retained for the measurement of Cl^- to allow correction for the entrained solution. The tubes were then reweighed to determine the amount of entrained solution. The adsorbed Cl^- ions were extracted by shaking the samples for 2 hours with 20 ml of 0.1*M* KNO_3. Chloride concentration was measured using a Tecator Flow Injection Analyser (Tecator Fiastar 5020 Analyzer, Box 70, S-26301 Höganäs, Sweden). Sorbed chloride was determined from the difference between the extracted chloride and the chloride in the entrained solution.

4.2.4.5 Column Experiment

For the main experiment the soil was initially wet to $\theta_n = 0.32$ and then carefully packed at a bulk density of 0.836 Mg m^{-3} into an acrylic column of 500 mm height and 125 mm internal diameter. The experiment was performed at a temperature of 298 K. A disk permeameter with the pressure head set at - 50 mm was used to establish unsaturated flow conditions, and to apply a solution of 0.032 *M* KCl to the upper end of

the soil column. To improve the uniformity of solute infiltration, contact between the disk permeameter and the soil was assured by using a small quantity of acid-washed fine sand. Holes near the base of the acrylic column allowed the egress of air pushed ahead of the infiltrating water. The steady-state flow rate was finally 0.031 mm s^{-1} and the total amount of solution applied was 140 mm.

For the purpose of monitoring water and solute movement through the soil column, two TDR-probes were used. The first was inserted vertically through the disk permeameter, as shown in Fig. 4.1. A special acrylic foot was glued inside the base of the permeameter. Holes were then drilled through both the permeameter base and the acrylic foot. Once the porous nylon membrane was set in place, a hole was cut in the membrane over the location of the holes for the TDR probe. The membrane edges were then sealed to the foot using hot-melt glue. The second probe was installed horizontally through holes drilled into the side at the acrylic column at a depth of 110 mm.

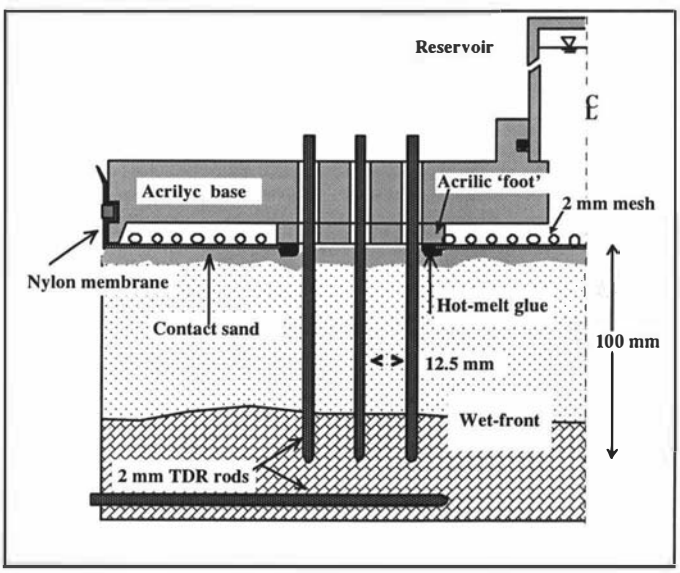

Fig. 4.1 Diagram of the combined TDR and disk permeameter set-up. The vertical section is bounded on the right by the central axis of the permeameter.

Larger holes were also cut in the wall of the acrylic column holding the soil. These holes in depth increments of 10 mm (ranging from 5 to 115 mm) allowed rapid

extraction of small soil cores (length of about 25 mm, internal diameter of 7 mm) at the end of the experiment. These samples were used for gravimetric determination of the water content, as well as the determination of resident concentration of chloride by extracting samples with deionised water at a ratio of 20 ml water to 0.6 g dry soil. The filtrates obtained were later analysed for chloride using a Tecator Flow Injection Analyser.

The unsaturated hydraulic conductivity function $K_w(\theta)$ was found using data from steady state flows and water contents at two pressure heads. A soil column similar to the one described above was infiltrated using a pressure head set at -20 mm and -50 mm. The final steady flow was considered to be the conductivity at that head and water content. A power-function $K_w(\theta)$ (Quadri *et al.*, 1994) was used, namely

$$K_w = K_s \left(\frac{\theta - \theta_a}{\theta_s - \theta_a} \right)^b \qquad [4.14]$$

where K_s is the saturated hydraulic conductivity [m s^{-1}], b is an empirical constant, and θ_s and θ_a are the saturated and antecedent water contents, respectively. With θ_s taken as 0.625 m^3 m^{-3}, the measured flow rates and θ values yielded a K_s value of 7×10^{-5} m s^{-1} and a b value of 10. At h_o = -20 mm, θ was 0.616 m^3 m^{-3}, while at h_o = -50 mm, θ was 0.599 m^3 m^{-3}.

The soil water diffusivity function $D_w(\theta)$ was evaluated using the following exponential expression scaled by the sorptivity (Brutsaert, 1979),

$$D_w(\theta) = \frac{\gamma S^2}{(\theta_s - \theta_n)^2} \exp\left(\beta \frac{\theta - \theta_a}{\theta_s - \theta_a} \right) \qquad [4.15]$$

where γ and β are interdependent constants, taken as 4.278×10^{-2} and 4, respectively (Clothier and White, 1981), and S is the soil's sorptivity [m $s^{-1/2}$]. The sorptivity was evaluated from the early-time infiltration rate using the square-root-of-time approach of

Smiles and Knight (1976). A value of S = 0.6 mm $s^{-1/2}$ was found for the repacked soil column at h_o = -50 mm and θ_n = 0.32.

The finite-difference numerical scheme used to model the flow of both water and reactive solute was that of Green and Clothier (1994), which used the functions of $K_w(\theta)$ and $D_w(\theta)$ given by Eq. [4.14] and [4.15], respectively. The chemical transport properties of λ, R and K_d were deduced through fitting-by-eye the numerical predictions to the TDR-measured rise in the concentration.

4.2.5 Results and Discussion

4.2.5.1 Water-Content Calibration

Results of the water content calibration are shown in Fig. 4.2, where the TDR-measured values of the dielectric constant (ε) are plotted against the gravimetrically determined volumetric water content (θ). An empirical calibration curve was obtained for the water content by fitting a quadratic function to the data, and was found to be

$$\theta = 0.119 + 1.7 \times 10^{-2}\, \varepsilon - 1 \times 10^{-4} \varepsilon^2 \,. \qquad [4.16]$$

This relationship deviates by about +0.1 m^3 m^{-3} from the curve suggested by Topp *et al.* (1980), which is shown as the broken line in Fig. 4.2. The deviation might be due either to the high organic matter content, or the low bulk density of Ramiha silt loam. Differences in the dielectric behavior of differently-textured soils have often been reported (Herkelrath *et al.*, 1991; Dasberg and Hopmans, 1992; Jacobsen and Schjønning, 1993). In their calibration measurements Jacobsen and Schjønning (1993) found that while bulk density, clay content and organic matter each influence the dielectric behavior of a soil, bulk density had the largest influence on ε.

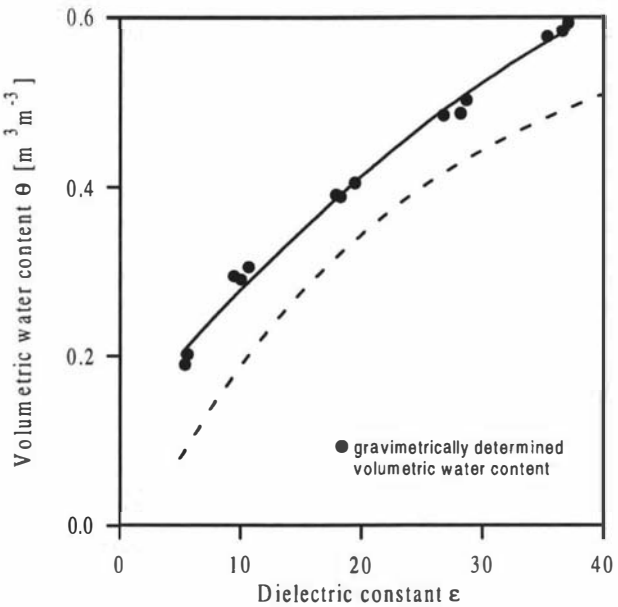

Fig. 4.2 Volumetric water content (●) determined gravimetrically vs. TDR-measured dielectric constant. Also shown is the fitted function (solid line), and the empirical relationship suggested by Topp *et al.* (1980) (broken line).

4.2.5.2 Solute-Concentration Calibration

Results of the solute calibration are shown in Fig. 4.3. Here the mean of the TDR-measured σ is plotted against the σ_w as measured by a conductivity meter of the extracted solution. During the calibration measurements, exchange between the native Ca^{2+} and the added K^+ is likely to have occurred. This cation exchange results in a decrease in the measured σ_w of the soil solution compared to the electrical conductivity of the added solution, by between 63 to 82 %, depending on the concentration of the added solute. However this decrease could also be due in part to an adsorption of Cl^-, or a double-layer effect (Rhoades *et al.*, 1989). The decrease shows the importance of measuring the electrical conductivity of the soil solution, instead of assuming it to be the same as that of the added solution.

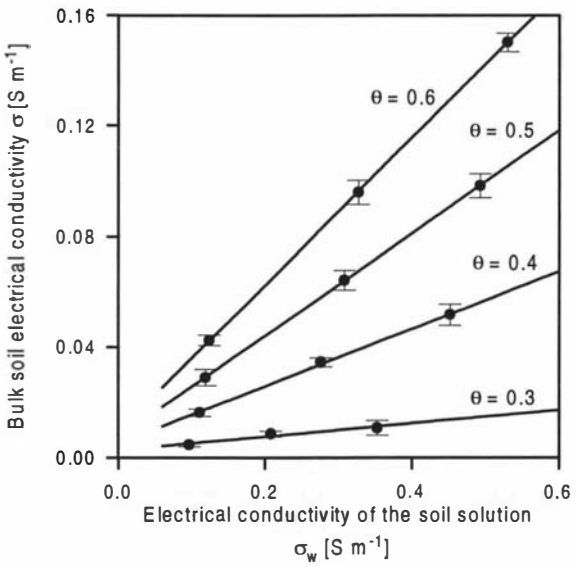

Fig. 4.3 TDR-measured bulk soil electrical conductivity (●) vs. electrical conductivity of the soil solution measured with a conductivity meter for different water contents of Ramiha silt loam. Also shown is the standard deviation (vertical bars) and the fitted relationship (solid lines).

The results show a linear relationship exists between the bulk soil electrical conductivity (σ) and the electrical conductivity of the pore water (σ_w) in the range of 0.1 to about 0.5 S m^{-1} at each volumetric water content (θ). This linearity deviates from previous results reported in the literature (Nadler and Frenkel, 1980; and Shainberg *et al.*, 1980) who found curvilinear behaviours for σ_w < 0.2 S m^{-1}. The deviation from linearity is probably influenced by clay content, Na^+ saturation (Shainberg *et al.*, 1980), water content and probe dimensions (Ward *et al.*, 1994). There also appears to be a relationship between θ and both the slope and the intercept of the lines relating σ and σ_w. On the basis of our data we parameterized the following relationship between σ, σ_w and θ, viz.

$$\sigma_w = \frac{\sigma - (0.0228\,\theta - 0.0042)}{(0.804\,\theta - 0.217)} . \qquad [4.17]$$

At low concentrations the electrical conductivity of the pore water (σ_w [S m^{-1}]) is linearly related to the concentration (C [mol L^{-1}]) of a particular salt solution. For a

KCl solution with concentrations ranging from 0.005 *M* to 0.05 *M*, Weast (1965) gives data implying that

$$C = -0.7 \times 10^{-4} + 7.6 \times 10^{-2}\ \sigma_w\ , \qquad [4.18]$$

while for $CaCl_2$ solution for the same concentration range the relationship is given by

$$C = -1.2 \times 10^{-3} + 9.4 \times 10^{-2}\ \sigma_w\ . \qquad [4.19]$$

Hence by measuring both θ and σ simultaneously, using TDR we are able to calculate σ_w using Eq. [4.17] and therefore estimate the solute concentration C by using either Eq. [4.18] or [4.19].

4.2.5.3 Column Experiment

4.2.5.3.1 Water Flow

The volumetric water contents measured by the horizontally- and vertically-placed TDR-probes during infiltration at h_o = -50 mm are shown in Fig. 4.4. A gradual increase in θ is seen for the vertically-installed probe-set. Here the average water content over the entire length of the rods is measured. As expected a more-abrupt rise in θ is measured by the horizontal probe, as this reflects the passage of the wet front past a depth of 110 mm. A relatively constant water content of 0.59 - 0.60 was reached after about 30 min (1800 s) in both cases. The TDR-measured water contents and those determined gravimetrically on subsamples at the beginning and the end of the experiment were within 0.01 $m^3\ m^{-3}$ for the vertical probe and 0.035 $m^3\ m^{-3}$ for the horizontal probe. Poor probe contact with the soil, prior to wetting, is a possible reason for the early underestimation of water content by the horizontal probe.

The solid lines in Fig. 4.4 are the prediction obtained using the numerical solution of equation [4.1] with the measured hydraulic properties. The agreement between the

measurements and the predictions is good for both probes, except for the slightly slower increase in θ before the final value of θ is reached. This discrepancy is probably due to locally-entrapped air (Peck, 1969), which the numerical model does not account for.

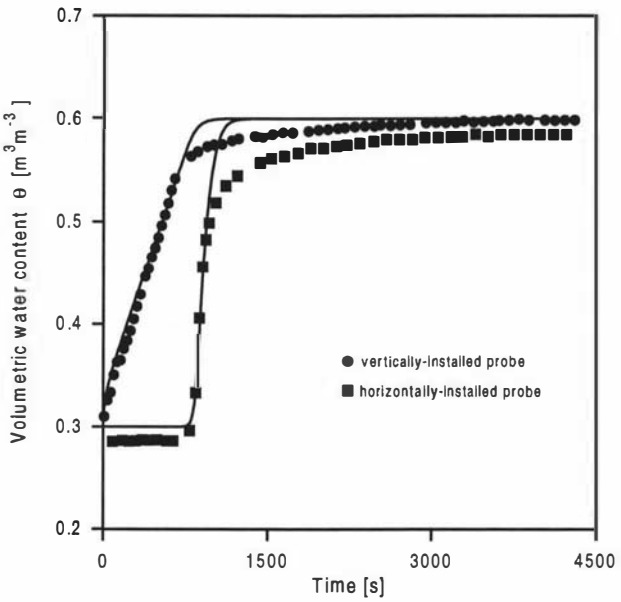

Fig. 4.4 TDR-measured water content for the vertically- (●) and the horizontally-installed probe (■) vs. time during infiltration. The solid lines are the predictions from the numerical solution of Richards' equation.

4.2.5.3.2 Chloride Movement

When a solution of potassium chloride invades a soil, with Ca^{2+} being the dominant exchangeable cation, we expect that exchange will occur between the calcium on the soil matrix and the added potassium ions. Therefore, until the exchangeable Ca^{2+} of the soil matrix is replaced, the invading front of the soil solution will contain dominantly Ca^{2+} and Cl^- ions. Only at longer times, when exchange equilibrium has been reached on the cation exchange sites, will the soil solution behind the invading front be dominated by K^+ and Cl^- ions, the influent species. The electrical conductivity of a 0.015 *M* $CaCl_2$ solution at 298 K is only 83 % of the conductivity of a 0.03 *M* KCl solution (Weast, 1965). Thus the leading edge of the invading solution, which contains $CaCl_2$ will have an electrical conductivity only 83 % of the resident solution concentration that will prevail at long times, which will consist of KCl. Figure 4.5 shows the corresponding rise in the resident chloride concentration for the horizontally-

installed TDR-probe, assuming that the soil solution consisted of $CaCl_2$ (filled squares) or KCl (open squares). These values were obtained from the measured bulk soil electrical conductivity using Eq. [4.17] and either Eq. [4.18] or [4.19]. The antecedent concentration of the soil solution as determined from σ_w measurements on the extracted soil solution was found to be 0.005 mol L^{-1}. Erroneous values greater than 0.005 mol L^{-1} were measured before the wet front reached the probe. These are represented by the crosses in Fig. 4.5 and are probably due to an underestimation of the antecedent water content near the beginning of the experiment (Fig. 4.4). The measured rise of solute concentration with time is of the classic sigmoid shape, at least in the early stages, with C_r reaching C_o after about 4000 s for the $CaCl_2$ curve [Eq. 4.19]. The further increase of C_r above C_o, when the $CaCl_2$ calibration equation is used is again represented by crosses. The final value of σ_w reached by the horizontal probe is 0.39 S m^{-1}. We attribute the apparently anomalous rise in C_r to a replacement of Ca^{2+} by K^+ in the soil solution at the probe depth.

The rise in solute concentration predicted by the numerical model is also shown in Fig. 4.5. Approximate values for the dispersivity (λ) and retardation (R), found by visually comparing many simulations to the measurements, were $\lambda = 2$ mm and $R = 1.2$. For this comparison only the data represented by the closed squares were considered. The simulation result is shown by the solid line. The agreement between the predictions and the experimental data is good over the range of applicability. Our deduced value for λ of 2 mm is similar to values given by Wagenet (1983) of between 2 to 4 mm for uniformly packed soil columns. The reasons for the observed solute retardation are discussed below.

The results obtained from the numerical solution were also compared with the analytical solution for steady-state water flow (equation A-2 of van Genuchten and Wierenga, 1986). This analytical solution is considered applicable to our experiment, since the water content was relatively constant once the wet front passed the probe. This occurred well before the leading edge of the solute front reached the probe depth. Furthermore it was assumed in the analytical solution, that molecular diffusion can be neglected for our experiment, as the pore water velocity was relatively high (De Smedt

and Wierenga, 1978). The analytical solution was fitted to the $CaCl_2$ data using a least square optimisation and is shown in Fig. 4.5 as the broken line. Values obtained for λ and R were 2.3 mm and 1.15 respectively, and are comparable to those values used in the numerical model. Hence we contend the numerical model is unlikely to be plagued by any large errors due to numerical dispersion. We are thus confident that our numerical model will work in the field, where transient water content effects may be longer lasting.

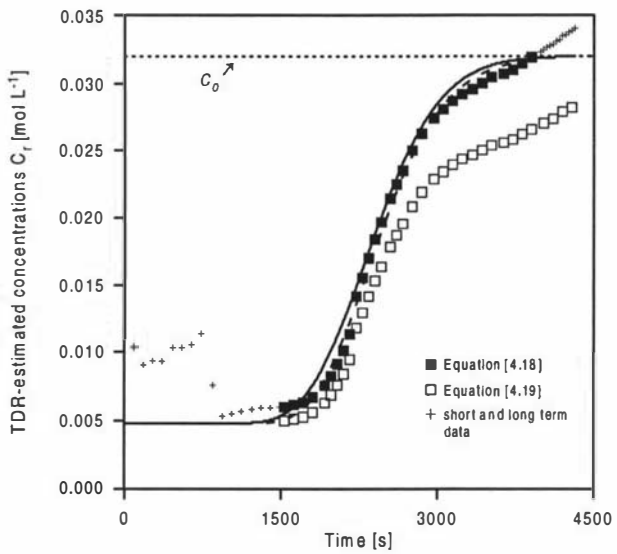

Fig. 4.5 The resident concentration estimated from the TDR-measured bulk soil electrical conductivity of the horizontally-installed probe during infiltration of KCl, using either Eq. [4.18] (□) or [4.19] (■). The fitted numerical solution of Eq. [4.4] is shown as the solid line and the analytical solution as the broken line. Also shown are short and long term data (+), which were not used for the fitting.

The rise in electrical conductivity of the soil solution (σ_w) for the vertically-installed TDR-probe is shown in Fig. 4.6. The gradual increase in σ_w is due to the fact that the TDR measures the average concentration over the entire 100 mm of the probe. Also shown in Fig. 4.6 are the predictions from the numerical model, assuming the soil solution contains either KCl (solid line) or $CaCl_2$ (broken line), again using the values of the transport parameters λ and R that were obtained from the horizontal probe. The predictions are based on the average concentration over the probe length, from which the average electrical conductivity of the pore water was then obtained, using either Eq.

[4.18] or [4.19], and assuming θ to be constant. As might be expected, the measured data first follow the expected behaviour of $CaCl_2$ (broken line), as the initial KCl soil solution would be dominated by the exchanged $CaCl_2$. However at later times the data approach the solid line for KCl, since at these longer times, more of the resident calcium is likely to have been leached beyond the probe depth.

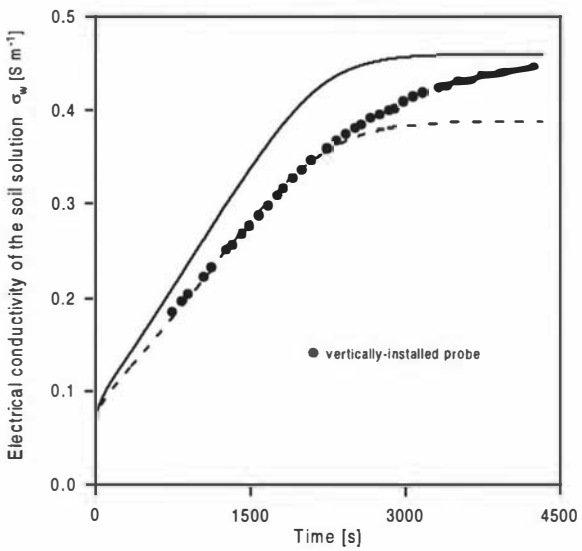

Fig. 4.6 The electrical conductivity of the soil solution calculated from the TDR-measured bulk soil electrical conductivity of the vertically-installed probe (●) during infiltration of KCl. The prediction from numerical solution of Eq. [4.4], assuming the soil solution to contain either $CaCl_2$ broken line) or KCl (solid line).

The reason for a retardation value R of 1.2, which implies a K_d of 0.143 L kg^{-1}, warrants further discussion. The Ramiha silt loam contains some allophanic material, and is therefore likely to have some positively-charged sites at the existing soil pH of 5.5. Therefore we would expect some chloride to be adsorbed onto anion exchange sites. Indeed, our measurements of chloride concentration in the soil solution extracted from soil samples taken at the end of the experiment indicated that some chloride had in fact been adsorbed. On average 13 % more chloride was present than would be expected if C_o was the concentration in the soil solution. However if another anion (e.g. nitrate or sulphate) were exchanged for the adsorbed chloride, there would be little effect on the electrical conductivity of the soil solution. This is because these anions have similar equivalent electrical conductivities (Weast, 1965). In contrast to miscible displacement studies where the actual chloride concentration is measured, the TDR technique would

not be able to detect the chloride adsorption and retardation. Only if the invading solution caused a change in the anion adsorption capacity (AEC) would the TDR electrical conductivity measurements detect any solute retardation. Thus independent measurements were made of the effect of the external solution concentration on the AEC of the Ramiha soil. The results are shown in Fig. 4.7.

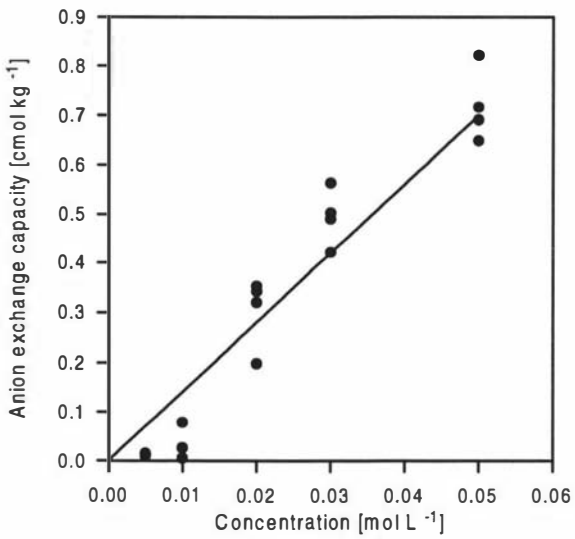

Fig. 4.7. The anion exchange capacity (●) measured for various concentrations of KCl in the soil solution. The solid line is the relationship between the anion exchange capacity and the external solute concentration with a slope of 0.14 L kg^{-1}.

Here it can be seen that the AEC is strongly dependent on soil solution concentration over the range of interest, namely 0.005 to 0.032 mol L^{-1}. Further the relationship, shown as the solid line in Fig. 4.7, is approximately linear, with a slope of 0.14 L kg^{-1}. Note that this is almost identical to the K_d value appropriate for an R value of 1.2.

4.2.6 Conclusions

The study has demonstrated that combining TDR and disc permeametry provides a useful tool for characterising water flow and chemical transport. The use of both vertically- and horizontally-installed TDR-probes can provide values for transport parameters as well as independent verification of these values. The importance of accurate measurement of θ is stressed, as this can have a large influence on the

calculation of the resident solute concentration. The dispersivity (λ) and the retardation (R) at the imposed pressure head of -50 mm were deduced to be 2.3 mm and 1.2, respectively.

In previous studies using TDR to measure solute movement in soil, it has been assumed that solute concentration is proportional to electrical conductivity. Any effects of cation or anion exchange on the TDR measurement of the soil electrical conductivity have been ignored. We have shown here how important these effects can be. When KCl was applied, even when enough solution had been added to the soil to make the chloride concentration in the soil solution similar to that in the applied solution, exchange of K^+ with Ca^{2+} was the apparent cause of the electrical conductivity of the soil solution being quite different to that of the applied solution.

This finding has a number of implications. One is that it is important that actual soil solution extracts be used when the TDR technique is being calibrated for soil solution electrical conductivity measurements. Another implication is that when the TDR is being used to measure solute movement in soil, cation (and sometimes anion) exchange needs to be taken into account. Preleaching with a calcium salt solution may therefore sometimes be appropriate. Alternatively, if the cation exchange sites are already calcium dominated, a calcium salt should be used as the tracer when solute movement parameters are being measured.

The method need not be restricted to laboratory studies as we have applied here. It should be possible to determine *in situ* not only the hydraulic properties that control infiltration, but also the chemical transport characteristics that determine the distribution of the associated solutes. We plan to carry out further investigations in the field using free-standing undisturbed pedestals that have been specially excavated to accept a disk permeameter on top. Here water and solute movement can be simply described one-dimensionally. Vertically- and horizontally-placed TDR-probes will again be used. Since water movement from the disk, will be transient, the numerical model will again be needed for the inverse simulation of the chemical transport properties.

Acknowledgments

The authors gratefully acknowledge the help provided by Dr.G.N. Magesan of Manaaki Whenua Landcare Research, Hamilton, and Nobiru Kozai, Kumamoto Prefectural Research Station, Japan. This research was funded by FRST contract CO9227.

4.3 TDR and Undisturbed Soil Columns of Manawatu Fine Sandy Loam

As a next step the use of TDR in combination with disk permeametry was assessed using undisturbed soil columns of Manawatu fine sandy loam. The experimental setup was the same as described in Section 5.2, except that one of the TDR probes was installed vertically through the disk permeameter as described in Section 4.2. Highly preferential flow of the applied chloride solution was observed in the effluent, as well as by TDR. Although the TDR probes were inserted into predrilled holes, vertical cracks might have developed during their insertion. Significant preferential flow is expected only in continuous vertical channels, which are at least 0.2 mm in diameter, or cracks of least 0.1 mm width and at pressure potentials above -150 mm (Scotter, 1978). As the solution was applied via a disk permeameter set to a pressure potential of -50 mm, cracks might be the reason for the observed preferential flow. Another possibility is preferential flow along the vertical probe (Zeglin *et al.*, 1992).

These results show that care must be taken when using vertically installed TDR probes in undisturbed soil columns. Often, insertion without significant side-effects may be difficult.

4.4 TDR Estimation of the Resident Concentration of Electrolyte in the Soil Solution

by Iris Vogeler , Brent E. Clothier , and Steven R. Green

From *Australian Journal of Soil Research*, 1997, 35, xx.

4.4.1 Abstract

In order to examine whether the electrolyte concentration in the soil solution can be estimated by TDR-measured bulk soil electrical conductivity, column leaching experiments were performed using undisturbed soil columns during unsaturated steady-state water flow. The leaching experiments were carried out on two soils with contrasting pedological structure. One was the strongly structured Ramiha silt loam, and the other the weakly structured Manawatu fine sandy loam. Transport parameters obtained from the effluent data were used to predict the transient pattern in the resident electrolyte concentration measured by TDR. The electrolyte concentration was inferred from the TDR-measured bulk soil electrical conductivity using two different calibration approaches; that resulting from continuous solute application, and the other by direct calibration. Prior to these, calibration on repacked soil columns related TDR measurements to both the volumetric water content, and the electrolyte concentration that is resident in the soil solution. The former calibration technique could be used successfully to describe solute transport in both soils, but without predicting the absolute levels of solute. The direct calibration method only provided good estimates of the resident concentration, or electrolyte concentration, in the strongly structured top layer of the Ramiha soil. This soil possessed no immobile water. For the less-structured layer of the Ramiha, and the weakly structured Manawatu soil, only crude approximations of the solute concentration in the soil were found, with measurement errors of up to 50%. The small-scale pattern of electrolyte movement of these weakly-structured soils appears quite complex.

Keywords: TDR calibration, solute transport, resident concentration, soil water content, soil structure.

4.4.2 Introduction

Time Domain Reflectometry (TDR) is a relatively new technique that possesses potential for studying solute transport through the soil (Kachanoski *et al.*, 1992; Wraith *et al.*, 1993; Vanclooster *et al.*, 1993, 1995). This technique relies on the measurement of the impedance (Z_L), or bulk soil electrical conductivity (σ), which can be related by calibration to the solute resident concentration (C_r). TDR calibration has been the prime topic of many studies, and it is already well known that the volumetric water content (θ), the electrical conductivity of the soil solution (σ_w), the surface conductance (σ_s), as well as the bulk density, and the soil temperature affect the TDR-measured bulk soil electrical conductivity. However, the overall effect of these various factors on σ, as measured by resistivity techniques, is not yet fully understood. Various approaches have been adopted to relate σ and C_r. These have been discussed in detail by Mallants *et al.* (1994; 1996), and Ward *et al.* (1994). Here only the direct calibration, using both repacked and undisturbed soil columns, and the continuous solute application approach are described. Both have potential to measure solute transport through undisturbed soil columns in the laboratory, and also directly in the field.

In the direct calibration approach, the TDR-measured impedance (Z_L) - or bulk soil electrical conductivity (σ) - is related to the concentration of the soil solution (σ_w) and the water content (θ). The calibration is generally performed on homogeneously repacked soil columns, in which both the soil structure and pore size distribution are disturbed. This change in structure and pore tortuosity is likely to affect the calibration function (Rhoades *et al.*, 1976; Nadler, 1981). Nadler (1991), however, found the effect of structural disturbance on σ-σ_w relations to be small. Briefly, soil samples are equilibrated to various water contents using different solution concentrations. Once a relation between σ, σ_w, and θ has been found, it should in theory be possible to study solute transport *in situ* under transient conditions. The first such direct calibration was presented by Rhoades *et al.* (1976). They used a four-electrode resistance technique. The calibration approach was based on a constant surface conductivity, a linear relationship between σ and σ_w, plus a tortuosity factor. However several investigators have found a dependency of the surface conductance on salt concentration and water

content (Cremers *et al.*, 1966; Nadler, 1981; Ward *et al.*, 1994). The latter was incorporated in our previous calibration (Section 4.2), and has also been discussed by Mallants *et al.* (1996).

Another approach involves a continuous solute application, by which solute is applied until a constant σ is reached. This asymptote is, in the absence of other information, then simply equated to the input concentration C_o. Thus it is assumed that the solute has spread uniformly throughout the soil. But in soils with immobile water, the equilibration time between the two water domains might be long, so that application of this method would require a long solute application time (Mallants *et al.*, 1996). However several experimental studies have used this continuous solute application method with TDR to obtain solute transport parameters from leaching experiments (Mallants *et al.*, 1994; Section 5.2). The approach is however restricted to steady-state conditions. In the field, water and solute transport are often transient in nature. This then makes the direct calibration method more suited for studying solute transport at the field scale, despite its attendant problems.

The purpose of this study was to determine if the electrolyte concentration in the soil solution could be estimated from the σ measured by TDR, as based on the direct calibration approach. Furthermore we compared various calibration approaches to monitor by TDR solute transport through undisturbed soil columns under unsaturated steady-state water flow. Two structurally different soils were studied: the Manawatu fine sandy loam, a soil classed by pedologists as being weakly structured, and the Ramiha silt loam, a soil classed as being strongly aggregated (Cowie, 1978; Pollok, 1975).

4.4.3 Theory

The theory for monitoring solute transport by Time Domain Reflectometry has already been reviewed in detail in Section 4.2, amongst others, so only salient features are repeated here. Briefly, the estimation of the solute resident concentration by TDR is based on the measurement of the dielectric constant (ε) and the impedance (Z_L) of the

soil. The dielectric constant can be used to calculate the volumetric water content (θ), using either the so-called "universal" relationship found by Topp *et al.* (1980), or by specific calibration. The impedance can be related to the bulk soil electrical conductivity by (Nadler *et al.*, 1991)

$$\sigma = K_G \, Z_L^{-1} \, f_c \, . \qquad [4.20]$$

Here K_G is a geometric probe constant which has been previously determined (Section 4.2), and f_c is a temperature-correction coefficient (see Table 15, U.S. Salinity Laboratory Staff, 1954).

4.4.4 Materials and Methods

The TDR used for the experiments was a 1502 C Tektronix cable tester (Tektronix, Beaverton, OR). Three-rod probes of length of 100 mm, diameters of 2 mm, and spacing between the center and outer rods of 12.5 mm, were used for all measurements. The probes were connected, via a 50 Ω coaxial cable and a multiplexer, to the cable tester. The cable tester was controlled by a laptop computer which automatically analysed for water content and bulk soil electrical conductivity.

Two soils with contrasting pedological structure were studied. One was the alluvial Manawatu fine sandy loam (a Dystric Fluventic Eutrochrept), a weakly structured soil. The other was the aeolian Ramiha silt loam (an Andic Dystrochrept), a strongly aggregated soil with variable charge due to volcanic ash addition. Description of both soils are given in Clothier *et al.* (1996). The Manawatu soil was taken from the herbicide strip in the Massey University Orchard. The Ramiha soil was taken under pasture. For each soil, two free-standing soil columns were carved from the soil profiles after removing the top 20 mm. These will be referred to as column A and B for the Manawatu soil, and column C and D for the Ramiha soil. Additional soil samples were taken for the calibration measurements.

The apparatus used for the leaching experiments on the intact columns has already been described in detail by Magesan *et al.* (1995), and the experimental procedure for the leaching experiments on the Manawatu soil is described in Section 5.2. Briefly, free standing soil columns were carved from the soil profile after removing the top 20 mm. Disk permeameters were used to apply first a solution of 0.0025 *M* $Ca(NO_3)_2$, and then a solution of about 0.025 *M* $MgCl_2$ to the columns. The preleaching with $Ca(NO_3)_2$ ensured steady state water flow and an uniform initial electrolyte concentration of the soil solution. These two salts were chosen because at the same concentration they have similar electrical conductivities (Robinson and Stokes, 1959). The concentrations were chosen to avoid nonlinearity with respect to C_r, which has been found for both low and high concentrations (Nadler and Frenkel, 1980; Ward *et al.*, 1994).

Table 4.1 Column data and model parameters obtained from the CDE.

Probe #	depth [mm]	θ [m^3 m^{-3}]	λ [mm]	R
Column A, Manawatu fine sandy loam, l = 340 mm				
1	190	0.402	38	1
2	290	0.370	38	1
Column B, Manawatu fine sandy loam, l = 295 mm				
3	140	0.438	36	1
Column C, Ramiha silt loam, l = 310 mm				
5	50	0.570	16	1.16
6	260	0.560	16	1.16
Column D, Ramiha silt loam, l = 270 mm				
7	50	0.576	23	1.19
8	220	0.590	23	1.19

l = length, λ = dispersivity, R = retardation factor

For the Manawatu soil the disk permeameters were set to a pressure potential head of -70 mm, which resulted in average flow rates of about 3 mm h^{-1}. To obtain similar flow rates the pressure potential head for the Ramiha soil was kept at -100 mm. The column length and water contents for the various columns are given in Table 4.1. Leaching with $MgCl_2$ for the Manawatu soil was continuous, but for the Ramiha soil leaching was interrupted after 36 h, and restarted again after a 12 h pause. As the Ramiha soil is a fully-mobile water soil, the pause in leaching was assumed to have, apart from some vertical redistribution within the soil column, no effect on solute transport. Solute transport was monitored by collecting the effluent at the bottom of the columns, and by

TDR probes inserted horizontally into the soil columns. Two probes were inserted into each column, the depths and probe numbers are given in Table 4.1.

Solute transport was modelled using the convection dispersion equation (CDE), and the solutions given by van Genuchten and Wierenga (1986) for flux concentrations (their A1), for the effluent, and resident concentrations (their A2) for the TDR data.

4.4.4.1 TDR Calibration

The calibration procedure for the Ramiha silt loam calibration has already been described in Section 4.2. Air dried, sieved soil (<2 mm) was stepwise brought to water contents ranging from 0.3 to 0.6 using KCl solutions of 0.01, 0.03, and 0.05 *M*. At each water content the soil was packed, at a bulk density of 0.84 Mg m^{-3}, into acrylic columns with a height of 250 mm and a diameter of 120 mm. The dielectric constant and the electrical impedance of the soil was measured by three-rod TDR probes inserted horizontally into these soil columns. After measurement, the water content was determined gravimetrically, as well as the electrical conductivity of the pore water by high speed centrifuging, and measurement of the electrical conductivity of the supernatant using a conductivity meter. The same procedure was now used for the calibration of the Manawatu fine sandy loam, but the soil was packed to a bulk density of 1.35 Mg m^{-3}, and only two concentrations, 0.005 and 0.025 *M* $MgCl_2$ and two water contents of 0.35 and 0.45 were used. The leaching experiments were performed in the same concentration range as the calibrations.

Additionally, calibration measurements for the Manawatu soil were carried out on undisturbed soil columns. Steel cylinders, 110 mm high and 100 mm in diameter, were used to enclose undisturbed pedestals of soil from adjacent to where the soil columns were taken for the leaching experiment. The metal of the cylinders did not have an effect on the TDR readings. The undisturbed soil cores were taken into the laboratory and wetted by capillary rise using again the two solutions of 0.005 and 0.025 *M* $MgCl_2$. After wetting, the samples were left to equilibrate in a pressure apparatus using two different pressures of 30 mbar and 2 bar. For each combination of concentration-

pressure, 4 replicate columns were used. For measuring ε and σ the TDR probes were installed vertically from the top. For each combination, duplicate measurements were made, giving 32 measurements in total. Again the gravimetric water content and the electrical conductivity of the pore water were determined, but only a single cylindrical soil sample around the probes was used.

4.4.5 Results

4.4.5.1 Water Content Calibration

The calibration curve for the ε-θ relationship for the Ramiha silt loam has already been given in section 4.2. Due to the high organic matter content and the low bulk density of 0.84 Mg/m^3 for this soil, a deviation of about + 0.1 m^3 m^{-3} was found between the relationship found and the curve suggested by Topp *et al.* (1980). For the Manawatu fine sandy loam, with a bulk density of 1.35 Mg m^{-3}, the relationship of Topp *et al.* (1980) was found to be adequate for the range $0.05 \leq \theta \leq 0.46$ m^3 m^{-3}. The maximum deviation was just 0.024 m^3 m^{-3}.

4.4.5.2 Solute Concentration Calibration

The relationship between the bulk soil electrical conductivity, the water content, and the electrical conductivity of the soil solution of repacked Ramiha soil was in Section 4.2 to be capable of description by,

$$\sigma_w = \frac{\sigma - (a\,\theta - b)}{(c\,\theta - d)}. \qquad [4.21]$$

where a, b, c, and d are constants.

The results, using the same approach for the Manawatu soil are shown in Fig. 4.8. Both the measurements obtained from the disturbed soil column (squares), and the undisturbed columns (circles) are given. Also shown are the standard deviations

(vertical bars) from the measurements on the disturbed soil columns. The water content in the undisturbed soil columns ranged from about 0.41 to 0.47 $m^3\ m^{-3}$, but only those samples of either 0.42 or 0.44 $m^3\ m^{-3}$ ($\pm$ 0.007) were used for the solute calibration. This resulted in 10 and 6 measurements for the two water contents. Linear relationships between σ and σ_w were found for the disturbed soil, and were assumed for the undisturbed soil columns at each water content. These relationships are shown on Fig.4.8. Using the same approach as described in Section 4.2 a relationship of the form of Eq. [4.21] was found between σ, σ_w, and θ for both the disturbed soil columns, and the undisturbed soil columns. As the values of a, b, c, and d in Eq. [4.21] are unique to each soil they are not explicitly given here.

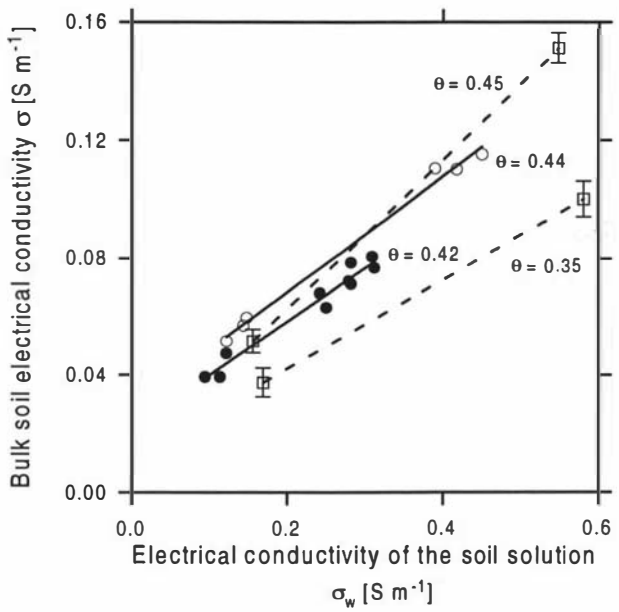

Fig. 4.8 TDR-measured bulk soil electrical conductivity vs. electrical conductivity of the soil solution measured with a conductivity meter for different water contents for Manawatu fine sandy loam using disturbed (❑) and undisturbed (○,●) soil columns. Also shown is the standard deviation (vertical bars) and fitted relationship (solid and broken lines).

The solute concentration, C, [mol l^{-1}] for $MgCl_2$ solution at concentrations ranging from 0.005 to 0.025 M can then be calculated from σ_w [S $m.^{-1}$] using data from Weast (1965) as

$$C = -1.3 \times 10^{-3} + 9.9 \times 10^{-2} \sigma_w . \qquad [4.22]$$

4.4.5.3 Leaching Experiments

Manawatu: The results of the leaching experiments on Manawatu fine sandy loam are described in Section 5.2. The effluent data were used to obtain parameters for the convection-dispersion equation of solute transport. The values for the dispersivity were 36 and 38 mm for Column A and Column B. These were then used to predict the resident concentrations of chloride (C_r) that should be measured using the continuous solute application method. Only one of the probes in Column B could be used as, for unknown reasons, the other gave unrealistically high measurements of the impedance. The results from the other probes are shown in Fig. 4.9. The agreement between the simulation and the TDR-inferred solute concentration, using the continuous solute application method, is good except for probe 2. Considering that the TDR measures only a small volume around the probe, whereas the effluent averages the concentration over the total area studied, this agreement is nonetheless heartening. Any variations in water content or salt concentration in the cross section can have an effect on TDR measured σ. However considerable replications would overcome this problem.

Also shown in Fig. 4.9 are the TDR-estimated relative concentrations of chloride using equation [4.21] and [4.22], with the constants found either from the calibration on repacked or undisturbed media. For column A, the C_r estimated from the calibration on disturbed soil (open squares) are higher than the input concentration, by up to about 50% for probe 3. These deviations could be due to a different soil structure or pore size distribution from that in the disturbed soil columns used for calibration, or perhaps due to small variations in probe soil contact. Furthermore, the C_r calculated from the relation for the undisturbed soil columns (open circles), are even higher. This could be due to the lower water content in this column compared to that used for the calibration (Table 4.1). Extrapolating the linear relationship found at θ of 0.42 and 0.44 $m^3\ m^{-3}$ might not have been appropriate. The overestimation of σ_w might hence be due to the assumption of linearity outside the calibration range. Yet for the probe in column B, the agreement between the prediction from the effluent and the TDR-estimated concentration is reasonable, whether using calibration on undisturbed or repacked media. We note that this soil column had a water content of 0.438, which is within the

range used in the calibration with undisturbed soil columns. Although the good agreement between TDR-estimated C_r and the prediction in column B might only be fortuitous, it seems that TDR can be used to measure solute resident concentrations, provided that calibrations have been carried out on undisturbed soil samples, and were within the water content and σ_w range.

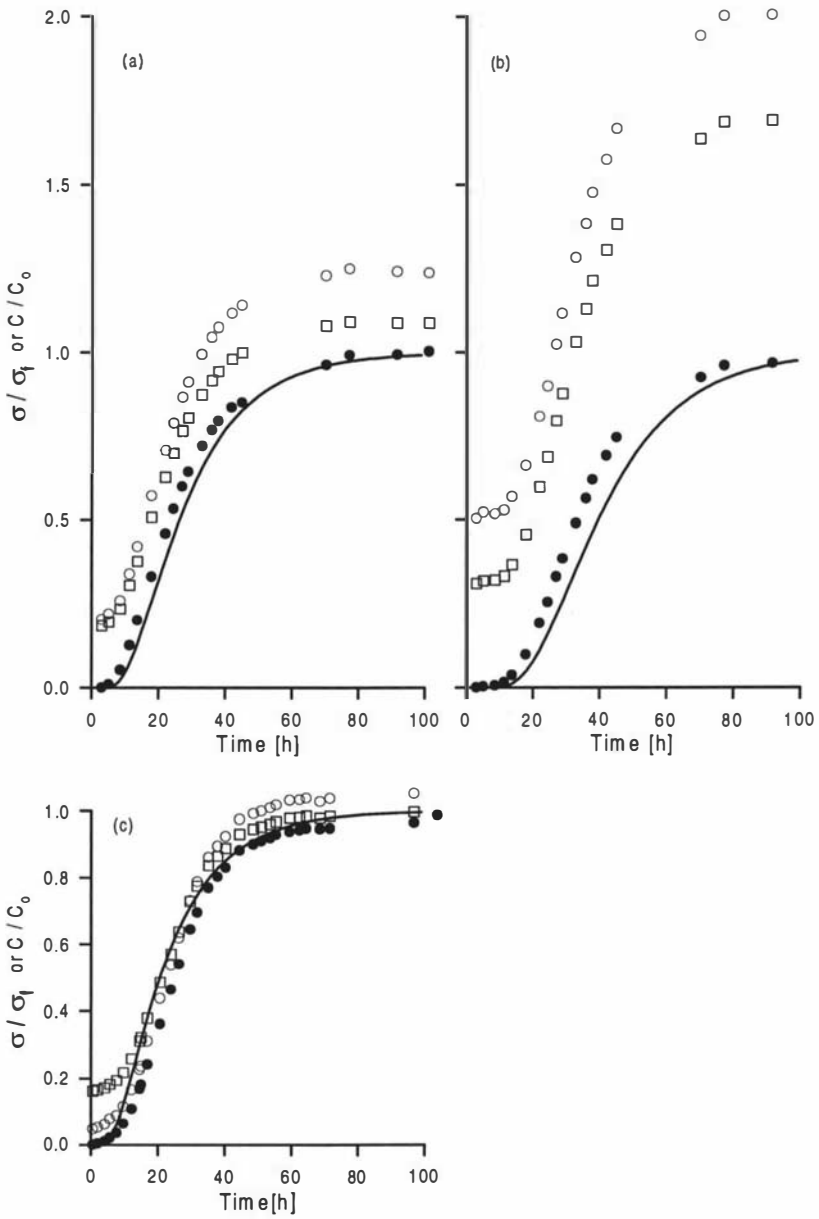

Fig. 4.9 Normalised bulk soil electrical conductivity as measured by TDR (●) and simulated curves (solid lines) for column A: (a) probe 1, (b) probe 2, and column B: (c) probe 3. Also shown are the normalised resident concentrations calculated from TDR measurements, and using Eq. [4.21] with values obtained from measurements on disturbed (□) or undisturbed columns (○), and Eq. [4.22].

Ramiha: The normalised effluent concentrations of chloride from the Ramiha soil in columns C and D, are shown in Fig. 4.10, together with the fits to the CDE. Dispersivities of 16 and 23 mm and were found for the two columns. Furthermore, a linearised retardation for the chloride of about 1.2 was obtained. This reaction is consistent with the value given in section 4.2, and is due to positively charged exchange sites at a pH of 5.5. The anion exchange capacity increases with a rise in the electrolyte concentration of the soil solution, such that the TDR should also detect this retardation.

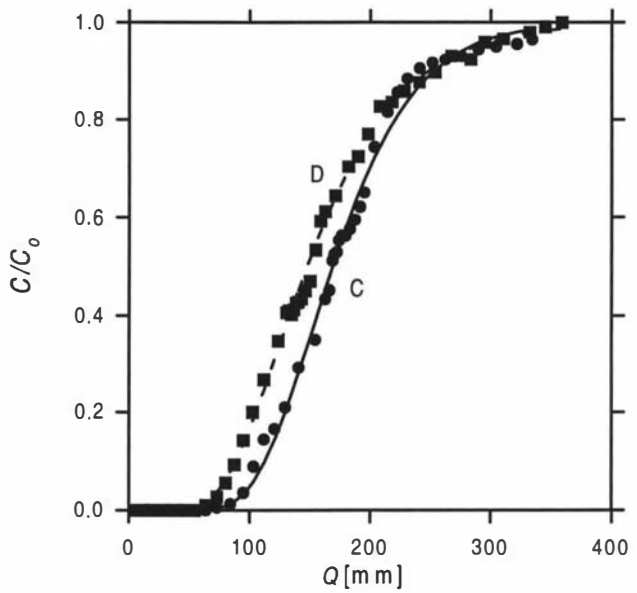

Fig. 4.10 Normalised anion breakthrough data and fitted curves using the CDE for column C (● and solid line) and column D (■ and broken line).

The dispersivities and the retardation factor so found, were now used to predict the resident concentration, again using the CDE, as should be measured by the TDR probes. The results are shown in Fig. 4.11. The somewhat minor variation in σ measured by probe 5 and 7 could be due to the decrease in water content of 0.028 and 0.017 $m^3\ m^{-3}$ close to the soil surface after interruption of leaching. For the lower probes the water content remained constant. Using the continuous solute application method, the agreement between the prediction and the measurements is again good for all 4 probes. The water content calculated from the TDR calibration on repacked columns (eq. [4.16]) were consistently 0.05 $m^3\ m^{-3}$ higher than the gravimetrically determined ones (Table 4.1). This could simply be due to a slightly higher mean bulk density (ρ_b) of 0.89 Mg m^{-3} found for the columns, compared to the calibration which was performed at a ρ_b of

0.84 Mg m^{-3}. This shows that the calibration curve is highly sensitive to ρ_b, and again stresses the need for care when using TDR calibration procedures. Consequently to calculate the normalised solute resident concentrations (C_r) the gravimetrically determined θ were used with Eq [4.21] and [4.22]. These are shown in Fig. 4.11 as the open squares.

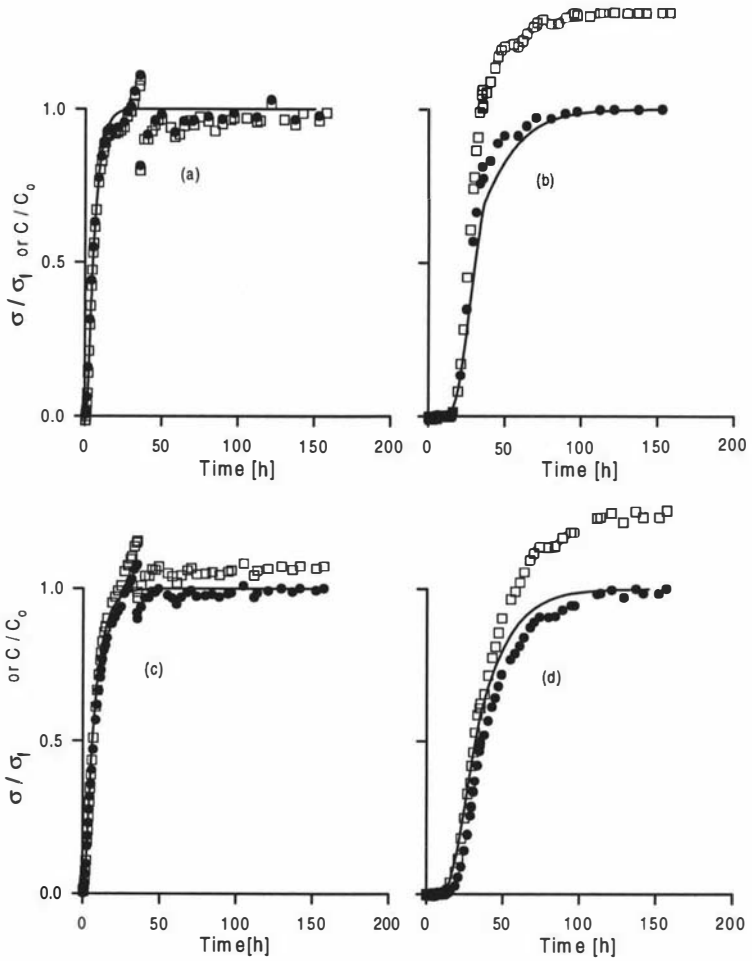

Fig. 4.11 Normalised bulk soil electrical conductivity as measured by TDR (●) and simulated curves (solid lines) for column C: (a) probe 5, (b) probe 6, and column D: (c) probe 7, and (d) probe 8. Also shown are the normalised resident concentrations calculated from TDR measurements, and using [4.21] and [4.22] (□).

The agreement between the prediction is good just for the two probes installed at 50 mm (probes 5 and 7), considering that θ changes due to interruption of leaching were ignored. For the two other probes installed at 260 and 220 mm, the calculated C_r is again far too high. This is again likely to be due to the local sensitivity of the TDR-

measured impedance or bulk soil electrical conductivity to soil structure, and perhaps bulk density immediately adjacent to the probe-rods. Both increase with depth. The structure of the Ramiha silt loam changes at a depth of 80 mm. The soil changes from strongly to medium developed aggregates, and the organic matter content decreases (Pollok, 1975). These changes in the soil profile are considered to explain the good agreement found for the upper probes, and the discrepancies found for the lower probes. The strongly developed structure in the top 80 mm appears to behave, in a electrolytic sense, similarly to a repacked soil. However the weaker pedological structure of the deeper profile apparently has quite an effect on the TDR-measured σ.

4.4.6 Conclusions

The TDR has been shown to be useful in estimating solute transport parameters, but only when the relative bulk soil electrical conductivity was used in the continuous solute application approach.

For two soils with contrasting pedological structure, the continuous solute application method performed well. However a drawback of this method is the need to ensure a constant water content and steady state flow. In the field however the water content is generally variable both in time and space. A further drawback is that this method does not provide an independent measure of the final resident concentration. Hence it is not possible to use the asymptotic values of C_r to infer anything about the degree of mobility of soil water. The success with the continuous solute application method, indicates that in some practical applications such a crude estimation might be sufficient. But for accurate predictions of resident concentrations, and solute transport under transient water flow further studies are needed on the various and local heterogeneities on TDR-measured σ and σ-σ_w-θ relationships. Separate calibrations for each layer might well always be necessary.

Caution has to be exercised when estimating electrolyte levels in the soil solution from TDR-measured σ using σ-σ_w-θ relationships obtained from disturbed soil columns.

Whereas this direct-calibration approach was found appropriate for the strongly aggregated layer of the surface Ramiha silt loam, it overestimated the resident concentrations in the less structured lower profile of the Ramiha soil. Also it failed to perform in the weakly structured Manawatu fine sandy loam. In a study on undisturbed saturated soil columns Mallants *et al.* (1996) also found that the reference impedance was underpredicted by 50% when using the direct calibration approach, based on independent calibration measurements in repacked soil columns.

Our results suggest a high sensitivity of the TDR-measured bulk soil electrical conductivity to the local soil structure, texture, and perhaps bulk density immediately surrounding the probes, and to the probe-soil contact. Similar findings were made by Vanclooster *et al.* (1995). In their study of solute transport through 1 m long monoliths they had to calibrate each probe separately. This was, in their case, attributed to changes in soil chemical properties within the soil profile.

It is interesting to note again that soils of weak pedological structure, *e.g.* the Manawatu, display quite complex hydraulic functioning (Clothier *et al.*, 1995). In contrast, soils of strongly developed structure, *e.g.* the Ramiha, can exhibit quite simple hydraulic functioning that is amenable to straight forward analysis (Clothier *et al.*, 1996). The TDR procedures used here reinforce the contrast between pedological structure and hydraulic functioning.

Acknowledgments

We thank Dave Scotter (Massey University, Palmerston North) for assisting with the experiments, and Arie Nadler (The Volcani Center, Institute of Soil and Water, Bet Dagan 50250, Israel) for helpful comments. This research was supported by the NSOF 96-170 "Partitioning of rootzone chemical into either uptake or despatch".

4.5 Overall Conclusions

The TDR method has been shown useful for monitoring solute transport through a repacked soil column under transient water flow (Section 4.2). Direct calibration was used, which related the TDR-measured impedance at various water contents to the pore water electrical conductivity in undisturbed soil columns. TDR probes installed both horizontally-and vertically ~~installed TDR-probes~~ were used successful. Furthermore the experiment demonstrated the effect of cation exchange reactions on the TDR-measured bulk soil electrical conductivity. This is important when the infiltrating solution is composed of cations different to those dominanting the exchange sites. In this case exchange reactions altered the electrical conductivity of the soil solution, which had a large effect on the TDR inferred solute transport parameters. The behaviour of chloride was simulated by coupling the water flow equation with the convection-dispersion equation. However the simulations were only reasonable when appropriate assumptions concerning the accompanying cation were made.

When TDR probes were installed vertically into undisturbed soil columns, highly preferential flow was observed. This probably resulted from cracks, which developed during their insertion. This demonstrates that, in some situations using vertically installed TDR probes in the field to monitor solute transport can lead to erroneous results.

In undisturbed soil columns of two contrasting soils, TDR only proved useful for monitoring solute transport if the continuous solute application approach was used (Section 4.4). However, this approach is limited to steady-state water flow, and problems arise in soils with mobile/immobile water fractions. Solute concentrations inferred from the TDR measured bulk soil electrical conductivity, and using the direct calibration approach, overestimated the resident concentrations in most cases. This was probably due to the high sensitivity of TDR measurements to soil structure, and bulk density immediately adjacent to the probe wires.

In conclusion, the TDR technique for monitoring solute transport in undisturbed soils has several problems associated with it. These include the effect of the soil structure, bulk density and the composition of the soil solution on TDR measured dielectric constant and impedance. Furthermore TDR measures only the total ionic concentration of the soil solution, not that of the individual ions. The technique seems therefore unsuitable for studying transport and exchange of reactive solutes.

Under steady-state water flow, the TDR-technique seems to be a valuable tool for determining solute transport parameters in undisturbed soil columns, as well as in the field. The use of TDR to monitor solute movement under transient water flow is hampered by a good understanding on how the TDR-measured impedance is influenced by soil structure and bulk density. But the continuous application method could overcome this, if some independent measure were made of the final concentration.

Chapter 5

5. Anion Movement Through Unsaturated Soil

5.1 Introduction

In Chapter 2 various approaches to characterise solute transport have been described and compared. It was concluded that the convection dispersion equation (CDE) seems a promising model to describe solute transport during unsaturated flow, but it still needs further testing. Apart from being relatively simple, transient water flow, as well as ion adsorption and exchange can be easily incorporated into the CDE. The leaching experiments described in this chapter were performed to test the ability of the CDE to describe anion movement under various water flow regimes. Also considered is the mobile/immobile water approach. Furthermore, the effect of the initial soil water and the vegetation on solute transport was studied.

In the previous Chapter, the TDR technique for studying solute transport through repacked and undisturbed soil columns was described. It was concluded that considerable replication of TDR instrumentation is needed to accurately describe solute transport, and there were certain problems with calibration. In this Chapter the more conventional method of using outflow breakthrough curves (BTC) to monitor solute movement is described for the same undisturbed soil columns. By using the BTC, average solute transport parameters over the entire soil column are obtained. These would be more spatially representative for solute transport compared to local measurements obtained by TDR probes. Furthermore, by collecting and analysing soil solution samples, solute exchange reactions between the soil solution and the soil matrix can be studied. These cannot be detected by TDR. The use of suction cups to study solute transport is also assessed.

The first paper describes leaching experiments on undisturbed soil columns of Manawatu fine sandy loam under a bare soil surface. These experiments were carried out to examine the effect of the water flow velocity on solute dispersion, and to test the validity of assuming a velocity invariant dispersivity. The second paper describes

leaching experiments performed on the same soil, but now under pasture. The effect of a short pasture, as well as that of the initial water content on solute transport is investigated. For these experiments a rainfall simulator was built. A picture of the experimental setup for the experiments described in Section 5.3 is shown in Fig. 5.1. Finally the approach of Bolt (1982) for describing dispersion, discussed in Section 2.5.3, is tested using the model parameters of the CDE and the MIM obtained from the various experiments.

The computer programs used in Section 5.2 were written in QuickBASIC, and are described in Appendix A. Examples of the various programs used in the following experiments are given in Appendix B, Programs 1-3. The computer program used in Section 5.3 was written in FORTRAN, and the solution was based on the Crank-Nicholson finited-difference scheme, which is described in detail in the 'WAVE' model by Vanclooster *et al.* (1994).

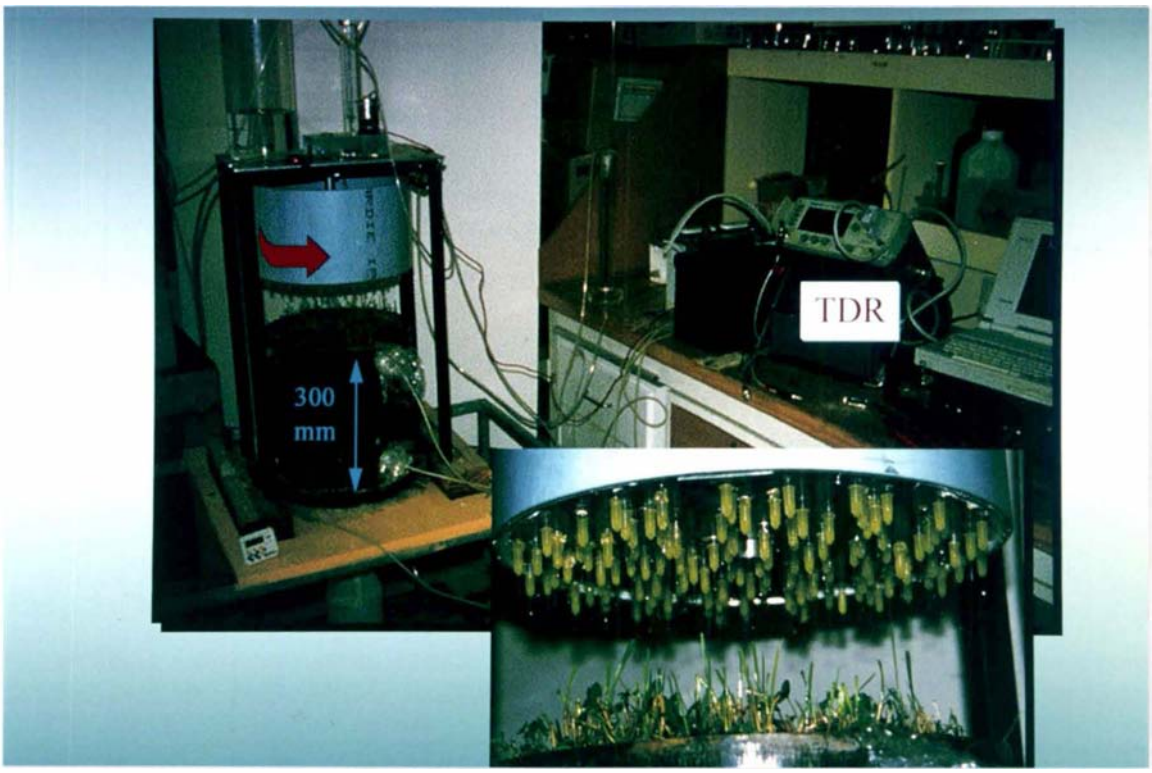

Fig. 5.1 Experimental setup for the experiments described in Section 5.3.

5.2 Anion Transport Through Intact Soil Columns During Intermittent Unsaturated Flow

by Iris Vogeler, David R. Scotter, Brent E. Clothier, and Russel W. Tillman

From *Soil Technology*, in press

5.2.1 Abstract

To assess the effect of varying water flow velocities on solute transport, leaching experiments were conducted on undisturbed soil columns of Manawatu fine sandy loam. A leaching apparatus, applying pressure heads of -80 mm or -3 mm to both ends of the columns, was used to infiltrate solutions of either $MgCl_2$, or $Ca(NO_3)_2$, at water flow rates of either 3 or 13 mm h^{-1}. Intermittent rainfall events were simulated by performing 3 consecutive unsaturated leaching events with no-flow periods interspersed. Solute transport was monitored by collecting effluent, and using suction cups and Time Domain Reflectometry. The convection-dispersion equation was found to simulate the anion breakthrough-curves well except for the short term concentration discontinuities observed when flow resumed after an interruption. Dispersivities obtained with the different measurement techniques and the two contrasting flow rates were similar, with values between 25 and 59 mm. A 10% difference between the flux and final resident concentrations was found, even after 1000 mm of infiltration over 13 days, attributable to anion exclusion from the double layer water of about 0.04 m^3 m^{-3}. The discontinuity after flow interruption could be simulated reasonably well using the mobile/immobile model with three different soil water domains assumed: "mobile", "immobile", and "exclusion".

5.2.2 Introduction

Practical relevance, combined with an unease concerning our present understanding, motivates research on solute movement through structured soil. At a microscopic level we know how convection and molecular diffusion can move water-borne solutes through soil. We know that the local interaction between these two processes produces what we call

hydrodynamic dispersion. But these microscopic insights are of limited value when we ask how a certain Darcy flux density of water might move a certain solute through a given soil.

Traditionally measurement of solute flow has involved either soil sampling, or the use of suction cups. Soil sampling is tedious and destructive. With suction cups one is not sure what mix of flux and resident concentration is being measured. The more recent advent of time domain reflectometry (TDR) avoids these two problems, but has other limitations associated with it, *e.g.* the small sampling volume, and the restriction to steady-state water flow. Here we describe unsaturated experiments on intact soil columns in which we realise measurement of anion and cation transport by TDR and suction cups, and by sampling effluent at the end of the column. These experiments allowed the assessment of suction cups and TDR as techniques for characterising solute flow in intact soil at realistic flow rates.

Most theoretical descriptions of solute flow involve the convection-dispersion equation (CDE), although other models, such as the stochastic-convective model of Jury (1982) have been used successfully to describe solute transport at the field scale. The CDE has often been found inadequate in structured soils under saturated flow conditions. In the field, however, such flow conditions are rare, especially in the more permeable macropore-hidden soils that are used for agriculture and water disposal. More common is unsaturated flow. Further testing of the CDE under such flow conditions is thus warranted. Seyfried and Rao (1987); Jardine *et al.* (1993); and Magesan *et al.* (1995) provide some experimental justification for the validity of the CDE under unsaturated flow conditions, but not for intermittent flow at different rates.

Where the CDE has been found inadequate the mobile-immobile model (van Genuchten and Wierenga, 1976) has often been used, where the soil water is arbitrarily divided into a mobile and a immobile fraction. This has sometimes resulted in significant improvements in modeling experimental laboratory and field studies of steady state and intermittent leaching events (Nkedi-Kizza *et al.*, 1983, Tillman *et al.*, 1991b). However

quantification of the separation between mobile and immobile water and solute transfer between these two domains merits further investigation (Clothier *et al.*, 1995).

Described here is a study conducted in the laboratory using intact columns of soil brought from the field to the laboratory. This approach allowed all the effluent moving though the soil to be collected at the base. Better control of the experimental conditions was possible than can be achieved in the field. The objective of the study was to assess the effect of various flow rates and intermittent leaching events on the transport and redistribution of inert solutes within the soil. To obtain the unsaturated water flows, pressure heads of either -80 mm or -3 mm were maintained at both ends of the columns. This resulted in steady water flows of about 3 and 13 mm h^{-1}. Redistribution of solute during intermittent rainfall events was simulated by performing three consecutive leaching events, with no-inflow periods between these of 12 hours and 7 days. We test the ability of the CDE, and the mobile/immobile model, to simulate these different leaching events. This paper describes the movement of anions. A later paper will describe the more complex cation transport under the same flow regimes.

5.2.3 Theory

Consider steady-state, one dimensional water flow through a uniform soil, as well as the transport of a conservative non-reactive solute being carried with that water. The CDE is then usually written (e.g. van Genuchten and Wierenga, 1986)

$$\frac{\partial C_f}{\partial t} = D_s \frac{\partial^2 C_f}{\partial z^2} - v \frac{\partial C_f}{\partial z} \qquad [5.1]$$

where C_f is the flux concentration in the soil solution [mol m^{-3}], t is time [s], z is depth [m], D_s is the dispersion coefficient [m^2 s^{-1}] and v is the average pore water velocity defined here as q_w/θ_e, where q_w is the Darcy flux density [m s^{-1}], and θ_e is the effective volumetric water content [m^3 m^{-3}]. We assume that hydrodynamic dispersion is much greater than longitudinal molecular diffusion, and that D_s can be approximated by

$$D_s = \lambda v \qquad [5.2]$$

where λ is the dispersivity [m] (Wagenet, 1983). Noting that t equals Q/q_w where Q is the cumulative infiltration [m] equation [5.1] may be written with Q as the temporal variable

$$\theta_e \frac{\partial C_f}{\partial Q} = \lambda \frac{\partial^2 C_f}{\partial z^2} - \frac{\partial C_f}{\partial z} \qquad [5.3]$$

If θ_e is found to be less than the measured volumetric water content θ_t, it would indicate that some of the soil water is not participating in the solute transport. We denote this non-participating water θ_x, defined as θ_t - θ_e.

Note that Equations [5.2] and [5.3] imply that solute movement expressed as a function of cumulative infiltration rather than time is independent of pore water velocity, and depends only on θ_e, λ and Q. This lack of dependence on real time implies that both lateral and longitudinal molecular diffusion are unimportant in terms of their observable effect on solute transport (Brusseau, 1993).

The boundary and initial conditions relevant to the study described here are for the soil to be initially free of the solute of interest, and then when Q equals zero the flux concentration changes to $C = C_o$ in the infiltrating solution. At some depth l, we are interested in the flux and resident soil solution concentrations, C_f and C_r respectively, as a function of cumulative infiltration. Then the solutions we require are (van Genuchten and Wierenga, 1986)

$$\frac{C_f(Q,l)}{C_o} = \frac{1}{2}\operatorname{erfc}\left(\frac{l - Q/\theta_e}{2(Q\lambda/\theta_e)^{1/2}}\right) + \frac{1}{2}\exp\left(\frac{l}{\lambda}\right)\operatorname{erfc}\left(\frac{l + Q/\theta_e}{2(Q\lambda/\theta_e)^{1/2}}\right) \qquad [5.4]$$

and

$$\frac{C_r(z,Q)}{C_r(z,\infty)} = \frac{1}{2}\text{erfc}\left(\frac{z-Q/\theta_e}{2(Q\lambda/\theta_e)^{1/2}}\right)+\left(\frac{Q}{\pi\theta_e\lambda}\right)^{1/2}\exp\left(\frac{-(z-Q/\theta_e)^2}{4Q\lambda/\theta_e}\right) -\left(1+\frac{z}{\lambda}+\frac{Q}{\lambda\theta_e}\right)\exp\left(\frac{z}{\lambda}\right)\text{erfc}\left(\frac{z+Q/\theta_e}{2(Q\lambda/\theta_e)^{1/2}}\right) \quad [5.5]$$

where $C_r(z, \infty)$ is the resident solution concentration after an effectively infinite amount of leaching with a solution of concentration C_o. Note that,

$$C_r(z,\infty) = C_o \qquad \text{if } \theta_t = \theta_e$$

$$C_r(z,\infty) = \frac{\theta_e}{\theta_t}C_o \qquad \text{if } \theta_t > \theta_e \quad [5.6]$$

The second model considered here is the mobile/immobile modification of the CDE (van Genuchten and Wierenga, 1976). In this model the effective soil water (θ_e) is divided into two domains: the "mobile" water (θ_m), and the "immobile" water (θi). Thus the total water content (θ_t) equals $\theta_m + \theta_i + \theta_x$. For non-reactive solute transport under steady state water flow, the solute transport equations for the mobile region of Tillman *et al.* (1991b) may be simplified to,

$$\theta_m\frac{\partial C_m}{\partial t} = q_w\lambda_m\frac{\partial^2 C_m}{\partial z^2} + D_i\theta_m\frac{\partial^2 C_m}{\partial z^2} - q_w\frac{\partial C_m}{\partial z} - \alpha\theta_i(C_m - C_i) \quad [5.7]$$

where C_m and C_i refer to the resident solution concentrations in the mobile and immobile regions, λ_m is the dispersivity in the mobile phase [m], α is the "diffusional" transfer coefficient for solute exchange between mobile and immobile regions [h^{-1}], and D_i the molecular diffusion coefficient of solute in the soil [$m^2\ h^{-1}$] given by (Tillman *et al.*, 1991b) as

$$D_i = 3.5\theta_t^2 D_o. \quad [5.8]$$

Here D_o is the diffusion coefficient in the bulk solution, which for a solution of $MgCl_2$ was estimated to be 3.6×10^{-6} m^2 h^{-1} (Robinson and Stokes, 1959).

The solute transport equation for the immobile region is given by,

$$\frac{\partial C_i}{\partial t} = D_i \frac{\partial^2 C_i}{\partial z^2} + \alpha \left(C_m - C_i \right) \qquad [5.9]$$

The above set of equations [5.7 to 5.9] for the mobile/immobile approach of the CDE was solved numerically using a similar procedure to that described by Tillman *et al.* (1991b). For no-inflow periods, q_w was set equal to zero in equation [5.7].

5.2.4 Materials and Methods

The soil studied is Manawatu fine sandy loam, a Dystric Fluventic Eutrochrept, taken from the herbicide-sprayed strip of a kiwifruit orchard. The top 20 mm of soil was removed and then two cylinders of soil about 120 mm in diameter were carefully carved *in situ*, and then removed. One core was 340 mm long, and will be referred to as column A. The other, column B, was 295 mm in length. Measurements on soil nearby gave a bulk density of 1.35 Mg m^{-3} and a specific surface area of 54 m^2 kg^{-1}.

A drawing of the leaching apparatus has already been published by Magesan *et al.* (1995), so only salient details are repeated. A disk permeameter sits atop each soil column to allow solution entry at some pre-set pressure potential. This is maintained by a bubbling tower and vacuum system. A similar apparatus underneath maintains the same pressure potential at the base, and allows routine collection of effluent aliquots. Except as indicated, the columns were kept at a pressure potential head of -80 mm. The columns were wrapped in polyethylene film to restrict evaporation. A suction cup 95 mm long and 3 mm in diameter was inserted horizontally into a pre-drilled hole 30 mm from the bottom of each soil column. A suction of 1.2 kPa (120 mm of water) was applied to the cup. This resulted in the cup collecting in total about 5% of the solution flowing through the soil column. Three-wire TDR probes, with rods 100 mm long, 2 mm in diameter, and 12 mm

apart, were inserted horizontally at depths of 190 mm and 290 mm in column A, and at 140 mm and 240 mm depth in column B. A jig allowed correctly-spaced holes to be pre-drilled for the TDR probes. A commercial cable tester controlled by a laptop computer was used to monitor the TDR probes and to analyse for soil water content and electrical conductivity. Details are given in section 4.2.

The first solution applied to the columns was 0.0025 *M* $Ca(NO_3)_2$. Pre-leaching with about 3 liquid-filled pore volumes of this solution brought the soil solution to an essentially uniform concentration and TDR-measured electrical conductivity. The infiltrating solution was then changed to 0.0235 *M* $MgCl_2$, and about 7 liquid-filled pore volumes of this solution was applied. The two salts used were chosen for their similar electrical conductivities (Robinson and Stokes, 1959). The two concentrations were chosen so the soil electrical conductivity would stay within the range measurable by TDR.

After leaching with the $MgCl_2$ solution, the treatment of the two columns diverged. Column A was rapidly sliced into 30 mm thick horizontal sections. The soil in each slice was homogenized and a sub-sample taken for gravimetric determination of water content. The extractions and chemical analyses described below were conducted on other moist sub-samples from each segment. Instead of it being immediately sectioned, column B was left for 7 days without a permeameter atop, so that there was no infiltration. The column was covered to prevent evaporation. Then another 1.5 pore volumes of the $MgCl_2$ solution was applied, again at a pressure head of -80 mm. The pressure head at the top and bottom of the column was then increased to -3 mm, and once the outflow rate had steadied to a new value, the infiltrating solution was changed to 0.0245 *M* $Ca(NO_3)_2$. After about 0.8 liquid-filled pore volumes of this solution had been applied, infiltration ceased for 12 hours, and then resumed until two more pore volumes had been applied. Column B was then sectioned and sub-sampled as described above for column A.

Chemical analyses were conducted on the effluent and suction cup samples taken routinely during leaching, and on soil extract samples at the conclusion of leaching. The soil solution from column A was extracted for chloride measurement by mixing 25 ml of 0.05 *M* K_2SO_4 solution with 2 g of moist soil. For column B the same extract was used, but

with a soil: solution ratio of 5g : 15 ml. The mixture was then shaken for an hour, centrifuged for 5 min at 8000 rpm, and filtered. Following Blakemore *et al.* (1987) for nitrate analysis, the soil was sub-sampled and extracted in the same way, except that the extracting solution was 2 *M* KCl. The soil : solution ratio was 5g : 15 ml for column A and 2g : 15 ml for column B. All samples were stored at 253 K until analyzed. Chloride was measured using a Tecator Flow Injection Analyzer, and nitrate using a Technicon Autoanalyser.

5.2.5 Results and Discussion

5.2.5.1 Water Flow and Storage

Table 5.1 Transport parameters obtained as described in the text

Data used	θ_e/θ_t [$m^3\ m^{-3}$]	λ [mm]
Column A ($\theta_t = 0.454$, $q_w = 3.1$ mm h^{-1})		
Outflow	0.91	38
Suction cup	0.96	26
TDR (190 mm depth)	0.80	43
TDR (290 mm depth)	0.80	38
Column B ($\theta_t = 0.431$, $q_w = 2.9$ mm h^{-1})		
Outflow	0.96	36
Suction cup	1.06	25
TDR (depth 140 mm)	1.15	25
Column B ($\theta_t = 0.478$, $q_w = 13$ mm h^{-1})		
Outflow	1.00	59
Suction cup	1.27	28

The gravimetric water contents measured at the time of final destructive sampling of the soil columns, and the independently-measured bulk density, allowed the volumetric water

content, θ_t, in each soil column at the conclusion of the experiment to be found. Table 5.1 gives the values. Volumetric water contents calculated from the final TDR measurements were within 3% of these values.

The measured outflow rate, which is the Darcy flux density q_w if the flow is steady, is shown as a function of Q in Figure 5.2. The flow rates were relatively stable. The average rainfall intensity in New Zealand is 5 mm h^{-1} (Tomlinson, 1992), so the rates achieved with a pressure head of -80 mm are not atypical of the Darcy flux densities that would occur in the field during rainfall. The gravity-induced redistribution, and the residual evaporation through the polyethylene that occurred when infiltration into column B was stopped on two occasions, meant that it took some time for the outflow rate to recover once infiltration resumed.

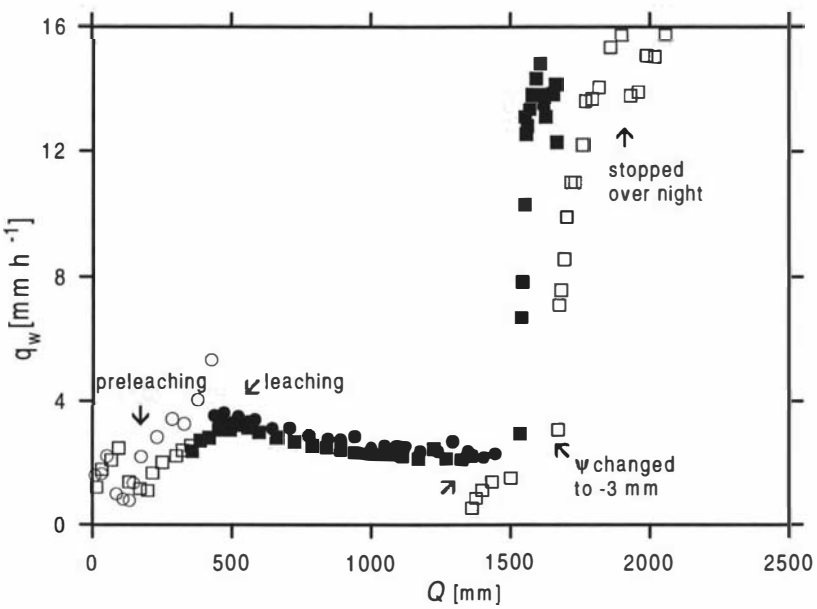

Fig. 5.2 Measured outflow flux density (q_w) as a function cumulative infiltration (Q) for columns A (○ and ●) and column B (□ and ■); open symbols indicate the infiltrating solution was $Ca(NO_3)_2$, closed symbols indicate $MgCl_2$.

5.2.5.2 Chloride and Nitrate in the Effluent and Simulation Results using the CDE

The normalized effluent concentration data for chloride at the flux density of about 3 mm h^{-1} are shown in Figure 5.3. Also shown are the fitted curves obtained using equation [5.4] and least-squares optimisation. The values found for the dispersivity and relative effective water content are given in Table 5.1. The average dispersivity value of 37 mm is an order of magnitude larger than the values typical of repacked soil (Wagenet, 1983), but similar to values found for intact soil by other workers (Seyfried and Rao, 1987; Magesan *et al.*, 1995). The θ_e / θ_t values in Table 5.1 show that the fitted water content values were 5 to 10% less than the measured values. This indicates that between 0.02 and 0.04 m^3 m^{-3} of the soil water was not accessible to the percolating chloride ions. This was probably due to anion exclusion from the double layer surrounding the colloids in the soil. An early study comparing tritium and chloride movement through repacked columns of the same soil similarly found 0.03 m^3 m^{-3} of soil water from which chloride was excluded (Scotter and Tillman, 1991).

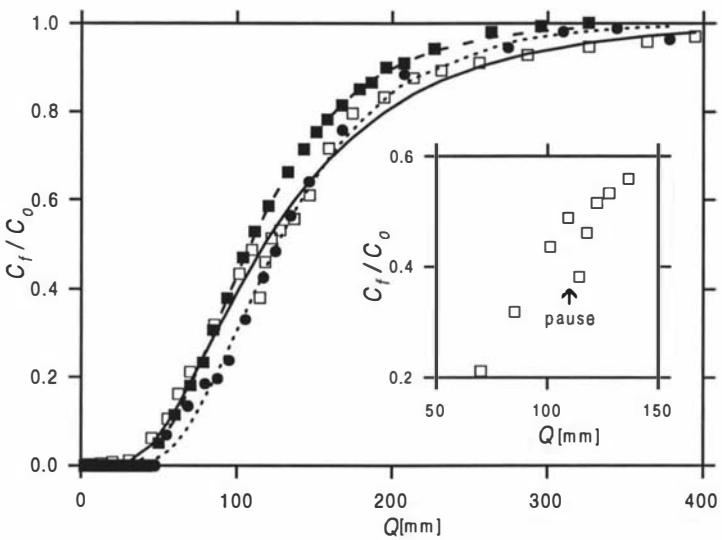

Fig. 5.3 Normalized anion breakthrough data and fitted curves using the CDE at the low flow rate for column A (● and dotted line) and column B (■ and dashed line), and for column B at the high flow rate (□ and solid line). The inset shows in detail the effect of the 12 h pause in leaching at the high flow rate.

Also shown in Figure 5.3 are the nitrate breakthrough data at the higher flux density of about 13 mm h^{-1} for column B. Figure 5.3 shows that at the higher flow rate more

leaching was needed before the effluent concentration approached the influent concentration. This could be due to either there being less time for molecular diffusion between faster and slower moving water at the greater flux density, or to more direct flow pathways in the slightly wetter soil at the higher flow rate. Nevertheless these quite similar BTC's obtained for the two different flow rates and the values in Table 5.1 indicate that the dispersivity is only slightly velocity dependent.

The one week pause in leaching had no effect on chloride concentration, because inflow and outflow concentrations were equal when it occurred. But the effect of the over-night pause during leaching at the high flux density appears in Figure 5.3 as a sudden drop in concentration at about Q = 110 mm. This can probably be attributed to transverse molecular diffusion between water which moved at different speeds during flow. If longitudinal diffusion had been the dominant process during the 12 h break, a sudden increase rather than a decrease in the effluent concentration would have been expected when flow resumed. Hu and Brusseau (1995) observed similar effluent concentration decreases following an interruption in the flow through a column containing porous spheres.

The fitted BTC for column B at the higher flow rate is also shown in Figure 5.3. The measured and predicted curves agree well except at Q values during the adjustment period between 110 and 210 mm. The discrepancy at these values is logically the result of the over-night pause in leaching. Unexpectedly a θ_e/θ_t value of 1.0 was obtained for the high flow rate. One might expect the percolating ions to "see" less of the soil water at the higher flow rate than at the lower flow rate. However the high value seems related to the over-night pause. When equation [5.3] was fitted using only the data collected before the pause in leaching, a θ_e/θ_t value of 0.95 was obtained, slightly lower than the value found for column B at the lower flow rate.

5.2.5.3 Resident Solute Concentrations and Simulation Results using the CDE

The resident soil solution concentrations at the end of leaching, inferred from the soil extracts are shown in Figure 5.4. For column A these are the chloride concentrations

measured at the end of leaching at the low flux density, and for column B they are the nitrate concentrations measured when leaching at the higher flux density ceased.

Average C_r / C_o values for the soil solution were found to be only about 0.90 for both, despite column A having being leached with over 1000 mm of chloride solution over a period of 13 days. This value is consistent with the 5 to 10% difference between the flux and resident concentrations implied by the θ_e / θ_t values in Table 5.1 and discussed above.

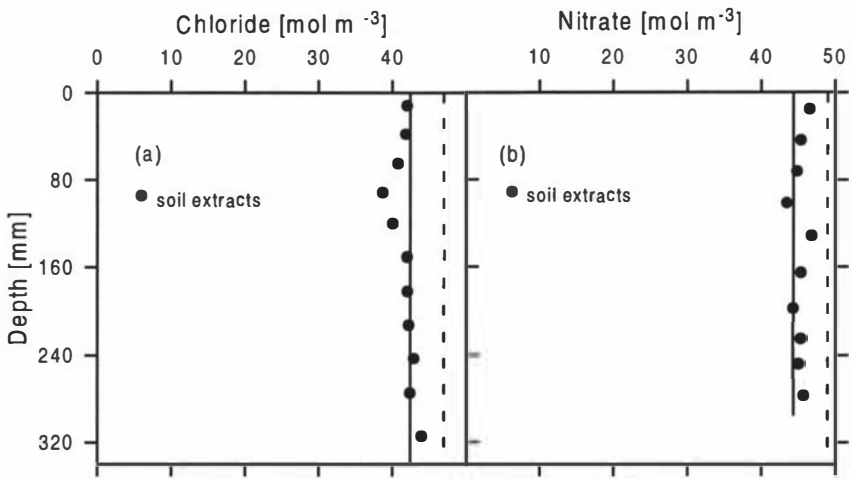

Fig. 5.4 Anion concentrations in the soil solution inferred from soil extracts (●) for column A (a) and column B (b). The broken lines show the concentration of the applied solutions, and the solid lines the predictions obtained from the MIM.

5.2.5.4 Characterising Anion Movement using Suction Cup Data

The suction cup data obtained at the lower flow rate are shown in Figure 5.5a. Also shown in Figure 5.5a are the flux concentrations at the suction cup depth calculated from equation [5.4], using the dispersivity values obtained from the effluent data. The measured and calculated values are in quite close agreement, indicating that the suction cup data could be used to describe chloride flow through the soil columns.

Equation [5.4] was also fitted using least-squares to the suction cup data. The θ_e / θ_t and λ values thus obtained are shown in Table 5.1. Note that, although the suction cups were

assumed to sample the flux concentration, the Pèclet number, defined as l/λ, was high enough for there to be little difference between the flux and resident concentrations except for the double layer effect. The dispersivity values were 30% lower than those obtained from the effluent data at the lower flow rate, and 50% lower at the higher flow rate. The dimensionless water contents were within 30% of the values inferred from the effluent data, but the discrepancies showed no consistent trend. Non-uniform flow in the soil columns, coupled with the relatively small sampling volume of the suction cups relative to the 120 mm column diameter, seems the most likely explanation for the differences observed.

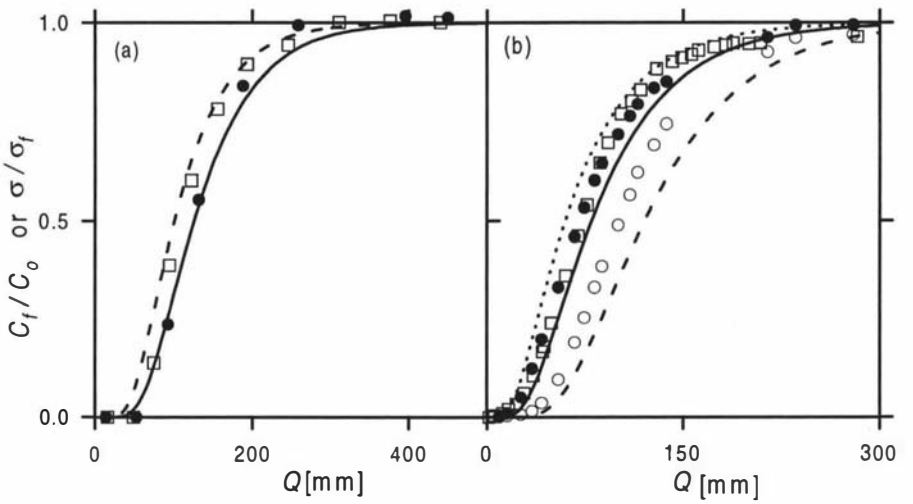

Fig. 5.5 (a) Normalised anion breakthrough data measured by suction cups and simulated curves for column A (● and solid line) and column B (□ and dashed line). (b) Normalised bulk soil electrical conductivity as measured by TDR and simulated curves for column A for TDR probe at 190 mm (● and solid line) and at 290 mm (○ and dashed line), and column B for TDR probe at 140 mm (□ and dotted line). The simulated curves were obtained using the dispersivities from the outflow data.

We conclude that provided the uncertainty inherent in the measurements is taken into account by adequate replication, suction cups can give reasonable estimates of the transport parameters for non-reactive ions like nitrate and chloride.

5.2.5.5 Characterising Anion Movement using TDR

The frequent TDR measurements of the soil's dielectric constant and impedance that were made during leaching with $MgCl_2$ solution were used to infer the bulk electrical conductivity of the soil, σ [S m^{-1}], as described in section 4.2. The measured values are shown in Figure 5.5b. These have been normalized to the final conductivity measured during leaching with the 0.025 *M* $MgCl_2$ solution, *viz.* σ_f . Only data for one probe for column B are shown, as for reasons which are not clear the other probe gave unreliable readings with unrealistically high attenuations. Given that the water content was constant with time, and that solutions with equal concentrations of $Ca(NO_3)_2$ and $MgCl_2$ have almost identical electrical conductivities, and further that between 0.0025 *M* and 0.025 *M* the electrical conductivity is almost linearly related to concentration (Robinson and Stokes, 1959), we can assume that the bulk electrical conductivity of the soil was linearly related to the resident chloride concentration in the soil solution. This in turn implies that σ/σ_f equals C/C_r (l,∞), provided leaching continued long enough for the resident concentration to reach its final value. Also shown in Figure 5.5b are the TDR readings predicted using Equation [5.5], with the λ and θ_e /θ_t obtained from the outflow data. Agreement is reasonable except for the probe at 290 mm in column A.

Equation [5.5] was also least-squares fitted to the TDR data, and the resulting parameter values are given in Table 5.1. The dispersivity values are within 30% of the values obtained from the effluent data. There was no consistent difference between the dispersivity values inferred from the shallow TDR probes, which were in about the middle of the columns, and the values inferred from effluent. Thus within the rather crude resolution of the TDR measurements, the dispersivity was length-wise invariant. The CDE appears valid.

As with the suction cup data, the inferred θ_e /θ_t values were not consistent. Again we attribute this to local variation in the water flux density, and the relatively small soil volume sampled by the TDR probes. An implication is that considerable TDR-replication is needed to obtain valid data. Thankfully this is often easily possible. When used to monitor vertical solute movement, vertical TDR probes would sample an even smaller

effective soil volume than the horizontal probes used here (Mallants *et al.*, 1994), if the flow paths are considered vertical.

5.2.5.6 Simulation using the Mobile/Immobile Model

In the mobile/immobile model, the soil water is generally separated into two phases, a mobile and an effectively immobile. But the mobility in the soil water could be visualised as an assemble of regions with different degrees of "mobility", and mass transfer coefficients. From both the flow interruption data (Fig. 5.3) and the resident concentration after an infiltration of 1000 mm, it seems that the soil water of the Manawatu fine sandy loam can be considered to comprise three different phases: a "mobile" (θ_m), a "quasi immobile" (θ_i) and a "totally immobile" (θ_x) phase. The "totally immobile" region is due to double layer exclusion of chloride, and not involved in solute transport. Solute is transported through the mobile region by convection and diffuses into the "quasi immobile" region. Although the size of θ_i is often considered to be dependent on the concentration of soil solution, the soil water content and the soil water flux (Nkedi-Kizza *et al.*, 1983, Kutílek and Nielsen, 1994), good results have been obtained in the laboratory and in the field by assuming a constant separation of these two domains (Tillman *et al.*, 1991b). The total immobile fraction for this soil was previously found to be 0.18 (Tillman *et al.*, 1991b), and this is assumed to comprise the "totally immobile" (θ_x) and the "quasi immobile" (θ_i) water fraction. From the resident concentration at the end of the experiment (Fig. 5.4) it was found that 0.04 $m^3\ m^{-3}$ of the soil's water could be classed as "totally immobile". This leaves 0.14 $m^3\ m^{-3}$ for the "quasi immobile" water fraction, and "mobile" water fractions ranging from 0.251 to 0.298. With these water fractions, the column B outflow data were used to parameterize α and λ_m by solving eqs. [5.7-5.9] numerically. By trial-and-error the values found were a dispersivity in the mobile phase (λ_m) of 20 mm, and a "diffusional" mass transfer coefficient (α) of 0.04 h^{-1}. The lower dispersivity found using this mobile/immobile approach compared to the one found using the CDE results from the separation of mechanical dispersion and diffusional exchange in the mobile/immobile model. The

dispersivity and the mass transfer coefficient obtained are of similar magnitude to the values of 12.5 mm and 0.028 h^{-1} found by Tillman *et al.* (1991b).

The measured and simulated normalised effluent concentrations of nitrate at the flux density of about 13 mm h^{-1} for column B are shown in Fig. 5.6. Although the model predicts a discontinuity in concentration after flow resumed, the concentration drop could not be simulated in its full extent. The underestimation is probably due to redistribution occurring during the interruption of flow. However the chloride breakthrough data for the two columns at the lower flux densities of about 3 mm h^{-1} were described reasonably well using the same model parameters.

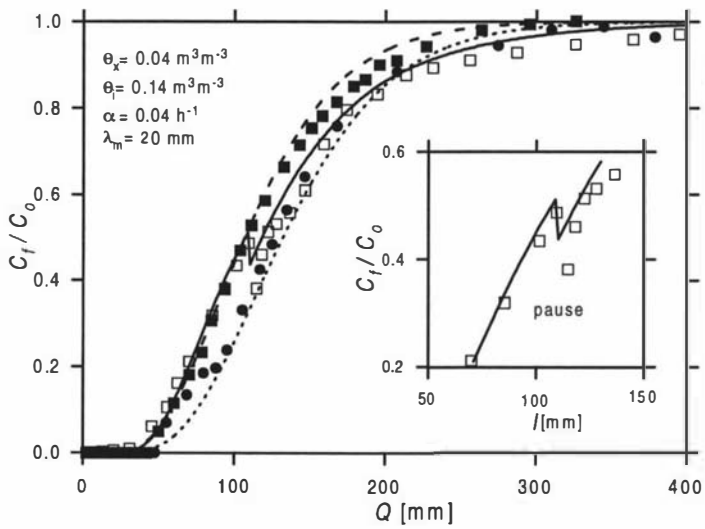

Fig. 5.6 Normalized anion breakthrough data and fitted curves using the mobile/immobile approach of the CDE at the low flow rate for column A (● and dotted line) and column B (■ and dashed line), and for column B at the high flow rate (□ and solid line).

The predictions of the resident concentrations of chloride for column A and nitrate for column B are shown in Fig. 3 as the solid line and are well described by this mobile/immobile approach. Simulations using this mobile/immobile approach are only slightly better then the ones obtained using the simpler CDE. Simulating solute transport through undisturbed soil columns of a stony soil, Schulin *et al.* (1987) also found only a slight improvement by using the mobile/immobile concept compared to the classical CDE.

However a direct comparison between the simulation using the CDE (Fig. 5.3) and the mobile/immobile approach (Fig. 5.6) is not justified, as the model parameters for the CDE were obtained by least square optimization for each column and show some variation (Table 5.1). In the mobile/immobile approach however the same values were used to simulate the effluent concentration data for both soil columns and flow rates.

5.2.6 Conclusions

During flow at Darcy flux densities of about 3 and 12 mm h^{-1} some variation in dispersivity values with flux density was observed. This variation is evident in the breakthrough curves of Figure 5.2, and the inferred dispersivity values in Table 5.1. Leaving aside the issue of depth dependence in the dispersivity, here it appears that for most practical applications, especially in the field, the CDE with a constant dispersivity can be deemed adequate.

The effect of a 12 h pause in leaching at 12 mm h^{-1} was a sudden drop in the effluent concentration when leaching resumed. However this drop was short-lived, and would not be significant at the scale of most field studies. The drop is consistent with some molecular diffusion from fast-moving to slower-moving water being much more important than longitudinal diffusion parallel to the direction of convective flow. Another possible cause is a change in the flow path geometry following the interruption in the flow (Roth and Hammel, 1996).

The difference observed between the final resident soil solution concentration and the final anion concentration in the influent and effluent, despite 1000 mm of leaching, indicated that about 10% of the soil water did not participate in anion transport. Anion exclusion from the diffuse double layer can explain this difference.

The more complex approach of the mobile/immobile model could describe the discontinuity after flow resumed. However the relatively small improvement gained compared to the CDE might not justify the use of the mobile/immobile approach, which

requires estimation of more model parameters. Further testing of this approach under different conditions in the laboratory and in the field is needed to assess its practical use.

The horizontally-inserted suction cups gave dispersivity and effective water content values within 30% to 50% of those inferred from the effluent measurements. The relatively small sampling volume of the suction cups would however appear to limit their usefulness, unless they are adequately replicated.

When suitable salts at suitable concentrations are used, horizontal TDR probes are able to measure the electrolyte level so that the soil's dispersivity and effective water content could be estimated as accurately as the suction cups. Again the small soil sampling volume seemed the main limitation to the usefulness of the TDR measurements. When using either suction cups or TDR probes in the field, considerable replication of the instrumentation, and perhaps longer cups and probes than those used here, would be needed.

5.3 Solute Movement through Undisturbed Soil Columns Under Pasture during Unsaturated Flow

by Iris Vogeler, David R. Scotter, Steven R. Green, and Brent E. Clothier

Submitted to *Australian Journal of Soil Research*

5.3.1 Abstract

Previous studies of solute movement concerning the influence of initial soil water content have led to apparently contradictory results. Here we describe some experiments which aimed to determine the effect of both pasture, and initial water content on solute movement. Solid $SrCl_2$, $CaCl_2$, and $Ca(NO_3)_2$ were surface-applied to undisturbed columns of a fine sandy loam under short pasture. The soil columns were 300 mm in both diameter and length. A rotating rainfall simulator delivered steady-state rainfall at about 10 mm h^{-1}. The leachate at the base was collected under suction and analysed, and one column was analysed for resident concentrations of strontium. Solute

transport could be accurately described by coupling Richards' equation with the convection dispersion equation, when ion exclusion or exchange were taken into account. The dispersivity was about 70 mm, only slightly higher than found previously for the same soil without vegetation. There was no significant difference in intrinsic behaviour when solute was applied to either an initially wet or a dry topsoil. The contrasting results from earlier published studies were probably due to incipient ponding and preferential flow. This will not usually occur in New Zealand pasture soils under typical rainfall intensities, but might under irrigation or when the soil structure is degraded. It is suggested soil cores need to have dimensions at least as large as the dispersivity if they are to encompass most of the variation in solute concentration.

Keywords: initial water content, transient and steady water flow, rainfall simulator, sample size

5.3.2 Introduction

Given the permeable nature of most of the soils, and a typical low rainfall intensity of 5 mm h^{-1} (Tomlinson, 1992), leaching in New Zealand is likely to occur predominantly under non-ponding unsaturated conditions. Thus one would usually expect the larger macropores to remain air-filled, and preferential flow to be avoided. Thus the convection-dispersion equation (CDE) would then successfully model solute movement through the soil. However, both in New Zealand and in other countries, the observed behaviour of surface-applied chemicals has often been at variance with the predictions from the CDE. For example, field studies by Saffigna *et al.* (1976) with potatoes in the U.S.A., and by Kanchanasut and Scotter (1982) with pasture in New Zealand, showed how interception by vegetation, and channelling by roots, caused surface-applied solute partly to remain near the surface, yet to move in part deeper into the profile. Other studies of surface-applied chemicals have shown that the soil water content of the topsoil can affect its subsequent leaching in contrasting ways. For example, in the U.K. White *et al.* (1986) found more leaching from initially dry soil cores than from prewet cores of clay soil. They attributed this lessening in preferential flow in the prewet soil to swelling reducing macropore size. In contrast, Tillman *et al.* (1991b) in New Zealand

found the potassium bromide they applied in 5 mm of solution to a sandy loam with a dry surface layer was quite immune to leaching, while the same amount of potassium bromide applied to a uniformly moist soil was not. They argued that the bromide in the 5 mm of solution was sucked into the smaller pores of the dry topsoil, where it was relatively isolated from subsequent irrigation. Prewetting avoided this behaviour. The results observed by Snow *et al.* (1994) in a lysimeter study on the same soil, also insinuated retention of solute within the immobile water near the soil surface, with subsequent slow movement from the immobile to the mobile water. Shipitalo *et al.* (1990) observed similar behaviour in a silt loam, and gave a similar explanation for it.

This study was conducted to clarify, under controlled conditions, some of these confusing results, particularly with regard to the effect of the initial water content on leaching behaviour. The importance of the sample size on measured solute concentrations is also demonstrated by comparing Sr^{2+} resident concentrations obtained from small soil cores, and from the bulk soil. Pasture-covered intact soil cores, 300 mm in both length and diameter, had chemical applied to their surface, and were then leached in the laboratory, using a rainfall simulator.

5.3.3 Theory

The experiments described here were carried out in the laboratory on vertical soil columns. For non-hysteretic one-dimensional flow infiltration and redistribution of water can be described by Richards' equation. Assuming that root uptake is negligible, the equation may be written as,

$$\frac{\partial \theta}{\partial t} = \frac{\partial}{\partial z}\left[D_w(\theta) \frac{\partial \theta}{\partial z} \right] - \frac{\partial K_w(\theta)}{\partial z} . \qquad [5.10]$$

where θ is the volumetric water content [$m^3\ m^{-3}$], D_w is the soil water diffusivity [$m^2\ s^{-1}$], K_w is the hydraulic conductivity [$m\ s^{-1}$], q_w is the water flux density [$m\ s^{-1}$], t is the time [s], and z is the depth [m].

The relevant initial and boundary conditions for leaching under steady rainfall are,

$$\begin{aligned} \theta &= \theta_n(z) \qquad t=0 \qquad 0 \le z \le l \\ q_w &= q_o \qquad z=0; t>0 \end{aligned} \quad , \qquad [5.11]$$

where θ_n is the initial water content [$m^3\ m^{-3}$], l is the column length [m], and q_o is the constant flux at the surface [$m\ s^{-1}$]. Eqs. [5.10] and [5.11] were solved numerically, using constitutive equations to describe both the soil water diffusivity and the hydraulic conductivity as a function of the soil water content.

The conductivity function $K_w(\theta)$ assumed was,

$$K_w = K_s \left(\frac{\theta - \theta_a}{\theta_s - \theta_a} \right)^b \qquad [5.12]$$

where b is an empirical constant, and θ_s is the near-saturated water content [$m^3\ m^{-3}$], and θ_a is a residual water content [$m^3\ m^{-3}$], and K_s is the hydraulic conductivity near saturation [$m\ s^{-1}$].

The soil's water-diffusivity function $D_w(\theta)$ was found using (Brutsaert, 1979),

$$D_w(\theta) = \frac{\gamma S^2}{(\theta_s - \theta_a)^2} \exp\left(\beta \frac{\theta - \theta_a}{\theta_s - \theta_a} \right) \qquad [5.13]$$

where γ and β are interdependent constants, taken as 4.278 x 10^{-2} and 4 (Clothier and White, 1981), and S is the soil's sorptivity [$m\ s^{-1/2}$] at θ_s and θ_a.

One-dimensional transport of solutes is described by the convection dispersion equation (CDE), which for nonreactive solutes under transient conditions is

$$\frac{\partial(\theta C_r)}{\partial t} = \frac{\partial}{\partial z}\left(\theta D_s \frac{\partial C_r}{\partial z} \right) - \frac{\partial(q_w C_r)}{\partial z} \qquad [5.14]$$

where C_r is the solute concentration in the resident soil solution [mol m^{-3}], and D_s is the diffusion-dispersion coefficient [m^2 s^{-1}]. It is assumed that molecular diffusion in the direction of flow is negligible, and that D_s is proportional to the average pore water velocity v (defined as q_w/θ) so,

$$D_s = \lambda v \qquad [5.15]$$

where λ is the dispersivity [m].

The soil is assumed initially to be free of the solute of interest, and application of chemical is simulated as a uniform concentration C_o being applied to the soil surface over a very short time interval, $0 < t < t_i$. This was followed by solute-free water at steady-state water flow. Thus for solute the appropriate initial and boundary conditions are,

$$\begin{aligned} &C_r = 0 \qquad 0 \le z \le l;\ t = 0 \\ &-\theta D_s \frac{\partial C_r}{\partial z} + q_w C_r = q_o C_o \qquad z = 0;\ 0 < t < t_i \\ &-\theta D_s \frac{\partial C_r}{\partial z} + q_w C_r = 0 \qquad z = 0;\ t > t_i \end{aligned} \qquad [5.16]$$

For the lower boundary condition it was assumed that the soil column was part of an effectively semi-infinite system, as suggested by van Genuchten and Wierenga (1986, p.1034).

Equations [5.10] through [5.16] were solved numerically using Newton-Raphson iteration for the water flow equation and a Crank-Nicholson scheme, with dispersion correction described by Gerke and van Genuchten (1993) for the solute flow. Comparison of the numerical and analytical solutions (van Genuchten and Wierenga, 1988) for movement of a pulse during steady-state water flow gave identical solutions, verifying the stability and convergence of the numerical solution. Equations to describe the hydraulic properties were derived from data of Clothier and Smettem (1990) for Manawatu fine sandy loam. The respective parameters were: S = 0.85 mm $s^{-1/2}$, K_s =

1.56×10^{-2} mm s^{-1}, θ_s = 0.455 m^3 m^{-3}, θ_a = 0.05 m^3 m^{-3}, and b = 12.1. Inputs for the computer program included the profile for the non-uniform initial water content with depth.

5.3.4 Materials and Methods

5.3.4.1 Column Experiments

The column leaching experiments were performed using Manawatu fine sandy loam under a pasture of predominantly ryegrass and white clover. The cores were taken from near where Clothier and Smettem (1990) carried out their experiments. Two free-standing undisturbed soil columns, with an internal diameter of 304 mm and 300 mm long were carefully carved in the field. After excavation and transport to the laboratory the soil columns, now protected by steel cylinders, were placed on a receptacle with a nylon mesh cover, which enabled application of a suction at the bottom of the columns. The pasture height was trimmed to 30 mm. Time Domain Reflectometry (TDR) probes of 150 mm in length were installed horizontally at depths of 50, 150 and 250 mm. These probes were used to monitor the water content during the experiment.

The two soil columns will be referred to as columns I and II. Both columns were preleached using a rainfall simulator, described below, with a solution of 0.0025 *M* $Ca(SO_4)_2$. Column I then received an application of solid $SrCl_2$ (60 g Cl m^{-2}), and Column II had an application of solid $Ca(NO_3)_2$ (60 g NO_3-N m^{-2}). This was immediately followed by further leaching with 0.0025 *M* $Ca(SO_4)_2$. The effluent was collected in aliquots. After a total infiltration of about 470 mm to each column, the rainfall simulator was removed, and gravity induced drainage was allowed to occur. For column I, the resident concentration of Sr^{2+} was measured. Five soil cores, 25 mm in diameter and 300 mm in length, were taken to test the spatial variability of Sr^{2+} in the soil column. These small cores will be referred to as subsamples. What remained of the soil column was then cut into 30 mm thick horizontal slices. Column II was placed into a climate room to allow dry-down of the soil by pasture root uptake. The temperature in the climate room was set at 20^0 C, and the daylight hours to 12 hrs. Daily measurements of the water content were made by TDR.

Transpiration by the pasture mainly resulted in water uptake from the upper part of the soil profile. Over an eight day period uptake, and some drainage, resulted in a decrease in θ, at a depth of 50 mm, from about 0.45 to 0.25 $m^3\ m^{-3}$. The water content, as measured by the lower two TDR-probes, remained nearly constant, with decreases of only 0.07 and 0.05 $m^3\ m^{-3}$. The pasture was then trimmed again to 30 mm, and an application of solid $CaCl_2$ (50 g Cl m^{-2}) was followed by 1 mm of 0.0025 *M* $Ca(SO_4)_2$ to dissolve the salt. After a further 24 h in the climate room, but without heating and lights, the column was taken back into the laboratory and once more leached with 0.0025 *M* $Ca(SO_4)_2$. After an infiltration of 960 mm the column was allowed to drain, and then cut into four horizontal slices. The leaching, following the application to the wet and then the dry soil surface, will be referred to as parts one and two of the experiment with column II.

5.3.4.2 Chemical Analysis

All soil samples were homogenised and weighed. Subsamples were then taken for gravimetric water content determination. This allowed the liquid-filled pore volume to be determined. The overall bulk density was calculated to be 1.33 Mg m^{-3}. The average volumetric water content during leaching was 0.40 for both columns, and so the equivalent length of water present was about 120 mm.

The effluent samples were analysed for chloride using a Tecator Flow Injection Analyser, and for nitrate-nitrogen using a Technicon Autoanalyser. Strontium in the soil was extracted by shaking 50 g of air-dry soil with 250 ml 1 *M* ammonium acetate (Thomas, 1982). Two sequential extracts were made, and these were combined prior to measuring. To estimate the spatial variability, the Sr^{2+} concentrations of the subsamples were also measured. Here 5 g of soil were extracted with 25 ml of ammonium acetate, and again two sequential extracts were made. The concentrations of Sr^{2+} in the extracts were analysed by atomic emission.

5.3.4.3 Rainfall Simulator

A rotating rainfall simulator, with hypodermic needles, similar to that of Bowman *et al.* (1994), was designed and built for the experiments. This is shown in Fig. 5.6a, and consists of a sprinkler reservoir (S), a pressure head regulator (P), and a water reservoir (R). The water head (H) in the sprinkler reservoir is controlled by a pressure head regulator, based on the Mariotte principle ($h_1 = h_2$). The cylindrical sprinkler reservoir, with a diameter of 310 mm and a height of 150 mm, has a plexiglass bottom with 120 holes drilled through it. Conical capillary tubes are inserted into the holes, and then replaceable hypodermic needles are attached. The 120 needles lie in concentric circles around the axis of the sprinkler reservoir (inset of Fig. 5.6). To prevent the needles from clogging there is a nylon mesh (40μm pores) over the base of the sprinkler reservoir, that is held in place by a c-clip wire under tension. The sprinkler reservoir is mounted to a DC motor, which sits on top of a steel frame, and rotates the entire sprinkler reservoir. This rotation is made to establish a more uniform rainfall application. The flow rate from the rainfall simulator can be altered either by using hypodermic needles of different sizes, or by imposing different water heads. For the experiments described here needles of 27 gauge were used, with a water head (H) of 60 mm. This resulted in average Darcy flux densities (calculated from the drainage) in the underlying soil of 9.8 mm h^{-1} ($\pm$ 0.4) for column I, and 10.5 mm h^{-1} ($\pm$ 1.3) for column II.

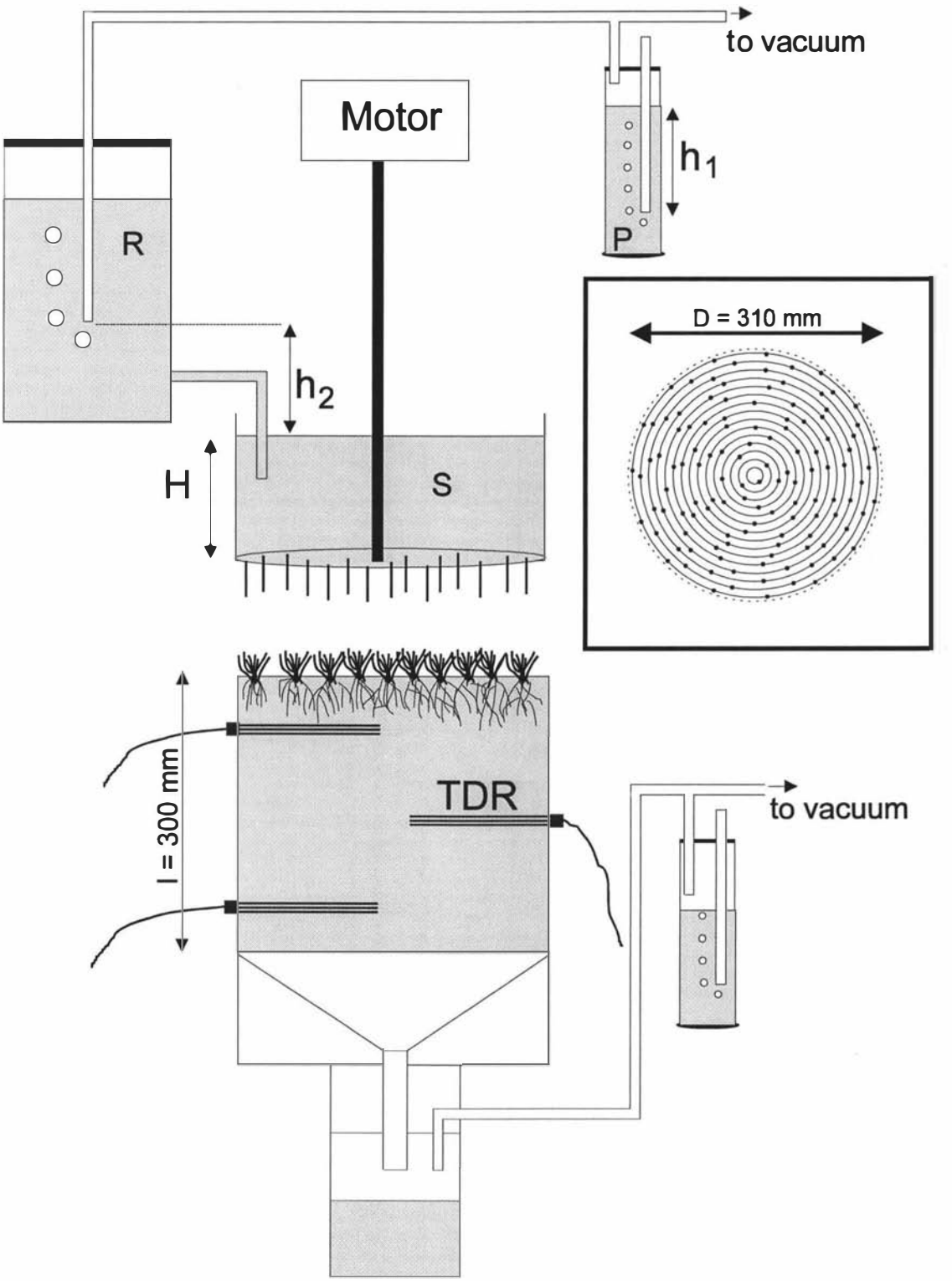

Fig. 5.7 Diagram of the rainfall simulator with sprinkler reservoir (S), pressure head regulator (P), and water reservoir (R). The pressure potential h_1 controls the water head (H) in the sprinkler reservoir.

To test the uniformity of the rainfall simulator 272 small containers with a diameter of 18 mm were placed underneath the reservoir assembly. The amount of water collected in each container was measured after a period of 2 hours. These volumes were then used to calculate the rainfall intensity in mm h^{-1}. The average rainfall over the two hours was 21.5 mm (± 2.6), which corresponds to a rainfall intensity of 10.75 mm h^{-1}. To evaluate the uniformity of distribution, Christiansen's uniformity coefficient (C_u) was calculated using (Heermann 1980),

$$C_u = \left(1 - \frac{\sum_{i=1}^{N} |x - \bar{x}|}{N \bar{x}} \right) 100 \qquad [5.17]$$

where x is the sample value, $\bar{x}$ is the mean value, and N is the number of observations. A uniformity coefficient of 90.3% was obtained, which is similar to those obtained by Andreini and Steenhuis (1990), which ranged from 90.7 to 96.6%.

5.3.5 Results

5.3.5.1 Anion Movement

The concentrations of chloride and nitrate in the effluent, normalised to the maximum concentration measured (C/C_{max}) are shown in Fig. 5.8 as a function of the cumulative infiltration Q. Recoveries for both chloride and nitrate calculated from the effluent data were between 97 and 99%. Also shown are the predictions from numerical solutions of the CDE. The data obtained from solute application to a wet soil surface were first fitted using least squares to the analytical solution of the CDE under steady state flow (Kreft and Zuber 1978, eq. 11). Dispersivities of 75 and 71 mm and mobile water contents of 90 and 96 % of the total water content were obtained for columns I and II, respectively.

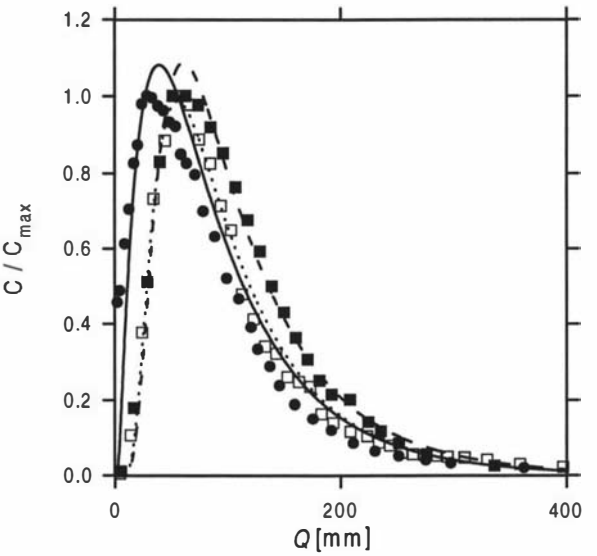

Fig. 5.8 Normalised anion breakthrough data and fitted curves using the CDE for Column I (□ and dotted line), and column II with solute either applied to a wet surface (■ and dashed line) or a dry surface (● and solid line) as a function of cumulative drainage Q.

The dispersivities are slightly higher than previously found values of between 36 and 59 mm for the same soil without vegetation (Section 5.2). The higher values could either be due to the vegetation, the larger column size, or just to spatial variability. Increasing mean dispersivities with increasing column length and area were also found by Parker and Albrecht (1987). The small fraction of the soil's water which is not participating in solute transport is consistent with earlier results (Section 5.2) after such long periods of infiltration, namely a years' rainfall. The "immobile" water fraction is probably due to anion exclusion from the diffusive double layer.

In the second part of the experiment with column II a pulse of calcium-chloride was applied to a dry topsoil. The normalised concentrations of chloride measured in the effluent are also shown in Fig. 5.8. Comparison between the solute breakthrough obtained when solute was applied to a wet soil surface, and when applied to the dry soil surface shows a slightly earlier occurrence of solute in the leachate from the dry soil. This is expected for there is less water to push ahead of the invading solute front. Also shown in Fig. 5.8 is the simulation for the dry soil obtained from the numerical solution of the CDE, using a dispersivity of 70 mm, and an effective water content of 96% of the final water content. The agreement between the measured data and the prediction is

good, suggesting that neither the dispersivity nor the "immobile" water content were influenced by the initial water content.

5.3.5.2 Resident Concentrations of Strontium

The Sr^{2+} concentrations per unit soil volume obtained from the large samples, as well as the 5 individually-analysed cores are shown in Fig. 5.9. The data obtained from the small cores show considerable variability, and they are quite different to the concentrations obtained from the large samples. For the individual cores, recoveries for Sr^{2+} ranging from 73 to 180 % were obtained, whereas the larger samples gave a recovery of 92%. Also shown in Fig. 5.8 are the simulations using the CDE in conjunction with cation exchange theory. The methodology described in Chapter 6 was used, where cation exchange is based on an equilibrium equation, in which a selectivity coefficient is used to describe the relationship between the cation species of interest in the soil solution and on the exchanger. The simulations were carried out using a selectivity coefficient of 1.0 for the homovalent (Ca^{2+} + Mg^{2+})- Sr^{2+} system, as suggested by Bruggenwert and Kamphorst (1982). Furthermore it was assumed that only 80 % of the cation exchange capacity (CEC) as measured by 1 *M* ammonium acetate displacement is involved in cation exchange reactions during leaching. This is the same percentage that was found for other cations in the experiments with the same soil described in Chapter 6. The agreement between the data and the simulations is reasonable, demonstrating the capability of the CDE, linked with cation exchange theory, to describe cation movement during unsaturated flow, as long as an appropriate CEC is used.

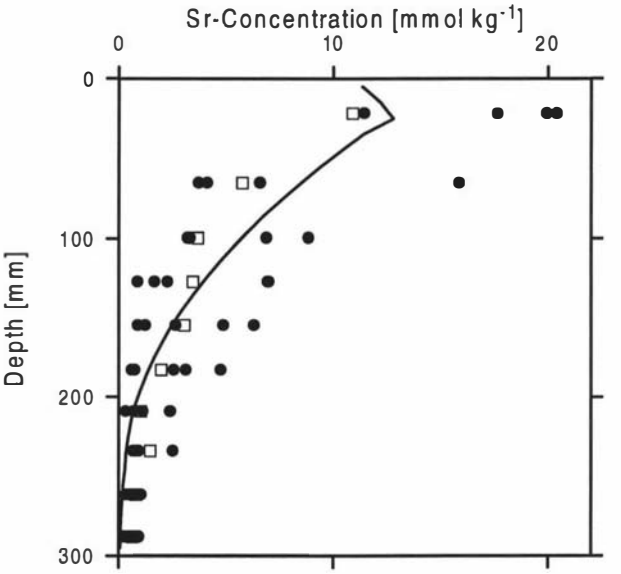

Fig. 5.9 Concentrations of Sr^{2+} in column I at the end of the experiment, as obtained from large samples (□) and subsamples (●). Also shown are the simulations using the CDE in conjunction with cation exchange theory.

5.3.6 Discussion

The question which arises is why our data did not exhibit preferential flow, and so could be adequately described by the CDE, in contrast to data from the earlier studies? Or to put it another way, why did the vegetation and initial soil water content have little effect on solute transport in our study, again in contrast to the earlier studies? The difference in the vegetation effect was probably just due to the length of the pasture. Our pasture was trimmed to about 50 mm height, shorter than that in the study of Kanchanasut and Scotter (1982). If the pasture had been longer, more interception and stem flow would have occurred, inducing a less uniform water flux density at the soil surface. This probably would have resulted in less uniform leaching, with some preferential flow, and with some of the applied chemical quite immune to leaching. It is interesting these effects were not observed with short pasture, as would be found after grazing.

Less obvious are the reasons for the contrasting results from this study and earlier studies concerning the effect of different initial water contents on the leaching of surface-applied chemicals. Incipient ponding and preferential flow probably occurred in

the clay soil used by White *et al.* (1986), due to its low matrix sorptivity and small hydraulic conductivity, even though their water application rate of about 12 mm/h was similar to ours. It is likely incipient ponding and some degree of preferential flow also occurred in the experiments of Shipitalo *et al.* (1990), as their rainfall simulator applied water at the high rate of 60 mm/h.

As our experiments and those of Tillman *et al.* (1991) were conducted on the same soil with similar short pasture cover, the contrasting leaching behaviour seems particularly significant. The main difference between the two experiments is in how the leaching water was applied. Tillman *et al.* (1991) used a hand-operated garden sprayer, with an time-averaged application rate of about 50 mm h^{-1}. The instantaneous rate was much higher than this however. They acknowledge that some local ponding occurred that would flowed into macropores. Some local ponding probably also occurred in the study of Snow *et al.* (1994). Thus in the soil near the surface the leaching environment was quite different to natural rainfall. This would seem to explain the preferential flow Tillman *et al.* (1991) observed; and suggests the results given here are more representative of what might happen under natural rainfall. Although we add the caveat that degraded topsoil structure can cause local ponding and preferential flow even at low rainfall intensities. Structure degradation can be caused, for example, by animal treading, or reduced humus levels, as occurs in orchard spray strips.

The large variability in the strontium concentration of the 25 mm diameter small cores indicates the scale at which hydrodynamic dispersion is occurring is larger than the core diameter. The measured dispersivity of about 73 mm provides an indication of this scale. It might be argued soil cores should be larger in volume than λ^3 if individual cores are to encompass most of the local variability in solute concentration.

5.3.6.1 Conclusions

At a rainfall intensity of 10 mm h^{-1}, the transport of surface applied chemicals through a fine sandy loam growing short pasture could be adequately described by combining the Richards' equation, the convection dispersion equation, and equations describing ion

exclusion or exchange. This was true whether the topsoil was wet or dry when the chemical was applied.

It is suggested the preferential flow reported in earlier studies was due to incipient ponding caused by high instantaneous water application rates. It is also suggested soil cores need to be larger in magnitude than λ^3 (where λ is about 73 mm in our experiments) for most of the local variation in solute concentration to be encompassed within each sample.

Acknowledgments

We thank Edward Young (Cranfield University, Silsoe, England) for helpful comments on an earlier draft of this paper. This research was supported by NSOF 96-170 "Partitioning chemical into either uptake or despatch".

5.4 Bolt's Approach and Anion Transport

The approach of Bolt (1982) to describe solute dispersion was introduced in Chapter 2. In this approach solute dispersion is described by a diffusion/dispersion length parameter, L_D. Assuming that longitudinal molecular diffusion is negligible, L_D is the sum of the dispersion length parameter, L_{dis}, and a mobile/immobile exchange length parameter, L_{mim}. It was shown how the parameters from the CDE and the MIM may be related to each other. Now a test is conducted of the validity of this approach using the model parameters obtained for the various column experiments described above in Sections 5.2 and 5.3. The parameters for the various columns are given in Table 5.2, where L_D (CDE) equals the dispersivity (λ) obtained by fitting the CDE to the data. The dispersion length parameter, L_{dis}, equals the dispersivity in the mobile water (λ_m) obtained from the MIM. Also given are the values for the mobile/immobile exchange length parameter, L_{mim}, calculated from equation [2.38], and L_D (MIM), as the sum of L_{dis} and L_{mim}. The values of the diffusion/dispersion length parameter L_D obtained from the CDE, and calculated from model parameters obtained from the MIM and using the

approach of Bolt, agree well for the columns with a bare soil surface (column A and B). Considering that the model parameters α and θ_i and L_{dis} for the two columns under pasture were not fitted, but taken from the columns under bare soil surface, the agreement between the L_D values obtained from the CDE and the MIM is also reasonable for the columns under pasture (column I and II).

Table 5.2: Parameters from column leaching experiments on Manawatu fine sandy loam using the CDE, the MIM, and Bolt's approach.

	Column A	Column B I	Column B II	Column I	Column II
q_w [mm h^{-1}]	3.1	2.9	13.1	9.8	10.5
θ_e [m^3 m^{-3}]	0.414	0.391	0.438	0.360	0.384
L_D (CDE) [mm]	**38**	**36**	**59**	**75**	**71**
θ_i [m^3 m^{-3}]	0.14	0.14	0.14	0.14	0.14
α [h^{-1}]	0.04	0.04	0.04	0.04	0.04
L_{dis} [mm]	20	20	20	20	20
L_{mim} [mm]	9	9	33	37	35
L_D (MIM) [mm]	**29**	**29**	**53**	**57**	**55**

The approach of Bolt (1982) seems to provide a reasonable picture of the microscopic processes inducing solute flow in the soil, provided solute movement is not strongly preferential.

5.5 Overall Conclusions

In the studies above, anion transport through a Manawatu fine sandy loam was described and modelled using the CDE and the MIM. The CDE describe the effluent data obtained from columns under bare soil and under pasture reasonably well. No significant difference in solute transport was found when solute was applied to initially wet or dry soil surface. The dispersivity was found to be only slightly velocity dependent, which means that for most practical implications in the field the use of a constant dispersivity would be appropriate. The dispersivities found under pasture were only slightly higher compared to those obtained from the columns without vegetation. It

was found that about 10% of the water did not participate in anion transport for non-adsorbed anions. This is probably due to anion exclusion from the double layer and results in accelerated leaching through the soil.

Flow interruption indicated some transverse molecular diffusion between faster and slower moving water, which cannot be described by the CDE. The use of the MIM with three different water fractions described the effluent data obtained from the interrupted leaching slightly better. Figure 5.10 shows a simplified picture of a soil which is considered as having "excluded", "quasi immobile", and "mobile" water. Convective flow of water and solutes occurs in the "mobile" water fraction only, and solute exchange between the "mobile" and the "quasi immobile" water occurs by diffusion, which is described here by a first order equation. Anions are excluded from some fraction of the soil water. The question arises as to whether such a picture of a soil is realistic, and if the use of the MIM is justified, or if the use of a simple model, such as the CDE is more appropriate?

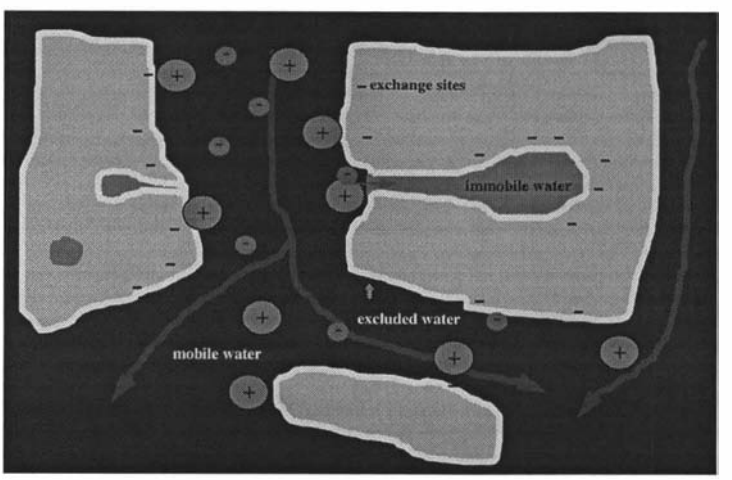

Fig. 5.10 Simplified picture of the soil with mobile, immobile and excluded water.

If the transport of the accompanying cations is considered, then it is necessary to consider exchange reactions between the cations on the solid phase and those in the soil solution. Exchange sites are assumed to be associated with both the "mobile" and the "quasi immobile" water domain, and cations are not excluded from the double layer.

The question which now arises is, how are the exchange sites partitioned between the different water domains? This will be assessed in the following chapter.

As with TDR, it is concluded that by adequate replication suction cups can be used to monitor transport of nonreactive solutes. The transport parameters inferred from the TDR data are consistent with the dispersivity being depth independent, at least over the column length of about 300 mm studied. This would imply convective-dispersive, rather than stochastic-convective solute transport. However it must be kept in mind that TDR measurements are highly sensitive to a relatively small soil volume and so plagued by local variabilities within the soil and the flow.

Chapter 6

6. Cation Movement Through Unsaturated Soil

6.1 Introduction

The previous Chapter dealt with the movement of anions through undisturbed soil columns in response to various water flow regimes. The studies were performed on Manawatu fine sandy loam under bare soil, and under pasture. For the Manawatu soil, the convection dispersion equation was found to describe the movement of anions well, and the mobile/immobile concept gave only slightly better predictions when leaching continued after flow interruption. Here the movement of the accompanying cations is described for the same undisturbed soil columns under bare soil. Also described is the movement of both anions and cations through undisturbed soil columns of Ramiha silt loam, and the differences in anion movement found for the two different soils is discussed.

In this chapter it is tested if the CDE coupled with exchange theory, and using the model parameters obtained for anion movement, can be used to describe cation movement. Furthermore it is examined if mobile and immobile regions with rate-limited diffusion to the exchange sites need to be considered when describing cation movement under transient water flow. Aa a previous experiment by Clothier *et al.* (1996) suggested that some of the adsorption sites might be "hidden" from the infiltrating solution, particular attention is given to the fraction of the cation exchange sites accessible to the infiltrating cation species. These issues are addressed in the paper below which has been submitted to the *European Journal of Soil Science*, and in a subsequent section.

Cation transport was modelled using the CDE in conjunction with cation exchange theory. Two different programs, for either homovalent or heterovalent exchange, were written in Quick BASIC, and are presented in Appendix A, Programs 4 and 5.

6.2 Cation Transport During Unsaturated Flow Through Two Intact Soils

By Iris Vogeler, David R. Scotter, Brent, E. Clothier and Russel, W. Tillman

Submitted to *European Journal of Soil Science*

6.2.1 Summary

Leaching experiments on 300 mm long undisturbed soil columns of two contrasting soils were performed to study the movement and exchange of cations. One soil was a weakly-structured alluvial Manawatu fine sandy loam, and the other a well-structured aeolian Ramiha silt loam. About 2000 mm of solutions of 0.025 *M* of $MgCl_2$ and $Ca(NO_3)_2$ were applied at unsaturated water flow rates of between 3 and 13 mm h^{-1}. Solute movement was monitored over several weeks by collecting effluent at the unsaturated base. In the Manawatu soil anion transport was influenced by exclusion from the double layer, whereas in the Ramiha soil anion adsorption occurred. Cation transport was described by coupling the convection-dispersion equation with cation exchange equations. Good simulations of the Mg^{2+} and Ca^{2+} concentrations in the effluent, and on the exchange sites were obtained if 80% of the exchangeable cations, as measured using the 1 *M* ammonium acetate method were assumed to be active. About 400 kg ha^{-1} of native potassium was leached beyond 300 mm in the alluvial soil, but only about 10 kg ha^{-1} leached from the aeolian soil.

6.2.2 Introduction

Leaching of reactive solutes has been well studied (Selim *et al.*, 1987; Brusseau and Rao, 1990), however most research has concentrated on a single species, with the adsorption isotherm described by some functional form. Less attention has been paid to the leaching of multiple cations, despite the importance of competition. Cation transport is controlled by exchange reactions between the soil solution and the exchange sites associated with the soil matrix (Schulin *et al.*, 1989). Early cation studies ignored competitive reactions between various cations in the soil system (Biggar and Nielsen, 1963; Lai *et al.*, 1978). Later work combined cation exchange theory, generally based on binary systems, with the convection-dispersion equation (CDE) (Robbins *et al.*,

1980), or the mobile-immobile model (van Eijkeren and Lock, 1984). The various approaches for incorporating cation exchange theory into solute transport models have been reviewed by Selim *et al.* (1990). Several authors have applied exchange theory to describe successfully cation transport in repacked soil columns (Persaud and Wierenga, 1982; Selim *et al.*, 1987; Schulin *et al.*, 1989; Bond and Phillips, 1990b; Grant *et al.*, 1995). Except for the work of Jardine *et al.* (1993) on strontium and cobalt leaching, cation transport during unsaturated flow through undisturbed soil seems to have escaped attention, despite unsaturated flow being the norm in field soils.

Models based on nonequilibrium cation exchange have often been found to give better results than models assuming equilibrium exchange with the CDE (Selim *et al.*, 1987; Schulin *et al.*, 1989). This is not surprising, given at least two more fitting parameters are involved. Contrasting opinions on the type of nonequilibrium can be found in the literature. While some authors assume spatial nonequilibrium (Schulin *et al.*, 1989), others attribute nonequilibrium to kinetically controlled chemical processes (Jardine *et al.*, 1993). The equations for both mechanisms are effectively of the same form. Regardless of the assumptions made, the accuracy of the various models depends on the availability of soil property data, which for cation transport include the cation exchange capacity and selectivity coefficients for the various systems. These properties are generally determined from independent measurements with mixed success. Alternatively they can be inferred from leaching experiments on undisturbed soil columns (Jardine *et al.*, 1988). The frequent failure of models using independently-derived parameters to predict cation transport, through even repacked soils (Schweich *et al.*, 1983) however suggests that more than non-equilibrium is involved.

Here we describe the movement of cations through two contrasting soils, an alluvial fine sandy loam and an aeolian silt loam. The soils have quite different cation exchange capacities, and also display different amounts of hydrodynamic dispersion during unsaturated flow (Chapter 5). Cation transport is described by coupling the convection dispersion equation with exchange theory. We consider what fractions of the cation exchange sites, as measured by the standard ammonium-acetate method, are involved in

solute transport of calcium and magnesium. Also we briefly describe the movement of the associated anions, and that of the indigenous potassium.

6.2.3 Theory

Reactive solute transport during steady-state flow is often described by the convention-dispersion equation, written here as,

$$\theta \frac{\partial C_s}{\partial Q} + \rho_b \frac{\partial S_s}{\partial Q} = \lambda \frac{\partial^2 C_s}{\partial z^2} - \frac{\partial C_s}{\partial z}. \qquad [6.1]$$

where θ is the volumetric water content, C_s is the soil solution concentration of ion species s [mol m^{-3}], Q is the cumulative infiltration [m], ρ_b is the bulk density [kg m^{-3}], S_s is the concentration of ion s on the solid phase of the soil [mol kg^{-1})], λ is the dispersivity [m], z is depth [m].

The most commonly used expression to describe the amount of a particular anion adsorbed (or excluded) by the soil assumes linear sorption over the concentration range of interest. Thus for anions we assume (Hutson and Wagenet, 1995)

$$S_s = K_d C \ , \qquad [6.2]$$

where K_d is the distribution coefficient [m^3 kg^{-1}], positive for adsorption, negative for exclusion. The effect of anion adsorption is then to retard or advance the movement of solute front by the factor R, defined as $1+ \rho_b / \theta K_d$. Given linear sorption, the solute front shapes are the same for both nonreactive and reactive solutes. In some soils the anion exchange capacity depends on the ionic strength of the soil solution. This has been observed in allophanic soils with variable charge above a characteristic pH (Parfitt 1980; Bolan *et al.* 1986). We then assume a linear relationship between K_d and the ionic strength (I) given by,

$$K_d = a\, I \quad . \qquad [6.3]$$

where a is some constant [$m^3\ kg^{-1}$].

Cation movement is described by incorporating an exchange model into the solute transport equation (Robbins *et al*, 1980). To avoid the complexity of multi-ion systems, cation exchange is modelled as a binary system, and this is done in one of two ways.

1. Homovalent exchange: The first is used when a homovalent system, with calcium and magnesium ions only, is considered. Then the exchange capacity is partitioned simply as

$$X_{CEC} = X_{Ca} + X_{Mg} \ , \qquad [6.4]$$

where X_{CEC} is the cation exchange capacity of the soil solids [$mol_c\ kg^{-1}$], and X_{Ca} and X_{Mg} are the charge concentrations of adsorbed calcium and magnesium respectively [$mol_c\ kg^{-1}$]. The exchange sites occupied by cations other than magnesium were assumed to be part of the X_{Ca} for the purpose of this analysis. Note that for bivalent cations S_s equals 2 X_s, where X_s is the charge concentration of the adsorbed cation species. The cation exchange capacity (CEC) is generally assumed to be constant (van der Zee and Destouni, 1992), however for variable charge soils the CEC increases with both the ionic strength (I) and pH (Parfitt, 1980; Bolan *et al.* 1986; Nahakara and Wada, 1994). We assume here a linear relationship between CEC and I. Here, where pH changes are only due to a change in I, the CEC can be given as a function of I,

$$X_{CEC} = c + d\, I \qquad [6.5]$$

where c and d are empirically-determined constants [$mol_c\ kg^{-1}$].

Cation exchange reactions are generally assumed to be instantaneous and reversible (Bond and Phillips, 1990a), which allows the use of equilibrium equations. Many such equations have been proposed, with the mass action, Kerr, Vanselow or Gapon

equations being perhaps the most common (Bohn *et al.*, 1985). As calcium and magnesium ions are both bivalent, in this case it matters little which equation is used. If it is assumed that the activities of calcium and magnesium are equal, and that the activities for both the solution and the adsorbed phase are proportional to their relative concentrations, then all four approaches mentioned above reduce to the simple linear equation

$$K_{\text{Ca-Mg}} = \frac{C_{\text{Ca}} X_{\text{Mg}}}{C_{\text{Mg}} X_{\text{Ca}}} , \qquad [6.6]$$

where $K_{\text{Ca-Mg}}$ is the dimensionless selectivity coefficient for calcium - magnesium exchange. We assume this to be constant over the concentration range of interest. Note that equation [6.6] implies a non-linear adsorption isotherm (e.g. relationship between C_s and S_s) when $K_{\text{Ca-Mg}} = 1$. So cation exchange not only retards movement, it also changes the shape of the breakthrough curve (or distribution with depth curve).

2. Heterovalent exchange: The second approach we use to model cation exchange is to describe the leaching of the native monovalent potassium that is initially present in the soil. Following US Salinity Lab Staff (1954) and Tillman and Scotter (1991a), we treat calcium and magnesium as a single species, and from the Gapon equation we get

$$K_{\text{K-CM}} = \frac{X_{\text{CM}} C_{\text{K}}}{X_{\text{K}} \left(C_{CM}\right)^{1/2}} , \qquad [6.7]$$

where $K_{\text{K-CM}}$ is the selectivity coefficient for potassium and the combined bivalent cations. The subscript K indicates potassium concentrations, and the subscript CM indicates calcium plus magnesium concentrations. The small fractions (< 5%) of the exchange sites occupied by of Na^{2+} were included in X_{CM} for the analysis. As Bohn *et al.* (1985) comment, the Gapon equation "adequately predicts cation-exchange behaviour over practical ranges for many soil systems". In this case, by adding in potassium, we get

$$X_{CEC} = X_{CM} + X_K \ . \qquad [6.8]$$

An explicit finite-difference scheme, similar to that used by Tillman and Scotter (1991a) was used to solve simultaneously the above set of equations (6.1-6.8), subject to the appropriate boundary and initial conditions described later.

6.2.4 Methods and Materials

Leaching experiments were performed on undisturbed soil columns under unsaturated flow conditions. The leaching apparatus used for the experiments has already been described by Magesan *et al.* (1995). Gravity-induced unsaturated flow was obtained by applying the same pressure head to both the top and bottom of the columns. Two different soils were studied. One was the alluvial Manawatu fine sandy loam (a Dystric Fluventic Eutrochrept), a weakly-structured soil with a bulk density of about 1.35 Mg m^{-3}, a relatively high cation exchange capacity (CEC), with mica as the dominant clay mineral of the clay fraction, and an organic matter content of about 3% (pers. comm. J.S. Whitton). The other was the aeolian Ramiha silt loam (an Andic Dystrochrept), a strongly-aggregated soil with a bulk density of about 0.89 Mg m^{-3}, a moderate CEC, a higher organic matter content of about 12% with a distinct decrease from 16.5 % in the upper soil profile to 6.2 % at a depth of 400 mm. There is also some allophanic material (Pollok, 1975), and mica-minerals (Parfitt *et al.*, 1984). Free standing soil columns 120 mm in diameter, with lengths ranging from 270 to 340 mm, were carved from the soil profile after removing the top 20 mm. The duplicate columns of each soil will be referred to as A and B for the Manawatu soil, and C and D for the Ramiha soil. Suction cups 95 mm long and 3 mm in diameter were inserted horizontally near the base of column A and B.

Disk permeameters set to a pressure head of -70 mm, resulting in average flow rates of about 3 mm h^{-1}, were used to apply first a solution of 0.0025 *M* $Ca(NO_3)_2$, and then a solution of about 0.025 *M* $MgCl_2$ to the columns. For columns A and B, leaching with $MgCl_2$ was continuous, however for columns C and D leaching was interrupted after an infiltration of 166 and 133 mm, and then restarted 12 h later. Columns A, C and D were

then sliced into 30 mm-thick horizontal sections and weighed. Lastly, subsamples were taken for gravimetric determination of water content and chemical analysis. Column B was left to equilibrate for 7 days before again being leached with the same solution. The pressure head at the top and bottom of the column was then increased to -3 mm, resulting in a flow rate of about 13 mm h^{-1}. The infiltrating solution was then changed again to 0.0245 *M* $Ca(NO_3)_2$. Throughout the experiment, effluent aliquots were collected, as were samples from the suction cups.

The cation exchange capacity (CEC) at the soil's pH was measured both on subsamples from the soil columns at the end of the experiment, and independently using soil samples taken from adjacent to where the soil columns were collected. The CEC was obtained by adding the adsorbed amounts of the individual cations K^+, Na^+, Ca^{2+}, Mg^{2+}. The quantities adsorbed were found by leaching with 1 *M* ammonium acetate (Blakemore *et al.*, 1987). Correction for the cation concentrations in the soil solution was performed by using a technique similar to that described by Elkhatib *et al.* (1987). This involved centrifuging subsamples of the soil straight after sampling, at 10000 RPM for 45 min. The concentrations of K^+ and Na^+ were determined by flame emission spectrophotometry, and those of Ca^{2+} and Mg^{2+} by atomic adsorption spectrophotometry. The soil solutions were extracted for chloride using 0.05 *M* K_2SO_4 and for nitrate using 2 *M* KCl. Chloride was measured using a Tecator Flow Injection analyzer, and nitrate using a Technicon Autoanalyser.

6.2.5 Results and Discussion

6.2.5.1 Cation Exchange Capacity and Selectivity Coefficients

The ammonium-acetate measured cation exchange capacity at soil pH, as a function of depth for the two soils is shown in Figure 6.1(a). For the Manawatu soil there is virtually no difference between the values found in the columns at the end of the experiment, and in the values measured on the samples taken adjacent to where the soil columns were taken.

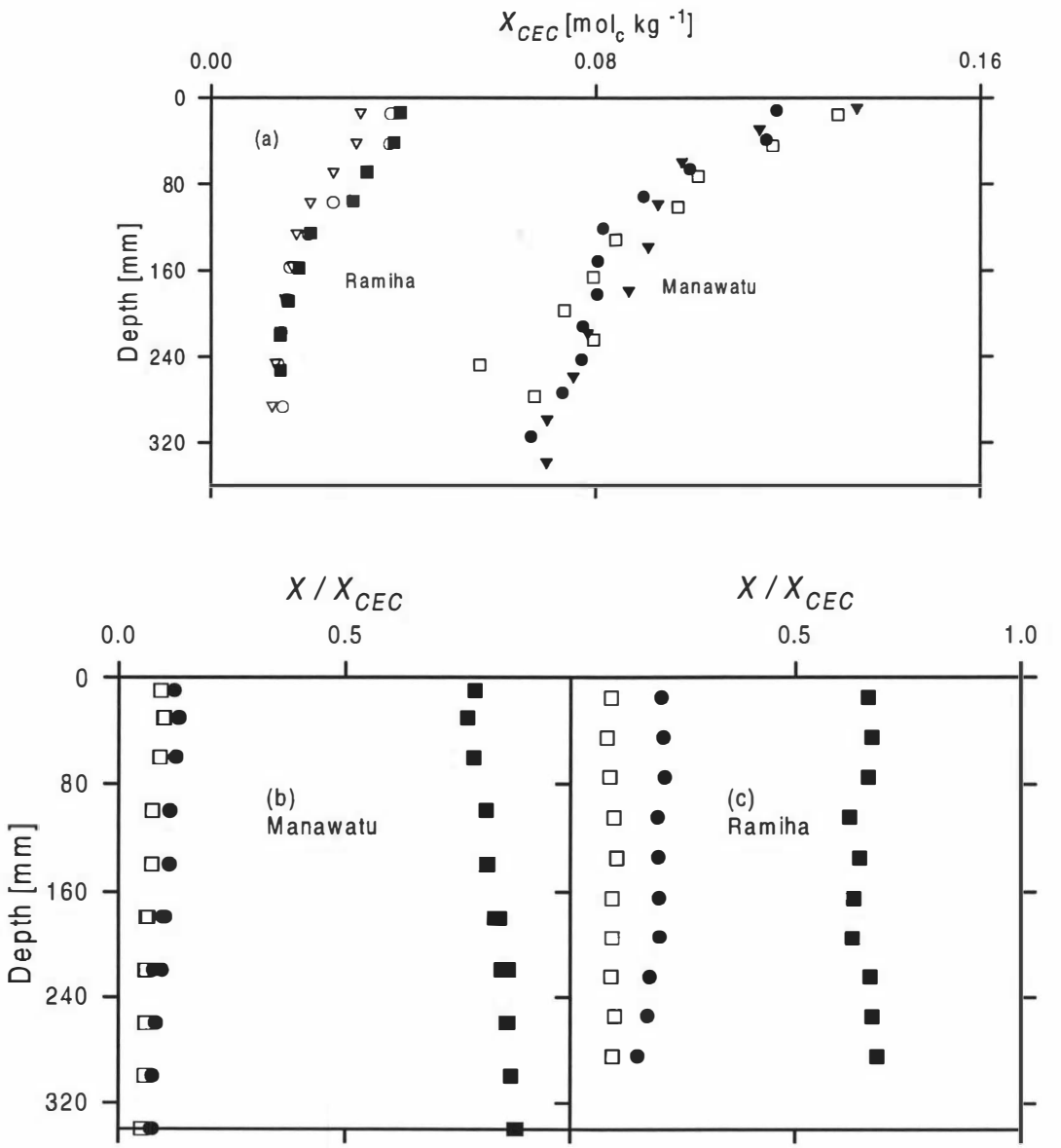

Fig. 6.1 (a) Ammonium-acetate measured CEC, at the soil's pH, as obtained for column A (●), column B(□), column C (○), and D (■), and independent measurements from the field for Manawatu (▼) and Ramiha (▽) soil as a function of depth. Figures (b) and (c) Initial relative concentrations of exchangeable cations from field measurements, Ca^{2+} (■), Mg^{2+} (●) and K^{+} (□).

As the ionic strength at the conclusion of the experiment was about 0.075, and in the other samples about 0.004, this indicates that the CEC was independent of the external soil solution concentration, at least over the range of interest. However in the Ramiha top soil, the cation exchange capacity increased with the external solution concentration.

In allophanic soils with variable charge, both anion (AEC) and cation (CEC) exchange capacity are dependent on both solution pH and ionic strength (Parfitt, 1980, Chan *et al.* 1980). Separate pH measurements in the Ramiha soil showed an increase from pH 4.9 when measured in 0.0025 *M* $Ca(NO_3)_2$ to pH 5.4 when measured in 0.025 *M* $MgCl_2$. The difference in CEC between the soil column samples and field soil samples is probably due to the combined effect of the differences in pH and solution concentration, as suggested by Chan *et al.* (1980). In both soils, the CEC decreased with depth, reflecting the decreasing organic matter. Note that the CEC of the Manawatu soil is approximately three times as high as that of the Ramiha soil. The average ammonium-acetate measured CEC of the Manawatu soil was found to be 0.088 $mol_c\ kg^{-1}$. For the Ramiha soil the average CEC increased from 0.020 $mol_c\ kg^{-1}$ at *I* of 0.003, to a CEC of 0.024 $mol_c\ kg^{-1}$ at *I* of 0.075. However the increase in CEC with solution concentration was confined to the top 100 mm of the soil. Similar increases in both cation and anion exchange capacity with increasing ionic strength (*I* ranging from 0.003 to 0.3) were found by Ishiguro *et al.* (1992) and by Katou *et al.* (1996) in allophanic andisols. The magnitude of the CEC has a great effect on the movement of surface applied cations, as will be shown later. The relative amounts of Ca^{2+}, Mg^{2+} and K^+ initially on the exchange sites were determined from measurements on the independently-taken soil samples, and these are shown in Figure 6.1(b) and (c). The dominant cation on the exchange sites was Ca^{2+} for both soils.

Figure 6.2 shows the measured relative concentration of cations on the exchange sites and also in the soil solution for the Manawatu soil. These are plotted in such a way that the selectivity constants in Equations [6.3] and [6.4] can be evaluated. The slope of the least-squares-fitted straight line through the origin gives the constant, presented in Equation [6.6]. The circles in Figure 6.2 represent measurements obtained from the column leaching experiments, and the triangles those obtained from independent measurements on the field samples. For evaluating the selectivity coefficients only the data from the columns were used as they were more consistent. The scatter in the field data for the binary Ca-Mg system (Figure 6.2a) might be due to interaction between Mg^{2+} and K^+ when they are at similar concentrations (Figure 6.1b). The relationships for the column data are approximately linear over the concentration ranges studied, which

justifies the assumption of constant selectivity coefficients. A $K_{Mg\text{-}Ca}$ value of 0.70 was obtained, which is within the range of values between 0.6 to 0.9 generally found (Freeze and Cherry, 1979). The stronger affinity of soil for Ca^{2+} has been attributed to hydration making the Mg^{2+} cation larger than Ca^{2+} (Bohn *et al.*, 1985). In the case of the K-(Ca+Mg) system a $K_{K\text{-}CM}$ value of 3.1 $(mol\ m^{-3})^{1/2}$ was found, which is about a third of the value found by Robbins *et al.* (1980), and suggests that this soil has a higher preference for K^+.

Due to the low soil solution concentrations of Ca^{2+} and K^+ in the Ramiha soil at the end of the leaching experiment, the above method for obtaining selectivity coefficients could not be used.

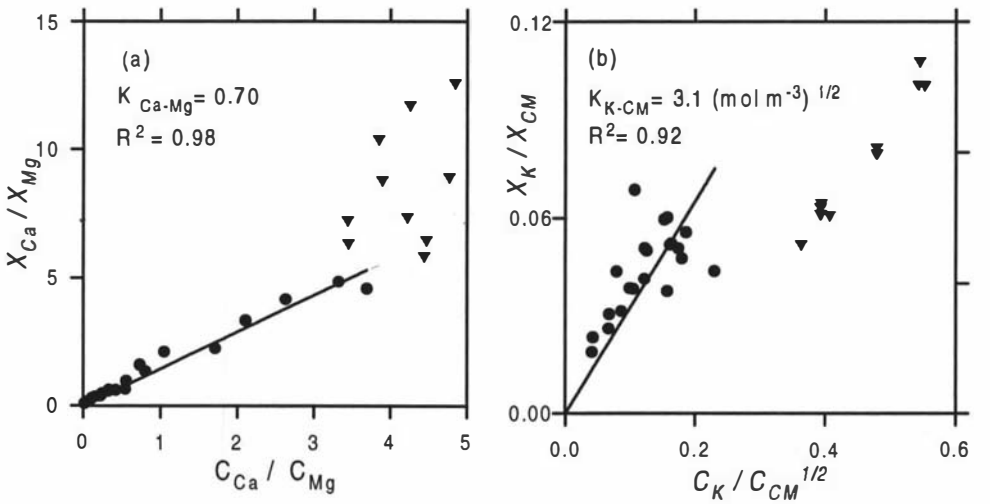

Fig. 6.2 Relative amounts of charge on the exchange sites balanced by different cations as a function of the relative concentration in the soil solution for (a) the Ca-Mg-system, and (b) the K-(Ca + Mg)-system for the Manawatu fine sandy loam. Circles present column data and triangles field data.

6.2.5.2 Anion Movement

The normalised anion concentrations measured in the effluent, after leaching started with either 0.025 *M* $MgCl_2$ or $Ca(NO_3)_2$ are shown in Figure 6.3. In the Manawatu soil, at a flow rate of about 13 mm h^{-1}, a drop in concentration was observed when leaching was interrupted for 12 h. This can be attributed to "immobile" water into which solutes

move by diffusion only (Chapter 5). For the Ramiha soil the rise in concentration was continuous, even when leaching was interrupted for 12 h.

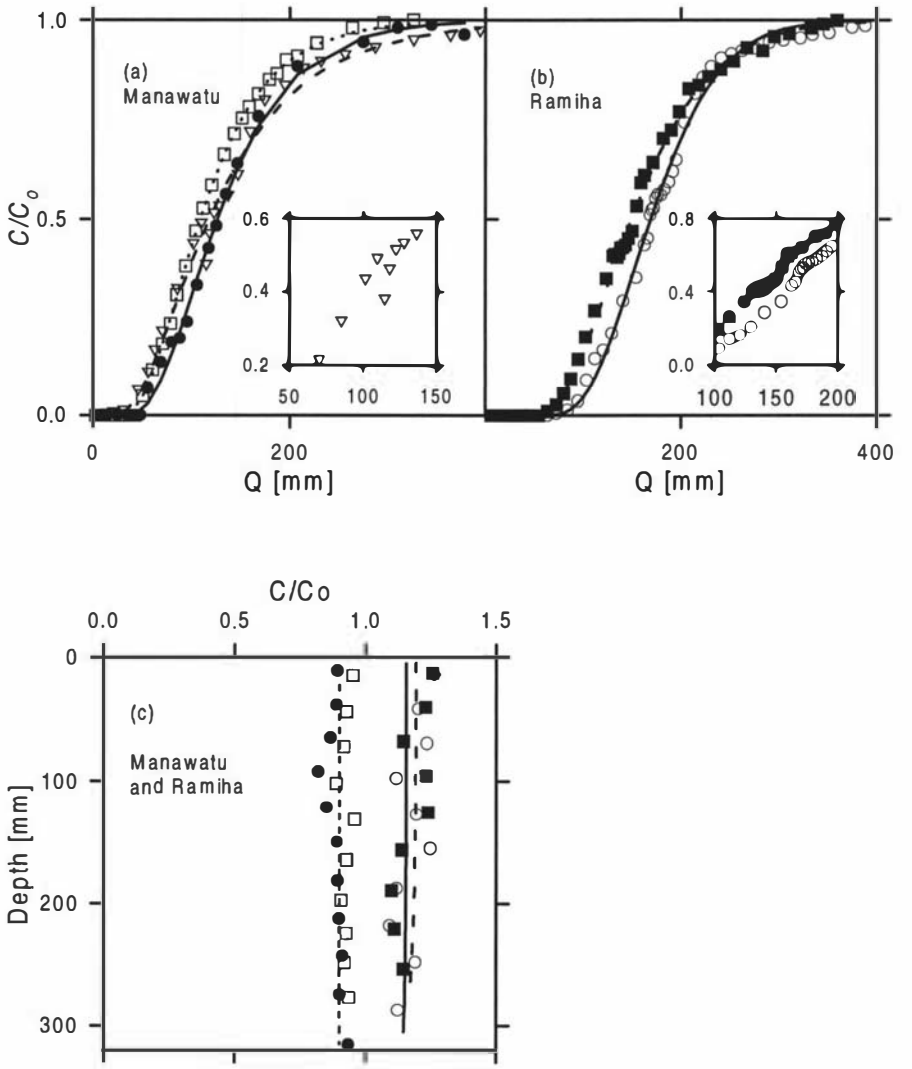

Fig. 6.3 Normalized anion breakthrough data during leaching and prediction using the CDE (a) for Manawatu soil column A (● and solid line), and column B (□, and dotted line for flow rate of 3 mm h^{-1}, and ▽ and broken line for flow rate of 13 mm h^{-1}), and (b) for Ramiha soil for column C (○ and solid line), and column D (■ and broken line). (c) resident anion concentrations as a function of depth for Manawatu soil for column A (●), and column B (□), and Ramiha soil for column C (○), and column D (■). Also shown are the predictions for column A and B (dotted line), and for column C (solid line) and column D (broken line). Insets give expanded views of the effect of the 12 h pause in leaching.

These different behaviours observed for the two soils might be due, in part, to the different flow rates during the intermittent leaching events, of about 2.5 mm h^{-1} for the Ramiha soil, and 13 mm h^{-1} for the Manawatu soil. In the Ramiha soil at the slow flow rate, diffusion into the "immobile" water was apparently fast enough to eliminate effectively the concentration gradients between the two water domains. In the Manawatu soil, however, under a faster flow rate, diffusion could not eliminate the concentration gradients during flow.

Apart from the flow rate, the spacings between domains of different mobilities might also determine the exchange between domains. If the Ramiha soil, a soil with a better structure, is then visualised as having closer connections between the mobile and immobile domains as compared to the Manawatu soil, it could be assumed that all the water in the Ramiha soil would appear mobile, as suggested by Clothier *et al.* (1996).

Retardation of chloride was observed in the Ramiha soil, presumably due to the presence of some allophanic material. A similar retardation was also detected by Time Domain Reflectometry as ionic strength increased (section 4.1), which implies that the anion exchange capacity increases with an increase in the external solution concentration. Furthermore, as even at low ionic strength of 0.003 and a pH of 4.9 some anion adsorption can be expected, it seems that at low ionic strengths exchange between Cl^- and the initially adsorbed anions is negligible. This would be the case for exchange with specifically adsorbed anions such as sulfate and phosphate (Marsh *et al.*, 1987). That sulfate can be retained preferentially relative to Cl^- was also found by Black and Waring (1979) in a study on soils containing allophane.

Also shown in Fig. 6.3 are the predictions using the CDE. Dispersivities found for the Manawatu soil were 38 mm (column A) and 36 mm (column B), with a K_d of -3.4×10^{-5} m^3 kg^{-1} due to anion exclusion. For the Ramiha soil dispersivities of 15 mm (column C), and 10 mm (column D) were found, and assuming linearly increasing adsorption with external solution concentration (Equation 3), values for a of 1.4×10^{-3} m^3 kg^{-1}, and 1.2×10^{-3} m^3 kg^{-1} for columns C and D, respectively. The different dispersivities found for these two soils are similar to the values found by

Magesan *et al.* (1995), and probably reflect the contrasting structures of these soils. Note, however, that erroneously assuming a constant K_d leads to higher values of the dispersivity. This shows the importance of accurately describing the adsorption processes when obtaining transport parameters such as the dispersivity.

The dimensionless resident soil solution concentrations at the end of leaching are shown in Figure 6.3c. Note that C_o is the anion concentration in the applied solution. For the Manawatu soil average C / C_o values of chloride (column A) and nitrate (column B) were found to be only about 0.90, despite column A having being leached with over 1000 mm of chloride solution. As the predicted lines show, this is consistent with anion exclusion from the diffuse double layer (section 5.2), and the negative K_d value found here from the breakthrough curves. In contrast, for the Ramiha soil average C / C_o values of about 1.2 were found, which are also consistent with predictions obtained using the positive K_d values inferred from the effluent data.

6.2.5.3 Calcium and Magnesium Outflow

The concentrations of Ca^{2+} and Mg^{2+} in the column effluent are shown in Figure 6.4. The increase in the total concentration of the invading solution and the simultaneous replacement of Ca^{2+} by Mg^{2+} on the exchange sites can be seen to result in an initial rise in the Ca^{2+} concentration of the effluent, followed then by a decrease. This phenomenon has been termed "the snow-plow effect" (Starr and Parlange, 1979), and is due to the increasing charge of the anions in the effluent solution being first balanced by calcium coming off the exchange sites, and then later by the applied Mg^{2+}. The peak concentrations of Ca^{2+} in the Manawatu soil were about twice as high as in the Ramiha soil. This reflects the different CECs for these soils (Figure 6.1a). Furthermore even after a total infiltration of 1000 mm of $MgCl_2$ into the Manawatu soil, the Ca^{2+} concentrations in the effluent are still relatively high, whereas in the Ramiha soil the Ca^{2+} concentrations in the effluent were less then 1 mol m^{-3} after just an infiltration of 500 mm of $MgCl_2$ solution. From the effluent data, the values for the resident concentrations in Figure 5, and the initial concentrations in Figure 1, the mass balance for Ca^{2+} and Mg^{2+} during the experiments was calculated to be between 99% and 104%.

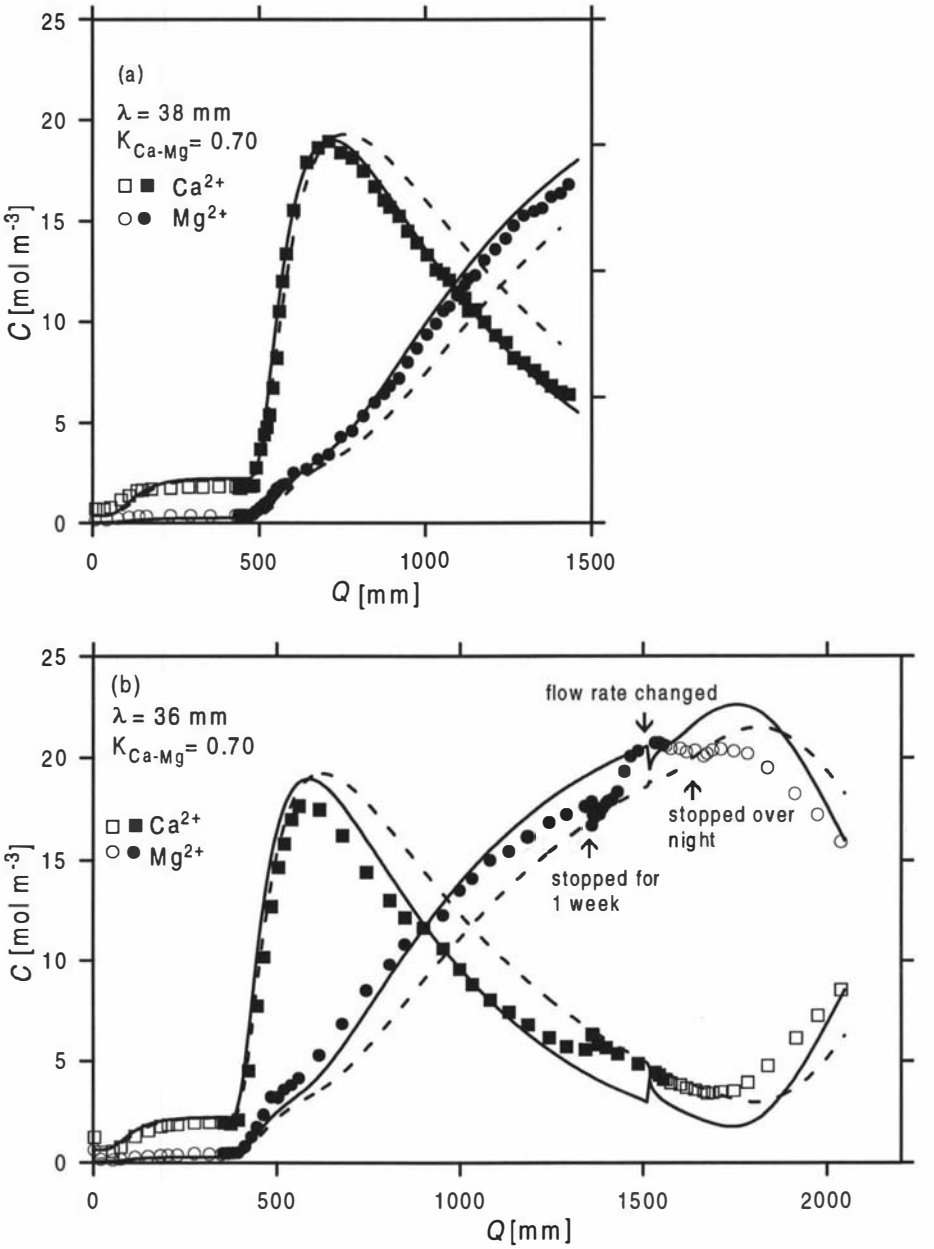

Fig. 6.4 Effluent concentrations of Ca^{2+} (□ and ■) and Mg^{2+} (○ and ●) as a function of cumulative infiltration Q (a) column A, and (b) column B of Manawatu fine sandy loam. Open symbols indicated leaching with $Ca(NO_3)_2$ solution and closed circles with $MgCl_2$ solution. Also shown are the simulations assuming the total measured CEC is involved (dashed lines) and only 80% of the ammonium-acetate measured CEC is involved (solid lines).

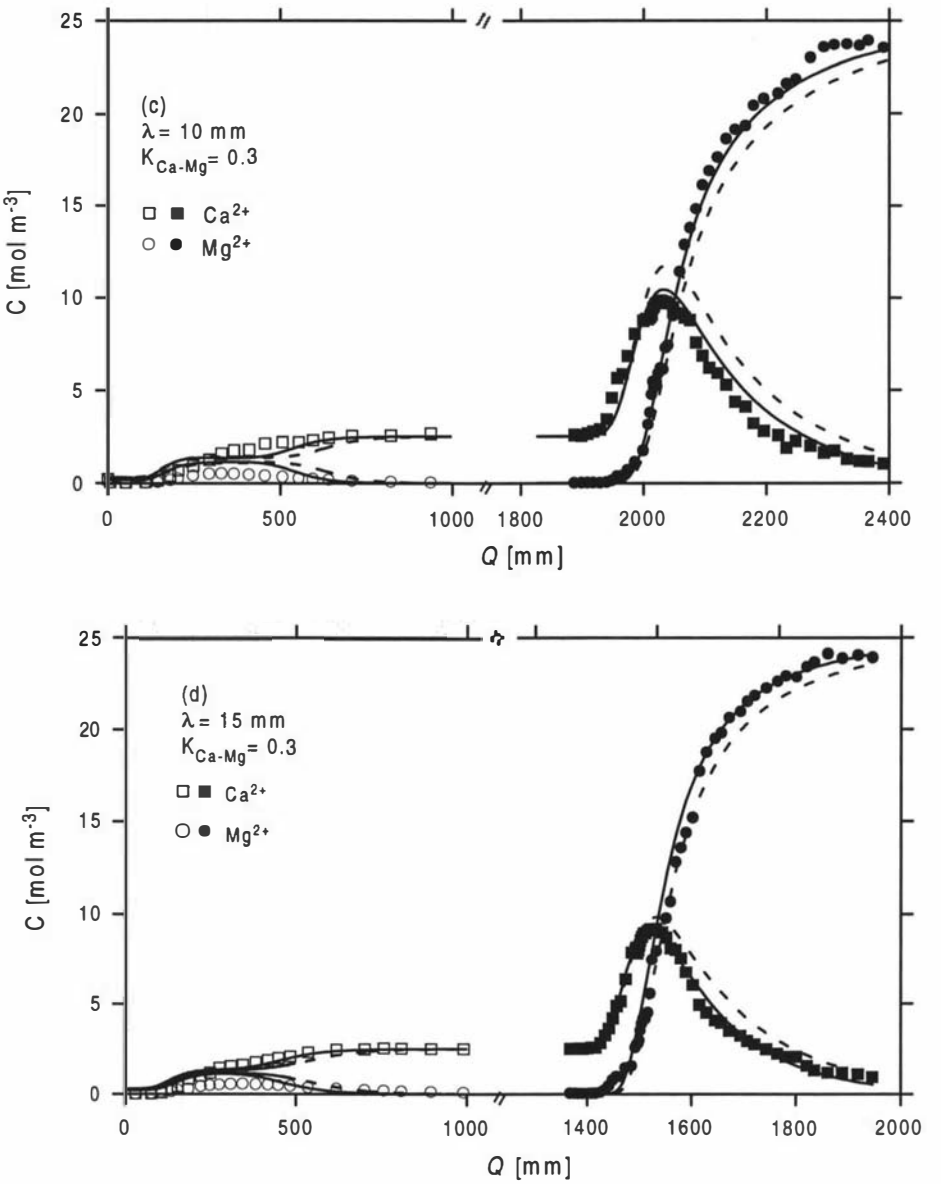

Fig. 6.4 Effluent concentrations of Ca^{2+} (□ and ■) and Mg^{2+} (○ and ●) as a function of cumulative infiltration Q (c) column C, and (d) column D of Ramiha silt loam. Open symbols indicated leaching with $Ca(NO_3)_2$ solution and closed circles with $MgCl_2$ solution. Also shown are the simulations assuming the total measured CEC is involved (dashed lines) and only 80% of the ammonium-acetate measured CEC is involved (solid lines).

The discontinuities in the outflow concentrations in Figure 4b when Q equals 1360 mm are due to the interruption of leaching for a week, suggesting that in the poorly-structured Manawatu soil a local disequilibrium remains between the mobile and immobile water during flow. This is consistent with the drop in anion concentration when leaching was interrupted for 12 h (Figure 6.3a). During the interruption of flow,

molecular diffusion reduced or eliminated this disequilibrium. A fraction of the cation sorption sites being at nonequilibrium has been postulated in many papers (Brusseau and Rao 1990; Schulin *et al.*, 1989; Selim *et al.* 1987).

Also shown in Figure 6.4 are the simulated concentrations, using the dispersivities found for the anion transport, and the selectivity coefficient of 0.7 for the Manawatu soil. For both soils, two simulations are shown. The first assumes that all the effective cation exchange capacity, as measured by the ammonium-acetate method, is "seen" by the percolating soil solution. The poor agreement with the measured values could suggest that the ammonium-acetate measurements overestimate the CEC, or that some exchange sites are not "seen" by the invading solution. However good agreement between measured and simulated data for the Manawatu soil was obtained when it was assumed that only 80% of the ammonium-acetate measured CEC was involved in cation exchange reactions, except after infiltration was interrupted for a week in column B. Perhaps redistribution and longitudinal diffusion during the week-long interruption are the reasons for this discrepancy. Note that during steady flow the CDE with an appropriate dispersivity can take into account effects of the local disequilibrium discussed above (Bolt, 1982).

For the Ramiha soil the selectivity coefficient was not measured independently. Optimization gave best agreement between measured and simulated data when a selectivity coefficient of 0.3, and again a CEC of 80 % of the ammonium-acetate measured value, was assumed. For the Ramiha soil the CEC was assumed to increase with the soil solution concentration as described by equation [6.5]. Due to the variable increase in CEC with depth (Figure 6.1), a separate relationship between CEC and I was used for each layer, with c ranging from 0.014 to 0.030 $mol_c\ kg^{-1}$, and d from 0.003 to 0.122 $mol_c\ kg^{-1}$. The lower selectivity coefficient ($K_{Ca\text{-}Mg}$) for the Ramiha soil compared to the Manawatu soil might be due to the higher organic matter content, and the allophanic material in the Ramiha soil (Hunsaker and Pratt, 1971). Robbins *et al.* (1980) quote a selectivity coefficient for Ca-Mg systems as low as 0.2 for a peat soil. In the Ramiha soil the selectivity for the Ca-Mg system may also be dependent on ionic

strength, as the model slightly overpredicts the concentration of Mg^{2+} in the effluent during preleaching. Selectivity coefficients that vary with the fractional coverage on the exchanger have occasionally resulted in better agreement between experimental data and predictions (Mansell *et al.*, 1988; Grant *et al.*, 1995).

The finding that not all the exchangeable cations, as determined by the ammonium-acetate method, are involved in exchange reactions during leaching with 0.025 *M* $MgCl_2$ warrants further discussion. The higher exchangeable cation content found by the ammonium-acetate method might be either an ionic strength effect, a pH effect, or both. The difference in ionic strength between the 0.075 in the leaching experiment, and the 1 in the ammonium acetate method might result in the dissolution of organic acids by ammonium acetate, which are insoluble at lower ionic strengths. These acids may contain replaceable Ca^{2+} in solution. Likewise the higher pH used in the ammonium-acetate method compared to the leaching experiments, might explain the different effective CEC values. Deviations between the exchangeable concentrations obtained from batch experiments and using the ammonium acetate method, and those inferred from column leaching experiments on repacked soil columns were also found by Schweich *et al.* (1983). They suggested that the deviations might be due to drying the soil and thereby destroying some organic matter. But they might also be due to the lower pH of 5 of the leaching solution.

According to Lanyon and Heald (1982) an overestimation of the cations participating in exchange reactions by the ammonium-acetate method was found in a study by Fisher (1963), with the amount of Mg^{2+} extracted by the ammonium acetate method exceeding that which equilibrated with a radioactive isotope of Mg^{2+}.

6.2.5.4 Resident and Solution Concentrations of Calcium and Magnesium

Figure 6.5 shows the final relative concentrations of (Ca^{2+} + K^{+}) and Mg^{2+} resident upon the exchange sites as a function of depth. In the Manawatu fine sandy loam, despite 1000 mm of $MgCl_2$ solution being applied over 13 days to column A, in the top 20 mm of the soil magnesium occupied only 92% of the exchange sites, as measured by

ammonium acetate extraction. This is consistent with the ammonium acetate method accessing calcium not seen by the invading solution. The degree of saturation with magnesium decreased with depth, and was only 62% at the bottom of the column. For column B the experiment concluded with 500 mm of $Ca(NO_3)_2$ being applied at about 12 mm h^{-1}, resulting in a decreasing Ca^{2+} saturation with depth.

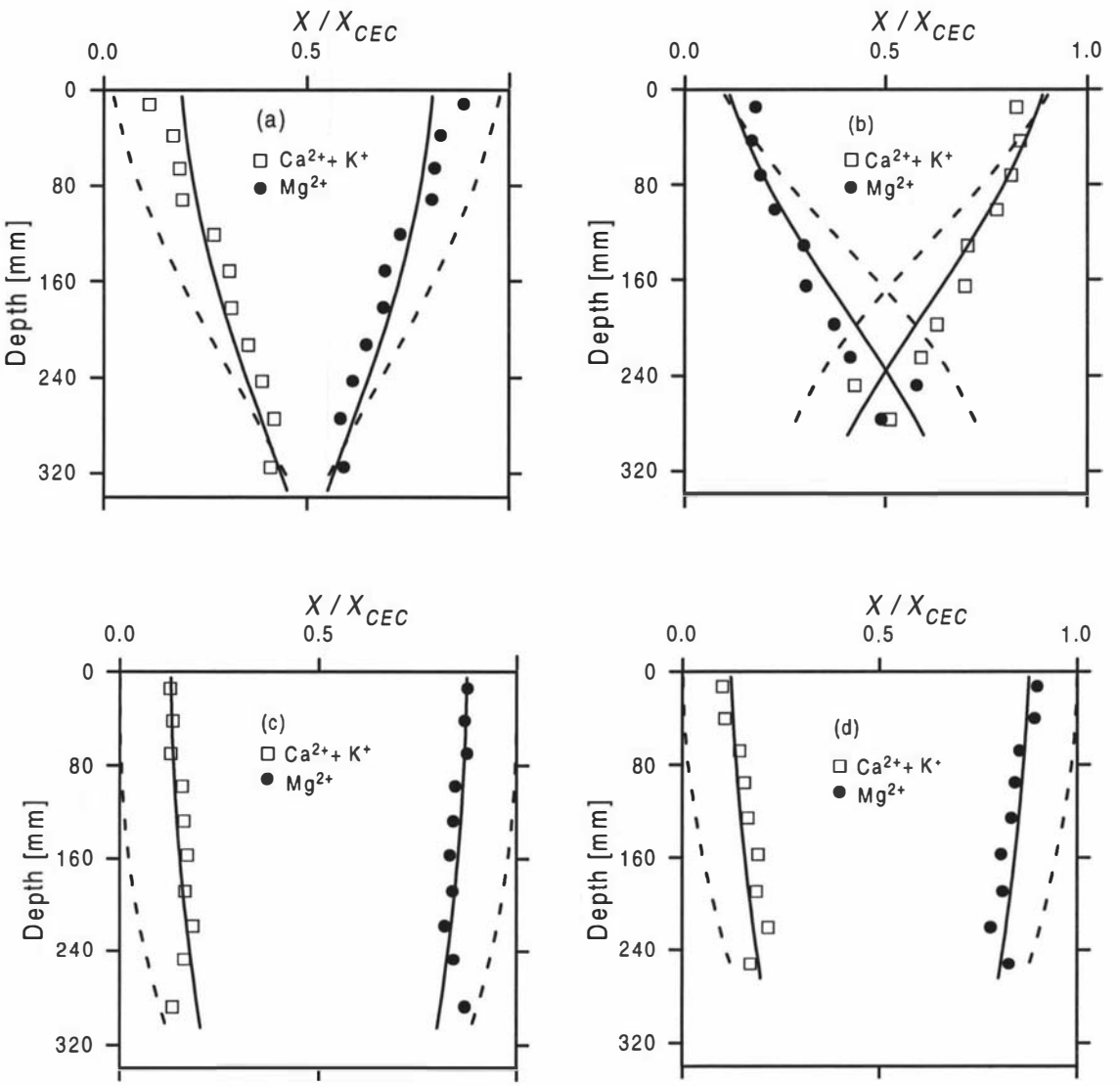

Fig. 6.5 Relative concentrations on the exchange sites of X_{Ca} (□) and X_{Mg} (●) at the end of the experiment for (a) column A, (b) column B, (c) column C, and (d) column D. Also shown are the simulations using 80 % of the measured CEC (solid lines) and 100% of the ammonium-acetate measured CEC (dashed lines).

In both columns of the Ramiha soil after leaching, magnesium occupied only about 85% of the exchange sites as measured using the ammonium-acetate method, the remaining exchange sites appeared to remain occupied by Ca^{2+} and K^{+}. It is more likely however that the ammonium-acetate method was extracting Ca^{2+} and K^{+} , which was not usually exchangeable.

Also shown in Figure 6.5 are the simulations assuming that all, and 80%, of the ammonium acetate measured CEC was active. Again the lower CEC estimates led to much better simulation of the final calcium plus potassium and magnesium distributions.

6.2.5.5 Suction Cup Measurements

The measured and simulated concentrations of calcium and magnesium from the suction cups of the Manawatu soil are shown in Figure 6.6. No suction cups were installed into the Ramiha soil.

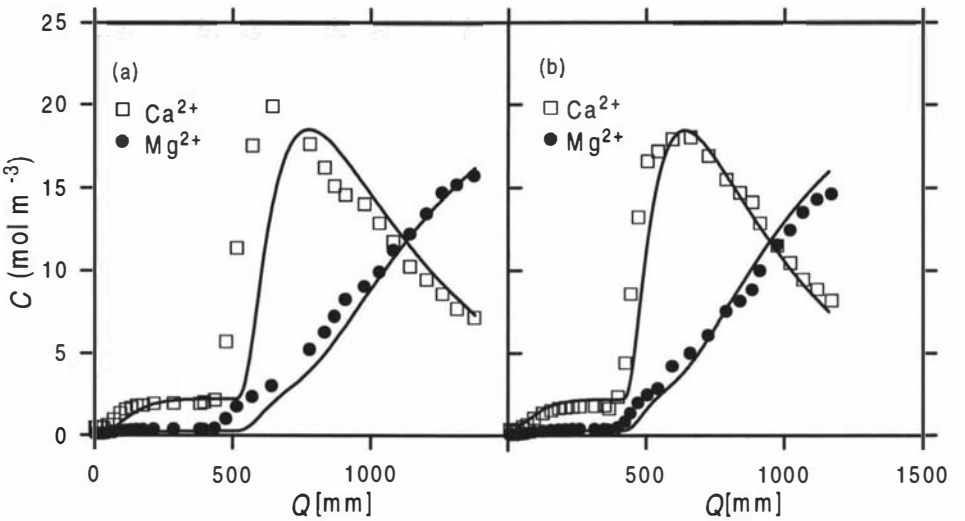

Fig. 6.6 Measured concentrations C from the suction cups for Ca^{2+} (□) and Mg^{2+} (●) as a function of cumulative infiltration Q for (a) column A and (b) column B. Also shown are the simulations using 80 % of the ammonium-acetate measured CEC.

The simulations assume that only 80% of the ammonium-acetate measured exchange sites are involved in cation exchange reactions. The agreement between the measured

and predicted values is reasonable for both columns, except for an initial underestimation of Ca^{2+} concentration for column A. This generally good agreement supports the applicability of suction cups for monitoring cation transport in this soil in the field under unsaturated flow conditions. Adequate replication would be needed to reduce the variability inherent in the use of small cups in a non-uniform porous medium.

6.2.5.6 Leaching of Potassium

Although potassium was not applied, the leaching of the indigenous K^+ was measured. The concentrations in the effluent, and on the exchange sites for both soils, are shown in Figure 6.7. The delay in the peak concentrations for K^+ in the Manawatu soil, relative to those for Ca^{2+} shown in Figure 6.4, is mainly due to the relatively high selectivity for K^+ at these low concentrations. This mechanism cannot however explain the differences between the duplicate columns. Potassium behaves differently to calcium and magnesium. Leaching can induce the release of significant amounts non-exchangeable K^+ (Kirkman *et al.*, 1994), with rate-limiting steps being involved (Sparks and Recheigl, 1982; Havlin *et al.*, 1985; Ogwada and Sparks, 1986). This delay has been attributed to a lack of immediate contact between the leaching solution and the soil particles, due to slow diffusion into or out of poorly expandable clay minerals, such as mica minerals. This rate-limited release of potassium probably explains the discrepancies found between the measurements and simulations in Figure 6.7a. It might also explain the discrepancies between the measurements and the simulations of the final resident concentrations shown in Figure 6.7(b). Due to the low K^+ concentration relative to the bivalent cations, the Gapon equation [6.7] implies an almost linear adsorption isotherm over the relevant concentration range. Thus potassium exchange just retards leaching, but does not effect the slope of the breakthrough curves or the resident distribution pattern.

Figure 6.7 also shows the very low concentrations of potassium in the leachate from the Ramiha soil compared to those in the Manawatu soil, despite Figure 6.1b indicating that the two soils have about the same fraction of the ammonium-acetate measured exchange sites occupied by potassium. Attempts to simulate the leaching of potassium from the

Ramiha soil showed that an unrealistic value of $K_{K\text{-}CM}$ was needed to simulate the measured concentrations.

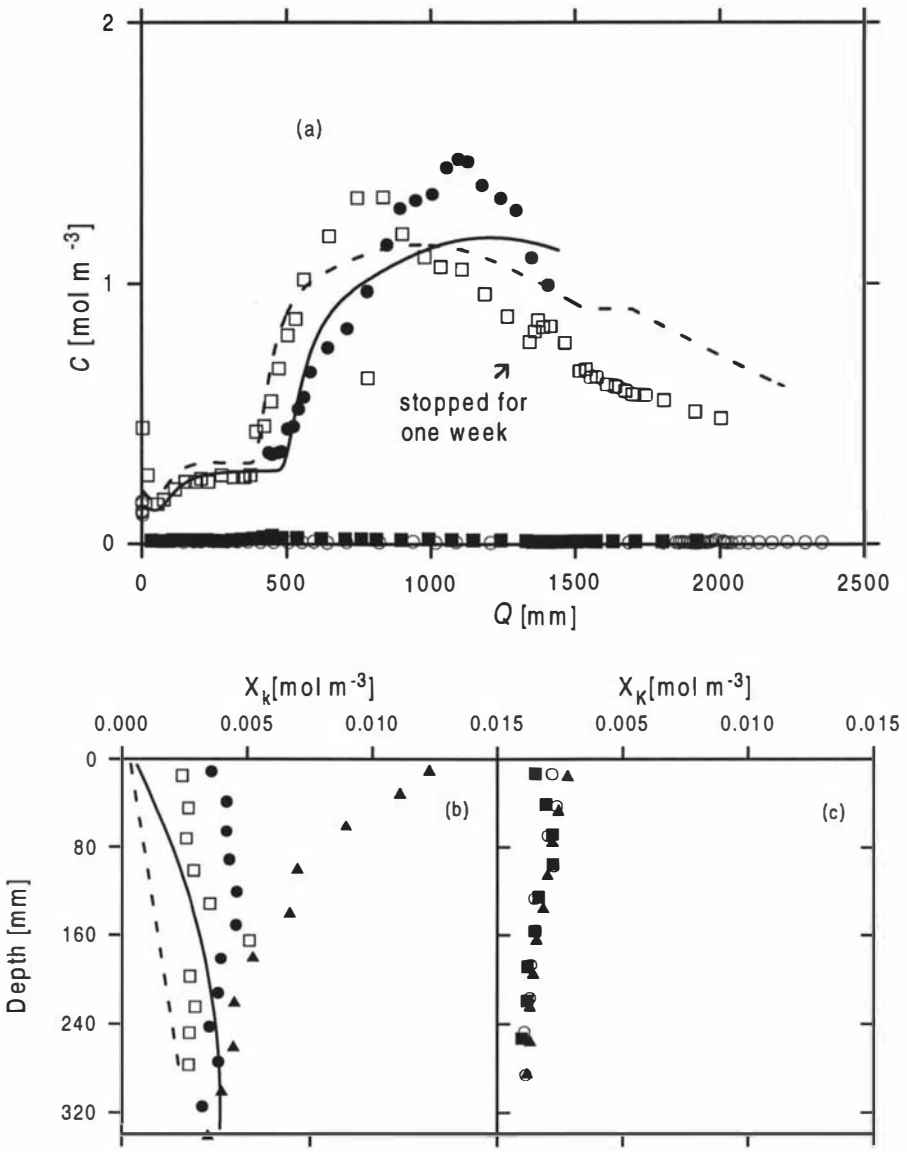

Fig. 6.7 (a) Effluent concentrations for K^+ during leaching with $Ca(NO_3)_2$ solution and $MgCl_2$ solution as a function of cumulative infiltration Q for column A (●), column B (□), column C (○), and column D (■). Also shown for the Manawatu soil are the simulations using 80% of the ammonium-acetate measured CEC, and a $K_{K\text{-}CM}$ value of 3.1 $(mol\ m^{-3})^{1/2}$. (b) Measured concentrations of K^+ on exchange sites for column A (●), column B (□), and initial K^+ concentrations for the Manawatu soil (▼). Also shown are the simulated concentrations for column A (solid line) and column B (broken line). (c) Measured concentrations of K^+ on exchange sites for column C (○), and column D (■),and initial K^+ concentrations for the Ramiha soil (▼).

Average recoveries for K^+ of 108% and 95% were calculated from the effluent and the initial and final resident concentrations for the Manawatu soil and the Ramiha soil, respectively. The high value for the Manawatu soil is consistent with the release of some non-exchangeable potassium. Whereas in the Manawatu soil about 350 to 530 kg K^+ ha^{-1} was leached during the experiment, only 5 to 12 kg K^+ ha^{-1} was leached from the Ramiha soil. Furthermore in the Ramiha soil, the measured exchangeable K^+ concentration (Figure 6.7b) stayed the same before and after leaching. The ammonium-acetate method seems to extract K^+ from the Ramiha soil, which is not truly present at the exchange sites. Martin and Sparks (1983) found similar behaviour for soils with a reasonable amount of vermiculite. They suggest that ammonium salts extract K^+ from specific sorption sites.

6.2.6 Conclusions

The important, and apparently original, finding of this study is that for permeable soils under realistic field flow rates, calcium and magnesium leaching can be simply described using the CDE, and a cation exchange equation. Local physical or chemical disequilibrium, if it occurs, does not need to be explicitly taken into account. However we found that the effective CEC was only 80% of that measured by displacing the soil cations with 1 *M* ammonium acetate solution.

The study also demonstrates the different mechanisms by which cations and anions interact with different soils, and how they affect ion movement. In the Manawatu soil anion exclusion accelerated leaching, whereas in the Ramiha soil anion adsorption retarded it. In the Manawatu soil the CEC was independent of ionic strength, whereas in the Ramiha soil the CEC changed with ionic strength, and this needed to be taken into account.

Leaching of indigenous K^+ was quite different for the two soils. Whereas in the Manawatu the invading $MgCl_2$ solution leached 350 to 530 kg ha^{-1}, in the Ramiha soil only 5 to 12 kg ha^{-1} was leached. The ammonium-acetate extractable K^+ provided a very misleading indication of the exchangeable K^+ in the Ramiha soil.

Acknowledgments

We thank Roger Parfitt of Landcare Research, Palmerston North and Nanthi Bolan of Massey University for helpful comments.

6.3 Cation Movement and the Mobile/Immobile Concept

Cation transport is often believed to be governed by nonequilibrium exchange reactions (Schulin *et al.*, 1989, Selim *et al.*, 1987; Jardine *et al.*, 1993), which are either attributed to a rate limited diffusion to exchange sites within the soil aggregates or to kinetically controlled exchange. In the previous chapter, the mobile/immobile concept (MIM) has been found to describe anion movement through undisturbed soil columns of Manawatu soil under intermittent leaching events only slightly better compared to the CDE (Section 5.2). In the following section the ability of the MIM to describe cation movement through the same soil columns will be assessed. Values for the excluded and immobile water fraction (θ_x and θ_i), the dispersivity in the mobile phase (λ_m), and the mass transfer coefficient between the mobile and the immobile phase (α) were those estimated from the anion data (Section 5.2).

To describe cation movement, an estimation on the distribution of the cation exchange sites between the mobile and the immobile domain is also required. The data were best described assuming that 60% of the exchange sites are associated with the immobile phase, and again assuming that only 80 % of the ammonium-acetate measured exchange sites were involved in cation exchange reactions. That more exchange sites are associated with the immobile phase can be expected, as immobile water is generally assigned to smaller pores, which have a larger surface area. The data and the simulations for the Manawatu soil, column A and B, are shown in Fig. 6.8a and b. Although the model predicts a discontinuity after the interruption of leaching for one week, the drop in concentration of Mg^{2+} and the simultaneous increase in Ca^{2+} could not be described in its full extend.

As for the simulation for anion transport (Section 5.2) little seems to be gained by using the mobile/immobile approach. Considering the additional parameters required for the MIM, which cannot be measured independently, it is concluded that the more simple CDE seems more appropriate for practical applications involving non-ponding unsaturated flow.

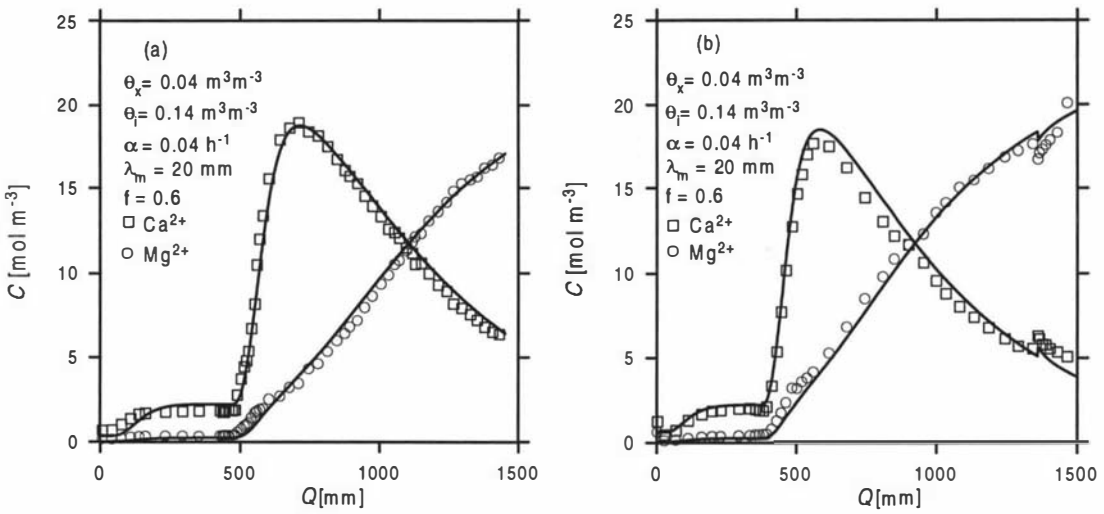

Fig. 6.8 Effluent concentrations of Ca^{2+} (□) and Mg^{2+} (○) as a function of cumulative infiltration Q (a) column A, and (b) column B. Also shown are the simulations using the mobile/immobile approach of the CDE and assuming only 80% of the ammonium-acetate measured CEC is involved (solid lines).

6.4 Overall Conclusions

From these results it can be concluded that cation transport can be described reasonably well using the CDE in combination with exchange theory, based on competitive exchange of two cation species. Assuming diffusion-controlled transfer between mobile and immobile regions resulted in only slightly better predictions for the Manawatu soil during intermittent leaching events. This small gain does not seem to justify the use of the mobile/immobile concept. In the Ramiha soil diffusion into the soil matrix does not seem to be a limiting step in ion transport, at least at the pore water velocities used.

All the cation exchange sites seemed to be accessible to the invading soil solution. This is consistent with the results obtained from the anion transport, where all the water, apart form the double layer water, was found to be involved in solute transport. However it seems that the 1 *M* ammonium acetate method overestimates the CEC involved in cation transport during leaching with solutions with an ionic strength of 0.075. Common ionic strength of soil solutions in New Zealand soils are about an order of magnitude lower than this (Edmeades *et al.*, 1985). So it is suggested that the CEC determined by the ammonium acetate method overestimates the exchange capacity involved in exchange reactions during cation transport in the field.

Chapter 7

7. General Conclusions

The three primary objectives of this study were; firstly to assess the ability of the convection dispersion equation to describe solute transport under various water flow regimes; secondly to study the effect of the initial water content and the vegetative cover on solute transport; and thirdly to assess the feasibility of using time domain reflectometry (TDR) to monitor solute transport. This concluding chapter summarises the findings.

Leaching experiments were performed on two contrasting soils, a weakly-structured Manawatu fine sandy loam, and a well-aggregated Ramiha silt loam. These two soils exhibit quite different solute transport behaviour. In the Manawatu soil anion exclusion from the double layer was observed, thereby accelerating the leaching of nonreactive anions, such as nitrate and chloride. In contrast, in the Ramiha soil anion adsorption was found. In this case, adsorption retards the leaching of all anions. Furthermore in the Ramiha soil, both the anion (AEC) and cation exchange capacity (CEC) increased with increasing external solution concentration. The CEC was constant in the Manawatu soil.

Flow interruption experiments showed that transverse molecular diffusion could effectively dissipate differences in solute concentrations between water flowing at different velocities in the Ramiha soil, but not in the Manawatu soil. These different behaviours might be in part due to the different water flow rate during the intermittent leaching events of about 2.5 mm h^{-1} for the Ramiha soil, and 13 mm h^{-1} for the Manawatu soil. But the local disequilibrium in the poorly structured Manawatu soil between "mobile" and "immobile" water is probably mainly due to a greater spacing between these two water domains in this soil. The well-aggregated Ramiha soil apparently has shorter diffusion distances between the "mobile" and the "immobile" domains, as compared to the weakly-structured Manawatu soil. Thus in the Ramiha soil all the water appears "mobile".

The experimental data were used to examine the capability of the convection dispersion equation (CDE) to describe solute transport under various water flow regimes. The applicability of the mobile/immobile concept (MIM) was also assessed.

The CDE could represent the observed anion concentrations in the effluent satisfactorily for both soils, provided anion adsorption, or exclusion were considered. Dispersivities (λ) found for the two different soils at water flow rates of about 3 mm h^{-1} under a bare soil surface were about 38 mm for the Manawatu soil and 13 mm for the Ramiha soil. These different values probably reflect the contrasting structure of the two soils. Nearly identical dispersivities were found for the duplicate columns of each soil. This suggests that most of the small scale heterogeneity was encompassed in the soil columns, which were about 120 mm in diameter, and about 300 mm in length.

Dispersivities in the Manawatu soil were found to be only slightly dependent on the water flow rate. Values inferred from the effluent data were 37 mm and 59 mm for the two contrasting flow rates of 3 and 13 mm h^{-1} in the same soil column. The higher value found for the higher flow rate is probably due to an increasing disequilibrium between "mobile" and the "immobile" water with increasing flow rate. Under steady-state water flow, the effects of local disequilibrium can be accounted for by using "appropriate" dispersivities. However the observed diffusional exchange between "mobile" and "immobile" water during flow interruption could not of course be described by the CDE.

Although the more complex MIM can, in principle, describe such situations, it gave only slightly better predictions compared to the CDE. Considering the additional transport parameters which need to be estimated in the MIM and the unresolved and perhaps unresolvable problem of how to estimate them, the use of the more simple yet approximately parameterised CDE seems preferable.

Movement of Ca^{2+} and Mg^{2+} could be described well by coupling the CDE with cation exchange theory. However only 80% of the cation exchange capacity (CEC) as measured by 1 *M* ammonium acetate displacement was involved in cation exchange reactions during

leaching with solutions with lower ionic strengths closer to those pertaining in the field. It seems that the ammonium-acetate method extracted Ca^{2+} and K^+ which are not usually exchangeable.

Leaching of indigenous potassium could not be accurately described by the CDE and exchange theory. This was probably due to the misleading indication of the exchangeable K^+ by the ammonium-acetate method in the Ramiha soil, and in the Manawatu soil rate-limited release of K^+ from mica minerals.

The initial water content did not affect the solute leaching behaviour in the unsaturated Manawatu soil. The CDE in conjunction with Richards' equation was used to successfully describe solute movement under transient water flow for both initially dry and wet soil conditions.

The CDE could also describe anion movement in the Manawatu soil under pasture. However before solute application, the pasture was cut relatively short. Leaching under longer pasture might have resulted in less uniform solute movement, due to interception and stem flow. The dispersivities (λ) found under pasture were slightly higher than those inferred from the bare soil experiments. Again nearly identical dispersivities were found for the duplicate columns which were both 300 mm in diameter and length. However high variations in solute concentrations were obtained from small soil cores, 25 mm in diameter taken from one of the columns. This suggests that samples need to be larger in volume than λ^3 if they are to encompass most of the local variabilities in solute concentration.

At water flux densities ranging from 3 to 13 mm h^{-1}, which are similar to common rainfall intensities in New Zealand, no preferential solute flow was observed in either soil. However under irrigation, or if the soil structure is degraded, preferential flow might occur due to incipient ponding. Clothier and Smettem (1990) suggest that incipient matrix ponding might occur at rainfall intensities of about 3-5 mm h^{-1} in the Manawatu fine sandy loam. This is in contrast to our observations, and probably due to some structure degradation as a result of grazing.

Important processes affecting solute movement not addressed here, but warranting further research, include the spatial variability at the field scale, biological transformation of solutes such as nitrate, the transport of multispecies ions in the soil solution (competitive exchange), and the role of various crops and their water extraction pattern on solute transport.

Time domain reflectometry (TDR) was found to be useful in monitoring solute transport under transient water flow through a repacked soil column. However in undisturbed soil columns TDR could only be used to estimate solute transport parameters when the relative bulk soil electrical conductivity was used. Measurement of the actual soil solution electrical conductivity, using an independently obtained calibration, was not possible. The method used, involving *in situ* calibrations, is limited to steady state water flow conditions. The inability to obtain a calibration transferable from one location to another is probably due to the high sensitivity of the TDR-measured bulk soil electrical conductivity to the local soil structure, and immediate bulk density. Further experiments are needed to investigate the effect of these soil properties on TDR-measured impedance. Just recently, Risler *et al.* (1996) proposed a new TDR-calibration procedure for transient conditions. This involves simultaneous measurements of the water content and the bulk soil electrical conductivity during cyclic wetting and drying at constant soil solution electrical conductivity. Although their study was confined to repacked soil columns, the method would seem to be applicable to undisturbed soil columns.

In summary, TDR seems a valuable tool for studying solute transport in the laboratory on soil columns, as well as in the field. However to obtain meaningful average transport parameters, considerable replication of instrumentation is required, which is easy-done with TDR. Limitations of TDR include calibration problems, the effect of exchange reactions on TDR-measured impedance or electrical conductivity, the restriction to nonreactive solutes unless adsorption is induced by an increase in sorption sites with increasing external solution concentration. Also there is a high sensitivity to a relatively small region close to the probe wires. This makes TDR sensitive to small air gaps around the probes and/or cracking of the soil. These may arise during installation or as a result of shrinking of soil during dry periods.

TDR measurements at different depths in the soil columns are consistent with solute in the surface soil being transported according to convective-dispersive flow. Howerver the small sampling volume of the probes meant that the TDR measurements were too variable to infer accurately the depth behaviour of solute transport. It remains unclear as to whether the CDE with a depth-invariant dispersivity may be extended to other depths, given mechanisms and scale are probably correlated. But regardless of mechanisms, profile variations in texture and structure will usually make this unlikely.

The overall conclusion of this study is that the convection dispersion equation seems adequate for describing the mean features of solute transport through undisturbed soil under both transient and steady-state unsaturated flow conditions. The initial water content and the short pasture did not significantly influence solute transport. The assumption of a velocity-invariant dispersivity seems reasonable for most practical applications. As long as an appropriate CEC is used, the CDE linked with cation exchange theory can be used to describe cation movement.

References

Addiscott, T.M., and Wagenet, R.J., 1985. Concepts of solute leaching in soils: A review of modelling approaches. *Journal of Soil Science*, 36, 411-424.

Amoozegar-Fard, A., Nielsen, D.R., and Warrick, A.W., 1982. Soil solute concentration distribution for spatially varying pore water velocities and apparent diffusion coefficients. *Soil Science Society America Journal*, 46, 3-9.

Andreini, M.S., and Steenhuis, T.S., 1990. Preferential paths of flow under conventional and conservation tillage. *Geoderma*, 46, 85-102.

Bajracharya, K., and Barry, D.A., 1993. Mixing cell models for nonlinear equilibrium single species adsorption and transport. *Journal of Contaminant Hydrology*, 12, 227-243.

Baker, J.M., and Allmaras, R.R., 1990. System for automating and multiplexing soil moisture measurement by time-domain reflectometry. *Soil Science Society of America Journal*, 54, 1-6.

Baker, J.M., and Lascano, R.J., 1989. The spatial sensitivity of Time Domain Reflectometry. *Soil Science* 147, 378-384.

Bear, J., 1972. *Dynamics of Fluids in Porous Media.* Elsevier Science, New York.

Beven, K.J., and German, P., 1982. Macropores and water flow in soils. *Water Resources Research* 18, 1311-1325.

Beven, K.J., Henderson, D.E., and Reeves, A.D., 1993. Dispersion parameters for undisturbed partially saturated soil. *Journal of Hydrology*, 143, 19-43.

Biggar, J.W., and Nielsen, D.R., 1962. Miscible displacement: II. Behaviour of tracers. *Soil Science Society America Proceedings*, 125-128.

Biggar, J.W., and Nielsen, D.R., 1963. Miscible displacement: V. Exchange processes. *Soil Science Society of American Proceedings, 27*, 623-627.

Biggar, J.W., and Nielsen, D.R., 1976. Spatial variability of the leaching characteristics of a field soil. *Water Resources Research*, 12, 78-84.

Black, A.S., and Waring, S.A., 1979. Anion adsorption by highly weathered soils. *Australian Journal of Soil Research*, 17, 271-282.

Blakemore, L.C., P.L. Searle, and B.K. Daly, 1987. *Methods of chemical analysis of soils*, NZ Soil Bureau Scientific Report 80, Lower Hutt, New Zealand.

Bohn, H., McNeal, B., and O'Connor, G., (ed.), 1985. Cation Retention. pp 153-181. In *Soil Chemistry*, 2nd edition, Wiley-Interscience Publication, John Wiley and Sons, Inc.

Bolan, N.S., Seyers, J.K., and Tillman, R.W., 1986. Ionic strength effects on surface charge and adsorption of phosphate and sulphate by soils. *Journal of Soil Science*, 37, 379-388.

Bolt, G.H., 1967. Cation-exchange equations used in soil science - A review. *Netherlands Journal of Agricultural Science*, 15, 81-103.

Bolt, G.H., 1982. *Soil Chemistry B. Physico-Chemical Models*, Elsevier, Amsterdam.

Bond, W.J., and Phillips, I.R., 1990a. Cation exchange isotherms obtained with batch and miscible displacement techniques. *Soil Science Society of America Journal*, 54, 722-728.

Bond, W.J., and Phillips, I.R., 1990b. Approximate solutions for cation transport during unsteady, unsaturated soil water flow. *Water Resources Research*, 26, 2195-2205.

Bowman, B.T., Brunke, R.R., Reynolds, W.D., and Wall, G.J., 1994. Rainfall simulator-grid system for solute transport studies using large, intact soil blocks. *Journal of Environmental Quality*, 23, 815-822.

Bresler, E., 1991. Soil Spatial Variability. *In Modeling Plant and Soil Systems*, Agronomy Monograph 31, Chapter 8, SSSA, Madison.

Bresler, G., and Dagan, G., 1979. Solute dispersion in unsaturated heterogeneous soil at field scale. II.: Applications. *Soil Science Society of America Journal*, 43, 476-472.

Bruggenwert, M.G.M., and Kamphorst, A., 1982. Survey of experimental information on cation exchange in soil systems, pp 141-203. In G.H. Bolt (ed.) *Soil Chemistry: B. Physico-Chemical Models*. Elsevier, Amsterdam.

Brusseau, M.L., 1993. The influence of solute size, pore water velocity and intraparticle porosity on solute and transport in soil. *Water Resources Research*, 29, 1071-1080.

Brusseau, M.L., and Rao, P.S.C., 1990. Modelling solute transport in structured soils: a review, *Geoderma*, *46*, 169-192.

Brutsaert, W., 1979. Universal constants for scaling the exponential soil water diffusivity? *Water Resources Research*, 15, 481-483.

Burns, I.G., 1974. A model for predicting the redistribution of salts applied to fallow soils after excess rainfall or evaporation. *Journal of Soil Science*, 25, 165-178.

Butters, G.L., and Jury, W.A., 1989. Field scale transport of bromide in an unsaturated soil. 2. dispersion modeling. *Water Resources Research* , 25, 1583-1589.

Cameron, D.R., and Klute, A., 1977. Convective-dispersive solute transport with a combined equilibrium and kinetic adsorption model. *Water Resources Research* 13, 183-188.

Campbell, G.S., 1985. *Soil Physics with Basics.* Transport Models for Soil-Plant Systems. Elsevier, Amsterdam. Science Publishers B.V.

Chan, K.Y., Geering, H.R., and Davey, B.G., 1980. Movement of chloride in a soil with variable charge properties. I. Chloride systems. *Journal of Environmental Quality*, 9, 579-582.

Clothier, B.E., Heng, L., Magesan, G.N., and Vogeler, I., 1995. The measured mobile water content of an unsaturated soil as a function of hydraulic regime. *Australian Journal of Soil Research,* 33, 397-414.

Clothier, B.E., Magesan, G.N., Heng, L., and Vogeler, I., 1996. In situ measurement of the solute adsorption isotherm using a disc permeameter. *Water Resources Research*, 32, 771-778.

Clothier, B.E., and Smettem, K.R.J., 1990. Combining laboratory and field measurements to define the hydraulic properties of soil. *Soil Science Society of America Journal*, 54, 299-304.

Clothier, B.E., Kirkham, M.B., and McLean, J.E., 1992. In situ measurement of the effective transport volume for solute movement through soil. *Soil Science Society of America Journal*, *56*, 733-736.

Clothier, B.E., and White, I., 1981. Measurement of sorptivity and soil water diffusivity in the field. *Soil Science Society of America Journal*, 45, 241-245.

Coats, K.H., and Smith, B.D., 1964. Dead-end pore volume and dispersion in porous media. *Society of Petroleum Engineering Journal*, 4, 74-84.

Cowie, J.D., 1978. *Soils and Agriculture of Kairarya County.* New Zealand Soil Bureau Bulletin 33 DSIR.

Cremers, A., van Loon, J., and Laudelout, H., 1966. Geometry effects of specific electrical conductance in clays and soils. *Clays Clay Mineralogy*, 14, 149-162.

Dagan, G., 1986. Statistical theory of groundwater flow and transport: pore to laboratory, laboratory to formation and formation to regional scale. *Water Resources Research*, 22, 120S-135S.

Dalton, F.N., 1992. Development of Time Domain Reflectometry for measuring soil water content and bulk soil electrical conductivity. In *Advances in Measurement of Soil Physical Properties: Bringing Theory into Practice*, SSSA Special Publication No. 30.

Dalton, F.N., Herkelrath, W.N., Rawlins, D.S., and Rhoades, J.D., 1984. Time-Domain Reflectometry: Simultaneous measurement of soil water content and electric conductivity with a single probe. *Science*, 224, 989-990.

Dalton, F.N., and van Genuchten, M.Th., 1986. The Time-Domain Reflectometry method for measuring soil water content and salinity. *Geoderma*, 38, 237-250.

Dasberg, S., and Dalton, F.N., 1985. Time Domain Reflectometry field measurements of soil water content and electrical conductivity. *Soil Science Society of America Journal* 49, 293-297.

Dasberg, S., and Hopmans, J.W. 1992. Time domain reflectometry calibration for uniformly and nonuniformily wetted sandy and clayey loam soils. *Soil Science Society of America Journal* 56, 1341-1345.

Davidson, J.M., and Chang, R.K., 1972. Transport of picloram in relation to soil-physical conditions and pore-water velocity. *Soil Science Society of America Proceedings*, 36, 257-261.

Davis, J.L., and Annan, A.P., 1977. Electromagnetic detection of soil moisture. *Canadian Journal of Remote Sensing* 3, 76-86.

Davis, J.L., and Chudobiak, W.J., 1975. In situ meter for measuring relative permittivity of soils. Paper 75-1A. *Geological Survey of Canada*. Energy, Mines and Resources of Canada, Ottawa.

De Smedt, F., and Wierenga, P.J., 1978. Approximate analytical solutions for solute flow during infiltration and redistribution. *Soil Science Society of America Journal*, 42, 407-412.

De Smedt, F., and Wierenga, P.J., 1984. Solute transfer through columns of glass beads. *Water Resources Research*, 20, 225-232.

De Smedt, F., Wauters, F., and Sevilla, J., 1986. Study of tracer movement through unsaturated sand. *Journal of Hydrology*, 85, 169-181

Dirksen, C., and Dasberg, S., 1993. Improved calibration of Time Domain Reflectometry soil water content measurements. *Soil Science Society of America Journal*, 57, 660-667.

Dyson, J.S., and White, R.E., 1987. A comparison of the convection-dispersion equation and transfer function model for predicting chloride leaching through undisturbed, structured clay soil. *Journal of Soil Science*, 38, 157-172.

Edmeades, D.C., Wheeler, D.M., and Clinton, O.E., 1985. The chemical composition and ionic strength of soil solutions from New Zealand topsoils. *Australian Journal of Soil Research*, 23, 151-165.

Elkhatib, E.A., Hern, J.L., and Staley, T.E., 1987. A rapid centrifuge method for obtaining soil solution. *Soil Science Society of America Journal,* 51, 578-583.

Elrick, D.E., and French, L.K., 1966. Miscible displacement patterns on disturbed and undisturbed soil cores. *Soil Science Society of America Proceedings*, 30, 153-156.

Elrick, D.E., Reynolds, W.D., Kachanoski, R.G., and Parkin G.W., 1993. Field measurements of water and solute transport parameters in soils. In D. Russo, G. Dagan (eds): *Water Flow and Solute transport in Soils* (ed..), Springer Verlag.

Engesgaard, P. and Christensen, Th.H., 1988. A review of chemical solute transport models. *Nordic Hydrology*, 19, 183-216.

Fellner-Feldegg, H., 1969. The measurement of dielectrics in the Time Domain. *The Journal of Physical Chemistry* 73, 616-623.

Freeze, R.A., and Cherry, J.A., (ed.), 1979. *Groundwater*. 604 pp, Prentice Hall, Englewood Cliffs, New Jersey.

Fisher, T.R., 1963. Measurements of adsorbed cations in soils employing radioactive isotope equilibration methods. *Dissertation Abstracts,* 23:2284.

Gardner, W.R., 1965. Movement of nitrogen in soil. In *Soil Nitrogen Agronomy* Monographs 10, eds. Bartholomew W.V., and Clark, F.E. Pub. ASA Wisconsin, pp 550-572.

Gardner, W.H., 1986. Water Content, 493-544. In A. Klute (Ed.), *Methods of Soil Analysis Part 1*. ASA, Madison, WI.

Gerke, H.H., and van Genuchten, M.Th., 1993. A dual-porosity model for simulating the preferential movement of water and solutes in structured porous media. W*ater Resources Research,* 29, 305-319.

Giese, K, and Tiemann, R., 1975. Determination of the complex permittivity from thin-sample Time Domain Reflectometry: Improved analysis of the step response waveform. .*Adv. Mol. Relax Processes* 7, 45-49.

Grant, S.A., Mansell, R.S., Bloom, S.A., and Rhue, R.D., 1995. Simulated transport of three cations through porous media: effect of different approaches to modelling cation exchange reactions. *Water Resources Research, 31*, 185-198.

Green, S.R., and Clothier, B.E. 1994. Simulating water and chemical movements into unsaturated soils. *The Phoenics Journal of Fluid Dynamics and its Application*, 7, 76-92.

Havlin, J.L., Westfall, D.G., and Olsen, S.R., 1985. Mathematical models for potassium release in calcareous soils. *Soil Science Society of America Journal*, *49*, 371-376.

Heermann, D.F. 1980. Fluid dynamics of sprinkler systems. Chapter 14 (pp. 583-618) in M.E. Jensen (ed.) *Design and Operation of Farm Irrigation Systems*, American Society of Agricultural Engineers, St Joseph, Michigan.

Heimovaara, T.J., 1993. Design of triple-wire Time Domain Reflectometry probes in Practice and theory. *Soil Science Society of America Journal*, 57, 1410-1417.

Heimovaara, T.J., and Bouten, W., 1990. A computer-controlled 36-channel Time Domain Reflectometry system for monitoring soil water contents. *Water Resources Research*, 26, 2311-2316.

Heng, L.K., White, R.E., Scotter, D.R., and Bolan, N.S., 1994. A transfer function approach to modelling the leaching of solutes to subsurface drains. II. Reactive solutes. *Australian Journal of Soil Research*, 32, 85-94.

Heng, L.K., and White, R.E., 1996. A simple analytical transfer function approach to modelling the leaching of reactive solutes through field soil. *European Journal of Soil Science*, 47, 33-42.

Herkelrath, W.N., Hamburg, S.P., and Murphy F., 1991. Automatic, real-time monitoring of soil moisture in a remote field area with Time Domain Reflectometry. *Water Resources Research*, 27, 857-864.

Hook, W.R., and Livingston, N.J., Sun, Z.J., and Hook, P.B., 1992. Remote diode shorting improves measurement of soil water by Time Domain Reflectometry. *Soil Science Society of America Journal*, 56, 1384-1391.

Hu, Q., and Brusseau, M.L., 1995. Effect of solute size on transport in structured porous media, *Water Resources Research*, 31, 1637-1646.

Hunsaker, V.E., and Pratt, P.F., 1971. Calcium magnesium exchange equilibria in soils. *Soil Science Society of America Journal*, 35, *151-152.*

Hussen, A.A., Warrick, A.W., and Musil, S.A. 1994. In situ method to determine hydraulic and transport parameters. p. 250. *In* Agronomy Abstracts. ASA, Madison, WI.

Hutson, J.L., and Wagenet, R.J., 1995. The application of chemical equilibrium in solute transport models. In *Chemical Equilibrium and Reaction Models.* SSSA 42, 97-112, Madison, WI.

Ishiguro, M., Song, K.C., and Yuita, K., 1992. Ion Transport in an allophanic andisol under the influence of variable charge. *Soil Science Society of America Journal*, 56, 1789-1793.

Jacobsen, O.H., and Schjønning, P. 1993. A laboratory calibration of time domain reflectometry for soil water measurements including effects of bulk density and texture. *Journal of Hydrology*, 151, 147-157.

Jardine, P.M., Jacobs, G.K., and Wilson, G.V., 1993. Unsaturated transport processes in undisturbed heterogeneous porous media: I. Inorganic contaminants. *Soil Science Society of America Journal*, 57, 945-953.

Jardine, P.M., Wilson, G.V., and Luxmoore, R.J., 1988. Modeling the transport of inorganic ions through undisturbed soil columns from two contrasting watersheds. *Soil Science Society of America Journal*, 52, 1252-1259

Jaynes, D.B., Logsdon, S.D., and Horton, R., 1995. Field method for measuring mobile/ immobile water content and solute transfer rate coefficient. *Soil Science Society of America Journal*, 59, 352-356.

Jury, W.A., 1982. Simulation of solute transport using a transfer function model. *Water Resources Research*, 18, 363-368.

Jury, W.A., 1983. Chemical transport modeling: Current approaches and unresolved problems. In SSSA Special Publication No. 11, SSSA and ASA, Madison, Wisconsin, p. 49-64.

Jury, W.A., Gardner, W.R., and Gardner, W.H., 1991. *Soil Physics*, 5th ed., John Wiley and Sons, Inc, New York, Chapter 7, 218-267.

Jury, W.A., and Roth, K., 1990. *Transfer Functions and Solute Movement through Soil*: Theory and Applications. Birkhäuser Verlag Basel.

Jury, W.A., and Scotter, D.R., 1994. A unified approach to stochastic-convective transport problems. *Soil Science Society of America Journal*, 58, 1327-1336.

Jury, W.A., Sposito, G., and White, R.E., 1986. A transfer function model of solute transport through soil I. Fundamental concepts. *Water Resources Research*, 22, (2), 243-247.

Jury, W.A., Stolzy, L.H., and Shouse, P., 1982. A field test of transfer function model for predicting solute transport. *Water Resources Research*, 18, 369-375.

Kachanoski, R.G., Pringle, E. and Ward, A., 1992. Field measurement of solute travel times using Time Domain Reflectometry. *Soil Science Society of America Journal*, 56, 47-52.

Kachanoski, R.G., Ward, A.L., and van Wesenberg, I.J., 1994. Measurement of transport properties at the field scale. *Transactions 15th World Congress of Soil Science*, Vol. 2a, Commission 1, Acapulco, Mexico.

Kanchanusut, P., and Scotter, D.R., 1982. Leaching patterns in soil under pasture and crop. *Australian Journal of Soil Research*, 20, 193-202.

Katou, H., Clothier, B.E., and Green, S.R., 1996. Anion transport involving competitive adsorption during transient water flow in an andisol. *Soil Science Society of America Journal*, 60, 1368-1375.

Khan, A.U.H., and Jury, W.A., 1990. A laboratory study of the dispersion scale effect in column outflow experiments. *Journal of Contaminant Hydrology*, 5, 119-131.

Kirkham, D., and Powers, W.L., 1971. *Advanced Soil Physics*. Wiley Interscience, Chapter 8, 379-420.

Kirkman, J.H., Basker, A., Supapaneni, A., and MacGregor, A.N., 1994. Potassium in the soils of New Zealand-a review. *NZ Journal of Agricultural Research*, 37, 207-227.

Kissel, D.E., Ritchie, J.T., and Burnett, E., 1973. Chloride movement in undisturbed swelling clay soil. *Soil Science Society of America Proceedings*, 37. 21-24.

Knight, J.H., 1988. In W.L. Steffen and O.T. Denmark (eds.) *Flow and Transport in the Natural Environment: Advances and Applications*, Springer Verlag, pp 17-29.

Knight, J.H., 1992. Sensitivity of Time Domain Reflectometry measurements to lateral variations in soil water content. *Water Resources Research*, 28, 2345-2352.

Kreft, A., and Zuber, A., 1978. On the physical meaning of the dispersion equation and its solution for different boundary conditions. *Chemical Engineering Science*, 33, 1471-1480.

Krupp, H.K., Biggar, J.W., and Nielsen, D.R., 1972. Relative flow rates of salt and water in soil. *Soil Science Society of America Proceedings*, 36, 412-417

Kutílek, M., and Nielsen, D.R., 1994. *Soil Hydrology*. Catena Verlag, Cremlingen-Destedt, Germany.

Lai, S-H., Jurinak, J.J., and Wagenet, R.J., 1978. Multicomponent cation adsorption during convective-dispersive flow through soils. *Soil Science Society of America Journal,* 42, 240-243.

Lanyon, L.E., and Heald, W.R., 1982. Magnesium, calcium, strontium and barium. In *Methods of Soil Analysis, Part 2. Chemical and Microbiological Properties.* 2nd ed. Agron. Monogr. 9 ASA, Madison, WI.

Lapidus, L., and Amundson, N.R., 1952. Mathematics of adsorption in beds. VI. The effect of longitudinal diffusion in ion exchange and chromatographic columns. *Journal of Chemical Physics*, 56, 984-988.

Ledieu, J., de Ridder, P., de Clerck, P., and Dautrebande, S., 1986. A method of measuring soil moisture by Time Domain Reflectometry. *Journal of Hydrology*, 88, 319-328.

Magesan, G.N., Scotter, D.R., and White, R.E., 1994. A transfer function approach to modelling the leaching of solutes to subsurface drains. I. Non-reactive solutes. *Australian Journal of Soil Research*, 32, 69-83.

Magesan, G.N., Vogeler, I., Scotter, D.R., and Clothier, B.E., 1995. Solute movement through two unsaturated soils. *Australian Journal of Soil Research*, 33, 585-596.

Mallants, D., Vanclooster, M., Meddahi, M., and Feyen, J., 1994. Estimating solute transport in undisturbed soil columns using time domain reflectometry, *Journal of Contaminant Hydrology, 17*, 91-109.

Mallants, D., Vanclooster, M., Toride, N., Vanderborght, J., van Genuchten. M.Th., and Feyen, J., 1996. Comparison of three methods to calibrate TDR for monitoring solute movement in undisturbed soil. *Soil Science Society of America Journal*, 60, 747-754.

Mansell, R.S., Bond, W.J., and Bloom, S.A., 1988. Multicomponent cation adsorption during convective-dispersive flow through soils: experimental study. *Soil Science Society of America Journal*, 52, 1533-1540.

Marsh, K.B., Tillman, R.W., and Seyers, J.K., 1987. Charge relationships of sulfate sorption by soils. *Soil Science Society of America Journal*, 51, 318-323.

Martin, H.W., and Sparks, D.L., 1983. Kinetics of nonexchangeable potassium release from two coastal plain soils. *Soil Science Society of America Journal*, 47, 883-887.

Mualem, Y., and Friedmann, S.P., 1991. Theoretical prediction of electrical conductivity in saturated and unsaturated soil. *Water Resources Research*, 27, 2771-2777.

Nadler, A., 1981. Field Application of the four-electrode technique for determining soil solution conductivity. *Soil Science Society of America Journal*, 45, 30-34.

Nadler, A., 1991. Effect of structure on bulk soil electrical conductivity (σ) using the TDR and 4P techniques. *Soil Science*, 152, 199-203.

Nadler, A., Dasberg, S. and Lapid, I., 1991. Time Domain Reflectometry measurements of water content and electrical conductivity of layered soil columns. *Soil Science Society of America Journal*, 55, 938-943.

Nadler, A., and Frenkel, H. 1980. Determination of soil solution electrical conductivity from bulk soil electrical conductivity measurements by the four-electrode method. *Soil Science Society of America Journal*, 44, 1216-1221.

Nakahara, O., and Wada, S.I., 1994. Ca^{2+} and Mg^{2+} adsorption by allophanic and humic andisol. *Geoderma*, 61, 203-212.

Nielsen, D.R., and Biggar, J.W., 1961. Miscible displacement in soils: 1. Experimental information. *Soil Science Society of America Proceedings*, 25, 1-5.

Nielsen, D.R., Biggar, J.W., and Simmons, C.S., 1981. Mechanisms of solute transport in soils. In I.K. Iskandar (ed.) *Modeling Waste Water Renovation*, Chapter 6, pp 115-135. John Wiley and Sons, New York.

Nielsen, D.R., van Genuchten, M.Th., and Biggar, J.W., 1986. Water flow and solute transport processes in the unsaturated zone. *Water Resources Research*, 22, 89S-108S.

Nkedi-Kizza, P., Rao, P.S.C., and Davidson, J.M., 1982. Ion exchange and diffusive mass transfer miscible displacement through an aggregated oxisol. *Soil Science Society of America Journal*, 46, 471-476.

Nkedi-Kizza, P., Biggar, J.W., van Genuchten, M.Th., Wierenga P.J., Selim, H.M., Davidson, J.M., and Nielsen, D.R., 1983. Modeling tritium and chloride 36 transport through an aggregated oxisol. *Water Resources Research*, 19, 691-700.

Novakowski, K.S., 1992. An evaluation of boundary conditions for one-dimensional solute transport. 1. Mathematical development. *Water Resources Research*, 28, 2399-2410.

Ogwada, R.A., and D.L. Sparks, 1986. Kinetics of ion exchange in clay minerals and soil: I. Evaluation of methods. *Soil Science Society of America Journal*, 50, 1158-1162.

Parfitt, R.L., 1980. Chemical properties of variable charge soils. In B.K.G. Theng (ed*) Soils with Variable Charge.* Soil Bureau, Department of Scientific and Industrial Research, Lower Hutt, New Zealand.

Parfitt, R.L., Saigusa, M., and Eden, D.N., 1984. Soil development processes in an aqualf-ochrept sequence from loess with admixtures of tephra, New Zealand. *Journal of Soil Science*, 35, 625-640.

Parker, J.C., and Albrecht, K.A., 1987. Sample volume effects on solute transport predictions. *Water Resources Research*, 23, 2293-2301.

Parker, J.C., and van Genuchten, M.Th., 1984. Flux-averaged and volume-averaged concentrations in continuum approaches to solute transport. *Water Resources Research*, 20, 866-872.

Parlange, J.Y., and Starr, J.L., 1977. Dispersion in soil columns: effect on boundary conditions and irreversible reactions. *Soil Science Society of America Journal*, 42, 15-18.

Parlange, J.Y., Barry, D.A., and Starr, J.L., 1985. Comments on "Boundary conditions for displacement experiments through short laboratory soil columns. *Soil Science Society of America Journal*, 49, 1325.

Passioura, J.B., 1971. Hydrodynamic dispersion in aggregated media: I. Experimental information. *Soil Science*, 111, 339-344.

Peck, A.J. 1969. Entrapment, stability and persistence of air bubbles in soil water. *Australian Journal of Soil Research*, 7, 79-80.

Persaud, N., and Wierenga, P.J., 1982. A differential model for one-dimensional cation transport in discrete homoionic ion exchange media. *Soil Science Society of America Journal*, *46*, 482-490.

Pollok, J.A., 1975. A comparative study of certain New Zealand and German soils formed from loess. Dissertation, Rheinische Friedrich-Wilhelms-Universität Bonn.

Quadri, M.B., Clothier, B.E., Angulu-Jaramillo, R., Vauclin, M., and Green, S.R. 1994. Axisymmetric transport of water and solute underneath a disk permeameter: Experiments and numerical model. *Soil Science Society of America Journal*, 58, 696-703.

Ramo, S., and Whinnery, J.R., 1958. *Fields and Waves in Modern Radio.* Wiley, New York, N.Y.

Rao, P.S.C., Rolston, D.E., Jessup, R.E., and Davidson, J.M., 1980. Solute transport in aggregated porous media. Theoretical and experimental evaluation. *Soil Science Society of America Journal*, 44, 1139-1146.

Resource Management Act, 1991, GPH Print

Rhoades, J.D., Manteghi, N.A., Shouse, P.J., and Alves, W.J. 1989. Soil electrical conductivity and soil salinity: new formulations and calibrations. *Soil Science Society of America Journal*, 53, 433-439.

Rhoades, J.D., Raats, P.A.C., and Prather, R.J., 1976. Effects of liquid-phase electrical conductivity, water content and surface conductivity on bulk soil electrical conductivity. *Soil Science Society of America Journal*, 40, 651-655.

Rhoades, J.D., and van Schilfgaarde, J., 1976. An electrical conductivity probe for determining soil salinity. *Soil Science Society of America Journal*, 40, 647-651.

Risler, P.D., Wraith, J.M., and Gaber, H.M., 1996. Solute transport under transient flow conditions estimated using time domain reflectometry. *Soil Science Society of America Journal*, 60, 1297-1305.

Robbins, C.W., Jurinak, J.J., and Wagenet, R.J., 1980a. Calculating cation exchange in a salt transport model. *Soil Science Society of America Journal*, 44, 1195-1200.

Robbins, C.W., Wagenet, R.J., and Jurinak, J.J., 1980b. A combined salt transport-chemical equilibrium model for calcareous and gypsifereous soils. *Soil Science Society of America Journal, 44*, 1191-1194.

Robinson, R.A., and Stokes, R.H., 1959. *Electrolyte Solutions*, p. 513, Butterworths, London.

Roth, K., Flühler, H., and Attinger, W., 1990a. Transport of conservative tracer under field conditions: Qualitative modelling with random walk in a double porous medium. In K. Roth, H. Flühler, W.A. Jury, and J.C. Parker (eds), *Field-scale Solute and Water Transport through soil.* Birkhäuser Verlag, Basel, Switzerland.

Roth, K., and Hammel, K., 1996. Transport of conservative chemical through an unsaturated two-dimensional Miller-similar medium with steady state flow. *Water Resources Research*, 32, 1653-1663.

Roth, K., and Jury, W. A., 1993. Modeling the transport of solutes to groundwater using transfer functions. *Journal of Environmental Quality*, 22, 487-493.

Roth, K., Jury, W.A., Flühler, H., and Attinger, W., 1991. Transport of chloride through unsaturated field soil. *Water Resources Research*, 27, (10), 2533-2541.

Roth, C.H., Malicki, M.A., and Plagge, R., 1992. Empirical evaluation of the relationship between soil dielectric constant and volumetric water content as the basis for calibrating soil moisture measurements by TDR. *Journal of Soil Science*, 43, 1-13

Roth, K., Schulin, R., Flühler, H. and Attinger, W., 1990b. Calibration of Time Domain Reflectometry for water content measurement using composite dielectricity approach. *Water Resources Research*, 26, 2267-2273.

Saffiggna, P.G., Tanner, C.B., and Keeney, D.R., 1976. Non-uniform infiltration under potato canopies caused by interception, stemflow and hilling. *Agronomy Journal*, 68, 337-342.

Schulin, R.A., Papritz, H., Flühler, H., and Selim, H.M., 1989. Calcium and magnesium transport in aggregated soils at variable ionic strength. *Geoderma, 38*, 311-322.

Schulin, R., Wierenga, P.J., Flühler, H., and Leuenberger, J., 1987. Solute transport through a stony soil. *Soil Science Society of America Journal*, 51, 36-42.

Schweich, D., Sardin, M., and Gaudet, J-P., 1983. Measurement of cation exchange isotherm from elution curves obtained in a soil column: preliminary results. *Soil Science Society of America Journal*, 47, 32-37.

Scotter, D.R., 1978. Preferential solute movement through larger soil voids. I. Some computations using simple theory. *Australian Journal of Soil Research*, 16, 257-267.

Scotter, D.R., and Ross, P.J., 1994. The upper limit of solute dispersion and soil hydraulic properties. *Soil Science Society of America Journal*, 58, 659-663.

Scotter, D.R., and Tillman, R.W., 1991. Movement of solutes associated with intermittent soil water flow. I. Tritium and bromide. *Australian Journal of Soil Research*, 29, 175-183.

Scotter, D.R., White, R.E., and Dyson, J.S., 1993. The Burns leaching equation. *Journal of Soil Science*, 44, 25-33.

Selim, H.M., Davidson, J.M., and Mansell, R.S., 1976. Evaluation of a two site adsorption-desorption model for describing solute transport in soils. Proceedings of 1976 Summer Computer Simulation Conference in Washington, D.C., pp 444-448.

Selim, H.M., Mansell, R.S., Gaston, L.A., Flühler, H., and Schulin, R., 1990. Prediction of cation exchange in soils using cation exchange reactions. pp 223-238. In K. Roth, H. Flühler, W.A. Jury, and J.C. Parker (ed.) *Field-Scale Water and Solute Flux in Soils*, Birkhäuser Verlag, Basel.

Selim, H.M., Schulin, R., and Flühler, H., 1987. Transport and ion exchange of calcium and magnesium in an aggregated soil. *Soil Science Society of America Journal*, 51, 876-884.

Seyfried, M.S., and Rao, P.S.C., 1987. Solute transport in undisturbed columns of an aggregated tropical soil: preferential flow effects. *Soil Science Society of America Journal*, 51, 1434-1444.

Shainberg, I., Rhoades, J.D., and Prather, R.J. 1980. Effect of exchangeable sodium percentage, cation exchange capacity, and soil solution concentration on soil electrical conductivity. *Soil Science Society of America Journal*, 44, 469-473.

Shipitalo, M.J., Edwards, W.M., Dick, W.A., and Owens, L.B., 1990. Initial storm effects on macropore transport of surface-applied chemicals in no-till soil. *Soil Science Society of America Journal*, 54, 1530-1536.

Skopp, J., Gardner, W.R., and Tyler, E.J., 1981. Solute movement in soils: Two region model with small interaction. *Soil Science Society of America Journal*, 45, 837-842.

Smiles, D.E., and Knight, J.H. 1976. A note on the use of the Philip infiltration equation. *Australian Journal of Soil Research*, 14, 103-108.

Snow, V.O., Clothier, B.E., Scotter, D.R., and White, R.E., 1994. Solute transport in a layered soil: Experiments and modelling using the convection-dispersion approach. *Journal of Contaminant Hydrology*, 16, 339-358.

Sparks, D. and Recheigl, J.E., 1982. Comparison of batch and miscible displacement techniques to describe potassium adsorption kinetics in Delaware soils. *Soil Science Society of America Journal*, 46, 875-877.

Sposito, G., White, R.E., Darrah, P.R., and Jury, W.A., 1986. A transfer function model of solute transport through soil. 3. The convection Dispersion Equation. *Water Resources Research*, 22, 255-262.

Starr, J.L., and Parlange, J.Y., 1979. Dispersion in soil columns: Snow plow effect. *Soil Science Society of America Journal*, 43, 448-450.

Thomas, G.W. 1982. Exchangeable cations. In A. Klute (ed) *Methods of Soil Analysis* Part II: *Chemical and Microbiological Properties*, 2nd ed. Agronomy No.9, ASA, Madison.

Tillman, R.W., and Scotter, D.R., 1991. Movement of solutes associated with intermittent soil water flow. II. Nitrogen and Cations. *Australian Journal of Soil Research*, 29, 185-196.

Tillman, R.W., Scotter, D.R., Clothier, B.E., and White, R.E., 1991. Solute movement during intermittent water flow in a field soil and some implications for irrigation and fertilizer application. *Agricultural Water Management*, 20, 119-133.

Tomlinson, A.I., 1992. Precipitation and the atmosphere, in *Waters of New Zealand*, edited by M. P. Mosely, pp.63-74, New Zealand Hydrological Society, Wellington.

Topp, G.C., and Davis, J.L., 1985. Measurement of soil water content using time-domain reflectometry (TDR): A field evaluation. *Soil Science Society of America Journal*, 49, 19-24.

Topp, G.C., Davis, J.L., and Annan, A.P., 1980. Electromagnetic determination of soil water content: Measurement in coaxial transmission lines. *Water Resources Research*,16, 574-582.

Topp, G.C. and Davis, J.L. and Annan, A.P., 1982. Electromagnetic determination of soil water content using TDR: I. Applications to wetting fronts and steep gradients. *Soil Science Society of America Journal*, 46, 672-678.

Topp, G.C., Yanuka, M., Zebchuk, W.D., and Zeglin, S., 1988. Determination of electrical conductivity using time domain reflectometry: Soil and water experiments in coaxial lines. *Water Resources Research*, 24, 945-952.

United States Salinity Laboratory Staff. 1954. *Diagnosis and improvement of saline and alkali soils.* U.S. Dep. Agri. Handbook 60.

Valocchi, A.J., 1985. Validity of the local equilibrium assumption for modeling sorbing solute transport through homogeneous soils. *Water Resources Research*,21, 808-820.

Vanclooster, M., Mallants, D., Diels, J., and Feyen, J., 1993. Determining local-scale solute transport parameters using time domain reflectometry (TDR). *Journal of Hydrology*, 148, 93-107.

Vanclooster, M., Mallants, D., Vanderborght, J., Diels, J., van Orshoven, J., and Feyen, J., 1995. Monitoring solute transport in a multi-layered sandy lysimeter using time domain reflectometry. *Soil Science Society of America Journal*, 59, 337-344.

Vanclooster, M., Viane, P., Diels, J., and Christiaens, K., 1994. WAVE. A mathematical model for simulating water and agrochemicals in the soil and vadose environment. Institute for Land and Water Management, Leuven, Belgium.

van der Ploeg, R.R., and Beese, F., 1977. Model calculations for the extraction of soil water by ceramic cups and plates. *Soil Science Society of America Journal,* 41, 466-470.

van der Ploeg, R.R., Machulla, G., and Ringe, H., 1995a. Ein Mischzellenmodell zur Abschätzung der Nitratauswaschung aus landwirtschaftlich genutzten Böden im Winterhalbjahr. *Zeitschrift für Pflanzenernährung und Bodenkunde*, 158, 365-373.

van der Ploeg, R.R., Ringe, H., and Machulla, G., 1995b. Late fall site-specific soil nitrate upper limits for groundwater protection purposes. *Journal of Environmental Quality*, 24, 725-733.

van der Zee, S.E.A.T.M., and Destouni, G., 1992. Transport of inorganic solutes in soil. In R.J. Wagenet, P. Baveye, and B.A. Stewart (eds.) *Interaction Processes in Soil Science.* Advances in Soil Science, Boca Raton, Fla.

van Eijkeren, J.C.M., and Lock, I.P.G., 1984. Transport of cation solutes in sorbing porous medium. *Water Resources Research, 20*, 714-718.

van Genuchten, M.Th., 1981. Analytical solutions for the movement of solutes. *Journal of Hydrology* (Amsterdam), 49, 213-233.

van Genuchten, M.Th., and Alves, W.J., 1982. Analytical solutions of the one-dimensional convective-dispersive solute transport equation. United States Department of Agriculture. *Agricultural Research Service*, Technical Bulletin No. 1661.

van Genuchten, M.Th, and Dalton, F.N., 1986. Models for simulating salt movement in aggregated field soils. *Geoderma*, 38, 165-183.

van Genuchten, M.Th., and Parker, J.C., 1984. Boundary conditions for displacement experiments through short laboratory soil columns. *Soil Science Society of America Journal*, 48, 703-708.

van Genuchten, M.Th., and Wierenga, P.J., 1976. Mass transfer studies in sorbing porous media. I. Analytical solutions. *Soil Science Society of America Journal*, 40, 473-480.

van Genuchten, M.Th., and Wierenga, P.J., 1977. Mass transfer studies in sorbing porous media. II. Experimental evaluation with tritium (^3H_2O). *Soil Science Society of America Journal*, 41, 272-278.

van Genuchten, M.Th., and Wierenga, P.J., 1986. Solute dispersion coefficients and retardation factors. In A. Klute (ed.) *Methods of Soil Analysis* Part I: Physical and Mineralogical Methods, 2nd ed. Agronomy No.9, ASA, Madison.

van Genuchten, M.Th., Gorelick, S.M., and Yey, W.W-G., 1988. Application of parameter estimation techniques to solute transport studies. Proceedings of the International Symposium on Water Quality Modeling of Agricultural Non-Point Sources, Part 2, Utah State University, Logan, Utah.

van Loon, W.K.P., Perfect, E., Groenevelt, P.H. and Kay, B.D., 1991. Application of dispersion theory to Time Domain Reflectometry in soils. *Transport in Porous Media*, 6, 391-406.

van Ommen, H.C., 1985. The "mixing-cell' concept applied to transport of non-reactive and reactive components in soils and groundwater. *Journal of Hydrology*, 78, 201-213.

von Hippel, A.R., 1954. *Dielectric Materials and Applications*, MIT Press, Cambridge, Mass.

Ward, A.L., Kachanoski, R.G., and Elrick, D.E., 1994. Laboratory measurements of solute transport using Time Domain Reflectometry. *Soil Science Society of America Journal*, 58, 1031-1039.

Wagenet, R.J., 1983. Principles of salt movement in soils. In D. W. Nelson *et al.* (ed.) *Chemical Mobility and Reactivity in Soil Systems*, Soil Science of America: Madison, Chapter 9, 123-140.

Weast, R.C. (Ed.) 1965. *Handbook of Chemistry and Physics*, 46th ed., p.D-81. The Chemical Rubber Co., Ohio.

White, R.E., 1985a. A model for nitrate leaching in undisturbed structured clay soil during unsteady flow. *Journal of Hydrology*, 79, 37-51.

White, R.E., 1985b. The influence of macropores on the transport of dissolved and suspended matter through soil. *Advances in Soil Science*, 3, 95-120.

White, R.E., Dyson, J.S., Gerstl, Z., and Yaron, B., 1986a. Leaching of herbicides through undisturbed cores of a structured clay soil. *Soil Science Society of America Journal*, 50, 277-283.

White, R.E., Dyson, J.S., Haigh, R.A., Jury, W.A., and Sposito, G., 1986b. A transfer function model of solute transport through soil. 2. Illustrative applications. *Water Resources Research*, 22, 248-254.

White, R.E., Thomas, G.W. and Smith, M.S., 1984. Modelling water flow through undisturbed soil cores using a transfer function model derived from ^3H_2O and Cl transport. *Journal of Soil Science*, 35, 159-168.

Wraith, J.M., Comfort, S.D., Woodbury, B.L. and Inskeep, W.P., 1993. A simplified analysis approach for monitoring solute transport using Time-Domain Reflectometry. *Soil Science Society America Journal*, 57, 637-642.

Yanuka, M., Topp, G.C., Zegelin, S., and Zebchuk, W.D., 1988. Multiple reflection and attenuation of Time Domain Reflectometry pulses: Theoretical considerations for applications to soil and water. *Water Resources Research*, 24, 939-944.

Zegelin, S.J., White, I., and Jenkins, D.R., 1989. Improved field probes for soil water content and electrical conductivity measurement using Time-Domain Reflectometry. *Water Resources Research*, 25, 2367-2376.

Zegelin, S.J., White, I., and Russell, G.F., 1992. A critique of the Time Domain Reflectometry technique for determining field soil-water content. In Advances in Measurement of Soil Properties: *Bringing Theory into Practice.* SSSA Special Publication No. 30.

Zurmühl, T., and Durner, W., 1996. Modeling transient water and solute transport in a biporous soil. *Water Resources Research*, 32, 819-829.

Appendix A

A.1 Numerical Solutions for the CDE used in this Study

Most of the experiments described in this study were simulated using Microsoft QuickBASIC computer programs. In the following section, the procedure for the various numerical solutions of the CDE for nonreactive and reactive solutes is described. The numerical solutions given here are based on an explicit finite-difference scheme. Examples of computer programs used are given in Appendix B.

A.1.1 Nonreactive Solutes

The solute flux density between the compartments of Fig. 2.8 (eq.[2.21]) under steady state water flow can be approximated for nonreactive solutes as,

$$q_{sn}^{j+1} = -\lambda_{eff}\, q_w \frac{C_{rn+1}^{j} - C_{rn}^{j}}{\Delta z} + q_w\, C_{rn}^{j} \qquad [A1]$$

where λ_{eff} is an effective dispersivity [m], that is used to correct for the numerical dispersion introduced by using a finite difference approach to approximate the convective flux. Here

$$\lambda_{eff} = \lambda - \lambda_{num} \qquad [A2]$$

where λ_{num} is the numerical dispersivity [m], which with $D_s = \lambda\, v$ and $v = q_w / \theta$, is given by (Campbell, 1985),

$$\lambda_{num} = \frac{1}{2}\left(\Delta z - \frac{q_w\, \Delta t}{\theta}\right). \qquad [A3]$$

The solute flux concentration $C_{f\,n}^{j+1}$ can then be calculated from eq [A1],

$$C_{f\,n}^{\,j+1} = \frac{q_{s\,n}^{\,j+1}}{q_{w\,n}^{\,j+1}} \qquad [A4]$$

and consideration of mass balance gives the total solute concentration M_n^{j+1} at time j+1 as

$$M_n^{j+1} = M_n^{j} + \left(q_{s\,n-1}^{\,j+1} - q_{s\,n}^{\,j+1}\right)\frac{\Delta t}{\Delta z} \,. \qquad [A5]$$

The solute resident concentration $C_{r\,n}^{\,j+1}$ then simply equals M_n^{j+1} / θ_n.

In the case of reactive solute, with adsorption described by a linear isotherm, solute resident concentrations in the soil solution are calculated as M / (θ / R), where R is the retardation coefficient, defined as 1+ ρ_b K_d / θ, and K_d is the distribution coefficient. Adsorption can be either constant throughout the profile, or depth dependent. In this later case K_d will be a function of depth.

Computer programs 1 and 2 in Appendix B are examples for numerical solutions for nonreactive solutes, following either a step change in input or an pulse input.

A.1.2 Numerical Simulations for the Mobile/Immobile Approach

For the numerical solution of the mobile immobile concept [eq.2.35], additional input parameters, such as the mobile and immobile water fractions (θ_m and θ_i), the mass transfer coefficient (α), and the dispersion coefficient (D_m) or dispersivity in the mobile phase (λ_m) need to be specified. The solute flux density (q_m) for the mobile water is found as,

$$q_{mn}^{\,j+1} = -\lambda_{meff}\, q_w \frac{C_{mn+1}^{\,j} - C_{mn}^{\,j}}{\Delta z} + q_w\, C_{mn}^{\,j} \qquad [A6]$$

where λ_{meff} is the effective dispersivity in the mobile phase and $C_{m\,n}^{\,j}$ is the concentration in the mobile phase of compartment n at time j [kg or mol m^{-3}].

The diffusional exchange (q_d) between the mobile and the immobile phase is given by,

$$q_{dn}^{j+1} = \left(C_{mn}^{\ j} - C_{in}^{j}\right) \alpha \Delta z \qquad [A7]$$

where $C_{i\ n}^{\ j}$ is the concentration in the immobile phase of compartment n at time j [kg or mol m^{-3}] and α is the mass transfer coefficient [s^{-1}].

Combining the above equations [A6 and A7] yields for the total solute concentration in the mobile and immobile phase,

$$M_{mn}^{\ j+1} = M_{mn}^{\ j} + \left(q_{mn}^{\ j+1} - q_{mn+1}^{\ j+1} - q_{dn}^{\ j+1} \right) \frac{\Delta t}{\Delta z} \qquad [A8]$$

and

$$M_{in}^{j+1} = M_{in}^{j} + q_{dn}^{j+1} \frac{\Delta t}{\Delta z} \qquad [A9]$$

and the total resident solute concentration equals the sum of the mobile and the immobile concentrations expressed per unit soil volume, M_{mn} and M_{in}.

The flux concentration C_f at the outlet end at the bottom of the notional layer (l) is calculated as,

$$C_{fl}^{\ j+1} = C_{ml}^{\ j+1} + C_{ml+1}^{\ j+1} \qquad [A10]$$

Computer program 3 in Appendix B is an example for numerical solution of the MIM.

A.1.3 Numerical Simulation of Cation Movement

The simulation of cation transport is here restricted to binary systems, notionally containing two cation species only. Either homovalent exchange, or heterovalent exchange with mono-and divalent cations is considered. Initial values required for the simulation include the anion concentration in the soil solution, the total mass of the

cations in the soil column, the cation exchange capacity as a function of soil depth, the bulk density, the volumetric water content, the water flow rate, and the dispersivity. The dispersivity can be obtained from the BTC's of the accompanying anions.

Homovalent system: Here we consider a system with calcium and another bivalent cation (magnesium or strontium). Values of the initially adsorbed concentration of Ca^{2+} ($X_{Ca\,n}^{j}$) and Mg^{2+} ($X_{Mg\,n}^{j}$), or Sr^{2+} ($X_{Sr\,n}^{j}$) and the cation exchange capacity ($X_{CEC\,n}^{j}$) are obtained from measured field values. Note that X denotes the charge concentration of the adsorbed cations. The cation exchange capacity is here assumed constant, an example of varying cation exchange capacity with external solution concentration is given in Chapter 6. The exchange sites are assumed to be occupied by Ca^{2+} and Mg^{2+} (or Sr^{2+}) ions only, so

$$X_{CEC\,n}^{j} = X_{Ca\,n}^{j} + X_{Mg\,n}^{j} \,. \qquad [A11]$$

The total cation initial concentration of Mg^{2+} plus Ca^{2+} in the soil solution (C_{Mg} and C_{Ca}) can be estimated from the monovalent anion concentration ($C_{ai\,n}^{j}$) in the first samples preleached (assuming only monovalent anions are present), as

$$\frac{C_{ai\,n}^{j}}{2} = C_{Ca\,n}^{j} + C_{Mg\,n}^{j} \,. \qquad [A12]$$

The exchange equation for the bivalent Ca-Mg system is given by (Robbins *et al.*, 1980),

$$\frac{C_{Mg}}{C_{Ca}} = \frac{1}{K_{Ca-Mg}} \frac{X_{Mg}}{X_{Ca}} \,. \qquad [A13]$$

Rearranging equations [A11 to A13], the initial solution concentration of Ca^{2+} is obtained as,

$$C_{Ca_n}^{\ j} = \frac{C_{a_n}^{\ j}}{1 + \left(\frac{1}{K_{Ca-Mg}} \frac{X_{Mg_n}^{\ j}}{X_{Ca_n}^{\ j}} \right)} \qquad [A14]$$

The initial concentration of Mg^{2+} can then be calculated using eq. [A11], and the initial total concentration of the individual cations ($M_{Ca_n}^{\ j}$ and $M_{Mg_n}^{\ j}$) from,

$$M_{Ca_n}^{\ j} = \theta\, C_{Ca_n}^{\ j} + \rho \frac{X_{Ca_n}^{\ j}}{2} \qquad [A15]$$

and

$$M_{Mg_n}^{\ j} = \theta\, C_{Mg_n}^{\ j} + \frac{X_{Mg_n}^{\ j}}{2} \,. \qquad [A16]$$

These initial values are computed in a subroutine of the program (Appendix B, Program 4)

The solute flux density of both Ca^{2+} and Mg^{2+} is calculated in a similar way as the anion flux [eq. 2.65] as,

$$q_{Ca_n}^{\ j+1} = C_{Ca_n}^{\ j} q_w - \lambda_{eff}\, q_w \frac{C_{Ca_{n+1}}^{\ j} - C_{Ca_n}^{\ j}}{\Delta z} \qquad [A17]$$

$$q_{Mg_n}^{\ j+1} = C_{Mg_n}^{\ j} q_w - \lambda_{eff}\, q_w \frac{C_{Mg_{n+1}}^{\ j} - C_{Mg_n}^{\ j}}{\Delta z} \qquad [A18]$$

The concentration of Mg^{2+} at the new time is obtained by combining the above equations [A11, A13, A15] to obtain the quadratic equation,

$$a_1 \left(C_{Mg_n}^{\ j+1} \right)^2 + b_1\, C_{Mg_n}^{\ j+1} + c_1 = 0 \qquad [A19]$$

where

$$a_1 = \theta\left(1 - \frac{1}{K_{Ca-Mg}}\right),$$

$$b_1 = \rho_b \frac{X_{CEC_n}^{\ j}}{2} - M_{Mg_n}^{\ j} - \frac{1}{K_{Ca-Mg}}\left(\rho_b \frac{X_{CEC_n}^{\ j}}{2} - 2M_{Mg_n}^{\ j} - M_{Ca_n}^{\ j}\right), \qquad [A20]$$

$$c_1 = \frac{1}{\theta K_{Ca-Mg}}\left(M_{Mg_n}^{\ j}\rho_b \frac{X_{CEC_n}^{\ j}}{2} - M_{Mg_n}^{\ j} M_{Ca_n}^{\ j} - M_{Mg_n}^{\ j} M_{Mg_n}^{\ j}\right)$$

The concentration of Mg^{2+} can then be calculated using the quadratic formula,

$$C_{Mg_n}^{\ j+1} = \frac{-b_1 \pm \sqrt{b_1^{\,2} - 4a_1 c_1}}{2a_1}. \qquad [A21]$$

The concentration of Mg^{2+} adsorbed at the new time is then found as

$$X_{Mg_n}^{\ j+1} = \frac{1}{\rho_b}\left(M_{Mg} - \theta C_{Mg_n}^{\ j+1}\right) \qquad [A22]$$

and the soil solution concentration of Ca^{2+} as

$$C_{Ca_n}^{\ j+1} = K_{Ca-Mg}\, C_{Mg_n}^{\ j+1} \frac{\left(\frac{X_{CEC}}{2} - X_{Mg_n}^{\ j+1}\right)}{X_{Mg_n}^{\ j+1}} \qquad [A23]$$

Combining these equations with the solute flux density equations yields the total concentration of Ca^{2+} and Mg^{2+} at the new time as,

$$M_{Mg_n}^{\ j+1} = M_{Mg_n}^{\ j} + q_{Mg_{n-1}}^{\ j+1} - q_{Mg_n}^{\ j+1}\frac{\Delta z}{\Delta t} \qquad [A24]$$

$$M_{Ca_n}^{\ j+1} = M_{Ca_n}^{\ j} + q_{Ca_{n-1}}^{\ j+1} - q_{Ca_n}^{\ j+1}\frac{\Delta z}{\Delta t} \qquad [A25]$$

Heterovalent system: Now we consider a system with monovalent and divalent cations, such as potassium, and calcium plus magnesium. We treat the Ca^{2+} and Mg^{2+} as a single species (CM). Then,

$$X_{CEC} = X_{CM} + X_K \qquad [A26]$$

The total cation concentration of Mg^{2+} plus Ca^{2+} and K^+ in the soil solution (C_{CM} and C_K) is then given by,

$$C_{ai\,n}^{\ j} = 2\,C_{CM\,n}^{\ j} + C_{K\,n}^{\ j} \qquad [A27]$$

and the equilibrium exchange equation is given by the Gapon equation (Robbins *et al.*, 1980),

$$K_{K-CM}\frac{X_K}{X_{CM}} = \frac{C_K}{\sqrt{C_{CM}}} \qquad [A28]$$

Rearranging equations [A26 to A28], the initial concentration of Ca^{2+} plus Mg^{2+} is obtained from,

$$C_{CM_n}^{\ j} = \frac{-b_2 \pm \sqrt{b_2^{\,2} - 4a_2c_2}}{2a_2} \qquad [A29]$$

where

$$a_2 = 4,$$

$$b_2 = -\left(4\,C_{ain}^{\,j} + \left(K_{CM-K} \frac{X_{Kn}^{\,j}}{X_{CMn}^{\,j}} \right)^2 \right), \qquad [A30]$$

$$c_2 = \left(C_{ain}^{\,j} \right)^2 .$$

The initial concentration of K^+ in the soil solution can then be obtained from [A27 and A29], and the initial mass from

$$M_{CMn}^{\,j} = \theta\, C_{CMn}^{\,j} + \rho_b \frac{X_{CM}}{2} \qquad [A31]$$

$$M_{Kn}^{\,i} = \theta\, C_{Kn}^{\,i} + \rho_b\ X_{Kn}^{\,j} . \qquad [A32]$$

The solute flux of Ca^{2+} plus Mg^{2+} and K^+ is calculated again as,

$$q_{CMn}^{\,j+1} = C_{CMn}^{\,j}\, q_w - \lambda_{eff}\, q_w \frac{C_{CMn+1}^{\,j} - C_{CMn}^{\,j}}{\Delta z} \qquad [A33]$$

$$q_{Kn}^{\,j+1} = C_{Kn}^{\,j}\, q_w - \lambda_{eff}\, q_w \frac{C_{Kn+1}^{\,j} - C_{Kn}^{\,j}}{\Delta z} , \qquad [A34]$$

and the concentration of Ca^{2+} plus Mg^{2+} and K^+ in the soil solution at the new time is obtained from

$$C_{CMn}^{\,j+1} = \frac{C_{CMn}^{\,j} - y}{y'} \qquad [A35]$$

$$C_{Kn}^{\,j+1} = x - 2\, C_{CMn}^{\,j+1} \qquad [A36]$$

where

$$x = M_{Kn}^{\,j} + 2\, M_{CMn}^{\,j} - \frac{\rho_b\, X_{CEC}}{\theta},$$

$$y = 4\theta \left(C_{CMn}^{\,j} \right)^2 - 2\, K_{CM-K}\, \theta \left(C_{CMn}^{\,j} \right)^{1.5} - 2\left(x\theta + 2\, M_{CMn}^{\,j} \right) \left(C_{CMn}^{\,j} \right) \qquad [A37]$$
$$+ K_{CM-K} \left(\theta x - M_{Kn}^{\,j} \right) \left(C_{CMn}^{\,j} \right)^{1/2} + 2\, M_{CMn}^{\,j}\, x$$

and y' is the derivative of y with respect to $C_{CM\,n}^{j}$.

Combining these equations with the solute flux equations yields the total concentrations of Ca^{2+} plus Mg^{2+} and K^{+} at the new time as,

$$M_{CM\,n}^{j+1} = M_{CM\,n}^{j} + q_{CM\,n-1}^{j+1} - q_{CM\,n}^{j+1} \frac{\Delta z}{\Delta t} \qquad [A38]$$

$$M_{K\,n}^{j+1} = M_{K\,n}^{j} + q_{K\,n-1}^{j+1} - q_{K\,n}^{j+1} \frac{\Delta z}{\Delta t} \qquad [A39]$$

Computer programs 4 and 5 are examples for numerical solutions for homovalent and heterovalent systems.

Another approach is the use of a Crank-Nicholson scheme, which is an explicit-implicit scheme. In this case, the solute flux is evaluated at the time t + (1/2 Δt), which makes the solution more stable. The computer programs used for simulating solute transport under transient water flow (section 4.2 and 5.4) are based on the Crank-Nicholson scheme. A detailed description of the Crank-Nicholson scheme for simulating solute transport is given for the 'WAVE' model by Vanclooster *et al.* (1994).

Appendix B

B.1 Program 1

```
'This program calculates the model parameters (Ds and v) for solutes applied as step
'change in input by least sum of squares optimization using equation [2.61], here for
'Column A, Manawatu fine sandy loam

INPUT " ENTER input filename: ", Inputfile$
INPUT " Enter output filename: ", Outputfile$
OPEN Inputfile$ FOR INPUT AS #1
OPEN Outputfile$ FOR OUTPUT AS #2

'INITIAL SECTION
'm is the number of points for which computation is carried out
'units m;h
'Input data: Q and  Cl C/Co data
'DD = estimated and calculated dispersion coefficient, vv = measured and calculated
'pore water velocity
'CLC = measured outflow concentration, Cex = simulated outflow concentration
'Q = cumulative outflow, qw = water flux density, m = number of points for which
'computation is carried out

DD = 290/1000: qw = 3.05/1000: L = 340/1000: m = 26: theta = .454: VV = qw / theta

DIM Q(m), t(m), CLC(m), Cex(m, 3, 3), SumSq(3, 3), Cr(m), D(3), v(3)
LSumSq = 1E+10
TSS = 0: delta = .05: Total = 0
FOR n = 1 TO m
      INPUT #1, Q(n), CLC(n)
      t(n) = Q(n) / qw
      Total = Total + CLC(n)
NEXT
Average = Total / m
FOR n = 1 TO m
      TSS = TSS + ((CLC(n) - Average) * (CLC(n) - Average))
NEXT
'DYNAMIC SECTION
DO UNTIL ABS(DD - D(1)) = 0 AND ABS(VV - v(1)) = 0
D(1) = DD
D(2) = DD + delta * 10
D(3) = DD - delta * 10
v(1) = VV
v(2) = VV + delta * 1
v(3) = VV - delta * 1
FOR u = 1 TO 3
FOR v = 1 TO 3
SumSq(u, v) = 0
FOR n = 1 TO m
```

```
'CDE solution
L = length
CM = (L - v(v) * t(n)) / SQR(4 * D(u) * t(n)): CP = (L + v(v) * t(n)) / SQR(4 * D(u) *
t(n))

P = v(v) * L / D(u)
A = 0: B = CM
exf = 0
IF B <> 0 THEN GOTO 101
exf = EXP(A): GOTO 105
101 CC = A - B * B: XX = ABS(B)
IF ABS(CC) > 170 AND B > 0 THEN GOTO 105
IF CC < -170 THEN GOTO 104
IF XX > 3 THEN GOTO 102
TT = 1 / (1 + .3275911 * XX)
Y = TT * (.2548296 - TT * (.2844967 - TT * (1.421414 - TT * (1.453152 - 1.061405 *
TT))))
GOTO 103
102 YY = XX + 1
Y = .5641896 / (XX + .5 / (XX + 1! / (XX + 1.5 / (XX + 2! / (XX + 2.5 / YY)))))
103 exf = Y * EXP(CC)
104 IF B < 0 THEN exf = 2 * EXP(A) - exf
105 term1 = exf / 2

A = P: B = CP
exf = 0
IF ABS(A) > 170 AND B < 0 THEN GOTO 205
IF B <> 0 THEN GOTO 201
exf = EXP(A): GOTO 205
201 CC = A - B * B: XX = ABS(B)
IF ABS(CC) > 170 AND B > 0 THEN GOTO 205
IF C < -170 THEN GOTO 204
IF XX > 3 THEN GOTO 202
TT = 1 / (1 + .3275911 * XX)
Y = TT * (.2548296 - TT * (.2844967 - TT * (1.421414 - TT * (1.453152 - 1.061405 *
TT))))
GOTO 203
202 YY = XX + 1
Y = .5641896 / (XX + .5 / (XX + 1! / (XX + 1.5 / (XX + 2! / (XX + 2.5 / YY)))))
203 exf = Y * EXP(CC)
204 IF B < 0 THEN exf = 2 * EXP(A) - exf
205 term2 = exf / 2
Cf = term1 + term2
Cr(n) = term1 + v(v) * SQR(.3183099 * t(n) / D(u)) * EXP(-CM * CM) - (1 + P + v(v)
* v(v) * t(n) / D(u)) * term2
Cex(n, u, v) = Cf
SumSq(u, v) = SumSq(u, v) + (CLC(n) - Cex(n, u, v)) * (CLC(n) - Cex(n, u, v))
NEXT
```

```
IF SumSq(u, v) < LSumSq THEN
      LSumSq = SumSq(u, v)
      DD = D(u)
      VV = v(v)
END IF
NEXT
NEXT
RSq = 1 - (LSumSq / TSS)
PRINT USING "#########.###"; LSumSq; DD; VV
LOOP

PRINT " t "; " Measured Cf "; " Predicted Cf "; "Predicted Cr"
FOR n = 1 TO m
PRINT USING "###.###"; t(n); CLC(n); Cex(n, 1, 1); Cr(n)
Q(n) = t(n) * qw
PRINT #2, USING "#####.###"; t(n); Q(n); CLC(n); Cex(n, 1, 1)
NEXT
PRINT USING "#######.#####"; LSumSq; DD; VV; RSq
CLOSE : END
```

B.2 Program 2

```
'This program calculates the model parameters (Ds and v) for solutes applied as pulse
'input by least sum of squares optimization using equation [2.62], here for Manawatu
'soil, column II under pasture.

CLS
INPUT " ENTER input filename: ", Inputfile$
INPUT " Enter output filename: ", Outputfile$
OPEN Inputfile$ FOR INPUT AS #1
OPEN Outputfile$ FOR OUTPUT AS #2

'INITIAL SECTION
'm is the number of points for which computation is carried out
'Q and  Cl C/Co data
'units m, h, concentrations in g m^-3, Mo in g m^-2
' DD = estimated and calculated dispersion coefficient, vv = measured and calculated
'pore water velocity
'CLC = measured outflow concentration, Cex = simulated outflow concentration
'Q = cumulative outflow, qw = water flux density, m = number of points for which
'computation is carried out
'Mo = pulse of solute applied


Mo = 60!
lambda = 75 / 1000: qw = 10.5 / 1000: z = 300 / 1000: theta = .402: m = 25

VV = qw / theta
DD = lambda * VV
pi = 3.416

DIM Q(m), t(m), CLC(m), Cex(m, 3, 3), SumSq(3, 3), D(3), v(3)
LSumSq = 1E+10
TSS = 0: delta = .1: Total = 0
FOR n = 1 TO m
    INPUT #1, Q(n), CLC(n)
    t(n) = Q(n) / qw
    Total = Total + CLC(n)
NEXT
Average = Total / m
FOR n = 1 TO m
    TSS = TSS + ((CLC(n) - Average) * (CLC(n) - Average))
NEXT
'DYNAMIC SECTION
DO UNTIL ABS(DD - D(1)) = 0 AND ABS(VV - v(1)) = 0
D(1) = DD
D(2) = DD + delta * .01
D(3) = DD - delta * .01
```

```
v(1) = VV
v(2) = VV + delta * .001
v(3) = VV - delta * .001

FOR u = 1 TO 3
FOR v = 1 TO 3
SumSq(u, v) = 0
FOR n = 1 TO m

'CDE solution

Cf = Mo / qw * z / 2 / SQR(pi * D(u) * t(n) ^ 3) * EXP(-(z - v(v) * t(n)) ^ 2 / 4 / D(u) /
t(n))
Cex(n, u, v) = Cf
SumSq(u, v) = SumSq(u, v) + (CLC(n) - Cex(n, u, v)) * (CLC(n) - Cex(n, u, v))
NEXT
IF SumSq(u, v) < LSumSq THEN
      LSumSq = SumSq(u, v)
      DD = D(u)
      VV = v(v)
END IF
NEXT
NEXT
RSq = 1 - (LSumSq / TSS)
PRINT USING "#########.###"; LSumSq; DD; VV
LOOP
PRINT " Q "; " Measured Cf "; " Predicted Cf "; "Predicted Cr"
FOR n = 1 TO m
Q = qw * t
PRINT USING "###.###"; Q(n); CLC(n); Cex(n, 1, 1)
PRINT #2, USING "#####.###"; Q(n); CLC(n); Cex(n, 1, 1)
NEXT
PRINT USING "#######.#####"; LSumSq; DD; VV; RSq
CLOSE : END
```

B.3 Program 3

```
'Numerical program to simulate the solute flux concentrations, based on the
'mobile/immobile model, here for Column B at the higher flow rate with flow
'interruption.
'units m, h and g m^-3

'"INITIAL SECTION
  DIM n AS INTEGER: CLS
  INPUT "ENTER Outputfilename:", Outputfile$
  OPEN Outputfile$ FOR OUTPUT AS #1

'nl = number of compartments, w = theta, wi = theta immobile, wm = theta mobile,
'ww = pore volume, dof = diffusion coefficient, msi = initial solute concentration,
'beta = dispersivity in 'mobile phase, ebeta = effective dispersivity,
'alpha = mass transfer coefficient, Q = cumulative outflow,
'ci = relative input concentration

  nl = 30: length = 295 / 1000: dt = .02: np = 5 - 1: nnp = 5
  dof = 3.6 / 1000 / 1000: ww = 0: t = 0: mout = 0
  alpha = .04: beta = 20 / 1000: qw = 13.1 / 1000: msi = 0
  dz = length / nl
  w = .438: wi = .14: wm = w - wi: pvl = length * w:  ww = w * length
  ebeta = beta - (dz - qw / wm * dt) / 2
  ci = 1

  DIM z(nl), ms(nl), msim(nl), msm(nl)
  DIM diff(nl + 1), disp(nl + 1), conv(nl + 1)
  FOR n = 1 TO nl
     z(n) = (n - .5) * dz
  NEXT

'"DYNAMIC SECTION
DO

'"STEP TIME
  t = t + dt: np = np + 1

'"CONTROL SECTION
  teff = t
  IF t * qw >= 110 / 1000 AND tstop = 0 THEN qw = 0: tstop = t
  IF t >= tstop + 12 THEN qw = 13.1 / 1000: teff = t - 12
  IF Q > 400 / 1000 THEN CLOSE : STOP

'"NITRATE
  conv(1) = ci * qw: diff(1) = 0: disp(1) = 0: diff(nl + 1) = 0: disp(nl + 1) = 0
  FOR n = 2 TO nl + 1
     conv(n) = msm(n - 1) / wm * qw
```

```
  NEXT
  FOR n = 2 TO nl
      diff(n) = (3.5 * w ^ 3 * dof) * (ms(n - 1) / w - ms(n) / w) / dz
      disp(n) = ebeta * qw * (msm(n - 1) / wm - msm(n) / wm) / dz
  NEXT
  FOR n = 1 TO nl
      vertdiff = diff(n) - diff(n + 1)
      interdiff = (msm(n) / wm - msim(n) / wi) * alpha * dz
      interdisp = disp(n) - disp(n + 1)
      msm(n) = msm(n) + (conv(n) - conv(n + 1) + vertdiff * wm / w - interdiff +
interdisp) *
      dt / dz
      msim(n) = msim(n) + (vertdiff * wi / w + interdiff) * dt / dz
      ms(n) = msim(n) + msm(n)
  NEXT
  mout = mout + conv(nl + 1) * dt
  IF qw > 0 THEN Cflux = conv(nl + 1) / qw ELSE Cflux = 0
'"OUTPUT
'"SCREEN PRINT
  IF np = nnp THEN
      np = 0
      Q = teff * qw
      PRINT USING "######.###"; t; teff; Q; Cflux
      IF Q > 0 THEN PRINT #1, USING "#######.###"; t; Q; Cflux
  END IF
LOOP
```

B.4 Program 4

```
'Numerical program to calculate the flux and resident concentrations for Ca2+ and Mg2+,
'here for Column A, Manawatu fine sandy loam
'units m, kg and hours, concentration mol m-3 (ie mmol/litre)

CLS
INPUT "ENTER Outputfilename:", Outputfile$
OPEN Outputfile$ FOR OUTPUT AS #1
INPUT "ENTER Outputfilename:", Outputfile$
OPEN Outputfile$ FOR OUTPUT AS #2

'nl = number of compartments, Q = cumulative outflow
'rhob = bulk density, qw = water flux density
'Cai = initial anion concentration, Cao = anion concentration of applied solution
'Cmgo and Ccao = Mg2+ and Ca2+ concentrations of applied solution, Kp = selectivity
'coefficient
'Xmgi and Xcai = initial concentration of Mg2+ and Ca2+ at adsorber.
'Mmgi and Mcai = initial total concentration of Mg2+ and Ca2+
'cfa = flux concentrations of anions, cresa = resident concentrations of anions,
'cfmg and cfca = flux concentration of Mg2+ and Ca2+

nl = 10: length = 340 / 1000: Cai = .8: Cao = 5: tmax = 543.6
theta = .454: qw = 2.69 / 1000: disp = 38 / 1000: rhob = 1350: dt = .05
tlpv = length / qw * theta: dz = length / nl
extra = 10: nll = nl + extra
counter = 0: maxcounter = 50
Kp = .7: Cmgo = 0: Ccao = 2.5

DIM CEC(nll), Xmgi(nll)

CEC(1) = .118: CEC(2) = .116: CEC(3) = .1: CEC(4) = .09: CEC(5) = .082:
CEC(6) = .08: CEC(7) = .08: CEC(8) = .077: CEC(9) = .073: CEC(10) = .067

FOR n = 1 TO extra
    CEC(nl + n) = .067
    NEXT

Xmgi(1) = .0166: Xmgi(2) = .0151: Xmgi(3) = .0122: Xmgi(4) = .0106:
Xmgi(5) = .0101: Xmgi(6) = .0086: Xmgi(7) = .0067: Xmgi(8) = .0062:
Xmgi(9) = .0052: Xmgi(10) = .005

FOR n = 1 TO extra
    Xmgi(nl + n) = .005
    NEXT


DIM Mmgi(nll), Mcai(nll), CoMg(nll), z(nll), CoCa(nll), Xcai(nll)
```

```
DIM Ca(nll), fa(nll), CECeff(nll), Mmg(nll), Mca(nll)
DIM Cmg(nll), fmg(nll), Cca(nll), fca(nll), Xmgieff(nll), Xmgeff(nll)

FOR n = 1 TO nll
    CECeff(n) = CEC(n) * 8 / 10
    Xmgieff(n) = Xmgi(n) * 8 / 10
    Xcai(n) = CECeff(n) - Xmgieff(n)
    z(n) = Kp * Xcai(n) / Xmgieff(n)
    CoMg(n) = (Cai / 2) / (1 + z(n))
    CoCa(n) = Cai / 2 - CoMg(n)
    Mmgi(n) = theta * CoMg(n) + rhob * Xmgieff(n) / 2
    Mcai(n) = theta * CoCa(n) + rhob * Xcai(n) / 2
    Ca(n) = Cai: Mmg(n) = Mmgi(n): Mca(n) = Mcai(n): Xmgeff(n) = Xmgieff(n)
NEXT

CLS : PRINT "Q", "fluxCa", "resCa", "fluxCmg", "fluxCca"

DO UNTIL t > tmax + .001
IF t > 162.4 THEN Cao = 47: Cmgo = 23.5: Ccao = 0

FOR n = 1 TO nll
    P = rhob * CECeff(n) / 2
    a1 = theta * (1 - 1 / Kp)
    b1 = P - Mmg(n) - 1 / Kp * (P - 2 * Mmg(n) - Mca(n))
    c1 = 1 / theta / Kp * (Mmg(n) * P - Mmg(n) * Mca(n) - Mmg(n) * Mmg(n))
    Cmg(n) = (-b1 + SQR(b1 * b1 - 4 * a1 * c1)) / 2 / a1
    Xmgeff(n) = 1 / rhob * (Mmg(n) - theta * Cmg(n))
    Cca(n) = Kp * Cmg(n) * (CECeff(n) / 2 - Xmgeff(n)) / Xmgeff(n)
NEXT

fa(0) = Cao * qw: fmg(0) = Cmgo * qw: fca(0) = Ccao * qw
fa(nll) = Ca(nll) * qw: fmg(nll) = Cmg(nll) * q: fca(nll) = Cca(nll) * qw

FOR n = 1 TO nll - 1
    edisp = disp - (dz - qw * dt / theta) / 2: IF edisp < 0 THEN STOP
    fa(n) = Ca(n) * qw - edisp * qw * (Ca(n + 1) - Ca(n)) / dz
    fmg(n) = Cmg(n) * qw - edisp * qw * (Cmg(n + 1) - Cmg(n)) / dz
    fca(n) = Cca(n) * qw - edisp * qw * (Cca(n + 1) - Cca(n)) / dz
NEXT
cfa = fa(nl) / qw: cfmg = fmg(nl) / qw: cfca = fca(nl) / qw
cresa = (Ca(nl) + Ca(nl + 1)) / 2
Q = qw * t

IF counter >= maxcounter THEN
PRINT USING "####.######"; Q; cfa; cresa; cfmg; cfca
PRINT #1, USING "####.######"; Q; cfa; cresa; cfmg; cfca
counter = 0
END IF
```

```
FOR n = 1 TO nll
      dM = (fa(n - 1) - fa(n)) * dt / dz
      Ca(n) = Ca(n) + dM / theta
      dM = (fmg(n - 1) - fmg(n)) * dt / dz: Mmg(n) = Mmg(n) + dM
      dM = (fca(n - 1) - fca(n)) * dt / dz: Mca(n) = Mca(n) + dM
NEXT
t = t + dt
counter = counter + 1
LOOP

FOR n = 1 TO 10
PRINT USING "####.#####"; n; Mmg(n); Cmg(n); Mca(n); Cca(n); Ca(n)
PRINT #2, USING "####.#####"; n; Mmg(n); Cmg(n); Mca(n); Cca(n); Ca(n)
NEXT
STOP
```

B.5 Program 5

```
'Numerical program to simulate the solute flux and resident concentration of Ca+Mg
'and K, here for Column A, Manawatu fine sandy loam
'units m, kg and hours, concentration mol m-3 (ie mmol/litre)

'Initial Section
CLS
INPUT "ENTER Outputfilename:", Outputfile$
OPEN Outputfile$ FOR OUTPUT AS #1
INPUT "ENTER Outputfilename:", Outputfile$
OPEN Outputfile$ FOR OUTPUT AS #2
'Note that C = calcium + magnesium here

'nl = number of compartments, rhob = bulk density, qw = water flux density
'cco = initial concentration of Ca+Mg, cko = initial concentration of K, kg = selectivity
'coefficient
'u = initial anion concentration, ccat = cation concentration
'Xki = initial concentration of K+ at adsorber, Xci = initial concentration of Ca2+ + Mg2+
'at adsorber
'Mki = initial total concentration of K+, Mci = initial total concentration of Ca2+ + Mg2+
'cfc = flux concentration of Ca2+ + Mg2+, cfk = flux concentration of K+
'mk and mc = total concentration of K+ and Ca2+ + Mg2+
'ck and cc = flux concentration of K+ and Ca2+ + Mg2+

nl = 10: length = 340 / 1000: cco = 2.5: cko = 0: tmax = 540
theta = .454: qw = 2.69 / 1000: disp = 38 / 1000: rhob = 1350
ccoiguess = .15: kg = 3.1: u = .8: dt = .005: dz = length / nl
edisp = disp - (dz - q * dt / theta) / 2: IF edisp < 0 THEN STOP
extra = 10: nll = nl + extra
counter = 0: maxcounter = 500

DIM CEC(nll), Xki(nll), Ccat(nll)
Ccat(n) = u / 2
CEC(1) = .118: CEC(2) = .116: CEC(3) = .1: CEC(4) = .09: CEC(5) = .082:
CEC(6) = .08: CEC(7) = .08: CEC(8) = .077: CEC(9) = .073: CEC(10) = .067

FOR n = 1 TO extra
    CEC(nl + n) = .067
    NEXT•

Xki(1) = .0125: Xki(2) = .0113: Xki(3) = .0088: Xki(4) = .0069: Xki(5) = .0067:
Xki(6) = .0054: Xki(7) = .0046: Xki(8) = .0045: Xki(9) = .004: Xki(10) = .0034

FOR n = 1 TO extra
    Xki(nl + n) = .0034
    NEXT
```

```
DIM Xkieff(nll), Xci(nll), z(nll), Mci(nll), Mki(nll), coci(nll), Coki(nll), ck(nll),
mk(nll), fk(nll)
DIM cc(nll), mc(nll), fc(nll), CECeff(nll)

FOR n = 1 TO nll
      CECeff(n) = CEC(n) * 8 / 10
      Xkieff(n) = Xki(n) * 8 / 10
      Xci(n) = CECeff(n) - Xkieff(n)
      z(n) = kg * Xkieff(n) / Xci(n)
      a2 = 4
      b2 = -(4 * u + z(n) * z(n))
      c2 = u * u
      coci(n) = (-b2 - (SQR(b2 * b2 - 4 * a2 * c2))) / 2 / a2
      Coki(n) = u - 2 * coci(n)
      Mci(n) = theta * coci(n) + rhob * Xci(n) / 2
      Mki(n) = theta * Coki(n) + rhob * Xkieff(n)
      mc(n) = Mci(n): mk(n) = Mki(n)
      cc(n) = ccoiguess
NEXT
 CLS : PRINT "Q", "fluxC", "fluxK", "CC(1)", "CK(1)"

'Dynamic Section
DO UNTIL t > tmax + .001
IF t > 162.5 THEN cco = 23.5

FOR n = 1 TO nll
P = rhob * CECeff(n)
g = (mk(n) + 2 * mc(n) - P) / theta
x = cc(n)
500    IF x < 0 THEN x = .001
      sqrx = SQR(x)
      y = 4 * theta * x * x - 2 * kg * theta * x ^ 1.5 - 2 * (g * theta + 2 * mc(n)) * x +
      kg * (theta *g - mk(n)) * sqrx + 2 * mc(n) * g
      diffy = 8 * theta * x - 3 * kg * theta * sqrx - 2 * (g * theta + 2 * mc(n)) + kg / 2 *
     (theta * g - mk(n)) / sqrx
      newx = x - y / diffy
      IF ABS((x - newx) / newx) > .01 THEN x = newx: GOTO 500
      cc(n) = newx: ck(n) = g - 2 * cc(n)
      NEXT
fk(0) = cko * qw: fc(0) = cco * qw
fk(nll) = ck(nll) * qw: fc(nll) = cc(nll) * qw
FOR n = 1 TO nll - 1
      fk(n) = ck(n) * qw - edisp * qw * (ck(n + 1) - ck(n)) / dz
      fc(n) = cc(n) * qw - edisp * qw * (cc(n + 1) - cc(n)) / dz
NEXT
cfk = fk(nl) / qw: cfc = fc(nl) / qw
Q = qw * t
IF counter >= maxcounter THEN
```

```
        PRINT USING "####.######"; Q ; cfc; cfk; cc(1); ck(1)
        PRINT #1, USING "####.######"; Q ; cfc; cfk
        counter = 0
        END IF

FOR n = 1 TO nll
        dM = (fk(n - 1) - fk(n)) * dt / dz: mk(n) = mk(n) + dM
        dM = (fc(n - 1) - fc(n)) * dt / dz: mc(n) = mc(n) + dM
NEXT
t = t + dt
counter = counter + 1
LOOP

FOR n = 1 TO 10
        PRINT USING "####.#####"; n; mk(n); ck(n); mc(n); cc(n)
        PRINT #2, USING "####.#####"; n; mk(n); ck(n); mc(n); cc(n)
NEXT
STOP
```